University of Glasgow

The phenotypic, genotypic and transcriptomic characterisation of a novel *Pseudomonas aeruginosa* small colony variant isolated from a chronic murine infection model

Submitted to the University of Glasgow for the degree of Doctor of Philosophy

Sharon C Irvine (BSc, MSc, MBChB, MRCP)

Institute of Infection, Immunity and Inflammation

College of Medical, Veterinary and Life Sciences

University of Glasgow

Acknowledgements

Firstly I would like to thank Dr Dan Walker for his supervision, support and enthusiasm throughout my PhD. Despite a difficult start to my fellowship, things were transformed under Dan's supervision. My thanks also go out to the rest of the Walker group, past and present who have been so much fun as well as inspirational. A special mention to Laura and Cameron for their invaluable help with my experiments.

I would also like to thank my secondary supervisor Dr Andrew Roe and all of the members of the Roe group for their help and support over the last 3 years. In particular James Connolly for his invaluable help with data analysis and Tom Parker for his help with experiments.

My research idea came from an incidental finding during Dr Hannah Bayes own research project. I would like to thank Hannah for all of her help and support throughout.
I am honoured to have been part of the microbiology team in Level 2 of the GBRC and feel that it is an ideal environment for a clinician to undertake a scientific PhD given the vast expertise within the department. I would like to thank each and every person on Level 2 of the GBRC for making this such an enjoyable experience.

Margaret from the electron microscopy department in the University of Glasgow has been fantastic in enabling me to produce high quality images of my work. Without her help this would not have been possible.

In addition I would like to thank Derek Brown from the reference laboratories for his help with the PFGE.

Furthermore I would like to acknowledge my collaborators in the DSMZ, Brunswick, Germany and in particular Dr Boyke Bunke and Cathrin Sproer for their amazing support throughout my project and their wonderful hospitality during my stay in Germany. Also a thank you to the Liverpool Centre for Genomic Research for their help in sequencing my DNA and RNA samples.

Many thanks to Medical Research Council (MRC) for their financial support and for accepting me on to this SCP3 Clinical Fellowship and to the University of Glasgow for enabling me to carry out this piece of research.

Abstract

Phenotypic change is a hallmark of adaptation of *Pseudomonas aeruginosa* to the lung during chronic infection in patients with cystic fibrosis (CF). Well-characterised phenotypic variants include mucoid and small colony variants (SCVs), the appearance of which is associated with disease severity. In this thesis, *P. aeruginosa* SCVs isolated from the murine lung following the establishment of chronic infection are characterised at the phenotypic and genetic level. The isolated SCVs are shown to closely resemble those isolated from CF patients and conversion to the SCV phenotype is accompanied by transcriptional changes that include upregulation of key virulence determinants and the oxidative stress regulon, suggesting that selection of the SCVs in the lung is driven by the host immune response to chronic infection. Using a combination of single-molecule real-time (PacBio) and Illumina sequencing we identified the genetic switch for conversion to the SCV phenotype as a large genomic inversion through recombination between homologous regions of two rRNA operons. The observations that a highly similar inversion is observed in a recently sequenced *P. aeruginosa* SCV isolate from a patient with cystic fibrosis and that genomic inversion in *S. aureus* can also drive conversion to an SCV phenotype, suggests this may be a common mechanism through which diverse bacteria adapt to the environment of chronically inflamed host tissue.

Author’s declaration

I hereby declare that this thesis is the result of my own work and has been composed for the degree of PhD at the University of Glasgow. All work presented was performed by myself unless otherwise stated and has not been submitted for any other degree at this or any other institution. All sources of information and contribution have been acknowledged in the text.

Sharon C Irvine

Abbreviations

AHL	Acyl homoserine lactones
AMR	Antimicrobial resistance
BAL	Bronchoalveolar lavage
BHI	Brain heart infusion broth
cAMP	Cyclic adenosine monophosphate
cDNA	Complimentary DNA
CF	Cystic fibrosis
CFTR	Cystic fibrosis transmembrane conductance regulator
CFU	Colony forming units
c-di-GMP	Cyclic diguanylate
COB	Columbia blood agar
COPD	Chronic obstructive pulmonary disease
CPA	Common polysaccharide antigen
dH_2O	Distilled water
DNA	Deoxyribonucleic acid
DNase	Dornase alpha/Pulmozyme
dNTP	Deoxynucleoside triphosphate
ECDC	European Centre for Disease Prevention and Control
EGTA	Ethylene glycol tetraacetic acid
EPS	Extracellular polymeric substances
ESBL	Extended spectrum beta-lactamase
FDA	Food and Drug Administration
GC	Guanine Cytosine
HCl	Hydrochloric acid
HIV	Human Immunodeficiency Virus
IV	Intravenous
LB	Lysogeny broth
LDH	Lactate dehydrogenase
LPS	Lipopolysaccharide
MDR	Multi-drug resistant

MH	Mueller-Hinton
MIC	Minimum inhibitory concentration
MMP	Matrix metalloproteinases
NaCl	Sodium chloride
MRSA	Methicillin-resistant Staphylococcus aureus
NLRC4	Nods-Like Receptor family, CARD domain containing 4
NGS	Next generation sequencing
OD600	Optical density at 600nm
OM	Outer membrane
ORF	Open reading frame
OSA	O-antigen-specific
PA	Pseudomonas aeruginosa
PacBio	Pacific Biosciences
PBS	Phosphate buffered saline
PCR	Polymerase chain reaction
PFGE	Pulse-field gel electrophoresis
PQS	Pseudomonas quinolone signal
PMN	Polymorphonuclear neutrophil
PVD	Pyoverdine
qRT-PCR	Quantitative real time PCR
QS	Quorum sensing
ROS	Reactive oxygen species
RNA	Ribonucleic acid
RPKM	Read per kilobase per million
SCV	Small colony variant
SEM	Scanning electron microscopy
SMRT	Single molecule real time
SNP	Single nucleotide polymorphism
TCA	Trichloroacetic acid
TEM	Transmission electron microscopy
TB	Tuberculosis
tRNA	Transfer RNA
TSB	Tryptone soya broth
T3SS	Type 3 secretion system
T4P	Type 4 pili

UK	United Kingdom
WHO	World Health Organisation

List of Figures

List of Tables

Table of Contents

Chapter 1 Introduction

1.1 Cystic Fibrosis

Cystic Fibrosis (CF) was first described in 1936 by Fanconi and further characterized by Andersen in 1938[1] and is the most prevalent, fatal single gene defect in the Caucasian population. Individuals of Northern European origin have the highest incidence of CF with about 1 in 2500 newborn children affected and a carrier frequency of 1 in 25[2]. Within the United Kingdom (UK), over 9,700 individuals have cystic fibrosis. The CF transmembrane conductance regulator (CFTR) gene, mapped on chromosome 7 encodes the gene responsible for CF which functions as a cAMP-regulated chloride ion channel[3]. CFTR is expressed in higher quantities in the tissues clinically affected by CF such as the sinuses, lungs, pancreas, liver, gastro-intestinal tract and reproductive tract making it a complex multi-system disease. The major cause of morbidity and mortality in this patient group is pulmonary infection and inflammation, which leads to progressive pulmonary failure. The most common pathogen in adult patients with CF is *Pseudomonas aeruginosa (P. aeruginosa)* which chronically infects most adult patients leading to irreversible respiratory demise[4].

The lungs of neonates with CF are pathologically normal, however infection and inflammation occurs early in life[4]. The initiating event for bacterial colonization remains poorly understood, however in early childhood infection with *Haemophilus influenzae* and *Staphylococcus aureus* is common[5]. Early infection leads to a florid inflammatory response with neutrophil recruitment and activation. Subsequently *P. aeruginosa* rapidly becomes the predominant organism and due to its ability to form complex drug resistant biofilms making this opportunistic pathogen almost impossible to eradicate[6] (see Figure 1-1). *P. aeruginosa* can be cultured from the sputum of approximately 80% of adults with CF over the age of 18. The definition of chronic *P. aeruginosa* infection is when 50% or more sputum samples test positive in a 12 month period for *P. aeruginosa*[7].

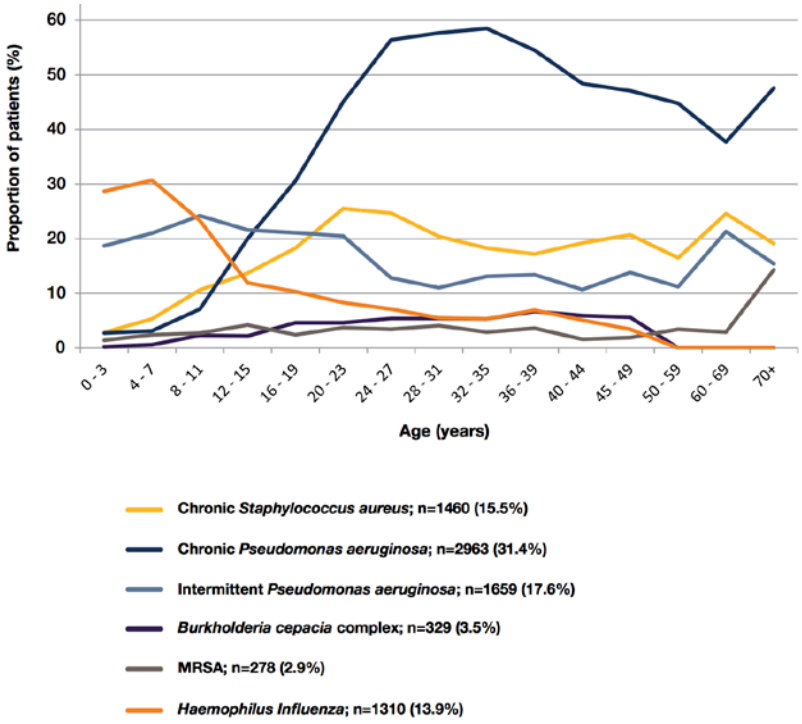

Figure 1-10-1 Bacterial burden in CF patients by age

Data gathered from the UK Cystic fibrosis registry annual data report 2014. The trend for *P. aeruginosa* infection is intermittent infection in approximately 25% of children under 15 years of age. (Taken from CF registry annual report 2014[8])

Later in the course of infection, further pathogenic bacteria including multi-resistant *Stenotrophomonas maltophilia*[9,10], *Burkholderia cepacia*[11–13], MRSA[14,15] and *Mycobacterium abscessus*[16] become increasingly problematic with failure of treatment and worsening outcomes[8].

1.2 *Pseudomonas aeruginosa*

P. aeruginosa is a Gram-negative, usually obligate aerobicfacultative anaerobic bacillus of the class Gammaproteobacteria. It is a ubiquitous environmental bacterium and opportunistic pathogen which normally inhabits the soil and aquatic environments, but is able to establish itself in vulnerable patients. It displays high levels of intrinsic resistance to many antibiotics and disinfectants, which makes it extremely difficult to eradicate. Serious *P. aeruginosa* infections are often nosocomial and the majority are associated with

significantly compromised host defences such as in neutropenia, severe burns or cystic fibrosis (Table 1-1).

Table 1-1 Common *P. aeruginosa* infections and risk factors[17]

Infection	Major risk factors
Soft tissue	Burns, wounds, ulcers, post surgery
Urinary tract	Use of urinary catheter
Bacteraemia	Immunocompromised in particular
Diabetic foot	Diabetes, impaired microvascular circulation
Respiratory/pneumonia	Elderly, COPD, bronchiectasis, cystic fibrosis, mechanical ventilation
Otitis externa	Tissue injury, water in ear canal
Keratitis	Extended contact lens wear, contaminated contact lens solution
Otitis media folliculitis	Poorly cleaned hot tubs

1.3 *Pseudomonas aeruginosa* pathogenesis and major virulence factors

Previous studies have revealed that *P. aeruginosa* isolated from acute infections differ significantly in phenotype from those isolated from chronic infections[18]. *P. aeruginosa* is endowed with a large genome containing over 5,570 predicted open reading frames (ORF's) and 6.3 million base pairs[19]. The *P. aeruginosa* genome is highly adaptable allowing it to rapidly colonise relatively hostile environments. As many as one in ten genes in the genome are involved in regulatory functions[20,21] and encode known or putative transcriptional regulators[22]. Studies of clinical and environmental strains have revealed that up to 90% of the genome is conserved between strains and very few single nucleotide polymorphisms (SNPs) seem to distinguish different strains, suggesting some phenotypic differences are likely to be due to changes in gene expression rather than genome sequence[23].

Isolates from acute infections express a wealth of virulence factors as outlined in Table 1-2 below whereas many isolates from chronic infections lack or produce low levels of some inflammatory features including pili and the type 3 secretion system (T3SS)[24]. Figure 1-2

outlines the interaction between the *P. aeruginosa* virulence factors and the host cells which allow cell adhesion, invasion and metabolism.

Table 1-2 Summary of *P. aeruginosa* virulence factors[25]

Pathogenic function	Cell-associated factors	Extracellular factors
Adhesion	Type IV pili Carbohydrate-binding proteins (lectins) Glycocalix Alginate slime (biofilm)	
Adhesion facilitation		Neuraminidase
Motility/Chemotaxis	Flagella (swimming), pili (twitching)	
Invasion		Elastase (LasB and LasA) Alkaline protease Haemolysins Cytotoxin (leukocidin) Pyocyanin pigment Siderophores
Toxinogenesis	Lipopolysaccharide (endotoxin) LecA and LecB lectins	Exotoxin A Type III effector cytotoxins – ExoS, ExoU, ExoT, ExoY Enterotoxin
Antiphagocytic surface properties	Slime layers Glycocalix Lipopolysaccharide	
Defense against serum bactericidal reaction	Slime layers Glycocalix	Protease enzymes
Defense against immune responses	Slime layers Glycocalix	Protease enzymes

Isolates from chronic patients more readily form biofilms and overexpress alginate, resulting in a mucoid phenotype[26]. Such altered virulence subsequently results in reduced immunostimulation and inevitably reduces clearance from the CF lung[6].

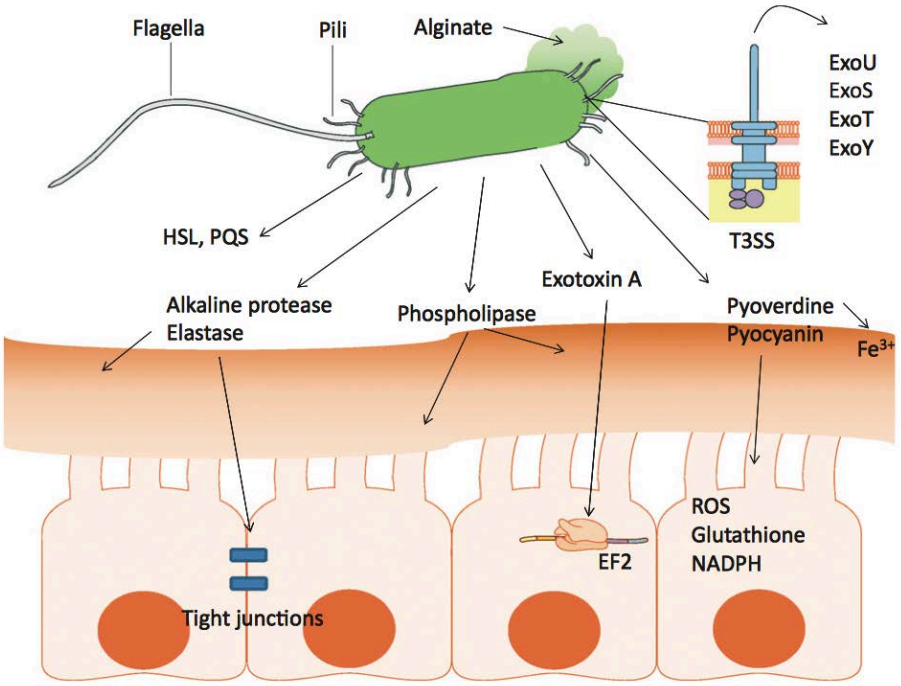

Figure 1-20-2 Virulence factors produced by *Pseudomonas aeruginosa*[17]

Main virulence factors produced by *Pseudomonas aeruginosa* and how these allow cell adhesion, invasion and metabolism. Taken from Gellatly with permission 2013[17].

1.3.1 Flagella and type 4 pili

Type 4 pili (T4P) are long protein fibres which provide the ability to adhere to chemically diverse surfaces including glass, metals and mammalian cells, promoting bacterial cell aggregation and virulence[27]. T4P are unique in mediating flagellum-independent, twitching motility[28,29]. Together with flagella, pili also facilitate swarming motility. They also provide a pivotal role in biofilm development, providing initial attachment to a surface therefore making them a major virulence factor in early infection. Often, T4P are downregulated in chronic infections[30].

Flagella are highly complex bacterial organelles with over 50 genes involved in their synthesis and function[31]. They are required for swimming motility and are well conserved between bacterial species and facilitate the acquisition of essential nutrients playing a role in the virulence of pathogenic organisms[32]. *P. aeruginosa* lacking functional flagella (Fla- mutants) have been shown to be less invasive than motile strains in a mouse burn infection model, with the addition of antiflagellum antibody also having a protective effect[31,33].

1.3.2 Quorum Sensing and Rhamnolipid Biosynthesis

Many bacteria use quorum sensing (QS) to monitor cell density and to coordinate their behavior[34] via small membrane-diffusible molecules called autoinducers (outlined in Fig 1-3). *P. aeruginosa* produces three autoinducers, two of which are acyl homoserine lactones (AHLs): 3-oxo-dodecanoyl homoserine lactone and butyryl homoserine lactone[35]. Recently it has been reported that *P. aeruginosa* produced a third intracellular signalling molecule, 2-hepatyl-3-hydroxy-4-quinolone designated the *Pseudomonas* quinolone signal[36,37] (PQS). To orchestrate the synchronous production of virulence factors and biofilm formation, *P. aeruginosa* depends on two major LuxI/R quorum-sensing systems[36,38], the Las and Rhl systems which act as global regulators of gene expression. Both regulatory proteins LasR and RhlR show high specificity and bind only their cognate signal molecule. Rather than working in parallel, the two systems form a hierarchy, with the Las system controlling the Rhl system. A small regulatory RNA-binding protein, RsmA negatively regulates the production of AHLs at the post-transcriptional level[35,39]. A non-coding RNA,second protein RsmZ (also known as RsmB), antagonises the action of RsmA[40,41], with overexpression of RsmZ resulting in loss of swarming behaviour[42].

The Rhl system controls the production of rhamnolipids which act as virulence factors and surface wetting agents, allowing easier flagellar motility over semi-solid surfaces[42]. The genes *rhlA, rhlB* and *rhlC* code for the enzymes that produce rhamnolipids. The genes which encode the rhamnosyls-transferase enzymes RhlA and RhlB are on the same operon and are strongly upregulated by the Rhl quorum-sensing signalling system[43]. A function of great importance is the fact that rhamnolipids cause release of LPS from the outer membrane resulting in increased surface hydrophobicity[44]. Within a biofilm community, rhamnolipids have an important role in maintaining non-colonised pores that are an essential part of the biofilm architecture[45].

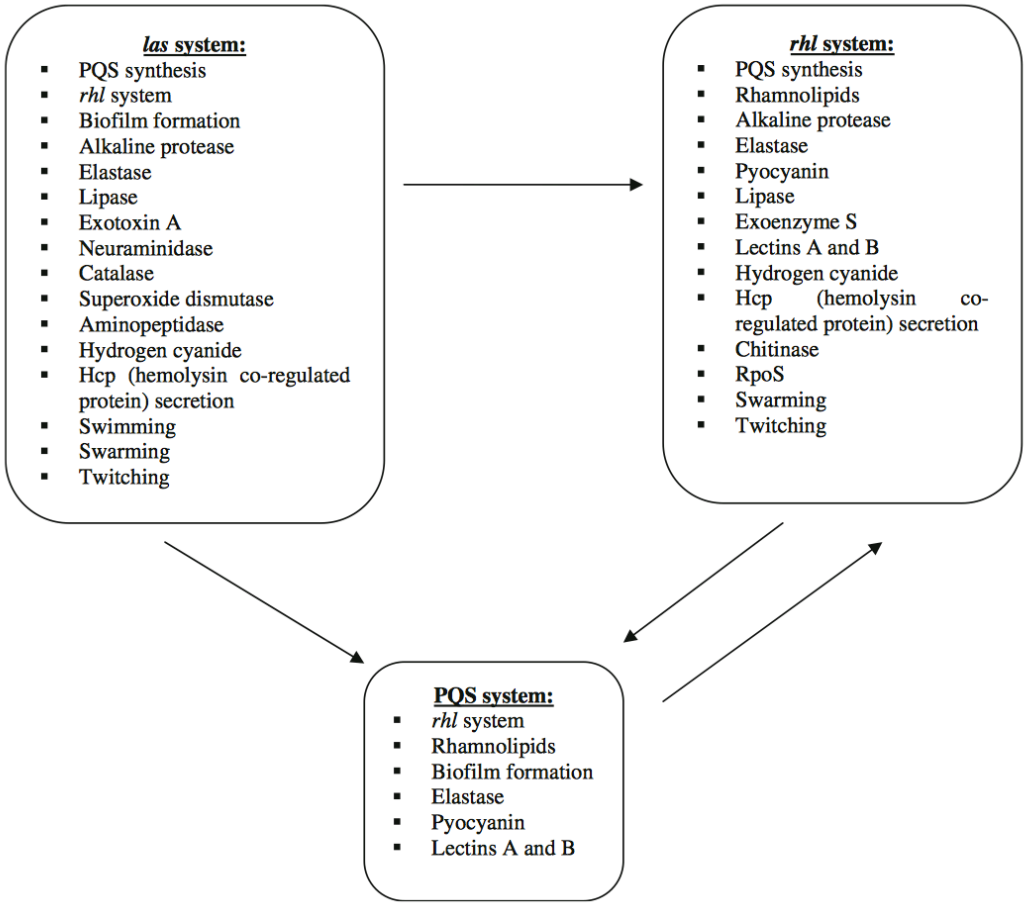

Figure 1-30-3 Quorum sensing regulators and their control

las and rhl are the two quorum sensing systems in Pseudomonas, which control expression of numerous genes. The Pseudomonas quinolone signal (PQS) provides a link between the las and rhl quorum sensing systems, strongly inducing rhl[39,46,47]. Taken with permission from Strateva 2011[25]).

Virulence factors which are regulated via this system include elastase, protease, exotoxin A, pyocyanin and siderophores[37,48–50], therefore strategies interfering with this cell-to-cell signalling system are potentially an innovative approach to combatting bacterial disease[51].

1.3.3 Biofilm Formation

Biofilms are microbial communities encased in an extracellular polymeric substances (EPS) which represents a protective mode of growth enabling microorganisms to survive in hostile environments facilitating the dispersion of seeding cells to colonise new niches[28,52].

It involves a coordinated and regulated transition from free-swimming planktonic bacteria to complex and highly differentiated communities of surface attached organisms (Fig 1-4). The formation of biofilms is intricately linked to QS[53]. Bacterial biofilms are implicated in chronic infections because they show increased tolerance to antibiotics and many disinfectant chemicals as well as the ability to resist phagocytosis and other components of the body's immune defence system[34]. Alginate is a well characterised component of *P. aeruginosa* biofilms although evidence suggests biofilm formation can also occur independently of alginate[28,54]. Early studies which examined the role of alginate in the initiation or maturation of biofilms focused on the mucoid phenotype from the CF lung, the basis of which is the overproduction of alginate. It was previously suggested that mucoid variants would most likely be responsible for biofilm formation in the CF lung and that the copious extracellular polysaccharide produced by these strains would play a protective role. A study by Wozniak in 2003[54] however suggested that in fact alginate is not a major constituent of the extracellular matrix of PA01 biofilms with the structural properties and antibiotic-resistance profiles of wild-type and *algD* mutant biofilms found to be indistinguishable[54].

Non-mucoid strains utilize primarily the Pel and Psl polysaccharide to form the extracellular matrix of the biofilm[55,56]. Regulation of Pel and Psl expression is complex, with multiple and intricate levels control. RpoS acts as a positive transcriptional regulator of *psl* gene expression[35]. Both the Gac-Rsm signal transduction pathway and QS have been suggested to positively regulate *pel* and *psl*[57].

The shift between motile and sessile states is under complex regulatory control, including the GacA/GacS two-component system which controls the translational repressor RsmA which directly affects biofilm formation via *pel*, *psl* and the second messenger cyclic-di-GMP (c-di-GMP)[35,58]. Additional studies have also identified and characterised YfiBNR as an important regulatory system involved in *P. aeruginosa* biofilm formation and in vivo persistence[59,60]. Activation of YfiN results in c-di-GMP production and consequent activation of several downstream targets affecting cell motility, exopolysaccharide production and induction of the Pel and Psl exopolysaccharides in particular.
Biofilms are highly heterogeneous environments with gradients of oxygen, nutrients and iron which may contribute to the slow growth of some bacteria in the biofilm and the upregulation of the stress response alternative sigma factor, RpoS, observed on transcriptional profiling[61,62]. Growth, protein synthesis and metabolic activity is high at

the surface of the biofilm however slow, impaired or no growth is observed in the centre of the biofilm which is one explanation for the reduced susceptibility of biofilms to antibiotics[63,64]. The centre of the biofilm is extremely limited in oxygen saturations which has been well documented and in fact these anaerobic conditions protect the *P. aeruginosa* strains growing in biofilms from killing by antibiotics[65]. Monotherapy with antibiotics is thus relatively ineffective at eradicating biofilm infections[66].

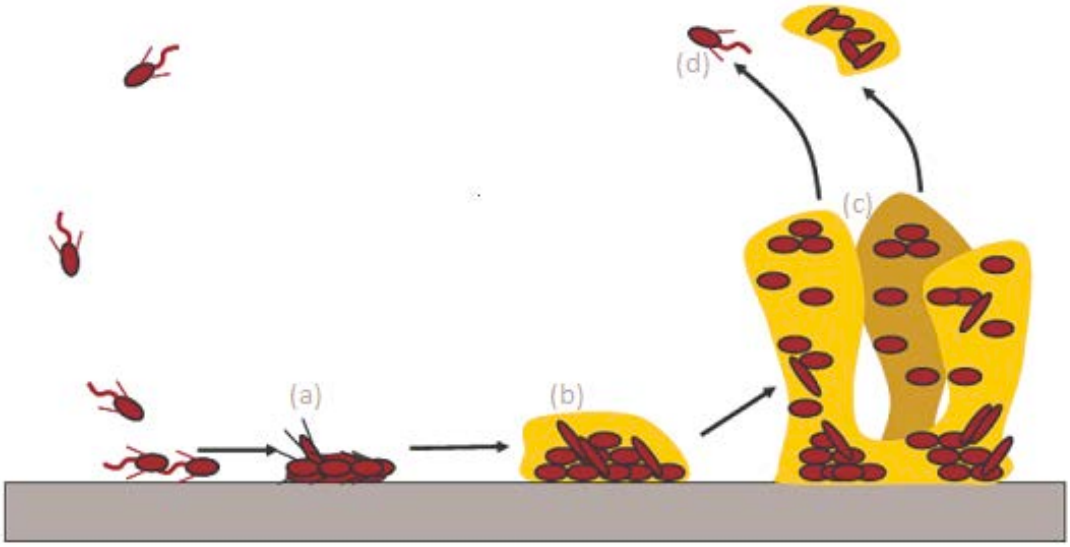

Figure 1-40-4. Process of biofilm formation
The process begins with (a) planktonic cells which adhere to a substratum, followed by (b) microcolony formation, (c) proliferation, maturation and mature biofilm formation and finally (d) detachment and reversion to planktonic growth.

1.3.4 Type 3 Secretion System

Type 3 secretion systems (T3SS) are produced by many pathogenic Gram-negative bacteria as a means of injecting toxins directly into the cytoplasm of eukaryotic cells. Cells of the innate immune system are thought to be the central target for T3SS intoxication allowing bacteria to evade clearance mechanisms, prevent phagocytosis and establish initial infection[67]. The injection of cytotoxins also leads to modulation of the actin cytoskeleton dynamics within the host cell, inhibiting mammalian DNA synthesis[68]. The role of T3SS in the unique setting of *P. aeruginosa* infection is controversial as studies have shown that isolates cultured from CF patients tend to secrete less T3SS effectors with increased duration of infection[69]. The T3SS of *P. aeruginosa* consists of

several proteins forming a macromolecular complex spanning the inner membrane, the periplasmic space, peptidoglycan layer, the outer membrane, the extracellular space and the host cell membrane (Figure 1-5).

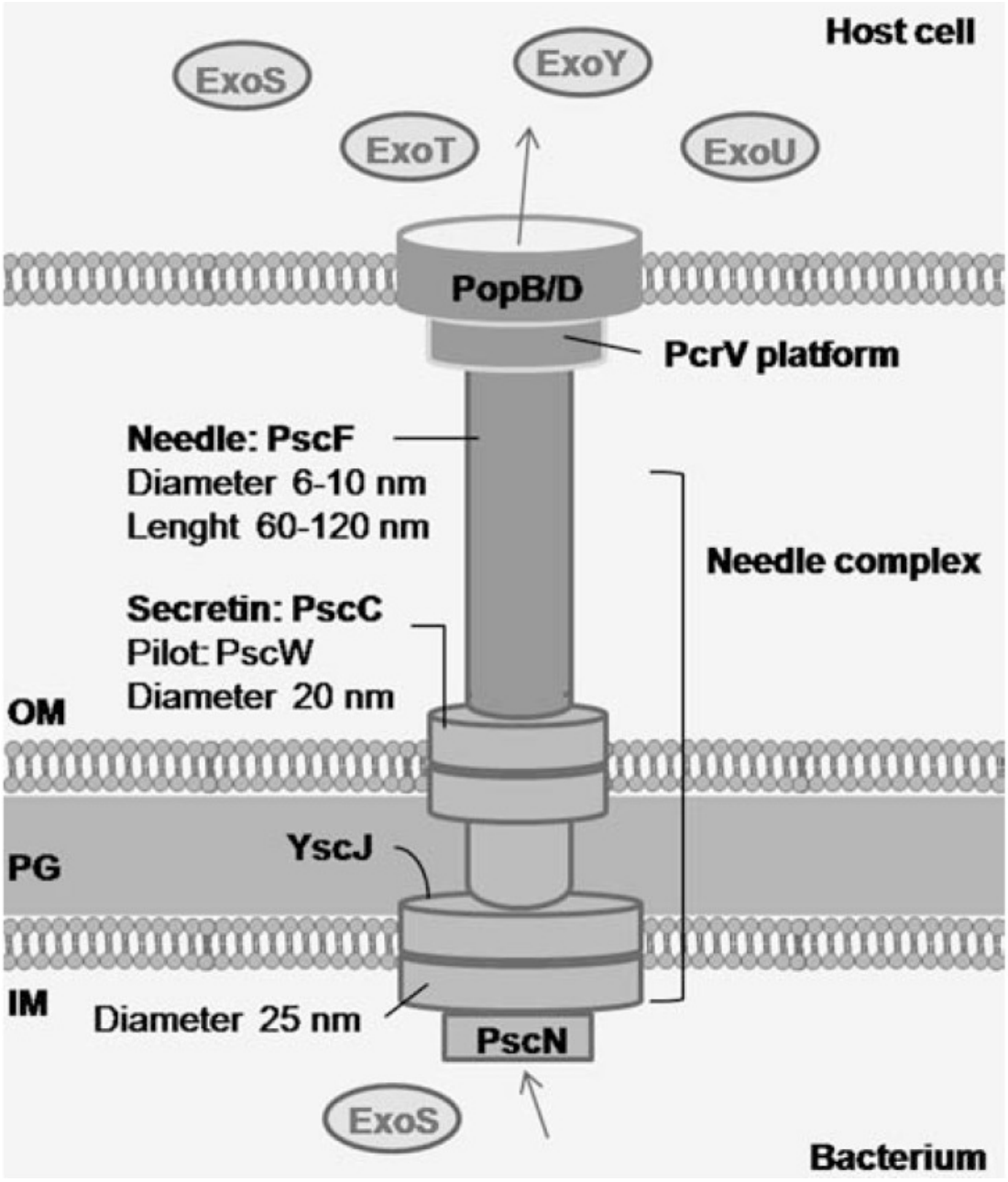

Figure 1-50-5 Type III secretion apparatus of *P. aeruginosa*

The main components making up the regulon: the needle complex and proteins involved in translocation, secretion, chaperone and effector functions. The four main effectors are shown, ExoS, ExoT, ExoU and ExoY. Taken with permission from Galle et al [70].

Thirty-six genes encoded in five different operons are involved in the biogenesis and regulation of the T3SS[71]. The complex regulon can be divided into five parts: proteins

constituting the needle complex, translocation of secreted proteins into host cells, proteins regulating the secretion process, chaperone proteins and effector proteins[72]. The needle-like appendage of the T3SS permits the translocation of proteins from the bacterium to the host through a pore formed in the cell membrane. Four effectors have been identified, ExoS, ExoT, ExoY and ExoU (Fig 1-5)[73–76] however most strains only posses three of the Exo effectors..

Type III secretion in *P. aeruginosa* is regulated at two levels: transcription of T3SS genes, via the transcription factor ExsA[70] and initiation of secretion itself. Transcription is induced upon activation of the secretion process allowing T3SS components to be produced at high levels when required[76]. Early studies revealed that ExsA is essential for full virulence in animal models of acute pneumonia in which alveolar instillation of ExoS producing *P. aeruginosa* strains led to severe alveolar damage when compared with mutant strains[77].

The T3SS has been shown to be a major reason for the cytotoxicity of the bacterium for a wide range of host cells. Comparison of the relative contributions of ExoS, ExoT and ExoU toxins to mortality, bacterial persistence and dissemination in a mouse model indicated that secretion of ExoU had the greatest impact[74]. In a mouse model of acute pneumonia it was found that secretion of ExoU was associated with a 40-fold decrease in the LD_{50} and in addition a significantly altered lung pathology[78]. Recent work has revealed that the increased virulence associated with ExoU secretion is the result of its phospholipase A2 activity, leading to cell death[79]. Additionally, the T3SS apparatus is itself a major cytotoxic factor independently of exotoxin translocation. It is associated with increasing inflammation and neutrophil recruitment into the airways[72] and therefore inhibiting the internalisation of *P. aeruginosa* into macrophages[80]. *P. aeruginosa* mutants with defective T3SS have been shown to be less virulent than their wild-type counterparts[75,81,82].

It has recently been shown that, via a functional T3SS, *P. aeruginosa* triggers the activation of an intracellular cytosolic sensor, NLRC4 (Nods-Like Receptor family, CARD domain containing 4)[83]. The NLCR4 detects the basal body rod component of the T3SS apparatus from a variety of bacteria including *Salmonella typhimurium*, *Burkholderia cepacia*, *Eschericia coli*, *Shigella flexneri* and *P. aeruginosa* [83–85]. Studies have shown that NLRC4-coupled inflammasome (a multimeric protein complex of innate immunity

involved in IL-18 and IL-1B secretion)[83] activation by T3SS leads to IL-8 secretion which increases neutrophil recruitment to the lung and subsequently lung injury[71].

1.3.5 Other virulence factors

The main role of proteases in *P. aeruginosa* virulence is thought to involve tissue penetration[86,87]. *P. aeruginosa* produces several extracellular proteases including LasA elastase (encoded by the *lasA* gene), LasB elastase (encoded by the *lasB* gene), alkaline protease (encoded by the *aprA* gene) and protease IV, all of which have been shown to play a major role during acute infection[88]. The participation of alkaline protease in systemic infections and tissue invasion is not entirely clear, however, it is known to play a substantial role in corneal infection[89]. LasA and LasB are regulated by the las quorum-sensing system and secreted via the type 2 secretion system[36]. They have elastolytic activity, degrading surfactant proteins and destroying elastin containing human lung tissue, resulting in pulmonary haemorrhages seen particularly in invasive *P. aeruginosa* infection[88]. Three other soluble proteins involved in invasion are also produced: a cytotoxin (previously named leukocidin) and two hemolysins which exert their major cytotoxic effects on lymphocytes, neutrophils and other eukaryotic cells[90].

Lipopolysaccharide (LPS) constitutes a physical barrier protecting the bacterium from host defences, mediating direct interactions with host cell receptors and antibiotic molecules[91–93]. It also acts as an endotoxin itself which initiates inflammation, host tissue damage and much of the pathology associated with bacteremia[91]. *P. aeruginosa* simultaneously produces two distinct LPS species, an O-specific antigen (OSA) and the common polysaccharide antigen (CPA)[94]. The CPA is composed of α-1-2, α1-3-linked D-rhamnose sugars and has been shown to be vital for attachment of the bacteria to respiratory epithelial cells[94]. Several studies have suggested that LPS contributes substantially to *P. aeruginosa* virulence including the toxic nature of LPS itself[95], development of serum resistance to LPS[96] and the fact that antibodies to LPS have been shown to be highly protective in animal models[97–99]. Studies on chronic infection in CF have also revealed that mean serum antibody titres to LPS correlate with duration of *P. aeruginosa* colonization and with disease severity as reflected by weight and vital capacity[100].

P. aeruginosa has a strong iron requirement and is able to excrete large amounts of two chemically unrelated siderophores, mainly pyoverdine (PVD) and to a lesser extent

pyochelin into its environment. They both function as powerful iron chelators allowing it to fulfill its nutritional requirements within the host which aims to limit iron availability to prevent bacterial growth[48,49,101]. In addition, *P. aeruginosa* also produces molecules which are directly and highly toxic to host cells. Pyocyanin, for example, is a toxic phenazine metabolite produced by *P. aeruginosa* which accelerates neutrophil apoptosis in vitro and is associated with reduced bacterial clearance from the lungs[102]. Pyocyanin is the most abundant phenazine and is present in significant quantities in the sputum of patients with cystic fibrosis and bronchiectasis whose lungs are colonised by *P. aeruginosa* [103]. The neutrophil-killing abilities of different *P. aeruginosa* strains correlate with their production of pyocyanin suggesting that phenazine-induced neutrophil apoptosis may be clinically relevant in the mechanism of *P. aeruginosa* persistence.[104,105] Pyocyanin is also responsible for causing oxidative damage to the host and mitochondrial electron transport disruption[105]. There is overwhelming in vitro and in vivo experimental data to support the argument the pyocyanin has important roles during *P. aeruginosa* -mediated pathogenesis[104–106]. *P. aeruginosa* also produces hydrogen cyanide which acts as a potent respiratory inhibitor due to its reactivity with cytochrome c oxidases and other metalloenzymes leading to the inhibition of aerobic respiration[107,108]. There is accumulating evidence for a role of cyanide in pathogenicity as a mediating factor in the paralytic killing of *Caenorhabditis elegans*[109].

1.4 *Pseudomonas aeruginosa* and Airway Infection

The lung is exposed to a constant bombardment of harmful inhaled agents and microorganisms. Several layers of defence in the healthy lung help prevent infection from inhaled or aspirated microorganisms. A combination of mechanical filtering, the innate mucosal immunity and circulating immune cells all participate in the clearance of microorganisms from the lung, usually at the cost of some degree of inflammation. A loss of any of these barriers frequently results in lung infection. Figure 1-6 below outlines the steps in initial colonisation of the lung followed by the establishment of acute and chronic infection.

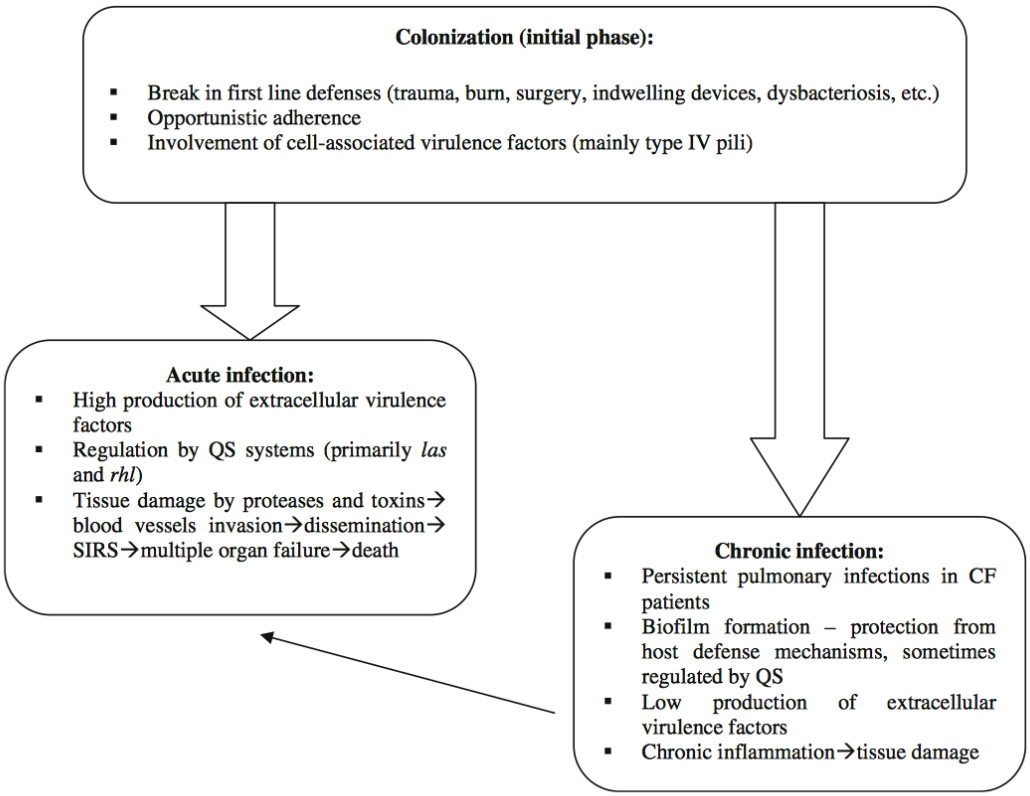

Figure 1-6 Stages of Pseudomonas lung infection

Lung infection is initiated by a break in the first line defences of the host, leading to colonisation. Acute infection results from high production of extracellular virulence factors and often multi-organ failure leading to death. Chronic infection is secondary to the more indolent persistence of bacteria in the lung and chronic inflammation as a result of biofilm formation. Taken with permission from Strateva et al, 2011[25]

P. aeruginosa is one of the most common pathogens causing respiratory infections of hospitalized patients. In CF patients, airway infection with *P. aeruginosa* leads to a broad spectrum of lung injury and pathological response. Acute lung injury, in comparison, which can lead to nosocomial necrotizing pneumonia is associated with a high incidence of morbidity and mortality[110]. Infection leads to destruction of the epithelium and bacterial invasion of the pulmonary vasculature with subsequent bacteraemia due to increased production of extracellular virulence factors (figure 1-6). Ventilator associated pneumonia generally demonstrates a mortality as high as 30%[110].

At the other extreme is the chronic and persistent airway infection seen in both cystic fibrosis and other chronic lung conditions where lung defence is damaged, including bronchiectasis. If not eradicated during the acute infection phase, *P. aeruginosa* can adapt to the lung environment to grow as a biofilm resulting in chronic infection (figure 1-6).

Typically, the bacteria isolated from an established chronic infection are less inflammatory and cytotoxic than the strains isolated years earlier from the same patient during the initial phase of infection[111]. Chronic *P. aeruginosa* lung infection in the form of structured biofilms is still highly problematic as it is generally not eradicable. CF patients often develop a *P. aeruginosa* lung infection by adolescence and can live with persistent infection for 20 years or more.

In CF, the thickened respiratory secretions, as a result of the CFTR mutation, prevents clearance of bacteria and impairs the immune response resulting in perpetual immunological stimulation[110]. As a consequence of persistent inflammation and impaired bacterial clearing, patients develop worsening suppurative lung disease. Small airways become obstructed with viscous mucus, organisms and inflammatory cells. An endless cycle of infection, inflammation and progressive endobronchial destruction and loss is established, leading to widespread fibrosis and bronchiectasis. Respiratory failure may finally develop with hypoxaemia and hypercapnia which is responsible for over 80% of CF-related deaths[5].

Outside CF, chronic infection with *P. aeruginosa* is also commonly seen in the setting of bronchiectasis and chronic obstructive pulmonary disease (COPD)[112,113]. The *P. aeruginosa* isolates from these conditions also share features to those seen in CF including the mucoid phenotype with increased mutation rates, increased antibiotic resistance and increased biofilm formation[114].

1.4.1 Immune Responses in Cystic Fibrosis

Absence of the CFTR function leads to chronic lung disease which is characterised by inflammation and persistent infection. There is significant controversy as to whether patients with CF have an intrinsic impairment in their immune response, which predisposes to pulmonary *P. aeruginosa* infection, with particular focus on neutrophil dysfunction[115–117]. The exact mechanisms are complex and only partially understood. Clinical data indicates that patients with CF have a normal immune response at sites other than the lung[118]. Alterations in the cellular components of the innate and adaptive immune system are likely to contribute to the impaired immune defence in CF lung disease.

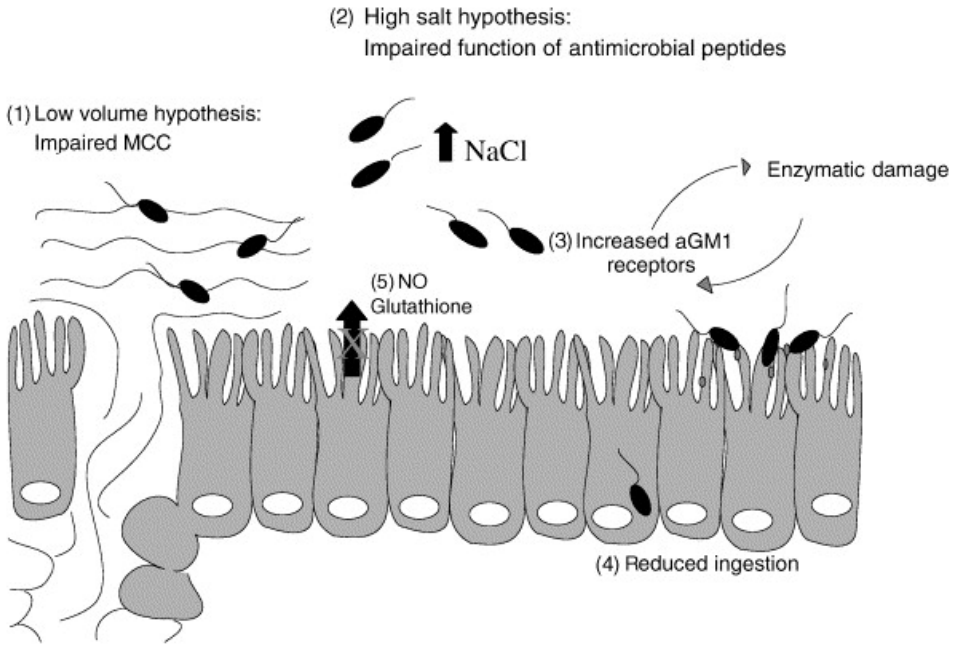

Figure 1-7. The suggested hypothesis to explain the predilection of *Pseudomonas aeruginosa* for the cystic fibrosis airway.

(1) Impaired mucociliary clearance (MCC) due to dehydrated airway surface liquid (ASL) and mucus. (2) The malfunction of antimicrobial peptides due to raised ASL salt content (3) An increased availability of bacterial receptors and the production of neuraminidase. (4) Defective internalization of bacteria by CF epithelial cells. (5) Low levels of defence molecules such as NO and glutathione. Image taken with permission from Davies et al, 2002[6].

There are three general components comprising the innate and adaptive immune defences in the respiratory tract (Figure 1-7): (1) the mucociliary escalator; (2) humoral component of surfactant proteins, defensins and other antimicrobial compounds; and (3) cellular component including epithelial cells, monocytes, macrophages, neutrophils, dendritic cells and lymphocytes.

1.4.2 Neutrophilic inflammation and lung injury

CF lung disease is dominated by neutrophilic airways inflammation, with high levels of neutrophils being recovered from airway fluid samples including sputum and broncoalveolar lavage (BAL). In addition, high levels of IL-8 are consistently found and is known to act as a major neutrophil chemoattractant[117,119]. IL-8 induced recruitment of

additional neutrophils to the airways results in release of neutrophil elastase[120,121] and the additional induction of IL-8 gene expression by bronchial epithelial cells, which establishes a chronic cycle of respiratory inflammation leading to poorer disease outcome[121–123]. Neutrophils induce lung damage via various mechanisms including release of matrix metalloproteinases (MMPs) which have the ability to degrade phagocytosed proteins. Neutrophil elastase is able to degrade a number of structural proteins including elastin, collagen, fibronectin and proteoglycan and also augments mucus secretion adding to airway obstruction[120,121].

1.4.3 B cell and T cell Responses

The role of B cell responses against pulmonary *P. aeruginosa* infection remains unclear. *P. aeruginosa* specific IgA and IgG are produced by CF patients in response infection and have been found to increase progressively as patients develop chronic infection[124,125]. Mice unable to produce secretory IgA in lung secretions were found to have a three-fold increase in mortality in response to acute *P. aeruginosa* infection[126]. Infection with *P. aeruginosa* is known to evoke a T cell response. In a murine model of acute *P. aeruginosa* infection, T cell immunity was found to develop and be important in host defence whereas humoral immunity was found to be dispensable[127].

1.5 Current Management of Cystic Fibrosis

Life expectancy in cystic fibrosis has improved dramatically in the last 4 decades, unfortunately, however, the majority of patients still die of respiratory failure with a mean predicted survival of 28 years[8]. The primary aim of therapy is to slow the progression of lung disease with meticulous daily management together with prompt, aggressive treatment of exacerbations to preserve lung function[2]. Figure 1-8 below highlights the improvement and reduction in chronic *P. aeruginosa* infection between 2008 and 2014.

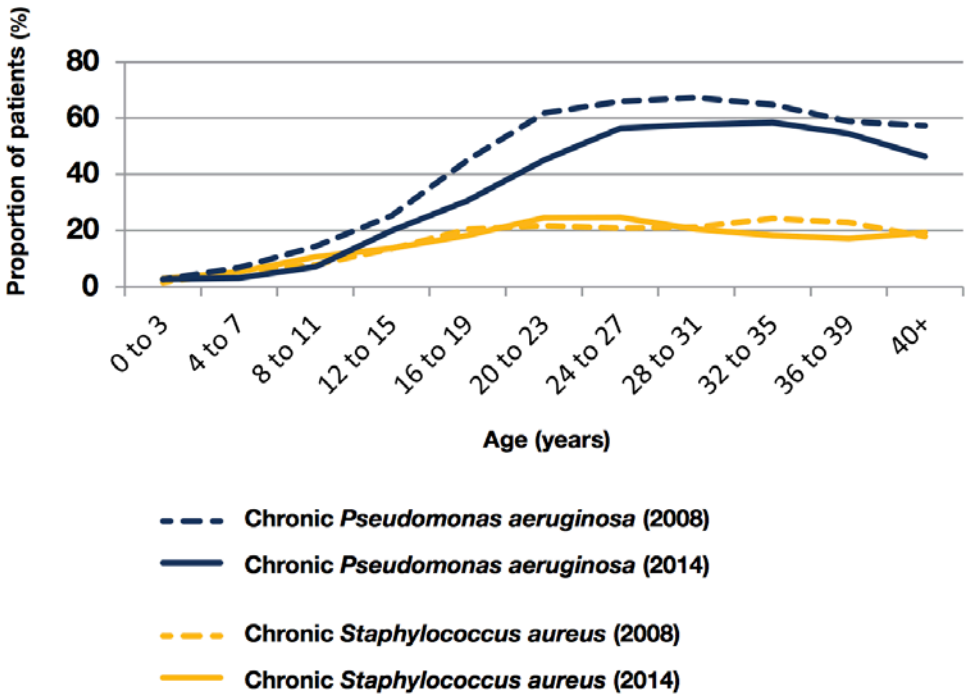

Figure 1-8. Proportion of patients with chronic *Pseudomonas aeruginosa* and *Staphylococcus aureus* infection over time

Data gathered from the UK Cystic fibrosis registry outlining the age at acquisition of *Pseudomonas aeruginosa* infection and subsequently lifelong persistence. Taken from CF registry annual report. 2014[8]

1.5.1 Antibiotic therapy

Antibiotic therapy for patients with CF is primarily directed at preventing, eradicating or controlling respiratory infections. Prompt use of antibiotics in these situations has been one of the major reasons for decreased morbidity and mortality over the last few decades. Detailed and up to date guidelines can be found at the Cystic Fibrosis Trust[8] website and also the European Cystic Fibrosis Society Standards of Care: Best Practice guidelines[2]. Briefly, treatment of *P. aeruginosa* infection begins with first isolates which are treated with a combination of oral ciprofloxacin and nebulised colistin for a period of 3 months. If the initial treatment of *P. aeruginosa* infection fails, or if patients become chronically infected, a combination of intravenous (IV) antibiotics is used. Although IV antibiotics have played a central role in the management of pulmonary infection in CF for 4 decades, there have only been two studies comparing their action against placebo[128,129]. The general principles of treatment of exacerbations depend on the clinician and the patient involved as well as the organism isolated from the sputum culture. The sensitivity pattern from the

organisms isolated from sputum and the clinical response shown by the patient is often discordant when there is infection with *P. aeruginosa*. First line treatment of *P. aeruginosa* comprise a β-lactam e.g. ceftazidime, meropenem, or an anti-pseudomonal penicillin (piperacillin-tazobactam or ticeracillin-clavulanic acid) combined with colistin or tobramycin. Nebulised colistin and tobramycin are widely used as long term treatments for patients chronically infected with *P. aeruginosa* and many clinicians will stop nebulised antibiotics whilst the patient is receiving IV antibiotics[8].

A number of different morphotypes of *P. aeruginosa* may be present in cultures from CF patients, which may complicate the useful interpretation of antibiotic sensitivity patterns. There is a concern that the use of a single antibiotic may be associated with increased levels of antibiotic resistance, hence the use of tailored combination therapy with antibiotics of differing mechanisms of action used[130–132].

Azithromycin is a macrolide antibiotic often used on a long-term basis in patients with chronic lung infections including CF, COPD and bronchiectasis. Azithromycin has well described anti-inflammatory properties with several studies showing that azithromycin alters macrophage phenotypes and inhibits inflammatory cytokine production[133–136]. A recent Cochrane review of the evidence revealed that addition of azithromycin to therapy doubled the rate of being free of exacerbations over 6 months compared to placebo. The need for oral antibiotics was also significantly reduced with azithromycin[137].

1.5.2 Channel Potentiators

The most common mutation responsible for the CF phenotype is the Phe508del mutation encoding the CFTR protein with approximately 45% of patients with cystic fibrosis homozygous for this allele[5]. The Phe508del mutation results in significantly reduced protein levels at the epithelial membrane and for those channels which do reach the membrane, the mutation also disrupts channel opening[5,138]. Together, these effects lead to minimal CFTR chloride transport activity. One approach to treating CF is to target the dysfunction of the CFTR channel in two specific steps: increase the amount of functional mutated CFTR and potentiation to increase channel opening[139].

Ivacaftor (Kalydeco) is an investigational CFTR potentiator and has been shown in numerous clinical studies to potentiate CFTR channel gating and enhance chloride

transport mainly in the G551D CFTR gating mutation, however may have a similar effect on all CFTR forms[140–142].

Lumacaftor is an investigational CFTR corrector that has shown in vitro to correct Phe508del CFTR misprocessing and ultimately increase the amount of cell-surface protein[143]. The combination of ivacaftor and lumacaftor in patients with CF who are homozygous for the Phe508del CFTR mutation has been shown in several studies to be associated with an increase in chloride transport than has either agent alone[143–146].

1.5.3 Mucolytics

Lower airway mucus accumulation is a key factor in CF lung disease by favouring chronic airway infection with *P. aeruginosa* and other Gram-negative organisms. There is characteristic airway inflammation which leads to bronchiectasis, progressive pulmonary function decline and eventually respiratory failure (see figure 1-9).

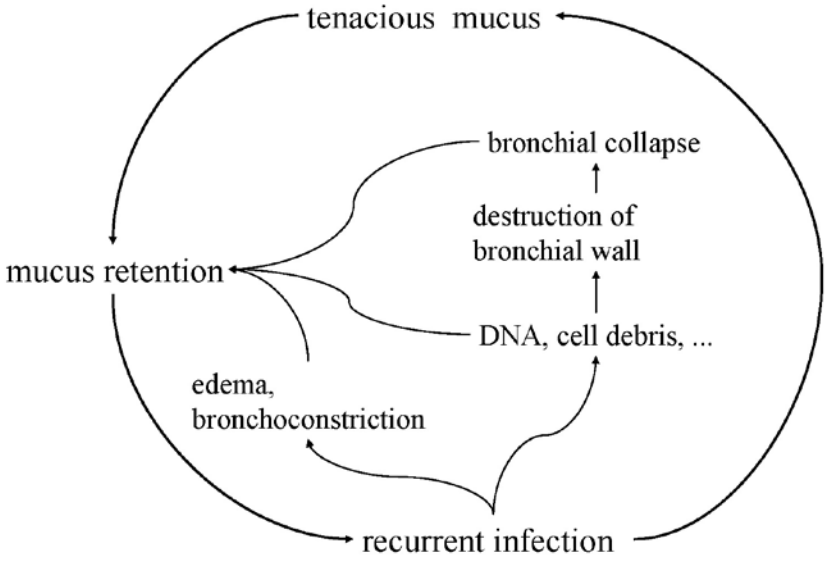

Figure 1-9 Cycle of mucus retention and recurrent infections.
Image taken from Tenke et al with permission[147].

Mucolytic agents break down the complex gel structure of mucus and therefore decrease its viscosity and elasticity. The only mucus degrading agent with proven efficacy in CF is

dornase alfa (DNase or Pulmozyme)[148,149]. As early as 1959, DNA was identified as being present in significantly higher quantities in sputum from CF patients compared to those with bronchiectasis resulting in increased sputum viscosity[150]. The source of DNA was identified as primarily leukocytes infiltrating the sputum as a result of infection with elevated DNA concentrations also being found in bronchoalveolar lavage fluid from infants with CF[111,151,152]. Dornase alpha specifically cleaves the extracellular DNA into shorter lengths which transforms the CF sputum into a flowing liquid[148]. Other mucolytics such as N-acetylcysteine have not been proven to be effective in CF patients[153].

1.5.4 Airway clearance techniques

In addition to the above therapies and nebulised saline solutions, chest physiotherapy uses airway clearance techniques to help clear excess mucus from the lungs. Once the lungs become productive of purulent sputum, airway clearance treatment is usually required on a daily basis and may be required up to three-four times during an exacerbation[154].

1.6 Phenotypic Variation in Chronic Infection

Phenotypic variation is a hallmark of adaptation to the host during chronic bacterial infection. Several studies have followed progression of Pseudomonas infection in patients with CF suggesting that a number of genotypic and phenotypic changes occur over time. The long term persistence of P. *aeruginosa* in the cystic fibrosis (CF) lung is characterized by the selection of a variety of genotypes and phenotypes that typically descend from one infecting *P. aeruginosa* clone via adaptive changes. *P. aeruginosa* isolates from a single patient may differ significantly in their specific morphotypes including mucoid, rough, smooth, dwarf, colourless, small colony variants and variants with visible autolysis or autoaggregative behaviour. These morphotypes may all differ significantly in their behaviours and antibiotic susceptibility patterns[155–157]. The changes seen in bacteria isolated from chronic infections typically include loss of flagellum and pili [158](required for adherence and type III secretion system function[159]), mutations in *mucA*, *mucB* or *mucD* resulting in transformation to the mucoid phenotype[160,161].

A phenotypic variant common to diverse bacteria is the small colony variant (SCV) which is characterised by reduced growth, increased adherent biofilm production[162], antibiotic resistance, hyperpiliation and atypical colony morphology. SCVs have been described for

a wide range of bacterial genera and species including *Staphylococcus aureus*, *Staphylococcus epidermidis*[163], *Streptococcus sp*[164,165], *Enterococcus*[166], *Listeria*[167], *Burkholderia*[12], *Salmonella*[168], *Vibrio*[169], *Shigella*, *Brucella*[170], *Lactobacillus*, *Serratia*, *Neisseria*[171] species and yeast[172]. *S. aureus* SCVs have been most extensively studied and their presence in persistent and recurrent infections is associated with a poor clinical and bacteriologic response to standard antimicrobial therapy in patients with abscess, chronic osteomyelitis, implantable prosthetic devices and bronchopulmonary infections[173–176]. Recently SCVs from *Enterococcus faecium* have been isolated from several patients. One case was thought to be due to epithelial cell invasion and subsequent intracellular persistence in the bladder in a patient with recurrent urinary tract infections[177]. A second case of an Enterococcus SCV was from a confirmed native heart valve endocarditis, likely due to SCV subpopulations with decreased sensitivity or resistance to the antibiotics given[178]. Chronic prosthetic joint infections are a major cause of morbidity and mortality following orthopedic surgery. There are many case studies focusing on the SCVs role in prosthetic infections, but also similar studies looking at gram-negative SCVs, including *Escherichia coli*[179]. In the case of *P. aeruginosa*, SCVs are commonly associated with chronic infection of the lung in patients with cystic fibrosis.

1.6.1 SCVs in Chronic infection of the CF lung

The opportunistic pathogen *P. aeruginosa* is responsible for chronic infections in the airways of cystic fibrosis (CF) patients leading to progressive decline in pulmonary function and inevitably respiratory failure. Over 2-years of follow up, *P. aeruginosa* SCVs were isolated from 38% of patients with CF infected with *P. aeruginosa* [180,181]. Compared with patients without SCVs, the presence of SCVs was associated with poorer lung function as well as increased daily inhaled antibiotic usage[180]. *P. aeruginosa* SCVs demonstrate features favouring chronic and persistent infection in the deeper airways including increased biofilm formation[11,155] which enables them to resist physical stress and antibiotic therapy and enables increased adherence to respiratory cells[155]. SCVs are able to grow preferentially in nutrient deplete conditions, which would favour the persistence in the CF lung and the ability to outgrow the wild-type phenotypes[182].

The exact mechanism behind the phenotypic switch to SCV has yet to be fully elucidated and research has shown that a number of different mutations can confer the SCV phenotype[47,60,182,183]. A recent study showed that a large scale chromosomal inversion

enabled conversion between a normal colony *S. aureus* (NCV) and a SCV isolated from the same patient, found presumably allowing it to switch its phenotype to adapt to the environment during chronic infection[184]. *S aureus* SCVs have been well studied in CF and are detected in about a quarter of patients[173,185]. The presence of *S. aureus* SCVs is independently associated with substantially worse outcomes and worse lung function[185,186]. Given the virulent properties of SCVs and their altered antibiotic susceptibility profiles, it is important to confirm their presence in the microbiology laboratory. Unfortunately, the mixed cultures obtained from sputum samples frequently makes the detection of SCVs very difficult. Figure 1-10 below demonstrates the marked difference in colony size between a normal colony variant and an SCV. Several studies have also suggested that the ability of granulocytes to uptake *S. aureus* SCVs is decreased. It can therefore be hypothesized that the specific environmental conditions present in the host suffering from CF (highly viscous mucous, hyperosmolarity, oxidative stress) may select for SCVs[186].

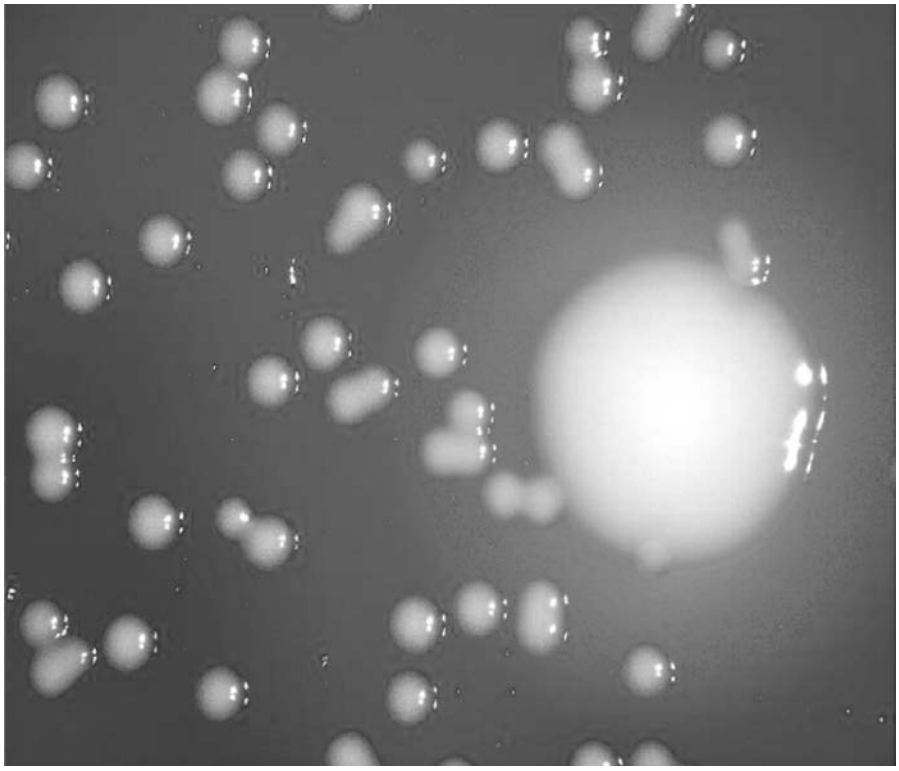

Figure 1-10 MRSA colony surrounded by SCVs

Image showing the difference in colony size and lack of heamolysis between the normal MRSA colony (large) and the SCV[187].

When *P. aeruginosa* moves from the environment to the CF airway, there are extensive nutritional and physiological changes for the bacterium to adapt to enabling it to survive in hostile environments. The immune system, constant antibiotic pressure, other respiratory microorganisms and osmotic stress resulting from the high viscosity of the mucus are important factors which influence adaptation.

When *P. aeruginosa* is faced with stressful conditions such as oxidative stress or antibiotic pressure, a fundamental transition in gene expression profile occurs[188–191]. During aerobic respiration, some electrons escape from the electron transport chain and generate reactive oxygen species (ROS). ROS have the ability to damage cellular structures, lipids, proteins and DNA resulting in loss of cell viability. As a consequence, cells have evolved complex enzyme systems such as superoxide dismutase (SOD) and catalase to eliminate the damaging mitochondria generated superoxides[188,192]. *P. aeruginosa* encounters several sources of oxidative and nitrosative stress during infection in the CF airway which can lead to increased bacterial mutation rates and select for variants that are able to survive in this environment[193]. A frequent phenotypic adaptation of *P. aeruginosa* in patients with CF is the conversion to the mucoid phenotype which results in overproduction of alginate and protection from the host immune response[194–196]. The most common mutations responsible for the mucoid conversion are found in the *mucA* gene. MucA normally limits the expression of the *algD* operon (which encodes the enzyme required for alginate synthesis) by sequestering the alternative RNA polymerase σ-factor σ^{22}. This inevitably leads to altered expression of numerous stress response and virulence associated genes[197]. During long-term colonisation of CF lungs, *P. aeruginosa* undergoes specific adaptation to the host environment and following prolonged persistence it develops small colony variants (SCVs) which display high intracellular c-di-GMP levels[59,60,182,198,199], enhanced biofilm formation, repression of flagellar genes, high fimbrial expression, resistance to phagocytosis and enhanced antibiotic resistance. The appearance of SCVs in the CF lung correlates with poor patient clinical outcome[12,156,185,200,201].

1.7 Antibiotic Resistance in *Pseudomonas aeruginosa*

'Antimicrobial resistance (AMR) within a wide range of infectious agents is a growing public health threat of broad concern to countries and multiple sectors. Increasingly, governments around the world are beginning to pay attention to a problem so serious that it threatens the achievements of modern medicine. A post-antibiotic era—in which common infections and minor injuries can kill—far from being an apocalyptic fantasy, is instead a very real possibility for the 21st century.[202]'

Bacterial infections remain a major health problem both within the UK and worldwide. In particular, the ability of bacteria to develop resistance against antibiotics is limiting the use of these drugs to treat bacterial infections. Resistance has spread around the world. MRSA has spread between continents[203] as have resistant strains of TB, malaria, HIV and pneumococci. Resistance to antibiotics is common and widespread across the globe. In Scotland, the Gram-negative pathogen *P. aeruginosa* shows resistance to mainline therapies such as Piperacillin-Tazobactam at 9.8% and cephalosporins of 8%[204]. Across Europe, the ECDC estimates that the human burden of the 6 most common drug-resistant bacteria alone is at least 25,000 deaths annually with an economic burden of greater than €900 million per year[205]. Moreover, the emergence of novel resistance mechanisms, such as the extended spectrum β-lactamases, highlights the rapid evolution of antibiotic resistance. There is thus an urgent need for therapies with modes of action distinct from conventional antibiotics.

1.7.1 Resistance Mechanisms in *Pseudomonas aeruginosa*

P. aeruginosa presents a serious therapeutic challenge for treatment of infections and selection of appropriate antibiotics is essential to optimizing clinical outcomes. Unfortunately *P. aeruginosa* has the ability to rapidly develop resistance to multiple classes of antibiotics even during the course of treatment, increasing morbidity and mortality significantly[206]. Patients with CF and bronchiectasis are exposed to prolonged and frequent courses of antibiotics throughout their lives which inevitably leads to intense selection pressure which drives antibiotic resistance[207,208]. Table 1-3 below outlines the major mechanisms by which bacteria develop antibiotic resistance. All known mechanisms of antibiotic resistance, namely intrinsic, acquired and adaptive, can be displayed by *P. aeruginosa*. Intrinsic resistance is imparted by low outer membrane (OM) permeability, expression of multi-drug efflux pumps and the occurrence of chromosomally

encoded antibiotic degrading enzymes (β-lactamases)[209–211]. Acquired resistance results from the transfer of genetic material encoding resistance genes, the accumulation of mutations in antibiotic targets and mutations in genes or regulators affecting intrinsic resistance mechanisms. Finally, adaptive resistance occurs when changing environmental conditions lead to increased resistance including *P. aeruginosa* growth in a biofilm.

Table 1-3. Mechanisms of bacterial antibiotic resistance.

Mechanism	Resistance class	Example(s)
Efflux pumps	Intrinsic	MexAB-OprM, MexCD-OprJ, MexEF-OprN, MexXY-OprM (cephalosporins, carbapenems, aminoglycosides, quinolones, ureidopenicillins)
Outer membrane impermeability	Intrinsic	OprF, OprD, OprB (carbapenems, aminoglycosides, quinolones)
β-lactamases	Intrinsic	AmpC (penicillins)
Targeted mutation	Acquired	DNA gyrase, DNA topoisomerase (quinolones) MexZ (quinolones, cefapimes, aminoglycosides)
Horizontal transfer	Acquired	Metallo- β -lactamases, ESBLs (penicillins, cephalosporins, carbapenems)
Membrane changes	Adaptive	Lipid A modification (aminoglycosides, polymyxins) AmpC upregulation (penicillins)

The outer membrane of gram-negative bacteria constitutes a semipermeable barrier that reduces the penetration of many classes of antibiotics. Specifically, the outer membrane in *P. aeruginosa* is only 8% as permeable to small molecules as the outer membrane of *Escherichia coli*[212]. To cross the *P. aeruginosa* outer membrane some antibiotics use porin channels such as the carbapenem-specific porin OprD[213,214]. Studies have proven that imipenem resistance in *P. aeruginosa* is associated with the loss of the porin OprD in combination with the activity of the chromosomally encoded β-lactamase AmpC, while overexpression of multidrug efflux pumps confers resistance to meropenem[213,214]. Reduced outer membrane permeability of vital antibiotics can arise from changes to the structure and composition of the PA outer membrane such as changes to the O-antigen, reduction in cell envelope Ca^{2+} and Mg^{2+} content or the covalent addition of 4-amino-L-arabinose to phosphate groups within the lipid A and core oligosaccharide moieties of LPS[215].

Efflux pumps are ubiquitous among Gram-negative and Gram-positive bacteria, transporting antibiotics and other toxins out of the bacterial cell[53,187,206,212].

1.7.2 Biofilms and Antibiotic Resistance

The ability of *P. aeruginosa* and many other bacteria to attach to wet surfaces and to each other, with subsequent differentiation into highly structured biofilms is considered a major virulence trait and enables chronic infection of the host[60,216,217]. The environmental stimuli that drive switching to the biofilm phenotype are poorly understood, however studies have shown that genetic diversity may arise by means of a mechanism involving the *recA* gene function[216]. It has been recognised for many years that 'dwarf' colonies can be isolated from the chronically infected CF lung and correlated with poor lung function[199,218]. *P. aeruginosa* biofilms can be up to 1000 times more resistant to antibiotics than bacteria in the planktonic (free living) state[209,216], are more inconspicuous to the immune system and provide physical protection from immune cells.

The development of antibiotic resistance in biofilm communities is not fully understood. Owing to the compact nature of biofilm structures, slow growth, nutrient limitation, activation of the general stress response and the protection conferred by the biofilm matrix polymers, natural and artificial chemical agents are unable to adequately attack and destroy infectious biofilm populations[219]. Growth, protein synthesis and metabolic activity are stratified in biofilms, with high levels at the surface and low levels in the centre. Very slow in situ growth rates in biofilms have been measured in the sputum of CF patients, with an average doubling time of 2-3 hours and the presence of a significant number of cells in stationary growth phase[191,209]. Use of β-lactam monotherapy in this setting is not effective at eradicating biofilm infections as these antibiotics are only effective against dividing *P. aeruginosa* cells.

The mutation frequency of biofilm-forming bacteria is significantly increased compared with planktonically growing isogenic bacteria with increased horizontal gene transfer in biofilms[220]. Biofilm-growing bacteria develop multidrug resistance against β-lactam antibiotics, fluoroquinolones and aminoglycosides by means of traditional mechanisms including enzymatic acquired resistance and recurrent mutations[221]. Bacterial cells present in biofilms may simultaneously produce enzymes which degrade antibiotics, have antibiotic targets of low affinity and overexpress efflux pumps with a broad range of

substrates. A high percentage of hypermutable *P. aeruginosa* isolates associated with antibiotic resistance have been isolated from CF patients[157,220,222,223].

The physical diffusion barrier in biofilms plays a pivotal role in biofilm resistance in *P. aeruginosa* via overproduction of β-lactamases in the matrix. These extracellular β-lactamases have the ability to inactivate the antibiotic as it penetrates, thereby protecting the deeper lying cells[191,224]. Sub-MIC concentrations of β-lactam antibiotics have been found to be responsible for the induction of increased alginate synthesis[225] in *P. aeruginosa* biofilms[226]. One of the only antimicrobial agents which is effective against the non-dividing dormant cells of the *P. aeruginosa* biofilm is colistin, whereas the metabolically active cells remain sensitive to ciprofloxacin. Combination therapy is often used and has shown to be effective in eradication of *P. aeruginosa* [227].

1.7.3 Persister Cells

All microbes are capable of producing a small subpopulation of dormant persister cells that are highly tolerant to killing by antibiotics. As the concentration of an antibiotic falls to sub-therapeutic levels, surviving persisters are able to re-establish the population resulting in relapsing chronic infection[66]. There are many studies outlining the presence of bacterial persisters and *Candida albicans* subpopulations that can remain viable at high concentrations of an antifungal agent.[228] Such subpopulations are not mutants, but rather phenotypic variants that can survive antimicrobial treatment. Drug tolerance appears to be a transient and reversible physiological state and when the antimicrobial agent is removed[229] these persisting microbial cells resume growth and become sensitive to antimicrobial agents[230].

1.7.4 Epigenetic Modification and Resistance

It is well established that many species of bacteria, including *P. aeruginosa* , *E.coli* and *S. enterica* exhibit resistance when they are exposed to successive steps of increasing concentrations of antibiotics[231]. One important finding in these studies is that there is often reversion back to the sensitive phenotype once the antibiotic pressure has been removed. This would be incompatible with a genetic mutation being the sole reason for this adaptive phenotype as the resistant phenotype would not be easily reversible. It has been suggested that a combination of epigenetic processes such as methylation and stochastic gene expression, may be driving the emergence of adaptive resistance[232–235].

1.8 Transcriptional Analysis and Next Generation Sequencing in mechanisms of resistance and adaptation

1.8.1 Transcriptome Analysis

Microbial transcriptome and metatranscriptome analysis is important for understanding host-pathogen immune interactions, predicting resistance to specific antibiotics, quantifying gene expression changes and tracking disease progression[236].

Although many different kinds of microbes evolve resistance, resistant bacteria are currently the greatest cause for concern. It is no coincidence that the nations with the strictest policies on antibiotic prescription (Scandinavia and Netherlands) have the lowest rates of resistance[237]. The molecular basis of antibiotic resistance is in many cases well understood and modern techniques have defined the stable genetic changes involved. However, the pathways by which bacteria evolve these resistance mechanisms remain unclear. Additionally, the significance of mutations in elements controlling gene expression will not be immediately apparent from genome sequencing alone, since change in expression of a global transcriptional regulator will produce dramatic changes in the overall bacterial gene expression profile[238,239]. These changes can underpin antibiotic resistance: for example, a number of recent studies have shown significant changes in global bacterial gene expression in response to antibiotic exposure. These have suggested generic bacterial defences that counter the end result of antibiotic treatment which is oxidative stress induced by reactive oxygen intermediates[240–243]. Bacteria counter this oxidative stress by upregulating specific genes such as the so-called stringent response[244] and through the induction of hydrogen sulfide[245].

Data from one of the initial transcriptome studies of the response of *P. aeruginosa* to iron indicated that 137 genes were upregulated secondary to iron depletion[246]. A further more systematic study was performed which addressed how the transcriptome changes when iron-starved *P. aeruginosa* cells were fed with iron. Most genes were found to be downregulated including genes involved in transport of small molecules and transcriptional regulators however it was noted that genes involved in virulence were upregulated, some of which may help the cells to overcome the host innate immune system[247]. There have also been several studies which look at how *P. aeruginosa* responds to varying levels of copper. Tietzel et al[248] identified a set of genes which form a core response of *P.*

aeruginosa to copper. Copper starvation under aerobic conditions led to downregulation of 132 genes, while only 10 genes were upregulated. In a further study the global response to sulphate starvation was addressed in a non-mucoid CF isolate and PAO1. Unlike PAO1, the CF isolate was shown to utilize mucin as a sulphur source. Several genes involved in the type III secretion system and exoenzyme S were also induced suggesting that cells recognize mucin as a sulphur source and also a host component[61]. Transcriptional profiling of osmotically stressed *P. aeruginosa* has also been studied[249] which led to the identification of a steady state osmotic shock regulon comprising 66 genes.

1.8.2 Environmental adaptation

In previous studies on global *P. aeruginosa* transcriptional profiles of biofilms, it has been shown that planktonic culture in exponential and stationary phase of growth and biofilm cultures show distinct patterns of gene expression indicating that biofilms are not just surface attached films in a stationary phase[52]. In a recent study by Dotsch et al[250], the differential gene expression was compared in mature *P. aeruginosa* biofilms as opposed to planktonic cells by the use of RNA sequencing technology, giving both qualitative and quantitative information on the transcriptome. The comparative analysis of gene expression in planktonic and biofilm cultures revealed simultaneously regulated genes in the stationary phase of planktonic cultures and in biofilms as well as a set of genes that were specifically regulated in biofilms. The latter included a large proportion of genes previously described to be biofilm regulated such as genes involved in type III secretion, adaptation to microaerophilic growth and the production of extracellular matrix components[250]. Quorum sensing has been implicated as an important step in the formation of ordered antibiotic-resistant biofilm communities. There have been several studies looking at quorum sensing mutants which has helped to identify a core set of 77 genes of the QS regulon that are positively regulated[34].

The versatility of *P. aeruginosa* in adapting to a wide range of environments including that of the human body is attributed to a large genomic repertoire consisting of a diverse set of genes encoding metabolic functions suited for proliferation in a wide range of environments. *P. aeruginosa* also has an impressive armament of virulence factors, explaining why this species is the most common human pathogen amongst the members of the genus Pseudomonas. Interestingly, virulence genes are highly conserved among different *P. aeruginosa* strains and are part of the core genome, leading to speculations that

some form of pathogenic interaction occurs in natural environments providing the evolutionary pressure for their maintenance. Rapid adaptation of bacteria to changing environments is accompanied by reprogramming of their regulatory networks to activate the expression of genes essential for their survival in the new environment while repressing those that are unnecessary or potentially deleterious. In a recent study by Wurtzel et al, RNA-sequencing was used to look at differential gene expression of *P. aeruginosa* grown at 28 and 37°C. The results revealed genes which were preferentially expressed at the body temperature, suggesting they play a role during infection. These temperature induced genes included the type III secretion system (T3SS) genes and effectors, as well as the genes responsible for phenazines biosynthesis[251].

Significantly, disruption of any of these pathways mentioned dramatically increased the susceptibility of the bacteria to a variety of antibiotics. Thus, drug targeting of these and related systems could offer novel therapeutic targets to treat antibiotic resistant bacteria. Although studies have been made of bacteria in different culture conditions, no studies have analysed changes in bacterial transcription that occur *in vivo* in response to antibiotic challenge. This is particularly important since growth of bacteria *in vivo* represents a totally different environment than the rich culture media used in laboratory studies[245].

1.9 Next Generation Sequencing technology

The next generation sequencing (NGS) technologies are revolutionary tools which have made remarkable achievements in genetics possible since the beginning of the twenty-first century. They produce great sequencing depth making them applicable to quantitative studies such as transcriptomic measurements.

In 1977, Frederick Sanger developed DNA sequencing technology based on the chain termination method, also known as Sanger sequencing[252,253]. The NGS technologies differ from the Sanger method in aspects of massively parallel analysis, high throughput and reduction in cost[254]. Recent advances in sequencing technology and bioinformatic interpretation have resulted in the availability of instruments that can be operated in a clinical environment. These technologies have many potential applications for the control of infectious disease outbreaks. In the recent 2014 Ebola outbreak in West Africa a new highly portable genome sequencer was used in the field (the MinION from Oxford Nanopore Technologies, Oxford) to track the evolution of the Ebola virus over the course

of the epidemic[255]. Previously, outbreaks have been difficult to identify in part due to limitations in molecular typing technology. Whole genome sequencing, in combination with phylogenetic analysis however are invaluable tools for epidemic investigation as they are able to identify exact transmission events and exclude cases mistakenly implicate by traditional methods[256–258].

Table 1-4 Comparison of NGS platforms. Table taken from Finseth et al with permission[257]

Platform	Chemistry	Read Length (bp)	Run Time	Advantage	Disadvantage
454 GS Junior (Roche)	Pyrosequencing	500	8 hours	Long read length	High error rate in homopolymer
454 GS FLX+ (Roche)	Pyrosequencing	700	23 hours	Long Read Length	High error rate in homopolymer
HiSeq (Illumina)	Reversible Terminator	2*100	2 days (rapid mode)	High throughput/cost	Short reads, Long run time
SOLiD (Life)	Ligation	85	8 days	Low error rate	Short reads, Long run time
Ion Proton (Life)	Proton Detection	200	2 hours	Short run times	Short reads
PacBio RS	Real-time sequencing	3000 (up to 15,000)	20 min	No PCR, Longest read length Can analyse methylation data	High Error Rate, high cost

Table 1-4 above outlines the main next generation sequencing platforms available and their main advantages and disadvantages.

Illumina have dominated the sequencing industry over the last few years and set the standards for high throughput massively parallel sequencing with the HiSeq 2000. Prior to the sequencing, the DNA samples are randomly fragmented during the library preparation step. The library is then amplified using PCR which has the potential to introduce amplification bias against AT or GC rich regions[259]. Illumina utilises sequencing by synthesis (SBS) technology using four fluorescently-labelled nucleotides to sequence tens of millions of clusters on a flow cell surface. During each sequencing cycle, a single

labelled deoxynucleoside triphosphate (dNTP) is added to the nucleic acid chain, which then acts as a terminator for polymerisation. The fluorescent dye is imaged to identify the base. The end result is highly accurate base by base sequencing that eliminates sequence-context specific errors and robust base calling across the genome[259].

Pacific Biosciences have developed a method for real time sequencing of single DNA molecules with a rate of several bases per second and read lengths into the kilobase range. This single-molecule, real-time (SMRT) technology utilises sequential base additions which are catalysed by each polymerase and detected with terminal phosphate linked fluorescent-labelled nucleotides.

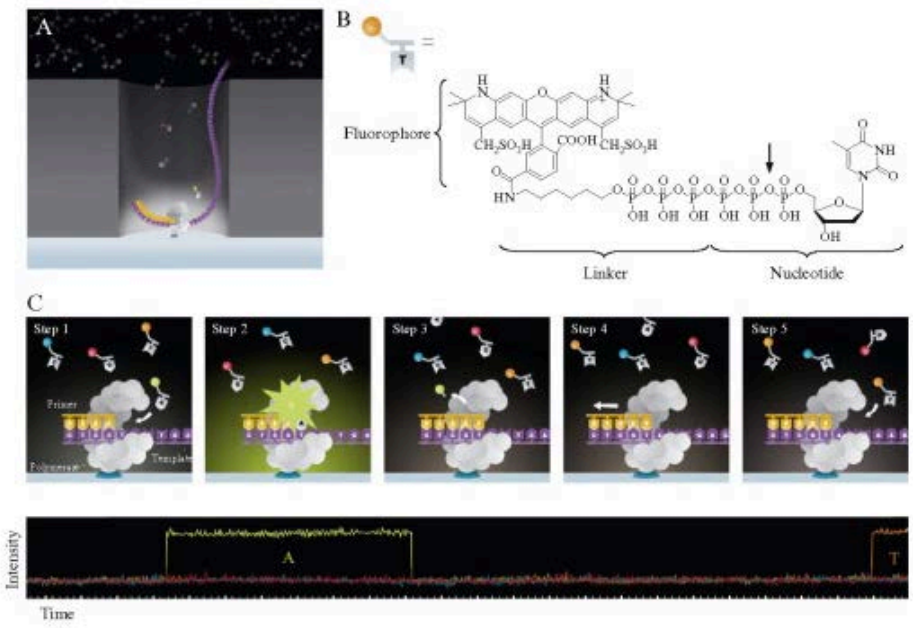

Figure 1-11 Principles of single-molecule, real –time (SMRT) DNA sequencing[260]
(A) Single DNA polymerase molecules and bound DNA template immobilized to the bottom of the array. (B) Molecular structure of the phospholipid linked nucleotides. The arrow indicates the α-β phosphodiester bond cleavage mediated by the DNA polymerase. (C) Step 1: DNA template/primer/polymerase complex is surrounded by diffusing phospholinked nucleotides which probe the active site. Step 2: Labelled nucleotide makes a cognate binding interaction with the template base in the DNA. Fluorescence is emitted continuously, giving rise to a detectable pulse in the fluorescence intensity time trace. Intensity of fluorescence indicates which base is incorporated. Step 3: The polymerase incorporates the nucleotide into the growing nucleic acid chain by cleaving the α-β phosphodiester bond, thereby subsequently releasing the pyrophosphate-linker-fluorophore. Step 4: The polymerase translocates to next template position. Step 5: The process repeats. Image taken from Korlach et al with permission[260].

The principles of SMRT DNA sequencing are outlined in figure 1-11 above. The technology uses a DNA polymerase to drive the reaction and images single molecules, which means there is no degradation of signal over time. The sequencing reaction ends when the template and polymerase dissociate[260,261]. The average read length from PacBio RS is about 3000bp but some may be 20,000 bp or longer. The SMRT approach has several advantages, specifically in relation to the long read length. With other technologies, the short read length and amplification bias can lead to fragmented assemblies whenever a repeat or poorly amplified area is encountered. *P. aeruginosa* genomes in particular are GC rich which results in poor amplification, repetitive regions and therefore poor quality sequencing. By combining the long reads of SMRT sequencing runs with the more accurate (in terms of nucleotide resolution) short reads of Illumina, the reads will span many more repeats and missing bases, closing many gaps and resulting in a highly accurate complete genome[262]. The long read lengths also have the ability to reveal complex structural variations present in the DNA such as large scale chromosomal rearrangements.

Methylation changes can also be detected from SMRT sequencing data due to the change in DNA polymerase kinetics as it moves along the template molecule[263]. From analysis of bioinformatics data the gene responsible for any given base modification can be matched to a sequence motif in which the modification lies, thus functional information emerges directly from the SMRT approach[263,264].

1.10 Aims

The evolution of phenotypic variants during infection enables microorganisms to evade immune defences, tolerate antibiotic treatment and persist in the host during chronic infection. Phenotypic change is a hallmark of adaptation of *P. aeruginosa* to the lung during chronic infection in patients with cystic fibrosis. Well characterised phenotypic variants include mucoid and small colony variants, the appearance of which is associated with disease severity. In the case of small colony variants, which form a highly adherent biofilm and show increased and antibiotic tolerance to some antibiotics, it has been suggested that the environmental pressures that select for SCVs may include antibiotics and a highly active host immune system. Here we show that *P. aeruginosa* small colony variants can be reproducibly isolated from the murine lung following the establishment of chronic infection in the absence of antibiotic pressure. This thesis also looks at optimisation of methods for bacterial RNA extraction from CF sputum samples for downstream transcriptomic analysis.

The three specific aims of this work were:

1. To phenotypically characterise and compare the SCV and original mucoid strain
2. To compare the transcriptome between the two isolates to establish changes in gene expression which may be accountable for the change in phenotype
3. To compare the whole genome sequence using a combination of techniques to establish a genetic mechanism behind the phenotypic switch

Chapter 2 Materials and Methods

2.1 Chemicals, growth media, buffers and strains

2.1.1 Chemicals

All chemicals used in this thesis were of analytical grade and purchased from Sigma-Aldrich, Fischer Scientific or Melford unless otherwise stated.

2.1.2 Growth media

Media used in this thesis was a combination of externally sourced agar plates, media prepared in the University of Glasgow and media prepared by myself in the laboratory.

Table 2-1 Self prepared media recipe (components per litre).

Lysogeny broth (LB) and minimal media were prepared in dH_2O using the recipes outlined. They were adjusted to pH 7.5 and sterilised by autoclaving. For preparation of the solid media, 15 g L^{-1} agar was added to the media prior to autoclaving.

Lysogeny broth (LB) Per litre	Minimal media Per litre
10 g Tryptone 5 g yeast 10 g NaCl	6.8 g Na_2HPO_4 3 g $KHPO_4$ 0.5 g NaCl 1 g NH_4Cl 2 ml glycerol 1 mM $MgSO_4$ 100 μM $CaCl_2$

Table 2-2 Externally sourced media

Media	Source
Columbia blood agar (COB)	Thermo Scientific (Oxoid Microbiology Products)
Chromogenic Pseudomonas agar	bioMérieux, UK
Chocolate Bacitracin	Thermo Scientific (Oxoid Microbiology Products)
CLED Agar	Thermo Scientific (Oxoid Microbiology Products)
Mueller Hinton agar (MHA)	Thermo Scientific (Oxoid Microbiology Products)
Tryptone soya broth (TSB)	Thermo Scientific (Oxoid Microbiology Products)
Sputasol	Thermo Scientific (Oxoid Microbiology Products)

Brain heart infusion (BHI) broth was made in the media department of the GBRC.

2.1.3 Buffers

Buffers were made using dH_2O, filter sterilised, autoclaved where necessary and stored at room temperature.

1x PBS solution was prepared as shown in Table 2.3

Table 2-3. Buffer recipe

Component	Quantity	Concentration
NaCl	8 g	137 mM
KCl	0.2 g	2.7 mM
Na_2HPO_4	1.44 g	10 mM
KH_2PO_4	0.24 g	2 mM

The mixture was made up to 800 ml in dH_2O and then adjusted to pH 7.4 with HCl before being made to a final volume of 1 litre. The buffer was then autoclaved and stored at room temperature.

2.1.4 Strains

The strains used in this study are described in Table 2-4 below.

Table 2-4. Strains used in this study

Strain of Pseudomonas	Genotype or relevant characteristics	Reference or source
PA01	Clinical isolate	Stover et al.[19]
NH57388A (NHMuc)	Clinical mucoid isolate	N. Hoffman, University of Copenhagen
SCV20265	Clinical small colony variant, human CF lung sample	Hanover Medical School[181]
SCVJan	Small colony variant from murine model	Murine model developed by Dr Hannah Bayes
SCVFeb	Small colony variant from murine model	Murine model developed by Dr Hannah Bayes
MUC	Mucoid isolate from mouse model infected with NHMuc	As above
GRI	Ventilator associated pneumonia clinical isolate	Glasgow Royal Infirmary microbiology laboratory
YH5	Paediatric cystic fibrosis isolate	Glasgow Royal Infirmary microbiology laboratory

2.2 Maintenance and growth of bacteria

2.2.1 Storage of bacterial strains

5 ml overnight cultures of bacterial strains were inoculated from a single colony on solid agar plates and grown overnight (~16 hours) in LB medium at 37°C with 220 rpm shaking. 0.5 ml of this culture was then added to a cryo-vial containing 1ml sterile glycerol (40%) and peptone (2%). The stocks were frozen at 80°C until required.

2.2.2 Bacterial colony morphology.

Colony morphology was obtained by plating strains onto COB Agar and LB agar. Plates were incubated at 37°C and 30°C to ensure no difference in morphology.

2.3 Murine agar bead infection model (Dr Hannah Bayes, University of Glasgow).

All mice were used between 12 and 16 weeks of age and of a C57BL/6 lineage. All procedures were carried out in accordance with UK Home Office regulations. The infection model was adapted from the protocol described by van Heeckeren *et al.* [265] *P. aeruginosa*-laden agar beads were prepared the day before inoculation, stored overnight at 4 °C, and a different bead preparation used for each experiment. *P. aeruginosa* -laden beads were stored on ice throughout the murine surgery. Following inoculation of *P. aeruginosa* -laden beads, the administrated inoculum was confirmed by homogenization and quantitative bacteriology on a further two aliquots of beads.

For inoculation of *P. aeruginosa* -laden beads, mice were anaesthetized using isofluorane via nose cone and the trachea exposed and cannulated (22G intravenous cannulae; BD Biosciences) under aseptic conditions. An average inoculum of $1x10^6$ CFU/50 µl per mouse was delivered. Animals were monitored closely post-operatively using a disease severity scoring system. An animal reaching a moribund end-point was culled. Daily weights were used as a further measure of disease progression and those with weight loss of greater than 20% of baseline weight were culled. Surviving animals were culled at 14-days post-procedure.

2.3.1 Pulmonary bacterial quantification and identification

Bronchoaveolar lavage (BAL) was performed aseptically with 1 ml sterile phosphate buffered saline (PBS) via transtracheal intubation. Lungs were removed aseptically and homogenized in 1ml PBS. BAL and homogenized lung tissue was plated on LBagar plates for morphology identification and serial dilution for quantification. Pulmonary bacterial burden was calculated from BAL plus right diaphragmatic lung homogenates. SCVs from murine samples were initially identified via typical morphology and via conventional laboratory methods including Gram stain, oxidase reaction and API 20NE (bioMérieux).

2.4 Culture of Clinical CF Sputum Samples

50 sputum samples were collected from CF patients in the adult CF cohort in the West of Scotland, attending out-patient clinic and undergoing an infective exacerbation to examine for presence of small colony variants of *P. aeruginosa*.
To the sputum sample, an equal volume of reconstituted Sputasol was added to the sample in the sterile universal. The mixture was vortexed until liquefaction was complete. The sample was then inoculated onto Colombia blood agar, chocolate bacitracin and CLED agar. The COB and chocolate bacitracin plates were then incubated in a CO_2 cabinet for 48 hours and the CLED incubated in an aerobic cabinet for 48 hours, both at 35°C.
The plates were analysed for the presence of SCVs and compared with the clinical report from the sample.

2.5 Phenotype and Virulence Characterisation

2.5.1 Growth curves.

Overnight culture of a tested strain was diluted 1:1000 in 10 ml of fresh LB broth and grown at 37°C with gentle shaking in a shaking incubator (IKA KS 4000i Control, 180 rpm). OD_{600} was measured at hourly intervals using a spectrophotometer (Eppendorf Bio Photometer). The experiment was performed with three biological replicates of each strain.

2.5.2 Reversion assay

Small colony variant isolates were inoculated into 5 ml BHI broth and incubated at 37°C, 200 rpm overnight. A 10 µl loop of the liquid overnight culture was then plated onto a Columbia blood agar plate and further incubated at 37°C overnight. Plates were examined at 24 and 48 hours to look for evidence of reversion back to the mucoid phenotype. One colony from the 48 hour culture was further inoculated into 5 ml BHI broth and incubated as before. This was repeated 14 times to examine whether reversion to mucoid phenotype would occur. The same assay was performed with the following variables:

1. LB instead of BHI
2. Minimal media instead of BHI

3. A range of incubation temperatures used; 21°C, 30°C, 42°C for cultures grown in LB, minimal media and BHI.

2.5.3 LPS extraction and analysis

A 5 ml overnight culture of each strain was set up in LB broth and incubated at 37°C in a shaking incubator at 200 rpm. 5ml of the cultures were then diluted 1:10 with LB and subsequently a 1.5 ml suspension made of the bacteria to obtain an OD_{600} of 0.5. The suspensions were centrifuged at 10,600 x g for 10 minutes and the supernatant removed and discarded. Extraction of LPS using the hot aqueous-phenol extraction method was performed as previously described[266]. LPS samples were then visualised by running samples on an SDS PAGE gel followed by staining using the SilverQuest Silver Staining kit (Life Technologies) as per the manufacturer's protocol.

2.5.4 Electron microscopy

For scanning electron microscopy the bacterial strains were grown on a coverslip in a petri-dish with LB broth at 37 °C for 36 hours. These were then washed in PBS, processed and stained using a paraformaldehyde-glutaraldehyde cocktail with alcian blue dye as previously described[267]. Both scanning electron microscopy (SEM) and transmission electron microscopy (SEM) were performed within the University of Glasgow.

2.5.5 Antibiotic susceptibility testing

2.5.5.1 E-test

The MIC for various antibiotics was determined using E-test strips (AB bioMérieux). A sterile cotton swab was immersed in 0.5 McFarland of tested bacterial culture before streaking on sterile Mueller-Hinton (MH) agar. In addition, the MICs were read at 24h and 48 h to take into account the slow growth of the SCVs.

2.5.5.2 Vitek II

Additional susceptibility testing was performed using the Vitek II as per the manufacturer's protocol. To ensure no contamination of the Vitek II antimicrobial

susceptibility card, purity was checked by plating on COB agar. Overnight cultures were grown on COB agar.

2.5.5.3 Microtitre Broth MIC

Antibiotic stocks were prepared by dissolving and diluting as per the manufacturer's instructions to 2X the maximum concentration required. Solutions were frozen until required.

Test strains were grown in LB broth until they reached an OD of 0.6 (10^4 to 10^5 CFU/ml). 100 µl of LB was dispensed into the wells of a 96 well microtitre plate. 100 µl of the appropriate 2X antibiotic solution was then added to the wells in column 1 of the 96 well plate. Using the multipipettor, antibiotic was mixed with the broth in column 1 and then 100 µl added to column 2. This procedure was repeated from columns 1 to 10. 100 µl was then discarded from column 10 rather than adding to column 11. Bacteria were then diluted to the appropriate inoculum size and poured into a sterile petri-dish. Using the multipipettor, 5 µl of bacteria were dispensed into wells in columns 11 to 1 in that order. Column 12 remains empty as a blank control. The bacterial cultures were then streaked onto LB agar to check purity. The plates were incubated at 37 °C for 18 and 36 hours. Following incubation they were read using an ELISA reader and MIC was taken as the lowest concentration of drug that reduces growth by more than 90%.

2.5.5.4 Microtitre Biofilm PEG Assay

Antibiotic test solutions were prepared in advance as above. Peg biofilms were produced as per the manufacturer's protocol for the Innovotech MBEC^{TM} Assay for high-throughput antimicrobial susceptibility testing of biofilms. The antibiotic challenge plate was set up as per the protocol using tobramycin, ceftazidime and ciprofloxacin. To determine the minimum inhibitory concentration (MIC), the challenge plate was then placed in a fresh 96-well microtitre plate and incubated at 37 °C for 18 and 36 hours. An automated plate reader was used to measure the OD_{650} and determine the MIC.

2.5.6 Motility assays

Swimming, swarming and twitching motility were assessed according to previous studies[158], except that the plates were incubated at 30°C for 48-72 hours and in the

twitching motility assay Coomassie blue was used instead of crystal violet to stain for evidence of motility.

2.5.7 Biofilm microtitre plate assay

Quantitative determination of biofilm production was performed with the use of a microtitre plate assay with crystal violet. Briefly, for each isolate, the overnight bacterial culture was adjusted with LB broth to match a turbidity of 0.5 McFarland standard. The suspension was subsequently incubated overnight at 37 °C. The solution was diluted 1:100 in LB and 200 µl aliquots were inoculated into three wells each of a 96-well sterile microtitre plate. The plates were incubated overnight at 37 °C in air, washed and stained with 0.1% crystal violet. The wells were then washed again and dried in air. They were then decolourised with acetone. The optical density was measured at 600 nm (Eppendorf Bio Photometer). This was repeated with a 48 and 72 h incubation time period for the SCV to allow for the slower growth phase.

2.5.8 Type III secretion assay

Secreted protein profiles for SCVJan and NH were analysed by SDS-PAGE and immunoblot analysis after specific induction of type III proteins following addition of the chelator EGTA to the TSB media. Overnight cultures of the strains were grown in 5 ml LB broth (37°C, 200 rpm). The OD_{600} of the overnight culture was measured and used to calculate the volume required to add to the pre-warmed inducing media to give an OD_{600} of 0.05. This was then incubated at 37°C, 200 rpm and disturbed as little as possible. The OD was measured until 0.8 reached, centrifuged at 3750 rpm 4°C for 10 minutes. The supernatant was decanted into a fresh falcon tube and pellet discarded. Precipitation was carried out as previously described[268] following addition of 1 ml of 99% trichloroacetic acid (TCA). Samples were stored overnight at 4°C then centrifuged at 3750 rpm, 4°C for 60 minutes. The supernatant was aspirated carefully and then the falcon tube drained upside to dry the pellet thoroughly. The pellet was then resuspended in 100 µl of 1.5 M Tris-HCL pH 8.8.

Specific antibodies for ExoS and ExoT were used and analysed using SDS-PAGE and Western blot hybridisation. Assay and analysis was performed as previously described[76,269].

2.5.9 *Galleria mellonella* killing assays.

Larvae were stored on wood chips at 4 °C. Overnight cultures of bacterial strains NH and SCVJan were grown in LB broth, diluted 1:100 in the same medium and grown to an optical density of OD_{600} of 0.3 to 0.4 as previously described[159,270]. Cultures were centrifuged and pellets were washed twice and resuspended in 10 mM PBS to an OD_{600} of 0.1. Serial 10-fold dilutions were made in PBS. Five-microliter aliquots of the serial dilutions were injected using a Hamilton syringe into *G. mellonella* larvae, via the hindmost left proleg as previously described[271]. Ten larvae were injected per dilution for each *Pseudomonas* strain tested. Larvae were incubated in 10 cm plates at 37 °C and the number of dead larvae scored 1 to 4 days after infection. For each strain, data from 3 independent experiments were combined. A larvae was considered dead when it displayed no movement in response to touch. A negative control was used in each experiment to monitor the killing due to physical injury or infection by pathogenic contaminants. Time to death was monitored every 24 h post infection. In any instance where more than one control larvae died in any given experiment, the data from infected larvae were not used.

2.5.10 LDH Release/Cytotoxicity Assay.

To investigate the effect of the *P. aeruginosa* strains on macrophages, J774A.1 cells were infected with NH and SCVJan. Bacteria were grown for 17 h to stationary phase in LB broth at 37 °C. Immediately prior to infection, the bacteria were diluted to exponential growth phase with culture medium lacking phenol red and the concentration determined by measuring the OD_{600}. Cells were grown, washed and infected as previously documented[73]**.** Cells were infected with test organisms and incubated for 4 h and 10 h. Lactate dehydrogenase release was determined using the Cytotox 96 cytotoxicity assay kit (Promega USA) as described in the manufacturer's protocol.

2.5.11 Catalase Activity Assay

Overnight cultures of the strains NH and SCVJan were grown in LB broth. 5 µl of each overnight culture was then transferred to a fresh 5 ml LB and grown to an OD of 0.6 in a shaking incubator at 37°C. Catalase standard curves were prepared as per the manufacturer's protocol using the OxiSelect™ Colorimetric Catalase Activity Assay Kit (Cell Biolabs, Inc). 10 µl of each sample was added to the initial well of a 96-well microtitre plate during the preparation of samples. This was performed in triplicate for

each sample. Plate absorbances were read at 520 nm and results calculated as per the manufacturer's protocol.

2.5.12 Pyoverdine Measurement.

The concentration of pyoverdine produced by the NH and SCVJan after overnight culture in LB broth was estimated spectrophotometrically from the absorbance at 405 nm as previously described[272].

2.6 Molecular Techniques

2.6.1 DNA Isolation

Two different methods to obtain purified bacterial genomic DNA from bacteria grown in broth cultures were tested. The Promega Wizard DNA Extraction Kit was compared with the QIAGEN DNeasy Blood and Tissue Kit as per manufacturer's protocol.

DNA was subsequently prepared for sequencing on Illumina HiSeq using QIAGEN DNeasy Blood and Tissue Kit as per manufacturer's protocol. Sequencing and initial bioinformatics were performed in the Centre for Genomic Research, University of Liverpool.

2.6.2 PFGE and Southern Blot Hybridization.

PFGE using genomic DNA was carried out as previously described[273], using CHEF DRII apparatus (Bio-Rad Laboratories) with an electric field strength of ~6 V/cm and a pulse time of 20 s for 18 h. To differentiate the restriction profile of the genomes of NH and SCVJan, Xba1, Spe1 and Avr2 enzymes were used for DNA digestion. Southern blotting hybridization was carried out as described previously[274].

2.6.3 RNA isolation.

2.6.3.1 RNA isolation from cystic fibrosis sputum samples

The initial goal of this thesis was to isolate RNA from *P. aeruginosa* from infected CF sputum samples for downstream transcriptome analysis. Given the dense, purulent nature

of these clinical samples and high percentage of human neutrophils and other pathogens this was a lengthy process in trying to optimise isolation protocols.

Sputum samples were obtained from a cystic fibrosis patient known to be colonised with *P. aeruginosa*. This was immediately placed on ice following collection into a sterile universal. On reaching the laboratory the sample was split into three aliquots of approximately 1 ml. Following a literature search of potential methods, it was decided to compare and optimise three different methods of extraction, isolation and purification. The initial essential step involves immediate protection and stabilisation of the RNA in the samples. In tube 1, 1ml of Trizol (ThermoFischer) was added to the sputum sample. Tube 2, 1 ml of RNA protect (Qiagen). Tube 3, 1 ml of RNAlater (Qiagen) was added. Samples were vortexed and stored at -80 °C.

Tube 2 was processed using RNeasy Protect Saliva Kit (Qiagen), according to the manufacturer's protocol. 14 µl of RNase free water was added to the final preparation. Purified RNA was quantified using a NanoDrop spectrophotometer.

Tube 1 was processed as previously described[275]. 3 volumes of Zirconia beads were added to the Trizol-sputum mixture. This was homogenized immediately for 10 min at L5 setting on the vortex. 266 µl of chloroform was added to the mixture, shaken vigorously for 15 s, incubated for 10 min at room temperature and then centrifuged at 12,000 g for 15 min at 4 °C. The aqueous layer was transferred into an RNase free tube. RNA was then purified using RNA Clean and Concentrator (Zymo) as per the manufacturer's protocol. In column DNA digestion was performed using in column DNase. 14 µl of RNAse free water was added to the final preparation. RNA was quantified using a NanoDrop spectrophotometer.

To confirm the presence of RNA from *P. aeruginosa* in the RNA extracted from the CF sputum sample, RT quantitative (Q) PCR was performed. cDNA was synthesized from total RNA by reverse transcriptase (RT) using AffinityScript (Agilent) as per the manufacturer's protocol. GyrB primers were used to detect presence of Pseudomonal DNA.

Ribosomal RNA depletion was carried out using Epicentre Ribo-Zero Magnetic Gold Kit (Epidemiology) as per the manufacturer's protocol. RNA was further quantified using a NanoDrop spectrophotometer and Agilent Picoanalyser.

In an attempt to further purify the microbial RNA, MEGAClear Transcription Clean up kit (ThermoFisher Scientific) was used as per manufacturer's protocol.

2.6.3.2 RNA Isolation from bacterial cultures

Following the optimisation of RNA isolation from clinical sputum samples, it was evident that the Trizol/Zirconia bead extraction method was superior.

RNA isolation was subsequently carried out on broth samples using the Trizol/Zirconia bead extraction followed by Zymo RNA Clean and Concentrator as initial results revealed a higher yield of RNA.

RNA isolation from the samples was performed in triplicate. Bacterial suspensions were grown to early stationary phase to an OD_{600} of 1.8 in LB broth at 37 °C in a shaking incubator. 2 ml of each suspension was pelleted at 12 000 g for 10 min. RNA was extracted from samples using a bead beating/chloroform extraction method as previously described[275]. The samples were digested with DNAse I for 1 h, in column as per the manufacturers protocol. Bacterial RNA was enriched using MICROBEnrich (Life Technologies) as per protocol.

Ribosomal RNA was depleted using Ribo-Zero Magnetic Gold Kit (Epidemiology) (Epicentre) as per manufacturer's protocol. The precipitated sample was resuspended in 20 µl of RNAse free water. The concentration of RNA was initially determined using a NanoDrop spectrophotometer followed by an Agilent Bioanalyser. cDNA was generated by using the methods from the Superscript Double-Stranded cDNA Synthesis Kit (Invitrogen) per manufacturer's instructions.

2.6.4 Quantitative real time PCR (qPCR)

cDNA was synthesised from total RNA by reverse transcription (RT) using AffinityScript (Agilent) as per manufacturer's protocol. Validation of differential gene expression was carried out using KAPA SYBR FAST Universal qRT-PCR master mix (KAPA Biosystems). Total RNA was extracted as above and was quantified using a NanoDrop

spectrophotometer. qRT-PCR was performed using a single reaction mixture; cDNA synthesis followed by qRT-PCR. Individual reactions were performed in triplicate to account for technical variation. qRT-PCR reactions were carried out using the ECO Real-Time PCR System (Illumina) according to the manufacturers specifications and data analysed as previous[276].

Forward primer: CCTGGTGGGTTTCCGTTCCT

Reverse primer: GATGTAGCTGGCCAGACCGT

Figure 2-1. GyrB primers used for qPCR.

2.6.5 Library Preparation and Illumina Sequencing

Ribosomal RNA deplete RNA was sent to Liverpool University Genomics Institute for cDNA library preparation and sequencing using the Illumina Hi-seq. cDNA libraries were prepared using the Paired End Sequencing Sample Preparation Guide (Illumina). Sequencing was performed using Illumina HiSeq at the Centre for Genomic Research, University of Liverpool.

2.6.6 SMART Library Preparation and Sequencing

SMRTbell™ template libraries were prepared according to the instructions from Pacific Biosciences, Menlo Park, CA, USA. Briefly, for preparation of 10 kb libraries ~10µg genomic DNA isolated from SCVJan, SCVFeb and NH was sheared using g-tubes™ from Covaris, Woburn, MA, USA according to the manufacturer´s instructions. 5-10 µg sheared genomic DNA was end-repaired and ligated overnight to hairpin adapters applying components from the DNA/Polymerase Binding Kit P4 from Pacific Biosciences, Menlo Park, CA, USA. Reactions were carried out according to the manufacturer´s instructions. SMRTbell™ template was Exonuclease treated for removal of incompletely formed reaction products. Conditions for annealing of sequencing primers and binding of

polymerase to purified SMRTbell™ template were assessed with the Calculator in RS Remote, PacificBiosciences, Menlo Park, CA, USA. SMRT sequencing was carried out on the PacBio RSII (PacificBiosciences, Menlo Park, CA, USA) taking one 180 min movie for each SMRT cell. In total 6, 6 and 5 SMRT cells were run respectively.

2.6.7 Genome assembly and annotation

2.6.7.1 Illumina reads

Initial read trimming and QC was performed in the Liverpool centre for genomics. Sequencing reads were mapped to the corresponding reference genome (annotated NH strain). Transcriptome analysis was done in triplicate comparison within CLC Workbench. For each, the RPKM was calculated as previously described[277]. Differentially expressed genes were called by performing $\chi 2$ test on the RPKM values and applying Bonferroni correction for multiple testing. Genes with adjusted p-values smaller or equal to 0.05 in both replicates were determined to be differentially expressed.

2.6.7.2 PacBio reads

Data from each SMRT Cell was assembled independently using the "RS_HGAP_Assembly.3" protocol included in SMRTPortal version 2.3.0 using default parameters. Each assembly revealed the fully resolved chromosome in one single contig. Each chromosome was circularized independently, particularly artificial redundancies at the ends of the contigs were removed and all chromosomes were additionally adjusted to *dnaA* as the first gene. Validity of each assembly was checked using the "RS_Bridgemapper.1" protocol. For the purpose of this study it has been confirmed for each of the (repetitive) rRNA operons that enough uniquely mapping long read exist spanning the whole repeat structure. Finally, each genome was error-corrected by a mapping of Illumina reads (paired end reads, 100 bp) onto finished genomes using BWA[278] with subsequent variant calling using VarScan[279]. A consensus concordance of QV60 could be confirmed for all of the three genomes. Finally, all genomes were annotated using Prokka 1.8[280]. All genome sequences were deposited in NCBI GenBank under Accession Numbers CP013477, CP013478 and CP013479. Illumina short read data has been deposited at EBI SRA under Accession Numbers ERS1005137, ERS1005138 and

ERS1005139. The shortened 16S rRNA gene for strains SCVJan and SCVFeb were confirmed by PacBio assembly as well as BWA mapping of Illumina reads against the final chromosome showing uniquely mapped reads only at that genome position.
Reads were also analysed for methylation changes in the genomes that may account for the change in phenotypes. This was performed using automated PacBio software.

2.6.8 Accessibility of biological resources

Strains of this study have been deposited at DSMZ under DSM 100776 - 100778.

Chapter 3 Phenotypic characterisation of isolated small colony variants

3.1 Introduction

The infection process in the CF airways is associated with extensive genetic adaptation and microevolution of the infecting bacteria. Previous studies have suggested the accumulation of mutations results in strains with phenotypes many of which are not observed among environmental isolates[3,126]. Phenotypes associated with poor outcome in the CF population include presence of mucoid and SCV strains. In the clinical laboratory mucoid strains generally receive most attention due to their size and ability to spread on agar plates, with subsequent overcrowding often hindering the identification of SCVs and other pathogenic bacteria which may be present. The change in phenotype allows the SCV strain to evade the host immune system and persist within the human host. The consequences of persistent bacterial infection include increased morbidity and mortality as well as potential spread to other individuals. During these persistent infections, a sub-population of bacteria (including the SCV form and persister cells[281–283]) are able to persist in a non-replicating and metabolically altered state, with increased protection against oxidative stress[188,284]. The SCV phenotype represents a unique pan-bacterial strategy associated with persistent infection. The most common phenotypic traits associated with the SCV includes enhanced biofilm formation and surface attachment[199,285], a slower growth rate, small colony size (stemming from autoaggregation)[59,60], infectious persistence and increased virulence[286,287]. SCVs are also usually non-motile, with flagellar motility absent in most SCVs to date[47,155]. Hyperpiliation has been reported for some strains although the distribution of this phenotype is unknown.

It has been shown in several studies that during the course of lung infections, selection pressure from the CF host mucosal environment and/or the extensive antibiotic pressure routinely applied in the infected host, leads to emergence of the SCVs and subsequent worsening outcomes and mortality[180,287].

One important aspect in the persistence associated with the SCV phenotype is their ability to form highly adherent biofilm. Once formed, biofilms are extremely difficult to eradicate as they show increased tolerance to both biocides and antibiotics as compared to planktonic microorganisms. Several studies have shown that bacteria within biofilms have greater than one thousandhundred-fold increase in tolerance to antibiotics when compared to the same bacteria in planktonic state[53,191,219].

The work in this chapter describes the phenotypic characteristics of SCVs that evolved during the course of a chronic infection of the murine lung, in the absence of antibiotic selection. Comparison of the phenotypic characteristics of the isolated SCVs with the parent mucoid strain used to initiate infection, indicate clear mechanisms of adaptation to the chronically infected lung and increased virulence of the SCVs.

3.2 Results

3.2.1 Isolation of SCVs from a murine model of chronic *P. aeruginosa* lung infection

P. aeruginosa SCVs are commonly isolated from patients with cystic fibrosis and have been isolated *in vitro* as well as from experimental infection models following aminoglycoside treatment[156,183,218]. A number of recent studies have suggested that there is a strong correlation between presence of SCV in the CF lung with increased mortality[155,193], poor lung function and decreased FEV1[180]. Therefore the identification and further investigation into the SCV phenotype is clinically important.

To determine if SCVs could be isolated from a model of chronic *P. aeruginosa* lung infection in the absence of antibiotic selection we utilized a murine model to mimic chronic pulmonary infection in CF patients[265] (Figure 3-1). In this model, animals were inoculated with *P. aeruginosa* strain NH57388A (NH) a mucoid clinical isolate, embedded in agar beads. NH has a known mutation in the gene encoding the anti-sigma factor MucA, that results in alginate overproduction[288,289].

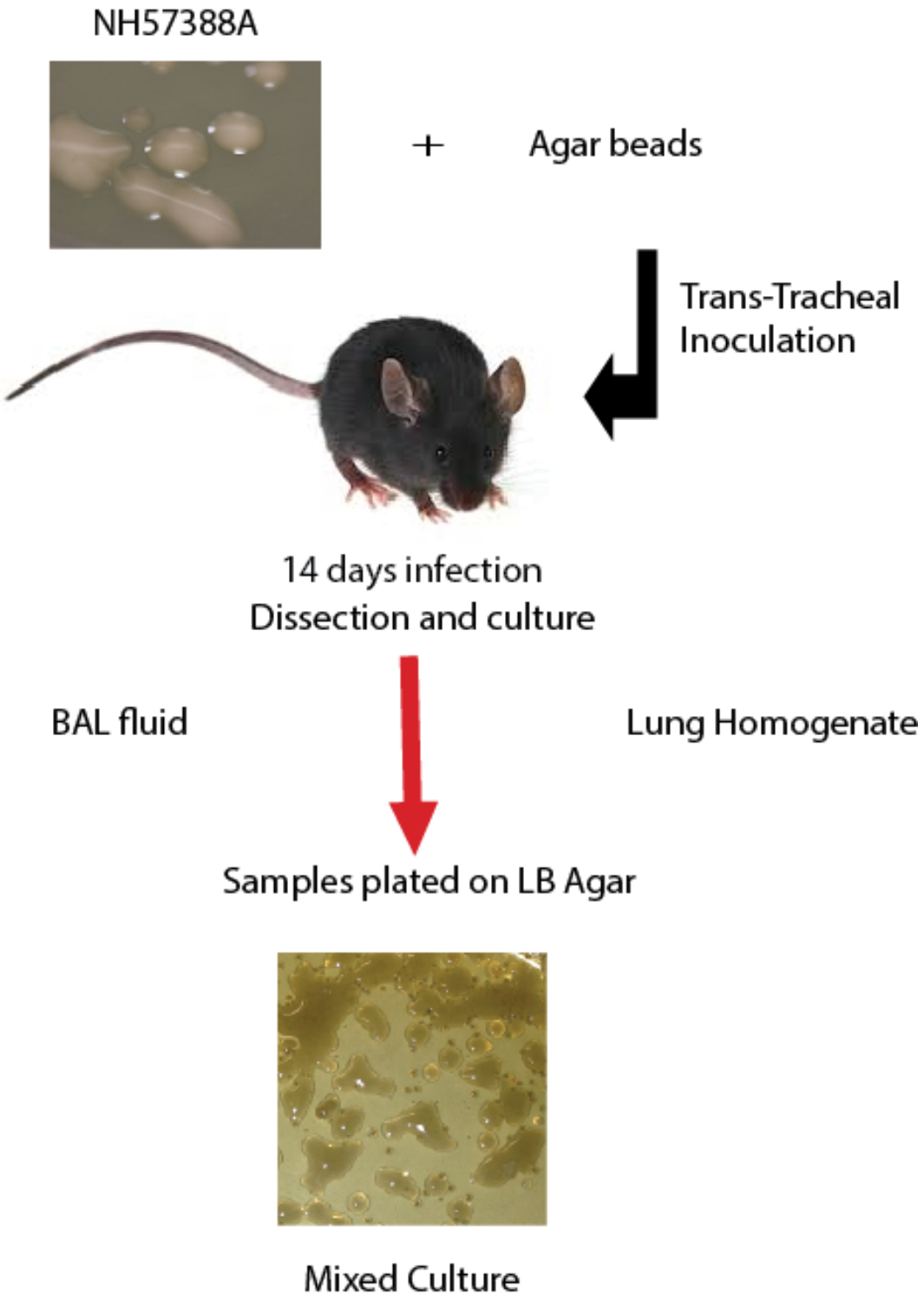

Figure 3-13-1. Recovery of small colony variants from a model of chronic *P. aeruginosa* lung infection

The mucoid clinical CF strain NH was inoculated into the mouse trachea, as described, to initiate chronic infection. After 14 days bacteria isolated from lung homogenate showed either the phenotype of the inoculated mucoid strain or a distinct small colony phenotype.

Fourteen-days post-inoculation with NH, mean chronic pulmonary infection rates were 43.3% (SD 21.3%; range 11.1-71.4%; results from 6 experiments with 7-10 surviving animals/group) with a median pulmonary bacterial burden of 1355 CFU/animal (IQR 182 – 3633). Recovered bacteria from lung homogenate samples obtained from animals remaining persistently infected following treatment with NH embedded beads displayed two distinct colony morphologies: typical large mucoid colonies identical in morphology to the inoculating strain and SCVs. The mucoid colonies were evident after 24 hours of growth on agar plates at 37°C with SCVs visible only after 48 hours of growth on agar-plates.

Overall SCVs were isolated from 17 out of 22 animals (77.3%) with chronic NH infection at 2 weeks post-inoculation and were seen in the presence of mucoid colonies in the majority of persistently infected animals (16 of the 17 animals). In animals developing SCVs these were most frequently isolated from lung homogenates (15 out of 17 animals; 88.2%) compared with bronchoaveolar lavage fluid (BALF) (9 out of 17 animals; 52.9%) (χ^2=20.9, p=0.0001). In addition, SCVs developed rapidly *in vivo*, with SCVs isolated from 75% of infected animals at 48 hours post-inoculation (N=4 animals). To determine if recovery of SCVs was a direct consequence of interaction with the host, NH-laden agar beads were incubated on agar plates at intervals from 24 hours to 2 weeks after bead formation, with this procedure performed on 3 separately produced batches of NH-laden beads. No SCVs were isolated from the beads at any time-point post-formation suggesting *in vivo* factor(s) act to induce SCV emergence in the infected lung.

3.2.2 Prevalence of SCV in the clinical setting

To establish the prevalence of *P. aeruginosa* SCVs in the CF cohort in Glasgow, 50 sputum samples from patients undergoing an infective exacerbation were cultured in parallel with their routine clinical culture in the microbiology laboratory in the QEUH, Glasgow. Following culture, plates were examined for evidence of SCV presence and compared with the clinical laboratory report to establish whether SCV presence is routinely reported.

P. aeruginosa SCVs were isolated from 7 out of 50 specimens. However, examination of the corresponding clinical reports showed that the presence of SCVs was not documented for any of the clinical specimens. This highlights the problems associated with CF microbiology as the plates are overgrown with mucoid strains of *P. aeruginosa* which reduces the ability to detect any other potential pathogen. Figure 3-2 shows an example of the plates from the clinical specimens and the difficulty in isolating single colonies.

a) b)

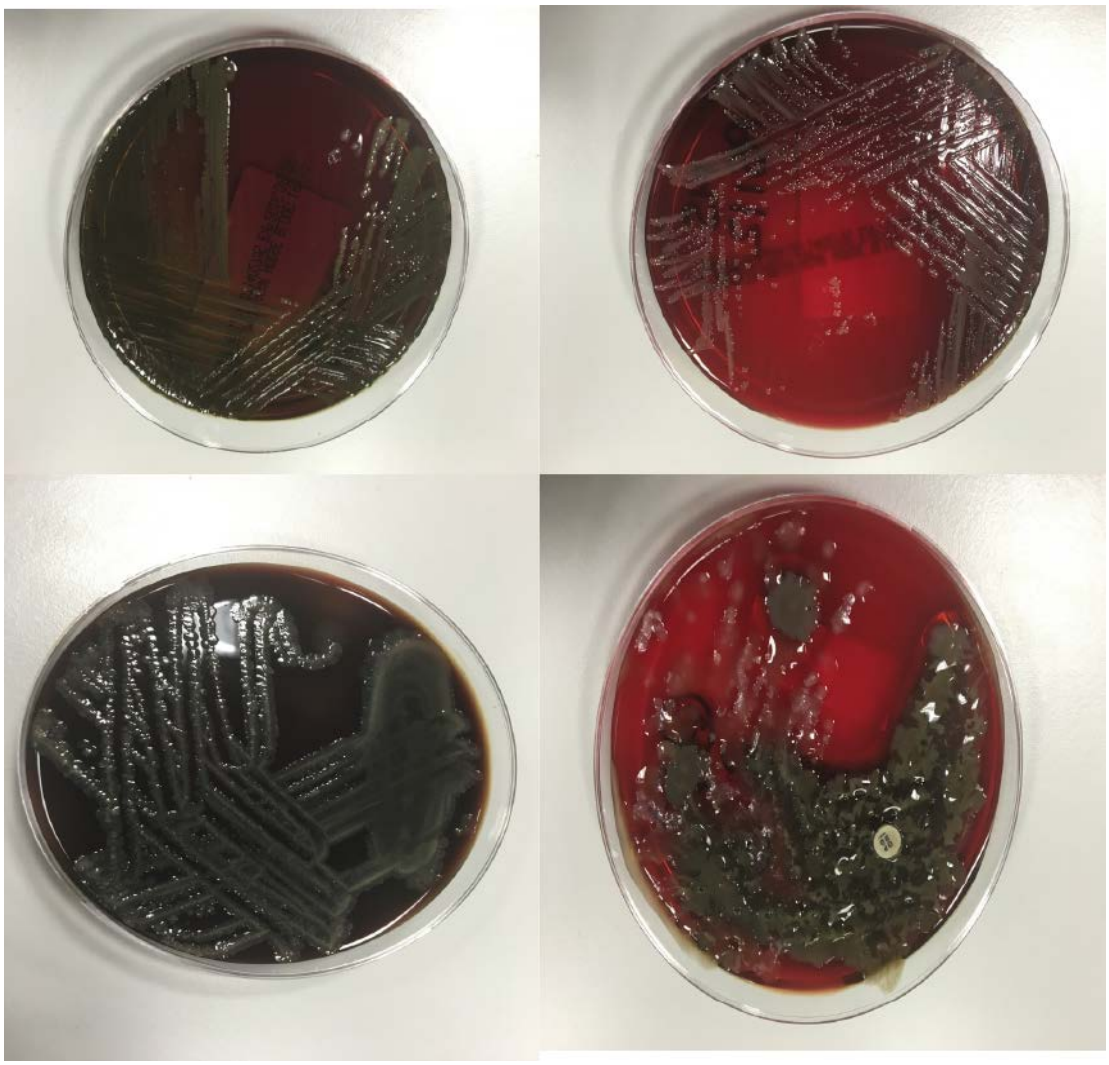

c) d)

Figure 3-23-2. Culture plates from clinical CF sputum samples

a) Heavy growth of *Serratia sp*, b) Heavy growth of mixed *P. aeruginosa* including SCV, c) Heavy growth of *P. aeruginosa* with *S. aureus* mixed in and d) Mixed *P. aeruginosa* including mucoid and SCV. Sputum processed using sputasol and plated onto Columbia Blood (COB) agar.

The cultures in Figure 3-2 are typical of sputum samples from chronically infected patients. The bacterial burden tends to be persistently high and the upper airways are always colonised with both Pseudomonas and coliforms due to the overuse of antibiotics in this cohort of patients.

3.2.3 Phenotypic characterisation

Both the mucoid parent strain, NH and SCVs isolated from the murine lung homogenate show colony morphologies that are common to isolates from the lungs of patients with CF, with colonies of recovered SCVs growing to approximately 2 mm after 48 hours (Figure 3-4a,b). Further phenotypic characterisation of one of these recovered SCVs (SCVJan) showed that like SCVs recovered from CF patients, SCVJan displays slow growth in liquid media with both an extended lag phase and a slower generation time compared with the parental strain (Figure 3-8). In addition it is highly adept at forming adherent biofilms on an abiotic surface (Figure 3-3, 3-4c). Transmission electron microscopy (TEM) analysis of NH and SCV biofilms, show that in contrast to the mucoid parent strain, SCVJan biofilms display a high density of highly adherent bacteria embedded in a dense network of extracellular material (Figure 3-3, 3-4c). This is in contrast to biofilms of NH, where bacterial density within the copious extracellular matrix is low and in addition, the mucoid biofilm is not adherent as it was removed from the glass slides with minimal washing. The identity of the extracellular matrix of *P. aeruginosa* SCVs is not well characterised, although is presumably key to their ability to form highly adherent biofilms, both on abiotic surfaces and in the lung during infection. Different drying techniques were used prior to obtaining an optimum image of the intricate biofilm network, as can be seen in figure 3-3 below.

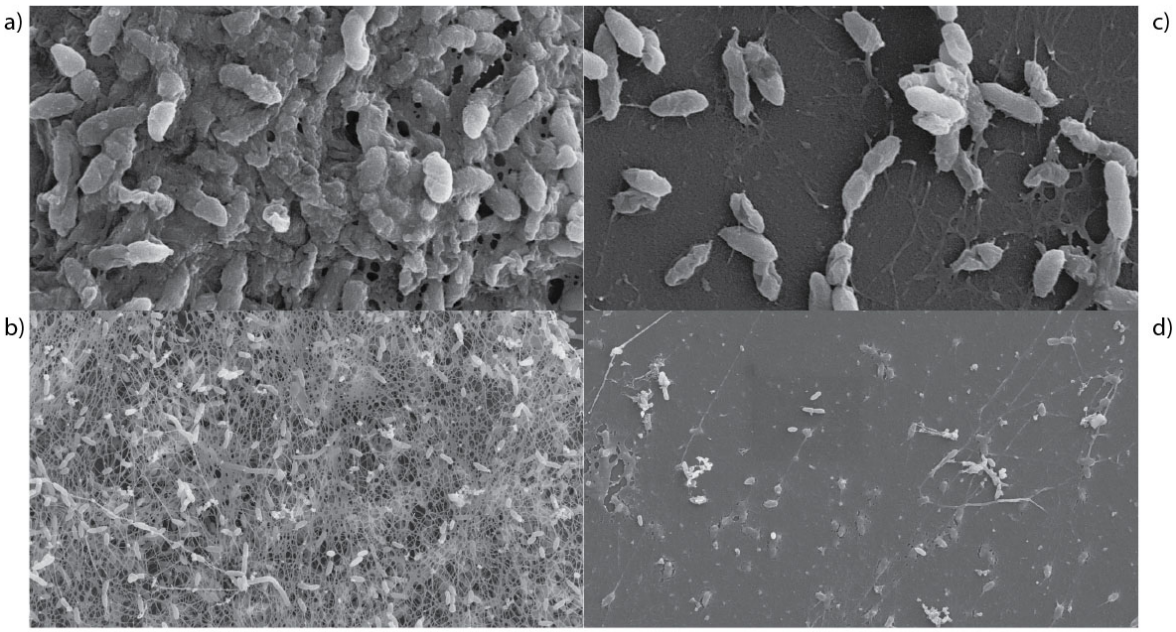

Figure 3-33-3. TEM images showing adherent biofilm on a glass coverslip

A) SCVJan biofilm fixed using 2.5% glutaraldehyde. B) SCVJan biofilm prepared using ethylene glycol and 1,2-pentanediol in place of classical dehydration methods. C) NH biofilm fixed using 2.5% glutaraldehyde. D) NH biofilm prepared using ethylene glycol and 1,2-pentanediol in place of classical dehydration methods.

Negative TEM staining showed that similar to SCVs isolated from some patients with CF, and in contrast to the mucoid parent strain SCVJan is hyperpilliated (Figure 3-4d). This characteristic may also enhance biofilm formation.

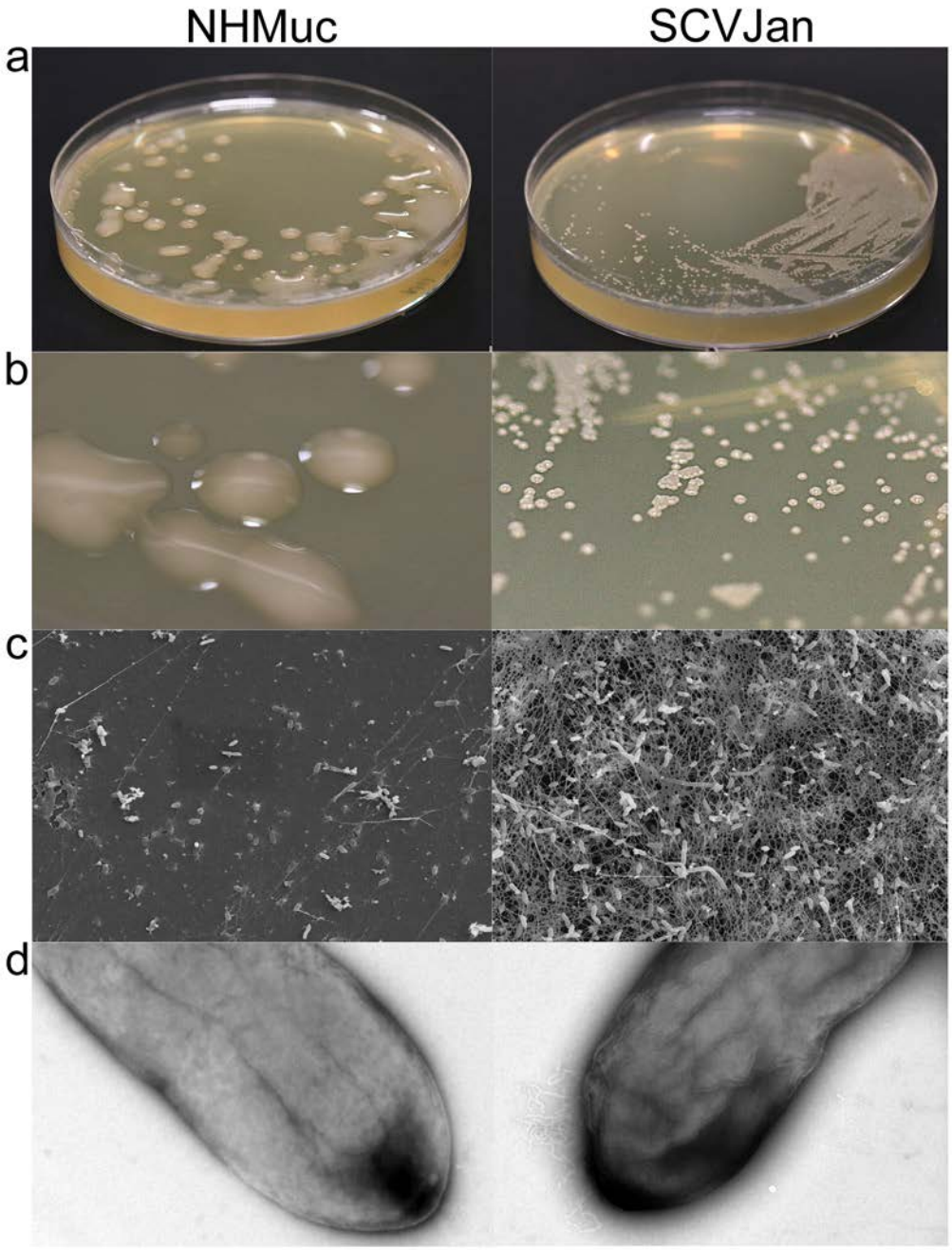

Figure 3-43-4 Phenotypic differences between NHMuc and SCVJan

a) and b) Growth of NH and SCVJan on LB agar at 37 °C after 48 hours. There are marked differences in colony size and morphology. c) SEM images of biofilm of NH and SCVJan grown on a glass coverslip for 24 h in LB broth at 37 °C. d) SEM image of NH and SCVJan with negative staining shows that in contrast to NH, SCVJan is highly pilliated.

3.2.4 *P. aeruginosa* SCV phenotype produces highly adherent biofilm

In addition to the EM images above (figure 3-3, 3-4) which clearly demonstrates the complex and intricate adherent biofilm produced by the SCV strain on the glass coverslip, a biofilm assay was performed to compare against control strains. Previous studies have implicated the mucoid strain as being most associated with biofilm production[54,290], however this study would suggest that the mucoid strain is unable to produce an adherent biofilm. Figure 3-5 below clearly demonstrates gross biofilm production by the SCV strain which has more residual crystal violet staining in the wells as compared to PA01. The mucoid strain has no adherent biofilm following a simple washing technique.

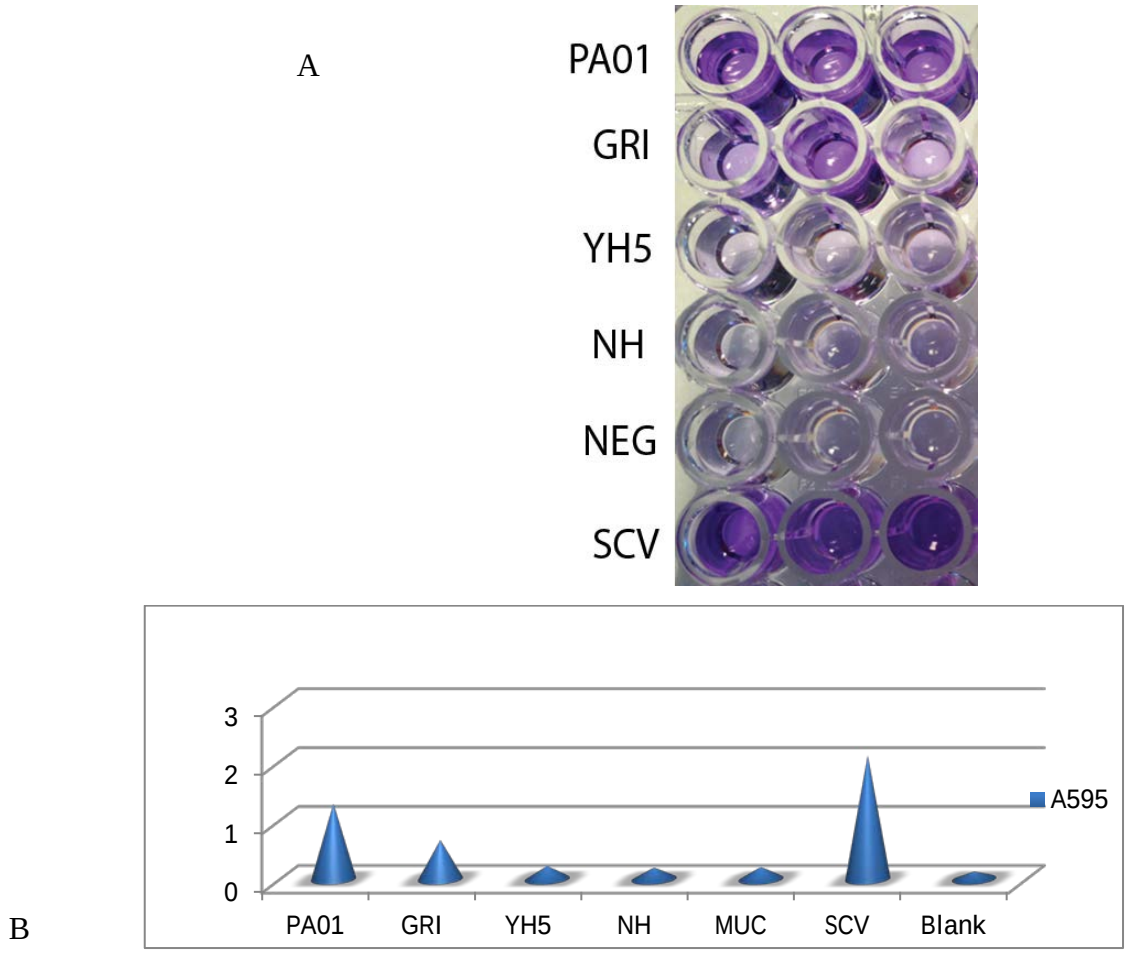

Figure 3-53-5. Microtitre biofilm assay

A. Comparing the three control strains (PA01, GRI and YH5) against the test strains NH and SCV PA01 is the generic control strain, GRI is a clinical strain from a patient with ventilator associated pneumonia and YH5 is a mucoid strain from a paediatric CF patient. B. The optical density of

crystal violet stain in the wells is directly proportional to the biofilm production as demonstrated by the A595 reading. .

Previous studies have suggested that formation of the SCV phenotype is associated with altered flagellar function and reduced motility. Often all three types of motility are affected, namely swimming, swarming and twitching motility. However, the parent NH strain is non-motile and no differences in swimming motility were observed for the SCV strains (Figure 3-6, 3-7) The differences in the EM images in Figure 3-4d above would suggest that the SCV has increased pili at the terminal end of the bacteria however this does not appear to affect motility (Figure 3-6, 3-7). This may be responsible for the formation of the highly adherent biofilm structure.

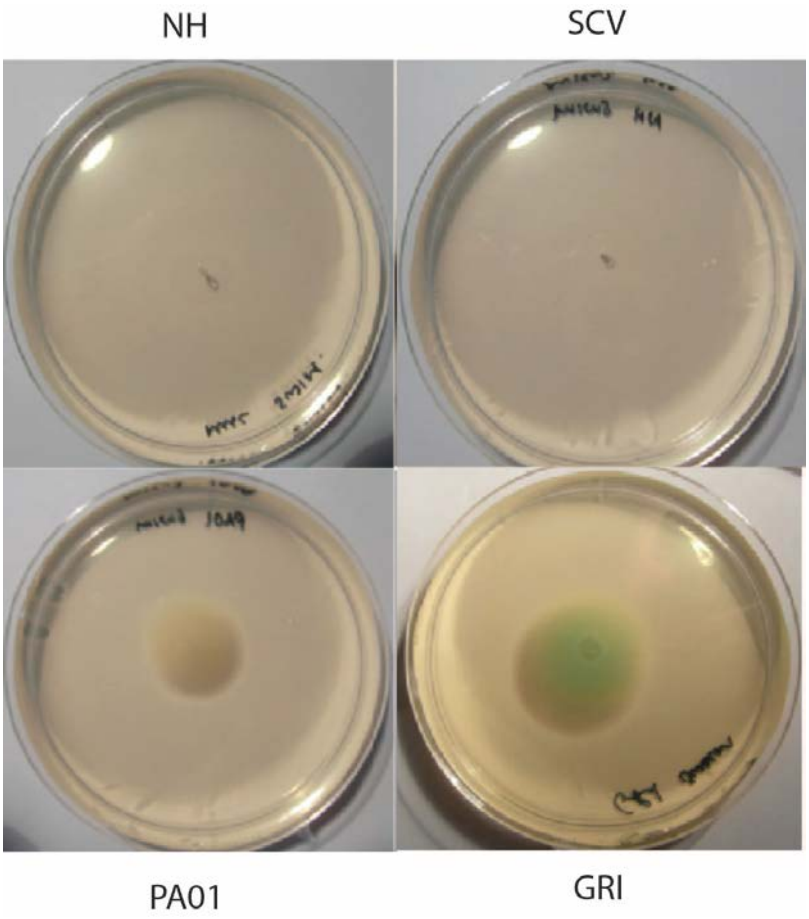

Figure 3-63-6. Swimming motility of the a) SCV strain and d)NH with c) PA01 and b) GRI as control organisms.

Tryptone swim plates (1% tryptone, 0.5% NaCl, 0.3% agar) were inoculated with a sterile toothpick and incubated for 16h at 25°C. Motility was then assessed qualitatively by examining the circular turbid zone formed by the bacteria migrating away from the point of inoculation. GRI

and PA01 are both non-mucoid strains. GRI is a clinical strain isolated from a ventilator associated pneumonia patient.

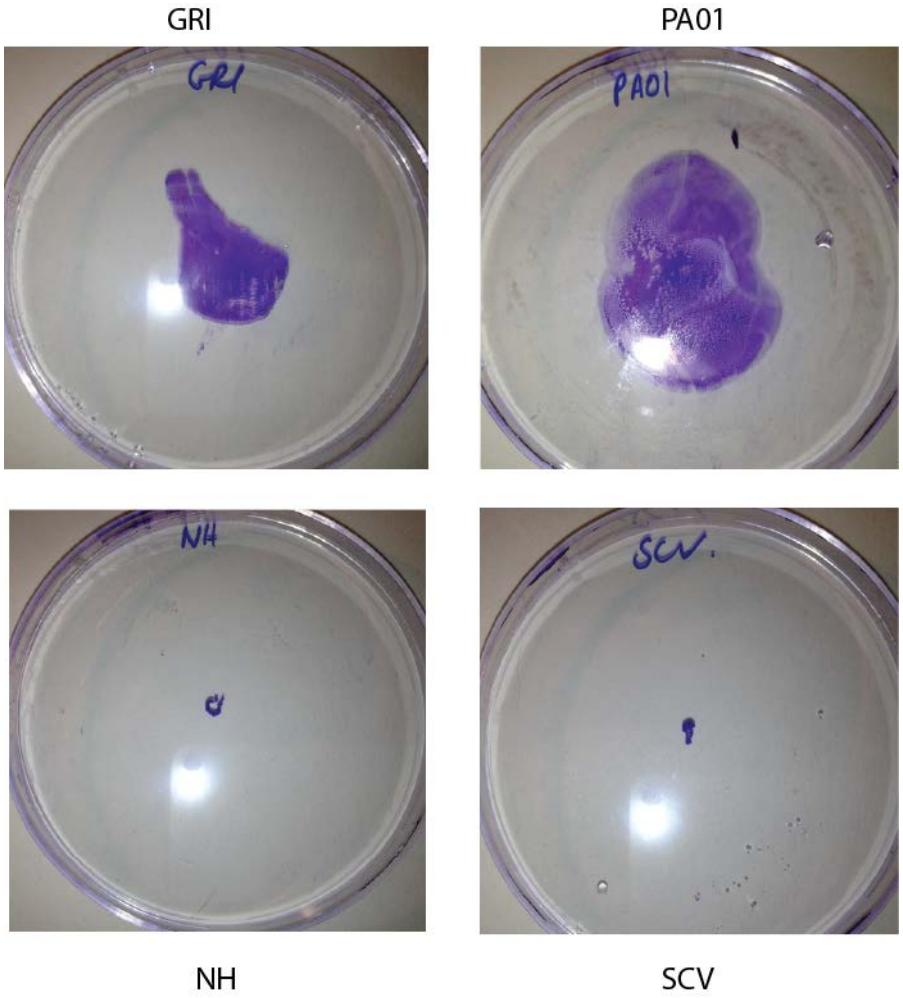

Figure 3-73-7. Twitching motilities of the control strains a) GRI and b) PA01 against the test strains c) NH and d) SCV

GRI and PA01 are both non-mucoid strains. GRI is a clinical strain isolated from a ventilator associated pneumonia patient. 1% LB agar plates were prepared. A sterile toothpick was then used to inoculate the agar plates in the centre of the agar through to the petri-dish with each test strain. Plates were incubated for 24 hours at 37°C. The twitching motility is represented by a halo of growth between the agar and the petri-dish. This was visualised by flooding the agar plate with crystal violet.

3.2.5 The phenotype of isolated SCVs is highly stable

Following repeated subculture of the SCV and mucoid strains under different growth conditions as described in section 1.15.2, reversion back to the wild-type morphotype was not observed. Samples were subcultured 10 times. Repeated subculture through BHI and minimal media at a range of temperatures from 21°C to 42°C over a two week period failed to revert the phenotype back to the mucoid morphotype. Previous studies have suggested that SCVs formed under antibiotic pressure in vitro are unstable and revert back the wild-type in as few as one passage[59].

The phenotype is also highly reproducible and was isolated from various mouse models during the course of the experiment. The reproducible and constant phenotypic change would suggest that the same genetic alteration has occurred each time, rather than small SNP's or insertions which would result in a slightly different result each time.

3.2.6 Isolated SCVs display a reduced growth rate and increased virulence

To further characterise the SCV phenotype, we performed various assays to establish the virulence potential in comparison to the mucoid wild type. A growth assay was performed which revealed an extended lag phase of growth in the SCV strain. For SCVJan an OD of 0.5 was achieved in 8 hours, in comparison to the mucoid strain which achieved an OD of 0.5 in 3 hours. This prolonged growth phase enables the bacteria to evade the immune system and also antibiotics which may target the growth and replication cycle of the bacteria[66,282].

The slow growth of the SCV also poses another significant diagnostic problem. The colonies appear over a prolonged incubation period and often go undetected in the clinical laboratory. To avoid misidentification, a prerequisite for the recovery and isolation of SCVs is the application of extended conventional culture and identification techniques. They become rapidly overgrown by the wild type morphotypes on agar and often they are deficient or reduced biochemical reactions. In addition, the slow growth rate of SCVs makes standardisation of susceptibility testing difficult because a slow growth rate alters diffusion times and affects automated systems which are reliant on a typically growth cycle.

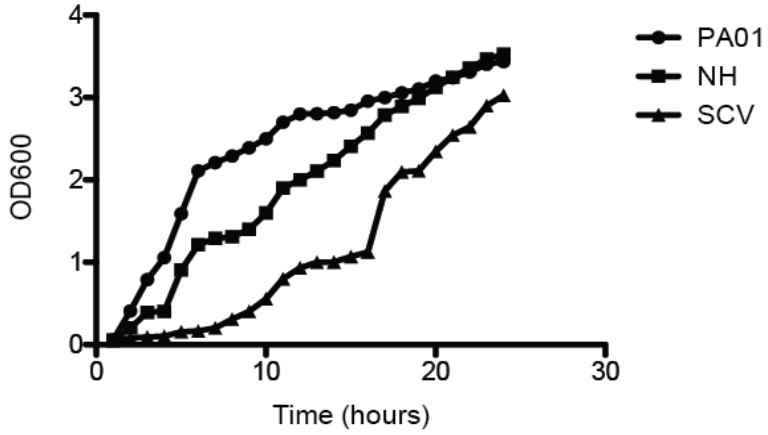

Figure 3-83-8. Growth curves

Revealing a slower growth phase in the SCV strain as compared to the NH and the control strain PA01. All isolates grown in LB broth and incubated for 24 hours at 37°C with OD_{600} recorded at 3 hourly intervals using a spectrophotometer.

An observation made when carrying out the growth curve analysis was the overproduction of pyoverdine by the SCV strain in LB broth both at both room temperature and 37°C (Figure 3-9). The SCV also developed the characteristic *P. aeruginosa* odour on incubation when compared to the mucoid strain. Production of siderophores including pyoverdine and pyochelin allows the bacteria to survive in hostile environments and chelate iron which promotes growth and survival[48,49]. These two siderophores are found to be important in biofilm formation and virulence[105,291].

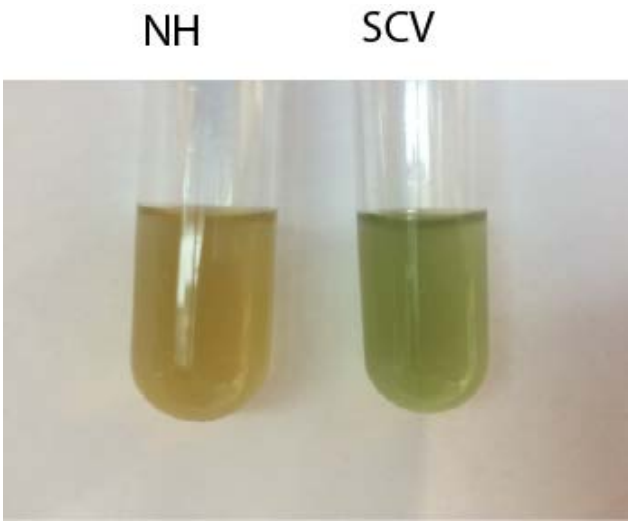

Figure 3-93-9. Pyoverdine production

The appearances of the NH and SCV strain inoculated into LB and incubated overnight at 37°C. The green colour of the SCV broth confirms increased pyoverdine production.

Because the toxicity of H_2O_2 released by phagocytes has been implicated in the innate immune responses, bacterial pathogens exploit catalytic enzymes to survive the host environments. A catalase assay, shown in figure 3-10a was performed to compare the amount of catalase activity in the SCV as compared to the NHSCV and establish whether it is more adapted to survive in the host environment.

The cytotoxic effects of SCV and NH on J774A.1 cells were determined by the quantification of lactate dehydrogenase (LDH) released in culture medium.
The SCV strain showed increased LDH release following infection of J774A.1 cells as shown in figure 3-10b. The increased LDH was observed after a 10 hour incubation period where the percentage of LDH released was 98% in comparison to only 40% in the mucoid strain. This is a highly significant finding and would suggest that the SCV has the potential to cause direct tissue damage at the site of infection in the host and may be responsible for the lung damage seen in CF.

To determine whether the SCV was more pathogenic to a host on direct infection, *Galleria mellonella* larvae were infected with each strain and observed post-infection for 72 hours. Phosphate buffered saline (PBS) was used for untreated controls. The results in Figure 3-10c show 82% mortality after 72 hours following infection with the SCV strain as compared to 63% mortality following infection with the mucoid strain.

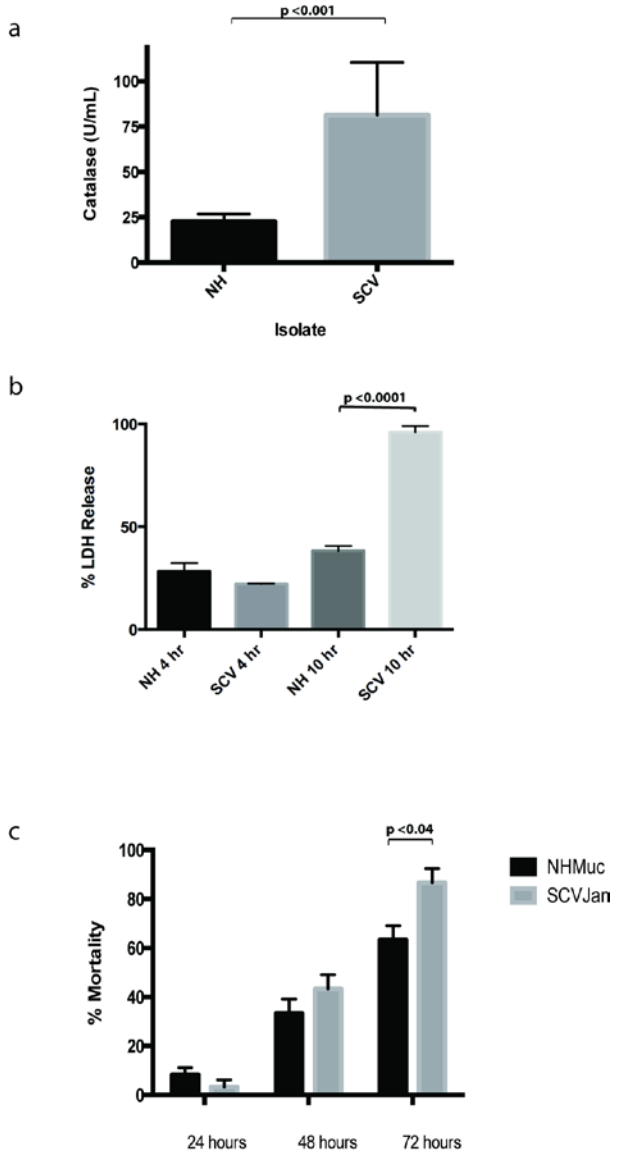

Figure 3-103-10. SCVJan displays increased virulence as compared to the NH strain

a) Catalase assay**.** Overnight cultures of bacterial strains were grown in LB broth, diluted 1:100 in the same medium and grown to an OD_{600} of 0.4. 20µl of each serial dilution of overnight culture were added to 3 wells in a 96 well plate to allow for average readings for each sample. Plate absorbance was read at 520nm.

b). LDH release assay. J774A.1 cells were infected with NH and SCV and LDH release was measured after 4hr and 10hr. Lactate dehydrogenase release was determined using the Cytotox 96 cytotoxicity assay kit (Promega USA) as described in the manufacturer's protocol.

c) *Galleria mellonella* killing assay. Five-microliter aliquots of the serial dilutions of each isolate were injected using a Hamilton syringe into *G. mellonella* larvae, via the hindmost left proleg. Death of the larvae was monitored over a 72 hour period.

To determine if the SCV displayed increased production of known virulence factors, a type III secretion system assay was performed to compare against the mucoid strain. PA01 and the GRI strain were used as controls as both were used in previous assays and known to express both ExoS and ExoT. During the initial protein purification steps it was clear that there was increased protein secretion in the SCV broth as can be seen from figure 3-11. Following centrifugation there was a large pellet formed in the Falcon tube.

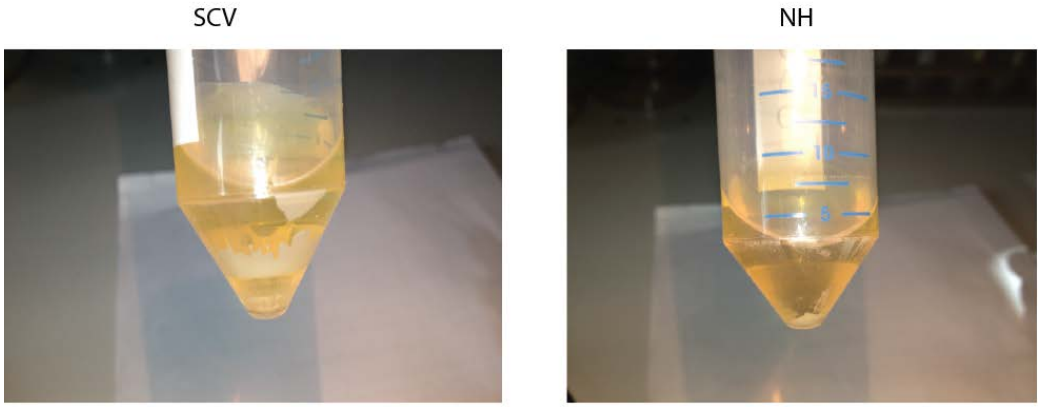

Figure 3-113-11. Type III Secretion protein production

Secreted proteins during the type III secretion assay can be directly visualised as a pellet following centrifugation.

Following protein purification and extraction, specific antibodies for ExoS and ExoT were used and analysed using SDS-PAGE and Western blot hybridisation. Figure 3-12 clearly shows expression of ExoS and ExoT by the SCV, with no evidence of a band from the mucoid strain. The type III secretion system facilitate bacterial pathogenesis by injecting proteins into the host cell and interfering with host cell function[71,159].

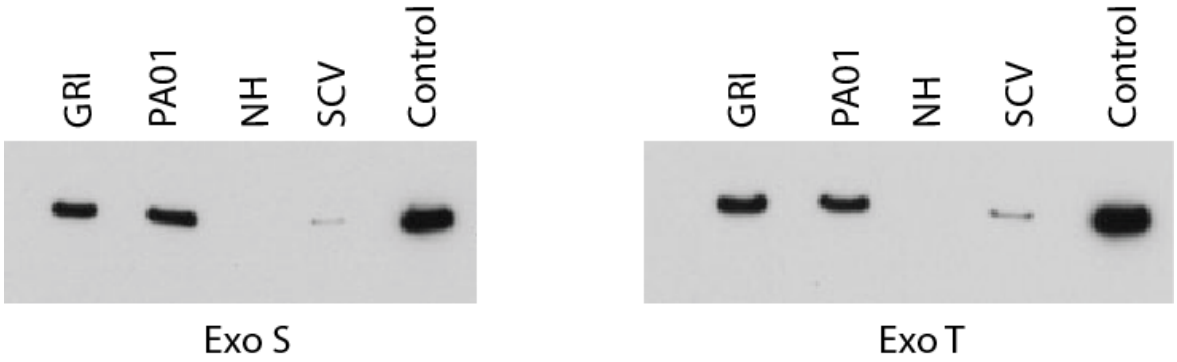

Figure 3-123-12. Type III secretion assay.

Western blot analysis following type III secretion assay. Secreted protein profiles for SCV, NH and the control strains (GRI and PA01) were analysed by SDS-PAGE and immunoblot analysis after specific induction of type III proteins. Specific antibodies for ExoS and ExoT were used and analysed using SDS-PAGE and Western blot hybridisation. Assay and analysis was performed as previously described

As in most gram-negative bacteria, the LPS of *P. aeruginosa* forms an integral part of the outer membrane and several studies suggest that LPS contributes substantially to its virulence[93,292]. LPS was extracted using the hot aqueous phenol method as previously described and the SDS-PAGE stained using silver staining to visualise the results. Figure 3-13 below shows that there is a no difference in the LPS banding pattern between the NH and SCV phenotypes.

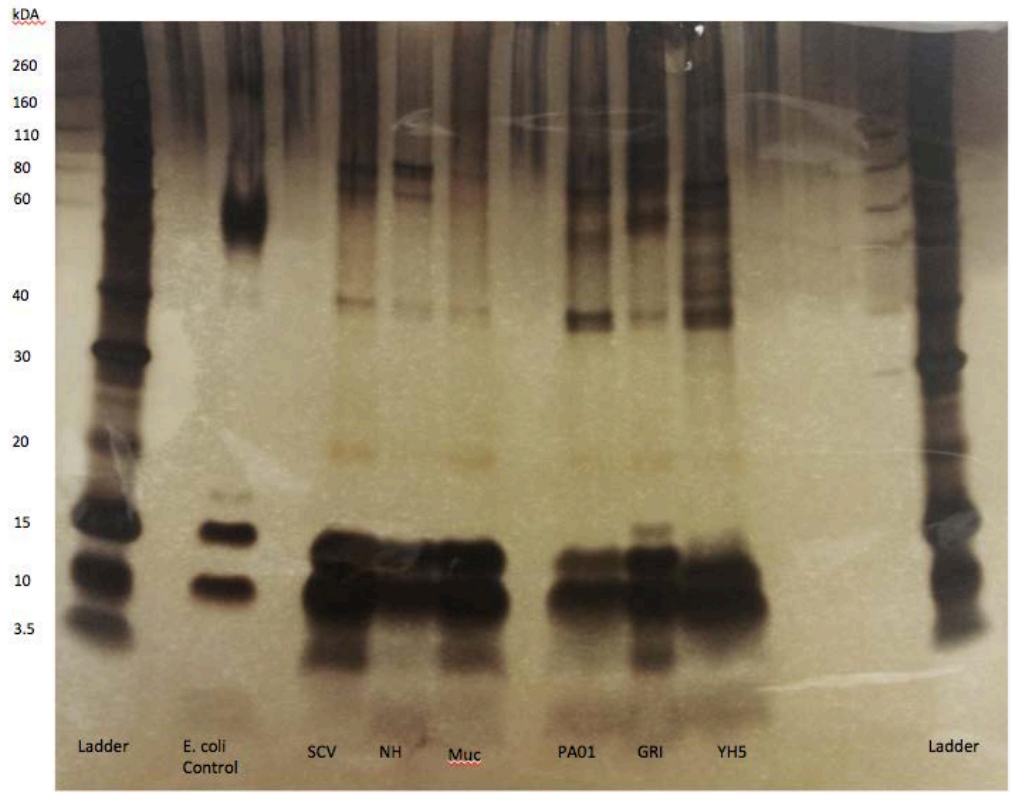

Figure 3-133-13 LPS characterisation

Silver stained SDS-PAGE gel of LPS from the different *P. aeruginosa* strains. Use of *E. coli* as a control strain in addition to PA01, GRI and YH5 strains. 15ul were separated on a 12% SDS-polyacrylamide gel and stained with Pro-Q Emerald 300 as per the manufacturer's instructions.

3.2.7 *P. aeruginosa* SCV phenotype shows increased susceptibility on regular antibiotic sensitivity testing methods but reduced susceptibility in the biofilm form

In contrast to previous reports, we did not observe a generally enhanced antibiotic resistance in the planktonic state on conversion to the SCV phenotype however when tested in the biofilm state, the SCV showed increased antibiotic resistance. This suggests that in the host these SCVs are more antibiotic resistant.[293,294] Indeed, in the planktonic state, relative to the parent strain, SCV displayed increased sensitivity to four of the 17 antibiotics tested and decreased sensitivity to only one (Table 3-1). This is a significant problem with antibiotic sensitivity testing in the clinical laboratory and does not correlate with the environment and growth state in the host. The slow growth rate of the SCV also adversely affects the interpretation of automated sensitivity testing, including the Vitek II. The incubation times are set within the platform and result in a time-out of the slow

growing SCV, or a false result suggesting the SCV is sensitive rather than resistant due to lack of growth.

Table 3-1. Antibiotic sensitivity pattern of SCV versus NH using Vitek II. Breakpoints as per EUCAST (European Committee on Antimicrobial Susceptibility Testing) guidelines. (Confirmation using E-test).

	NH		**SCV**	
Antimicrobial	MIC	Interpretation	MIC	Interpretation
Temocillin	>/= 32	R	>/= 32	R
Ticarcillin	>/= 128	S	>/= 128	R
Ticarcillin/Clavulanic Acid	>/= 128	R	>/= 128	R
Piperacillin/Tazobactam	>/= 128	R	>/= 128	R
Cefotaxime	>/= 64	R	>/= 64	R
Ceftazidime	32	R	32	R
Imipenem	2	S	</= 0.25	S
Meropenem	2	S	</= 0.25	S
Amikacin	32	I	16	S
Gentamicin	>/= 16	R	>/= 16	R
Tobramycin	2	S	</= 1	S
Ciprofloxacin	2	I	2	I
Minocycline	>/= 16	R	>/= 16	R
Tigecycline	>/= 8	R	>/= 8	R
Chloramphenicol	32	R	>/= 64	R
Colistin	</= 0.5	S	</= 0.5	S
Trimethorpim/Sulphamethoxazole	40	R	40	R

To further investigate the fact that previous studies suggest SCVs have increased resistance to most antibiotics used in clinical practice, three commonly used antibiotics for CF exacerbations were used to determine MICs in liquid culture and minimum biofilm eliminating concentration (MBEC) Table 3-2 below shows a clear increase in resistance of the SCV to these three antibiotics when grown in the biofilm state and would also suggest that the sensitivity results being produced in the clinical laboratory have limited clinical meaning.

Table 3-2 Antibiotic sensitivity pattern comparing SCV and NH using broth microdilution and PEG biofilm assays (MBEC™).

Antibiotic	SCV MIC		NH MIC	
	Broth	MBEC™	Broth	MBEC™
Ciprofloxacin	2	4	2	2
Tobramycin	1	6	1	2
Ceftazidime	32	64	32	32

3.3 Discussion

This work demonstrates that during the course of infection in a murine model of CF, the SCV form of a mucoid *P. aeruginosa* strain evolves naturally during the course of infection and is able to effectively colonise the lung tissue. In this case, the isolated SCV has a stable phenotype and shows increased virulence when compared to the mucoid parent strain. The initial phenotypic analysis would suggest that SCVs are more virulent, able to produce subacute, persistant, recurrent and antibiotic resistant infections.

Bacterial phenotypic switching is considered to be an insurance policy against harmful environmental change including exhaustion of nutrients or antibiotic therapy.[233,281] A unique feature of the CF lung is the recovery of different *P. aeruginosa* morphotypes from a single sputum sample, with up to six different colonial variations present. All six morphotypes including SCVs have been isolated from post mortem lung specimens[180,218], but despite the clear association with these strain and poor outcomes, attention remains focused on the most common mucoid phenotype in the clinical laboratory setting. SCVs have been well described for >100 years as previously discussed[295] yet their significance has been limited by the fact that their occurrence in clinical specimens is rarely reported. From the routine culturing of the sputum samples obtained from 50 CF patients undergoing an infective exacerbation, we were able to identify all of these six morphotypes. Given that there is a strong correlation between the presence of SCV's and worsening outcomes[218,287,296], the identification and reporting of these organisms is of paramount importance. The appearance of the SCV, being small, rough and atypical in colour means that these colonies will most often be ignored in a mixed culture in the clinical laboratory. The phenotypic characterisation of the SCV illustrates that these SCV's isolated during the murine model of infection are similar and consistent with SCV's isolated from CF patients. The slow growth rate observed in the SCV allows the bacteria to persist in the host, evading the immune system and antibiotic pressure. In a laboratory setting, marked antibiotic tolerance can be produced by starving bacteria of nutrients[244]. This starvation also occurs during infection where nutrients are limited and when bacteria adopt the biofilm form of growth where there is a dense population of bacteria and limited diffusion due to the intricate network. The starvation is thought to result in a growth arrest and subsequent inactivity of the antibiotic targets; thus if targets are inactive, quinolones will produce less DNA breaks, aminoglycosides less protein mistranslation and β-lactams will cause lower levels of peptidoglycan accumulation triggering lysis. This slow growth also

results in misidentification and difficulty in culturing in the clinical laboratory setting given that the automated sensitivity methods including VitekII have a short incubation and run time set for typical *P. aeruginosa* growth phase.

As found in other studies[28,199,297,298], the SCV produces a highly adherent and intricate biofilm on prosthetic material and therefore host lung tissue. Biofilm growth selects for P. aeruginosa colony morphology variants that have biofilm related phenotypes, namely hyperadherence to abiotic surfaces. Previous studies implicated the mucoid morphotype as the one responsible for significant biofilm production causing human disease[265,289,299]. The results of this study however would argue against this and although the alginate hyperproduction results in a large volume of extracellular material which may form a physical layer on the lung structures, it would appear that the SCV strain is the one which adheres to the tissue and would be highly significant in the direct tissue damage and colonisation of a prosthetic device[298], intravenous line or catheter.

Electron microscope images from the single bacteria suggest that the SCV is hyperpiliated in comparison to the mucoid strain. This hyperpiliation may be in part responsible for its ability to produce the highly adherent biofilm seen on EM. There were no clear differences in swimming, swarming or twitching motility between these two strains which previous studies have shown[30,44,158]. Previous studies have suggested that formation of the SCV phenotype is associated with altered flagellar function and reduced motility. In this study, the parent mucoid strain and the SCV were both found to be non-motile. This may be in part due to the alginate hyperproduction of the mucoid strain and difficulty interpreting the results in this setting.

Phenotypic switching has been linked with persistence in host tissue, treatment failure and the development of persistent infections for a variety of bacteria[229,281,282,300]. It is not clear whether the switch is a constitutive process selected for in vivo or occurs only in response to particular environmental triggers including the antibiotic gentamicin[201,301]. Previous studies suggest that there is expansion of the SCV subpopulation under selective pressure, which can then revert back to the wild-type phenotype when the pressure is removed. These SCVs are thought to have unstable changes allowing them to revert back easily[233]. SCVJan in comparison was found to be a stable phenotype with no reversion back to the wild-type despite significant attempts.

Further characterisation of the SCV revealed that it displayed similar growth characteristics to those previously described[47,165,199]. The lag phase was 8 hours in comparison to the mucoid strains 3 hour period. As already discussed, this poses a significant diagnostic problem requiring extended incubation in the clinical laboratory and use of manual sensitivity testing methods, which are not validated for these organisms. The observed production of pyoverdine during routine incubation of the SCV in LB broth clearly demonstrates the increased virulence potential of this organism. As a free-living organism, *P. aeruginosa* is able to excrete large amounts of the siderophores pyoverdine and pyochelin into its environment which both function as powerful iron chelators[302,303]. To meet its needs for iron, the bacteria must compete with the host for iron which is tightly bound to host proteins therefore this would suggest that the SCV is more adept at utilising host iron supplies for survival. Further evidence to suggest the SCV is more suited to the hostile environment is highlighted in the fact that the SCV displays increased catalase activity, increased cytotoxicity in the LDH release assay, expression of the Type III secretion system and increased mortality when inoculated into the *Galleria mellonella* model. Previous studies have suggested that mucoid *P. aeruginosa* strains produce more cyanide than the non-mucoid strains which may result in an increase in pathogenicity in the human host[108,109]. In this study we observed an immediate toxic effect following injection of the mucoid strain which may be related to the cyanide, however when washed cells were injected, the SCV demonstrated an increased killing potential.

Several studies have suggested that oxidative stress selects for phenotypic diversification in vitro and it has since been speculated that oxidative stress similarly causes phenotypic variation in vivo[162,222,304]. The increased catalase activity seen in the SCV would support this theory. The Type III secretion system and its secreted protein products are considered to be a major virulence factor of *P. aeruginosa* and other gram negative bacterial pathogens. After attachment to the eukaryotic host cells, the type III secretion system enables these bacteria to inject effector proteins directly into the cytosol of the host cells[73,159]. In this study we demonstrated expression of the ExoS and ExoT proteins by the SCV in particular. To test if this upregulation was biologically meaningful, we determined the in vitro cytotoxicity by using the murine macrophage cell line J774 and the *Galleria mellonella* model. These two assays confirmed an increase in the cytotoxic effects of the SCV compared with the mucoid parent strain. It is generally accepted that the habitat of a chronically infected CF lung selects for less virulent *P. aeruginosa* strains[305,306].

Previously, isolates from CF patients were reported to produce lower levels of protease, elastase and exotoxin A[307] and lower levels of type III secretion proteins such as ExoS and ExoT[81]. The results of this study however, contradict this finding and show that the SCV under study here displays increased type III secretion mediated virulence.

In this study we demonstrated that routine clinical microbiology laboratory antibiotic sensitivity testing (VitekII and E-tests) fail to identify the increased antibiotic resistance of the SCV phenotype. By comparing the MIC of common anti-Pseudomonal antibiotics using the standard methods against peg biofilm cultures, it was evident that the SCV biofilm is highly resistant to most antibiotics. The structure of the wild-type and the SCV biofilms may have an effect on the ability of antibiotics to effectively eradicate bacteria in this stage and should be taken into account when interpreting laboratory generated antimicrobial sensitivity patterns.

3.4 Conclusions and future work

Overall, the phenotypic differences between the NH strain and the SCVJan strain begin to reveal the importance of in vivo diversification for *P. aeruginosa* and the ways in which it differs from in vitro observations. Given the observed differences in phenotype and virulence between the two strains, and the fact that this phenotypic switch seems to be a mechanism utilised by most bacteria, it would follow that a common genetic mechanism was responsible. There have been numerous studies suggesting possible mechanisms behind the switch[182,285,293,308], however nothing consistent in the literature. The next step aimed to genetically characterise the phenotypic switch and to establish a mechanism which may be common to all bacteria allowing them to set up and form chronic infection in the host.

Chapter 4 Genotypic characterisation

4.1 Introduction

4.1.1 Genetic basis of *P. aeruginosa* adaptation in infection

The advent of next generation sequencing has resulted in an explosion of prokaryotic genome projects. The first completely sequenced strain of *P. aeruginosa* was the laboratory strain PAO1[19] which revealed a genetic complexity including a large number of secretion and efflux systems, consistent with its ability to thrive in a wide variety of environments. The assembled genome sequence was found to be in excellent agreement with the physical map of the *P. aeruginosa* genome[309,310] with the exception of an inversion of over a quarter of the genome in the PAO1 isolate relative to DSM-1707, the PAO1-derived isolate previously mapped. The inversion seems to have resulted from homologous recombination between the *rrnA* and *rrnB* loci which are orientated in opposite directions and separated by 1.7 Mbp. Earlier observations have suggested that similar large-scale genome rearrangements between oppositely orientated ribosomal DNA loci in *E. coli* and *S. typhimurium* have led to the proposal that these reversible genome rearrangements may have important adaptive significance[311]. Since then, numerous *P. aeruginosa* genomes have been sequenced, including PA14[271] which is a more virulent strain and has additional genes clustered into genomic islands, but a core set similar to that of PAO1. The sequence of the Liverpool Epidemic Strain LESB58[189] indicated that both the core genome and the genomic islands are involved in *in vivo* competitiveness.

Adaptation, of *P. aeruginosa* to the lung during chronic CF infection can also be driven by point mutation as in the well characterised phenotypic switch from a nonmucoid to a mucoid phenotype, which results in copious amounts of the capsular polysaccharide alginate being produced[289].

Several studies using PFGE have identified a large-scale genome rearrangement which may be responsible for a change in phenotype of different bacterial species[184,312]. The study by Schmidt and subsequent next-generation sequencing of PAO1 in particular suggests that the bacterial chromosomes are able to invert at the *rrn* loci.

Several SCVs have been sequenced and recently the complete genome sequence of a highly adherent *P. aeruginosa* small colony variant (SCV20265) was published[181]. This SCV was isolated from the lung of a CF patient in the Hanover Medical School together

with a clonally identical wild-type. Phenotypically, it was noted to be hyper-piliated, exhibit increased twitching motility and capacity for biofilm formation and express elevated levels of cyclic diguanylate monophosphate (cyclic-di-GMP). The assembled SCV20265 genome consists of a circular chromosome, 6,725,183 bp which exceeds 10 of the 13 currently sequenced *P. aeruginosa* strains.

P. aeruginosa has a large number of genes devoted to command and control systems including environmental sensors and transcriptional regulators. These regulatory genes modulate the diverse genetic and biochemical abilities of this bacterium in changing environmental conditions. Several studies have suggested specific mutations which may be implicated in the SCV phenotype[59,60,182,183,293,313]. The majority of work has focused on *S. aureus* SCVs and several studies suggest that the presence of mutator strains leads to the SCV phenotype in particular defects in the mutator gene *mutS*.[183] In this study however, sequencing of the *mutS* gene failed to indicate a specific mutation. Further work looking at the emergence of phenotypic variants upon mismatch repair disruption in P. aeruginosa revealed the emergence of new morphotypes when the *mutS* gene was inactivated[314]. These variants displayed altered antibiotic sensitivity, altered motility and behaviour and increased pyoverdine and pyocyanin production. Several groups suggest that the SCV morphotype is strongly linked to elevated levels of cyclic-di-GMP, a ubiquitous bacterial second messenger able to regulate the transition between motile and sessile lifestyles[59,60,182,313]. Further, genetic experiments indicate that YfiN-mediated induction of the Pel and Psl exopolysaccharides plays a pivotal role in the SCV morphotype. Disruption of either exopolysaccharide operon leads to a partial phenotype, whereas disruption of both systems produced colonies with wild type morphology[55,182]. The GacS/GacA (global activator of antibiotic and cyanide synthesis) regulatory system is another pathway thought to be involved in the SCV phenotype[285,308,315]. This system regulates the expression of virulence factors, metabolism genes, motility proteins and stress tolerance genes. The response regulator GacA also plays a key role in biofilm formation and maturation. Sequencing technology has advanced significantly in the last 20 years. From the introduction of Sanger sequencing in 1975 through to PCR based sequencing, pyrosequencing and most recently next generation sequencing, it is now routine practice to produce complete bacterial genomes rapidly and at low cost. Illumina have dominated the sequencing industry over the last few years and set the standards for high throughput massively parallel sequencing with the HiSeq 2000. There are several problems with the Illumina sequencing technology, firstly the amplification steps may introduce a false bias

and secondly, the read lengths of only 100 bp do not allow for the identification of large scale genetic rearrangements. Pacific Biosciences have developed a method for real time sequencing of single DNA molecules with a rate of several bases per second and read lengths into the kilobase range. This technology allows for the identification of large-scale rearrangements however is less sensitive in the detection of SNPs. Combination of the results from the two platforms allow for a highly accurate and complete finished genome. Having established that SCVs phenotypically similar to those isolated from CF patients could be obtained from our *in vivo* model in the absence of antibiotic selection, we sought to understand the genetic basis of this phenotypic change.

4.2 Results

4.2.1 MLST reveals closest identity to DK2 strain

Given that the NH strain was a clinically obtained strain from the Netherlands which had never been previously sequenced, we aimed to establish its place in the *P. aeruginosa* lineage prior to genome analysis. Following Illumina sequencing of both the NH and SCV strains, we performed an MLST search against all of the sequenced strains on Genbank. This revealed that out of all the whole-genome sequenced strains, the most closely related strain by MLST is DK2, sharing 3/7 alleles as seen in Table 4-1 below. DK2 is a highly adapted pathogenic strain which was sampled over 35 years ago from CF patients attending the Copenhagen CF clinic at the University Hospital[316].

Table 4-1 MLST results

Revealing the most closely related strain to the NH and SCV is DK2 which shares 3/7 alleles. By use of the MLST Web server, the strains which we sequenced using Illumina Hi-Seq were typed. Shown are the names of the loci of the MLST scheme, the percentage of nucleotides that are identical in the best matching MLST allele in the database. Note that for a perfectly matching allele the percentage of identity will be 100%.

	acs	sro	gua	mut	nuo	pps	trp
RP73	98%	99%	100%	99%	99%	99%	99%
DK2	99%	99%	100%	99%	100%	99%	100%
M18	99%	99%	99%	99%	100%	99%	99%
LESB58	98%	99%	100%	99%	100%	99%	99%
PAO1	99%	99%	99%	99%	100%	99%	99%

4.2.2 Illumina HiSeq and PFGE fail to identify genetic differences between the mucoid and small colony variant

We initially performed Illumina HiSeq whole-genome sequencing and genomic comparison (using multiple genome alignment pipelines) between NH and the two separate SCVs (SCVJan and SCVFeb) isolated from independent in vivo experiments. However, despite their gross phenotypic differences, this analysis failed to identify any genetic differences between the SCVs and the parent strain. QC was performed in Liverpool

Genomics after processing and trimming of the reads. The read coverage was excellent for each sample, with an average of 15 million reads per sample and complete genome coverage, see table 4-2 below.

Table 4-2 Samples showing read length following Illumina HiSeq sequencing.

Average of 15 millions reads obtained with excellent coverage of the entire genome.

Sample	Total number of individual reads	Reads aligned	Coverage (assuming 6.3 Mb genome)
SCVJan	17933333	95.53%	284x
SCVFeb	16079082	95.71%	255x
NH	13791071	94.5%	218x

The Illumina HiSeq was chosen because of its genome coverage and high quality data. Based on the recent finding in *S. aureus* that switching between the normal colony and SCV phenotype is mediated by a reversible inversion of a large portion of the genome[184], we utilised PFGE technology with three different restriction enzymes in an attempt to identify a large scale genetic rearrangement (Figure 4-1). However, no genetic differences between the strains were identified using this approach. PFGE technology is limited in the fact that the restriction enzymes may fail to cut the genome at sites that will result in differences in the fragment size.

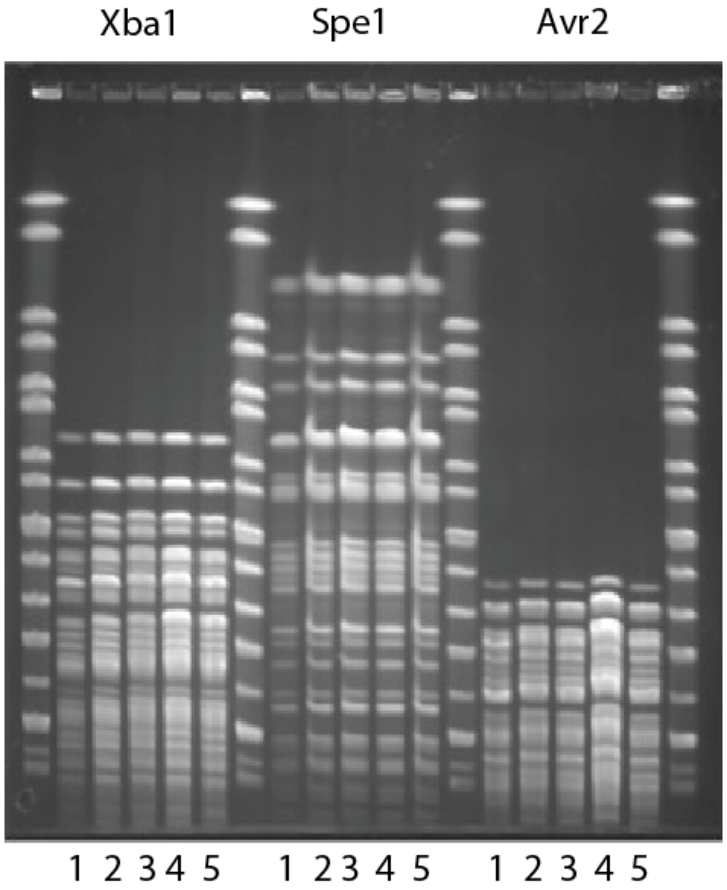

Figure 4-14-1. PFGE analysis of the SCV and NH genomes.
This analysis revealed no differences in band pattern between isolates. Three restriction enzymes were used, XbaI1, SpeI1 and AvrII2. Lanes 1 and 2 correspond to NH, lanes 3 and 4 correspond to SCVJan and lane 5 corresponds to SCVFeb.

4.2.3 PacBio analysis reveals a large-scale chromosomal rearrangement

In order to further investigate the genetic basis of conversion to the SCV phenotype we utilised the ultra-long reads produced by single-molecule real-time PacBio sequencing to attempt to identify any large scale genome rearrangements. The read data from the PacBio was combined with Illumina to provide a highly accurate, complete closed circular genome.
Using this technique we identified a large scale genomic inversion accompanying conversion from the parent mucoid to SCV phenotype in both SCVJan and SCVFeb (Figure 4-2).

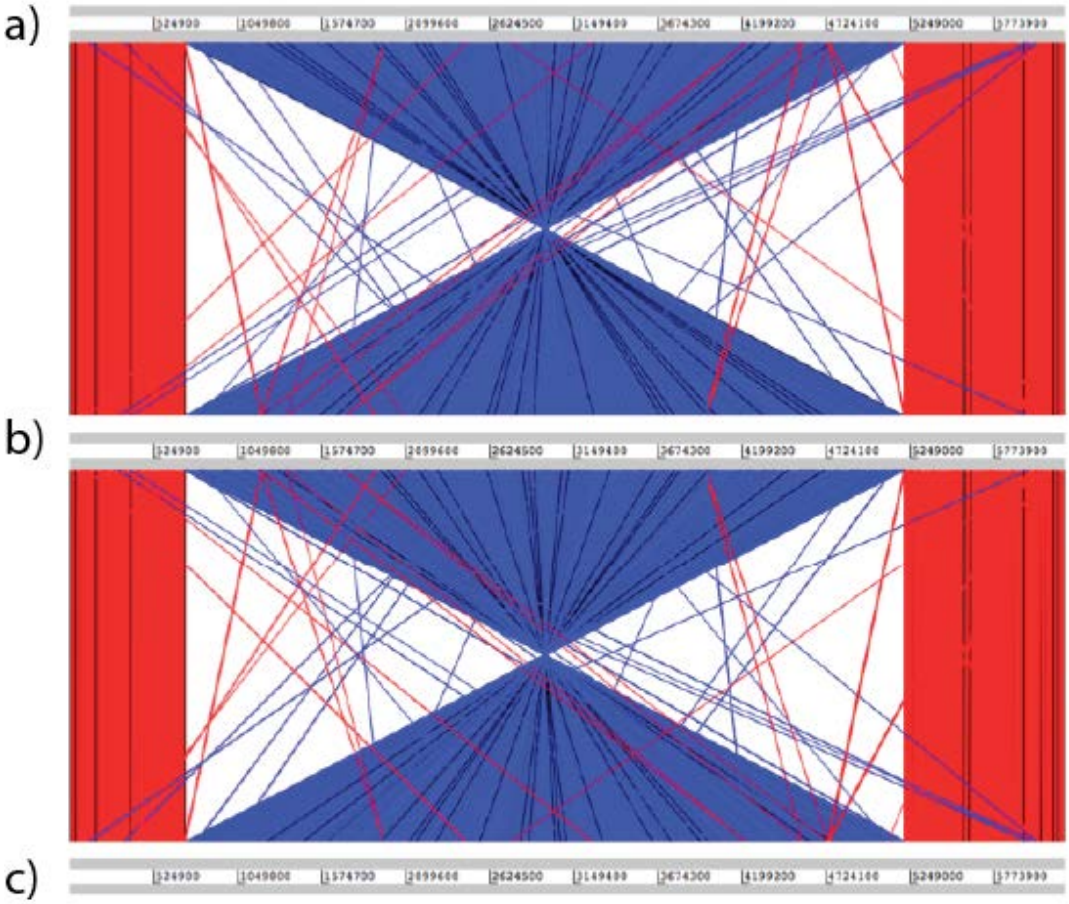

Figure 4-24-2 Alignments of genomes

a) SCVJan, b) NH and c) SCVFeb showing large scale genome inversion which is conserved between top a) and bottom c) SCV strains.

Closer inspection of the genome sequence identified the start and end points of the inversion, which for both SCVJan and SCVFeb begins at the first rRNA operon (0.72 Mbp) and ends at the third rRNA operon (5.21 Mbp). Exact chromosomal breakpoints were identified in the corresponding 16S rRNA genes by performing a MAUVE breakpoint analysis (Figure 4-3).

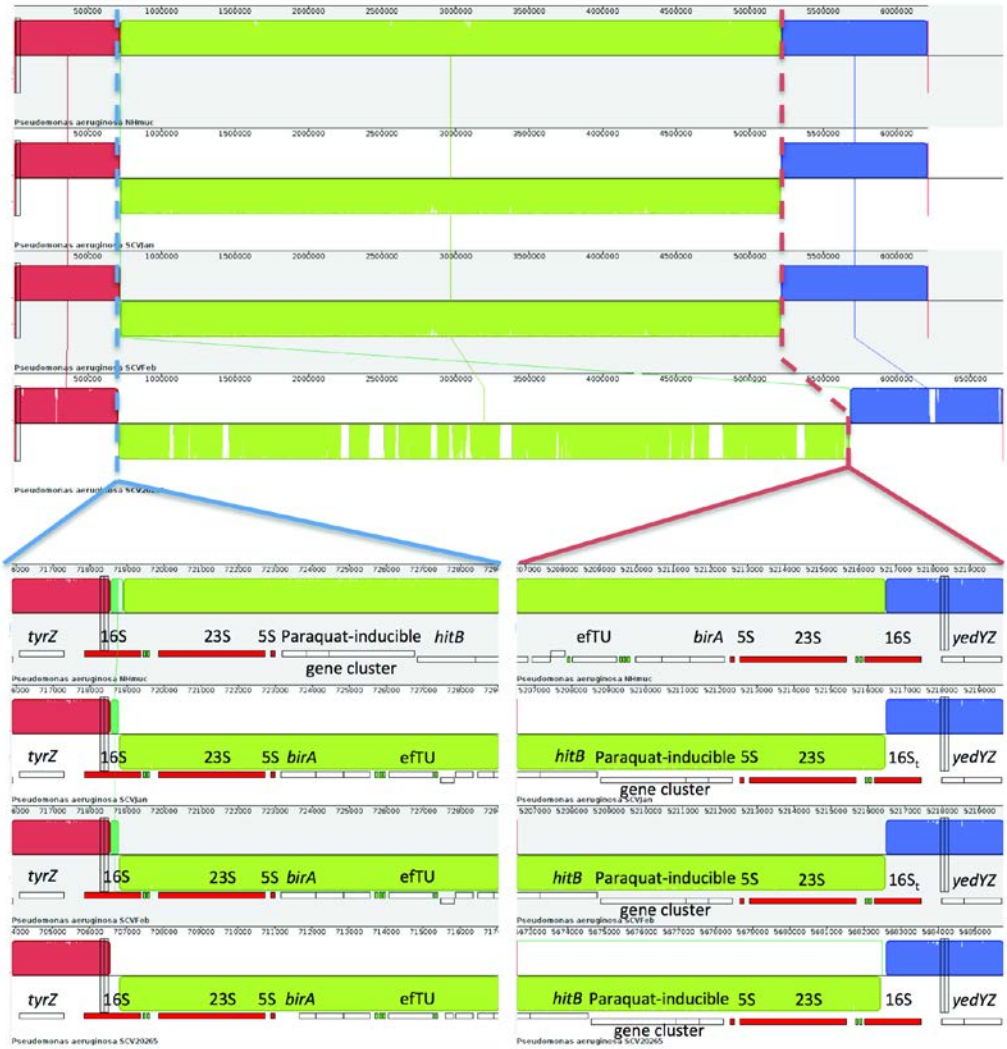

Figure 4-34-3. A common large scale chromosomal inversion in three *P. aeruginosa* strains is the genetic basis of conversion to the SCV phenotype.

From top to bottom strains NHMuC, SCVJan, SCVFeb and SCV20265 are displayed. Dashed lines indicate the inversion breakpoints present in the 16S rRNA genes. An inversion with highly similar breakpoints is present in the genome of strain SCV20265 a SCV isolated from a patient with CF. Within strains SCVJan and SCVFeb a unique truncated version of the 16S rRNA gene ($16S_t$) could be resolved, which could not be detected in strain SCV20265.

Furthermore, genome analysis revealed a 250 bp shortened 16S rRNA gene ($16S_t$) in both SCV strains, which is reflected in the reduced genome sizes of the SCVs (SCVJan 6,213,026, SCVFeb 6,213,029; Figure 4-4b) compared to the parent strain, NHmuc (6,213,276 bp; Figure 4-4a).

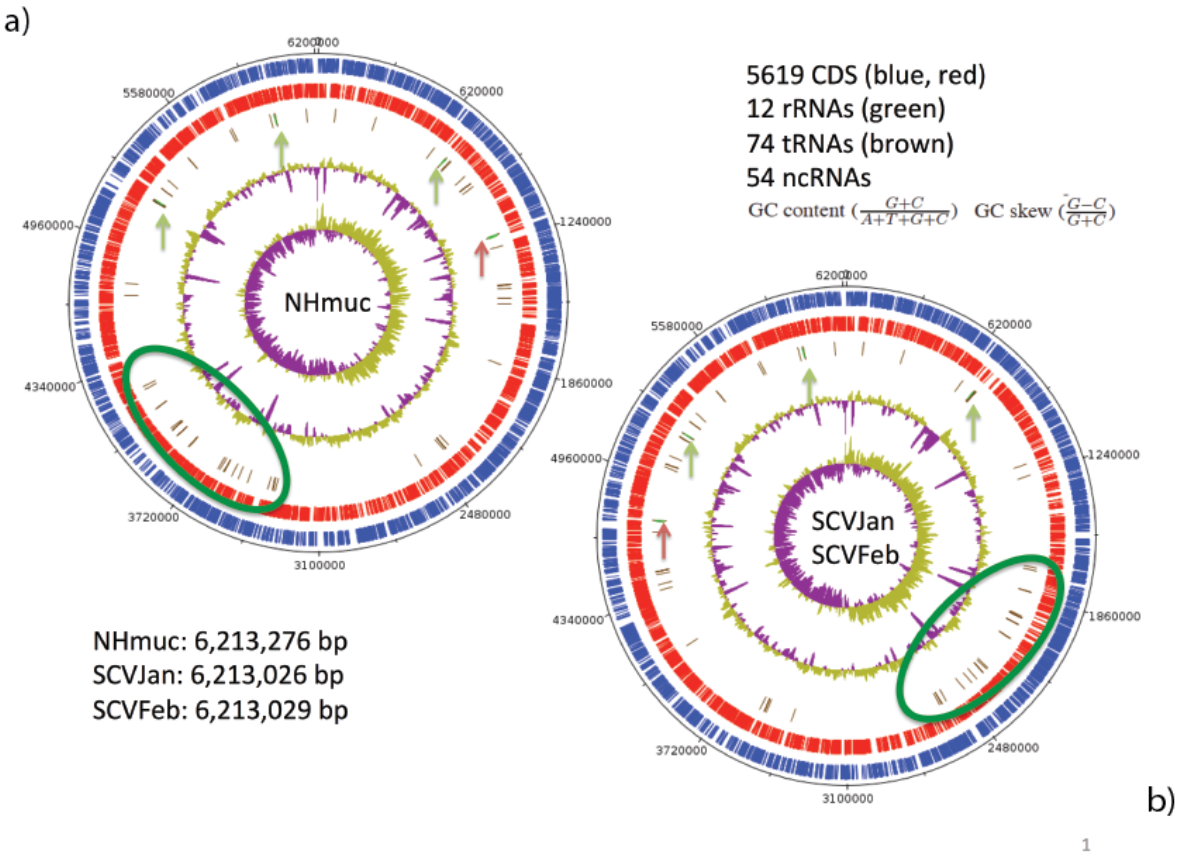

Figure 4-44-4 Chromosomal maps of *P. aeruginosa* NHmuc (a) and SCVJan/SCVFeb (b). The circular genomes of both strains are shown. Genomes of both SCV strains are 250 bp smaller compared to the parental strain NHmuc. Exact genome sizes are given in lower left corner. In blue (circle1) genes lying on the forward strand are shown and in red (circle 2) those on the reverse strand. In circle 3 tRNA genes are shown in brown, often clustered together with green rRNA genes, which have been additionally marked by vertical arrows. The red arrow shows the transposition of rRNA operon 3 in addition to that of a large tRNA region (green ellipse) due to the described chromosomal inversion. Circle 4 shows the GC content, whereas in circle 5 a GC skew is shown. Number of CDS, rRNAs, tRNAs and ncRNAs are identical in all strains (upper right corner according to GenBank submission). This map has been created using DNAplotter[317] (Carver *et al.*, 2009).

A >16S_full_length

agagtttgatcatggctcagattgaacgctggcggcaggcctaacacatgcaagtcgagc
ggatgaagggagcttgctcctggattcagcggcggacgggtgagtaatgcctaggaatct
gcctggtagtgggggataacgtccggaaacgggcgctaataccgcatacgtcctgaggga
gaaagtgggggatcttcggacctcacgctatcagatgagcctaggtcggattagctagtt
ggtggggtaaaggcctaccaaggcgacgatccgtaactggtctgagaggatgatcagtca
cactggaactgagacacggtccagactcctacgggaggcagcagtggggaatattggaca
atgggcgaaagcctgatccagccatgccgcgtgtgtgaagaaggtcttcggattgtaaag
cactttaagttgggaggaagggcagtaagttaataccttgctgttttgacgttaccaaca
gaataagcaccggctaacttcgtgccagcagccgcggtaatacgaagggtgcaagcgtta
atcggaattactgggcgtaaagcgcgcgtaggtggttcagcaagttggatgtgaaatccc
cgggctcaacctgggaactgcatccaaaactactgagctagagtacggtagagggtggtg
gaatttcctgtgtagcggtgaaatgcgtagatataggaaggaacaccagtggcgaaggcg
accacctggactgatactgacactgaggtgcgaaagcgtggggagcaaacaggattagat
accctggtagtccacgccgtaaacgatgtcgactagccgttgggatccttgagatcttag
tggcgcagctaacgcgataagtcgaccgcctggggagtacggccgcaaggttaaaactca
aatgaattgacgggggcccgcacaagcggtggagcatgtggtttaattcgaagcaacgcg
aagaaccttacctggccttgacatgctgagaactttccagagatggattggtgccttcgg
gaactcagacacaggtgctgcatggctgtcgtcagctcgtgtcgtgagatgttgggttaa
gtcccgtaacgagcgcaacccttgtccttagttaccagcacctcgggtgggcactctaag
gagactgccggtgacaaaccggaggaaggtggggatgacgtcaagtcatcatggcccttа
cggccagggctacacacgtgctacaatggtcggtacaaagggttgccaagccgcgaggtg
gagctaatcccataaaaccgatcgtagtccggatcgcagtctgcaactcgactgcgtgaa
gtcggaatcgctagtaatcgtgaatcagaatgtcacggtgaatacgttcccgggccttgt
acacaccgcccgtcacaccatgggagtgggttgctccagaagtagctagtctaaccgcaa
gggggacggttaccacggagtgattcatgactggggtgaagtcgtaacaaggtagccgta
ggggaacctgcggctggatcacct

B >16S_truncated

agagtttgatcatggctcagattgaacgctggcggcaggcctaacacatgcaagtcgagc
ggatgaagggagcttgctcctggattcagcggcggacgggtgagtaatgcctaggaatct
gcctggtagtgggggataacgtccggaaacgggcgctaataccgcatacgtcctgaggga
gaaagtgggggatcttcggacctcacgctatcagatgagcctaggtcggattagctagtt
ggtggggtaaaggcctaccaaggcgacgatccgtaactggtctgagaggatgatcagtca
cactggaactgagacacggtccagactcctacgggaggcagcagtggggaatattggaca
atgggcgaaagcctgatccagccatgccgcgtgtgtgaagaaggtcttcggattgtaaag
cactttaagttgggaggaagggcagtaagttaataccttgctgttttgacgttaccaaca
gaataagcaccggctaacttcgtgccagcagccgcggtaatacgaagggtgcaagcgtta
atcggaattactgggcgtaaagcgcgcgtaggtggttcagcaagttggatgtgaaatccc
cgggctcaacctgggaactgcatccaaaactactgagctagagtacggtagagggtggtg
gaatttcctgtgtagcggtgaaatgcgtagatataggaaggaacaccagtggcgaaggcg
accacctggactgatactgacactgaggtgcgaaagcgtggggagcaaacaggattagat
accctggtagtccacgccgtaaacgatgtcgactagccgttgggatccttgagatcttag
tggcgcagctaacgcgataagtcgaccgcctggggagtacggccgcaaggttaaaactca
aatgaattgacgggggcccgcacaagcggtggagcatgtggtttaaagggctacacacgt
gctacaatggtcggtacaaagggttgccaagccgcgaggtggagctaatcccataaaacc
gatcgtagtccggatcgcagtctgcaactcgactgcgtgaagtcggaatcgctagtaatc
gtgaatcagaatgtcacggtgaatacgttcccgggccttgtacacaccgcccgtcacacc
atgggagtgggttgctccagaagtagctagtctaaccgcaaggggacggttaccacgga
gtgattcatgactggggtgaagtcgtaacaaggtagccgtaggggaacctgcggctggat
cacct

Figure 4-54-5 Multifasta files containing the 16S rRNA sequences per strain.

A) The full length 16S rRNA sequence (NH: all four 16S, SCV: 1st, 2nd and 4th 16S)

B) in the SCVs both 16S with the locus_tag 4870 are identically truncated as shown above.

Prediction of rRNA secondary structure of the truncated sequences of the SCVs using RNAfold indicates that the truncated rRNA species does not adopt a fold similar to the wild-type rRNA (Figure 4-5).

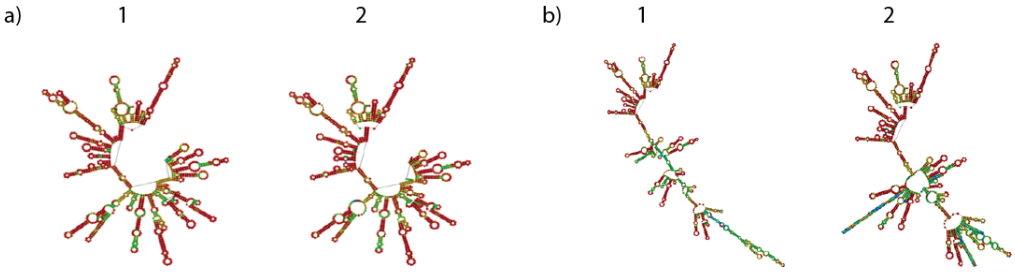

Figure 4-64-6. Detailed secondary structure models of the rRNA molecules.
a) 1 and 2 represent the 2 16S rRNA from the NH strain, b) 1 and 2 represent the 2 16S rRNA from the SCV. This analysis was performed using RNAfold.

There were no further differences in the number of protein coding genes (5619), rRNAs (12) or tRNAs (57) between SCVs and the parent strain. No SNPs could be identified in protein coding genes. Interestingly, comparison of the SCVJan and SCVFeb genomes with that of an SCV (SCV20265) isolated from a CF patient[181], which has recently been sequenced by PacBio sequencing, revealed an almost identical chromosomal inversion. However, in the case of SCV20265 the inversion was not accompanied by truncation of the 16S rRNA gene in the third rRNA operon (Figure 4-3).

4.2.4 Methylation differences between the SCV and NH strains are not observed

Epigenetic modifications affect a broad range of biological processes including gene expression, host-pathogen interactions, DNA damage and repair, environmental response and the inheritance of traits from one generation to another[318]. Changes in gene expression are known to occur through epigenetic modifications, with DNA methylation and histone modification being the most studied of these changes[233,319–321]. Gene expression can be controlled through the action of repressor proteins that attach to silencer regions of the DNA. These epigenetic changes can be controlled through the action of repressor proteins which attach to silencer regions of DNA. Recent work has also shown that adaptive antibiotic resistance in bacteria requires epigenetic inheritance and heterogeneity of gene expression patterns associated with the production of porins and efflux pumps[320].

Epigenetic changes do not affect the structure of the DNA or the nucleotide sequence and therefore are not identified using most NGS technology. To date, detection of modified bases has not routinely been a component of sequence analyses and it has posed significant technical challenges. Single Molecule, Real Time (SMRT) Sequencing directly detects epigenetic modifications by measuring kinetic variation during base incorporation. Using the PacBio SMRT portal software, we analysed the sequence data using the modification and motif protocol for any evidence of DNA modification which is shown below in Figure 4.6. This analysis compares the modification signal to an additional computational model for three modification types: 6-mA, 4-mC and Tet-converted 5mC. Coverage requirements vary with modification type, due to differences in their kinetic signatures, specifically detection of native 5-mC requires higher coverage to achieve reliable detection. There was no evidence of any methylation differences between SCVJan, SCVFeb or the parent strain NH. Modified bases would be represented as a distinct red cloud outwith the normal curve seen in the figure 4-6 below.

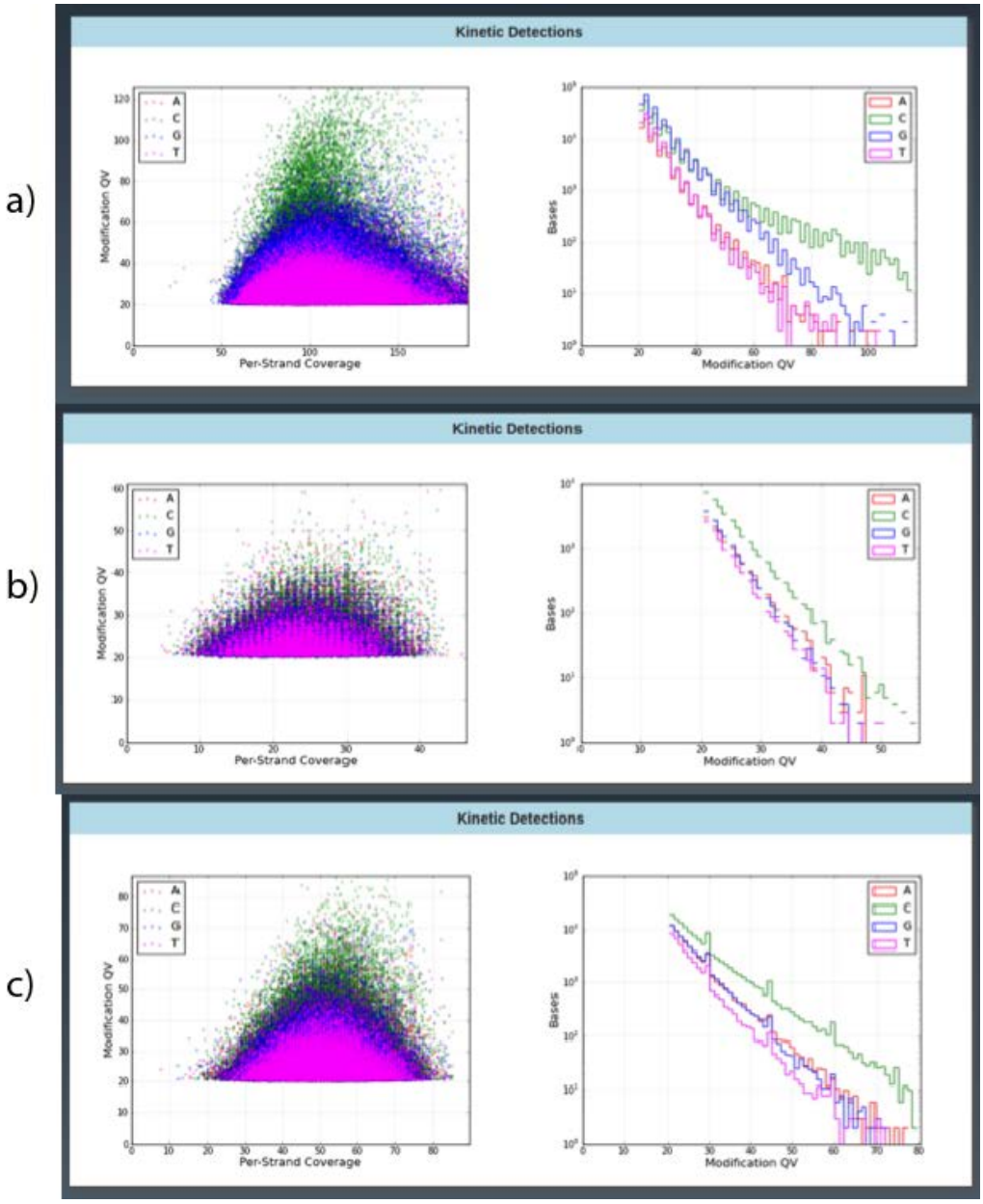

Figure 4-74-7. Methylation profiles of a) NH, b) SCVJan and c) SCVFeb.

Analysis was performed using the PacBio software. Using the PacBio SMRT portal software, we analysed the sequence data using the modification and motif protocol for any evidence of DNA modification. This analysis compares the modification signal to an additional computational model for three modification types: 6-mA, 4-mC and Tet-converted 5mC. Coverage requirements vary with modification type, due to differences in their kinetic signatures, specifically detection of native 5-mC requires higher coverage to achieve reliable detection.

4.3 Discussion

Previous studies aiming to identify the genetic basis for SCV conversion and phenotypic variation have suggested a range of SNPs and specific metabolic pathways may be involved in this phenotypic change. However, there is little consistency in the literature and specific genetic changes associated with conversion to the SCV phenotype during infection remain to be established [47,164,183,184,293,313]. Several studies have suggested the SCV phenotype may be the result of either thymidine auxotrophy caused by mutations in the thymidylate synthase gene[322] or an interruption in the electron transport chain, specifically resulting from an absence of menadione or hemin biosynthesis and metabolism[173,322]. Given the consistent phenotype seen in the SCVs between different bacterial strains and the recent identification of a genome inversion as the genetic basis for SCV conversion in an S. aureus strain[184], it would seem plausible that genome rearrangements may be a common mechanism of SCV conversion.

A key strength of our study was the availability of the parent strain used to establish infection for sequencing. This allowed a meaningful comparative genetic analysis to be performed enabling the determination the genetic basis of conversion to the SCV phenotype. Surprisingly, SNPs and INDELs were not identified in the SCV genome by Illumina sequencing and single-molecule real-time sequencing was subsequently used to show that the two sequenced SCVs carried a large genomic inversion within 16S rRNA genes. Genome rearrangements are known to have a profound effect on the organismal phenotype, affect gene expression and can result in loss of gene function when a rearrangement breakpoint occurs inside a reading frame[21,310]. *P. aeruginosa* is well known for its ability to alter the size and structure of its genome and although it possesses a relatively conserved core genome, insertions and deletions result in genomes ranging from 5.2 Mb to 7 Mb dramatically diversifying the genetic capacity of this species[323,324]. A number of studies have shown that a high proportion of CF P. aeruginosa isolates contain large chromosomal inversions[310,325], which may be selected for in that specific ecological niche as the resulting phenotype has features allowing it to survive in the environment of the chronically infected lung.

Appropriate maturation and folding of the 16S rRNA during 30S subunit biogenesis is known to be vital for translational fidelity[326–328]. The truncated genomes observed on analysis revealed a 250 bp shortened 16S rRNA gene ($16S_t$) in both SCV strains, which is reflected in the reduced genome sizes of the SCVs (SCVJan 6,213,026, SCVFeb 6,213,029) compared to the parent strain. This may partially explain the differences seen in gene expression as compared to the mucoid strain. This truncation may also explain why the SCV phenotypes in the strains isolated are stable, with no reversion back to the wild type strain from this in vivo experiment.

Although no methylation changes between the SCV and NH strain were observed, there are other epigenetic changes which could be responsible in part for the genome inversion and the phenotypic switch. Epigenetic changes represent heritable changes in gene expression without a change in the DNA sequence. Recently additional complexity was added to the epigenetic landscape by the discovery of a crucial role of small RNAs, non-coding RNAs, microRNAs and RNA-binding proteins in dynamic changes of the chromatin structure and spatial organisation of the genome inside the nucleus[329–332].

4.4 Conclusions and future work

The mechanistic details of how the observed genomic inversion lead to the coordinated expression changes observed here is currently not known, but the observation that a clinical SCV strain (SCV20265) obtained from the lung of a CF patient strain recently sequenced using the same strategy of combining SMRT and Illumina sequencing possesses a similar 16S rRNA based inversion, indicates that this inversion may be a clinically relevant route to the SCV phenotype (Figure 4-3). Other large scale genome rearrangements including large chromosomal inversions have previously been described in *P. aeruginosa* but these were not associated with conversion to the SCV phenotype. A reversible genomic inversion has also recently been shown to mediate the reversible conversion between normal colony and SCV phenotypes in *S. aureus*. However, in the case of the SCVs isolated in our work the SCV phenotype is stable and revertants to the parent phenotype were not observed.

In conclusion, we have shown here a *P. aeruginosa* SCV has originated in the lungs of an animal with chronic colonization with this microbe and that the observed phenotype would appear to result from a large chromosomal inversion. SCVs have a clear selective advantage in the context of the CF lung, and a better understanding of the drivers that produce the genomic rearrangement observed in this study may provide alternative therapeutic approaches to prevent the appearance of such damaging phenotypic variants.

Chapter 5 Transcriptomic Characterisation

5.1 Introduction

5.1.1 Transcriptomic adaptations during chronic infection

The versatility of *P. aeruginosa* in adapting to a wide range of environments including that of the human body is attributed to a large genomic repertoire consisting of an extremely diverse set of genes which encode metabolic functions suited for proliferation in environments with a wide range of available nutrients[19,223,333]. Rapid adaptations to changing environments by bacteria is accompanied by reprogramming of their regulatory networks to activate the expression of genes essential for their survival in the new environment while repressing those that are unnecessary or potentially deleterious. At the transcriptional level, this can be achieved by responding to various environmental cues that are often mediated by specific signal transduction pathways. A number of new regulatory mechanisms have been uncovered based on the activities of non-coding RNA[239,334,335]. Riboregulation, or RNA-based regulation is now recognised as an important mechanism for control of gene expression as it enables alteration of the translation of mRNA and transcript turnover[336,337].

There have been recent advances in sequencing technology allowing more accurate quantification of RNA levels in bacteria (RNA-seq) providing significant advances over the previous microarrays[338,339]. High throughput sequencing of cDNA libraries has the potential to study transcription at the single nucleotide level and therefore yield more detail on RNA transcripts present in a population of microbial cells. It does, however, remain a challenge as compared to eukaryotic mRNA, since bacterial mRNAs do not have a poly-A tail and hence cannot be isolated from other RNA sources by hybridisation to immobilised poly-T[236]. In addition, bacterial RNA samples usually contain up to 80% rRNA and tRNA and the residual mRNA component has a very short half-life and is hence unstable[340]. A further limitation of these studies is that the sequencing technologies employed to date are unable to distinguish between *de novo* transcription and post-transcriptional events as they only record the levels of RNA (cDNA) present, a weakness shared with microarray technology. Removal of the rRNA and tRNA may have an unknown adverse effect on the composition of the total RNA fraction and results in a biased cDNA library. During the construction of the cDNA libraries steps include amplification of the cDNA and hence there is the potential to introduce an over-representation of shorter transcripts in the libraries constructed for sequencing.

During chronic CF infection, *P. aeruginosa* strains often acquire mutations which cause them to undergo a phenotypic switch from a non-mucoid strain to a mucoid strain. The resulting production of alginate aids the organism in the evasion of phagocytosis and in resistance to neutrophils and macrophages and also antibiotic resistance[107,289]. One major regulator of alginate biosynthesis is the transcriptional regulator AlgR which belongs to the two-component signalling system superfamily. AlgR regulates various virulence factors including twitching motility, biofilm formation, quorum sensing and hydrogen cyanide production[62,226,341]. On the other hand, studies have shown that the SCV is implicated in increased mortality and morbidity in CF patients due to the increased persistence potential. It would seem that SCVs are selected for during the course of chronic infection due to a fitness advantage in this unique environment. Several studies have focused on the link to the second messenger cyclic-di-GMP (c-di-GMP) related system and the association that elevated levels are associated with a sessile and cooperative lifestyle[59,287,313]. On the contrary, low levels of c-di-GMP promote a unicellular, free-swimming lifestyle. The c-di-GMP system is controlled by activation of the YfiBNR regulatory system[182,313] therefore it would be interesting to compare the transcriptome between the two phenotypically different strains in this study to establish whether these previously investigated pathways are upregulated in this phenotypic switch. Biofilm formation is also previously described in the literature to be under the control of the LasR-Lasl and RhlR-Rhll cell density quorum sensing (QS) systems and a large number of the two-component regulatory systems[38,342,343].

In this study we have shown that in fact the SCV phenotype is likely to play a major role in the disease process in CF patients as relative to the parent strain isolated SCVs show increased cytotoxicity towards epithelial cells and display increased antibiotic resistance in the biofilm state. The mechanism behind the switch to this SCV phenotype would potentially enable us to develop novel therapies to target these virulent phenotypes.

In this chapter we compare the global transcriptome of the two SCV strains with the NH mucoid strain in an attempt to elucidate a mechanism behind the phenotypic switch.

5.2 Results

5.2.1 Over 554 genes are differentially expressed between the SCV and NH phenotypes

To determine the transcriptional changes associated with conversion to the SCV phenotype, we performed RNA sequencing (RNA-Seq) analysis of the parent strain, NH, and two SCV strains (SCVJan and SCVFeb isolated from independent *in vivo* experiments) grown in LB broth. RNA-Seq data for all strains was collected in triplicate and data for SCVJan and SCVFeb were combined to compare with NHMuc. Prior to transcriptome analysis, quality control of the total reads was performed on CLC Workbench to ensure comparable read coverage between strains. Figure 5-1 outlines the total read coverage following total RNA sequencing of the different strains, with an average of 18 million reads in certain parts of the genome in all strains apart from slightly lower values of 10 million in SCVFeb. It can also be clearly visualised that the gene expression differs significantly between the SCV and NH strains, with increased expression across the genome in the NH strain.

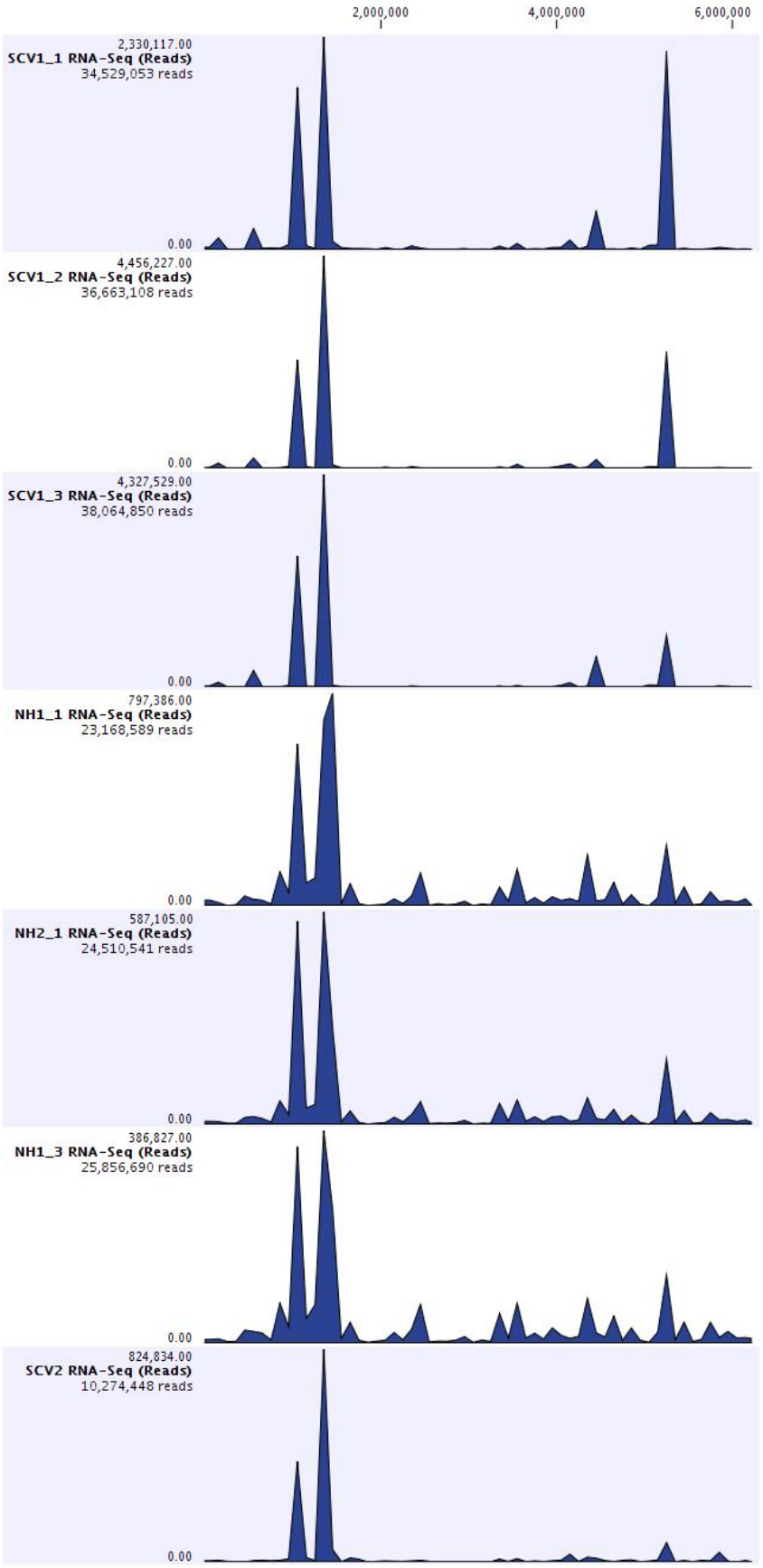

Figure 5-15-1. Transcriptome read coverage

Comparison of transcriptome reads data and coverage across entire genome between NH, SCV1 and SCV 2. Results show a similar coverage pattern between both SCVs in comparison to NH.

The Volcano plot in Figure 5-2 demonstrates global increase in total gene expression in the NH strain as compared to the SCV.

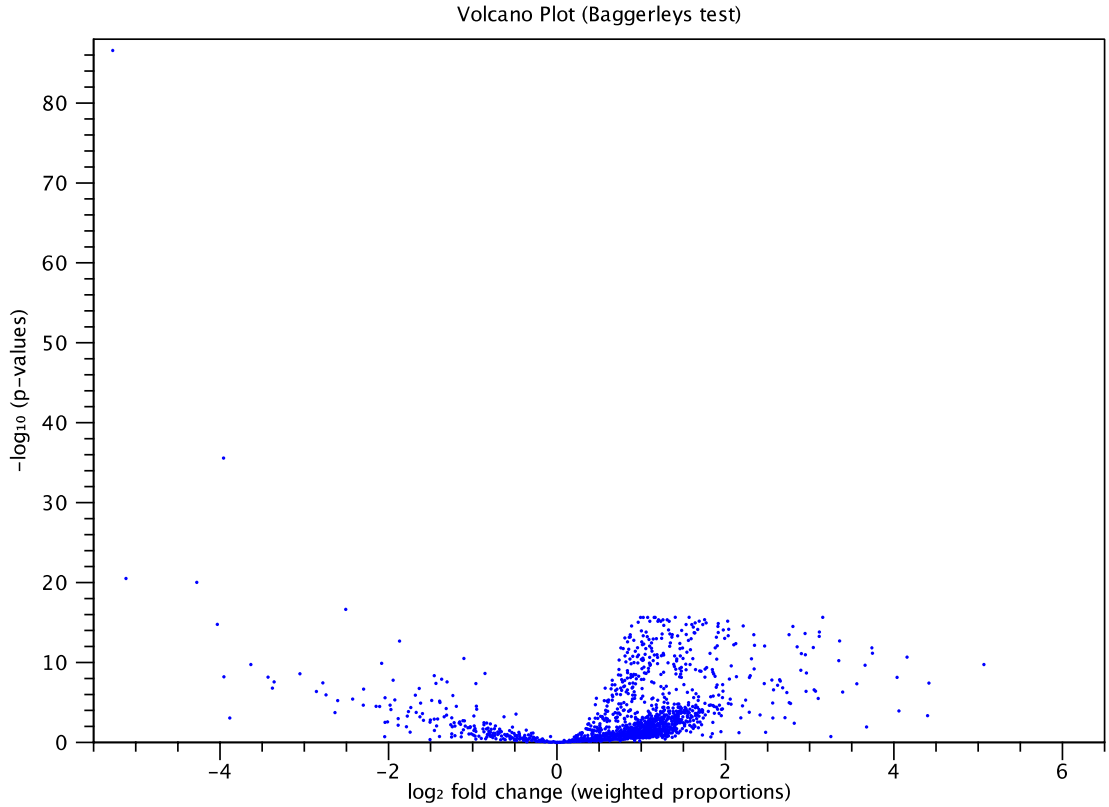

Figure 5-25-2. Volcano plot of SCV versus NH transcriptome data

Differential gene expression between SCV and NH strains. Gene expression is upregulated in NH compared to SCV.

The box plots in Figure 5-3 display an overall gene expression value following statistical correction. The expression values all follow a similar distribution which allows for accurate data interpretation and analysis.

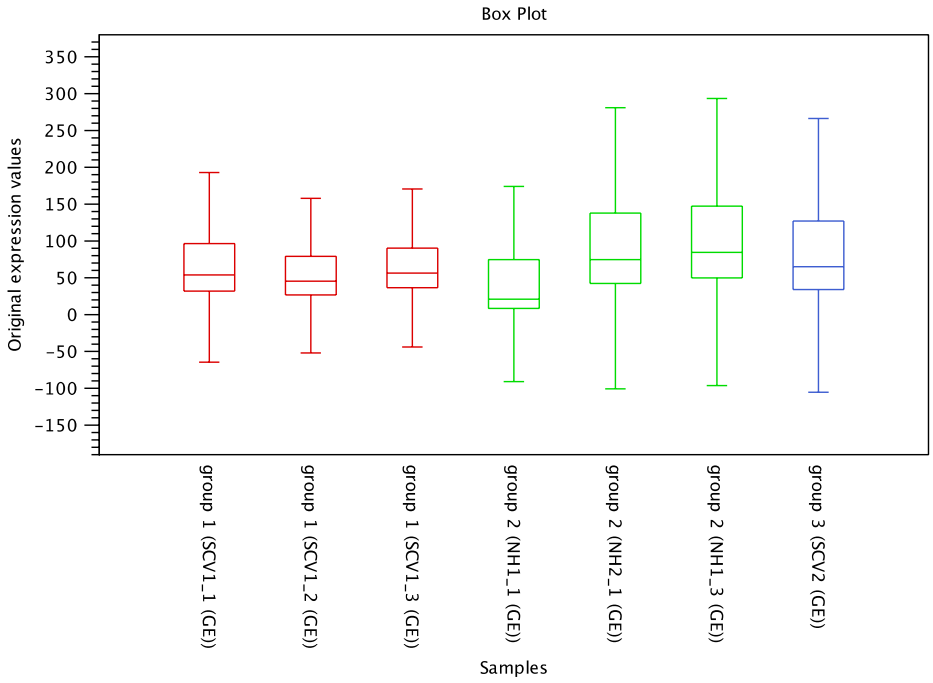

Figure 5-35-3. Box plot of original gene expression values

Total gene expression for SCV1 (SCVJan), SCV2 (SCVFeb), and NH. Similar levels observed in the box plot ensure adequate read coverage prior to analysis.

In order for a gene to be classified as differentially expressed, two criteria had to be fulfilled: the average change in expression (n-fold) must be >2 and the P value must be <0.05 (one-way analysis of variance). Relative to NHMuc, 190 genes showed >2-fold upregulation and 364 genes showed >2-fold downregulation in SCVJan/SCVFeb.

5.2.2 Differential expression of genes revealed downregulation of genes involved in growth and metabolism whereas genes involved in oxidative stress and iron acquisition were upregulated

Major functional classes of genes downregulated in SCVJan/SCVFeb include those involved in energy metabolism, amino acid and protein biosynthesis, DNA replication and recombination and cell wall/LPS/capsule biosynthesis, which together are consistent with the slow growth rate observed for SCVs (Figure 5-4). Notably, genes encoding heat shock proteins and other molecular chaperones (IbpA, GrpE, HtpG, ClpB, DnaK, GroES, DnaJ and ClpX) are highly represented among the most strongly downregulated genes in the SCVs (Table 5-2).

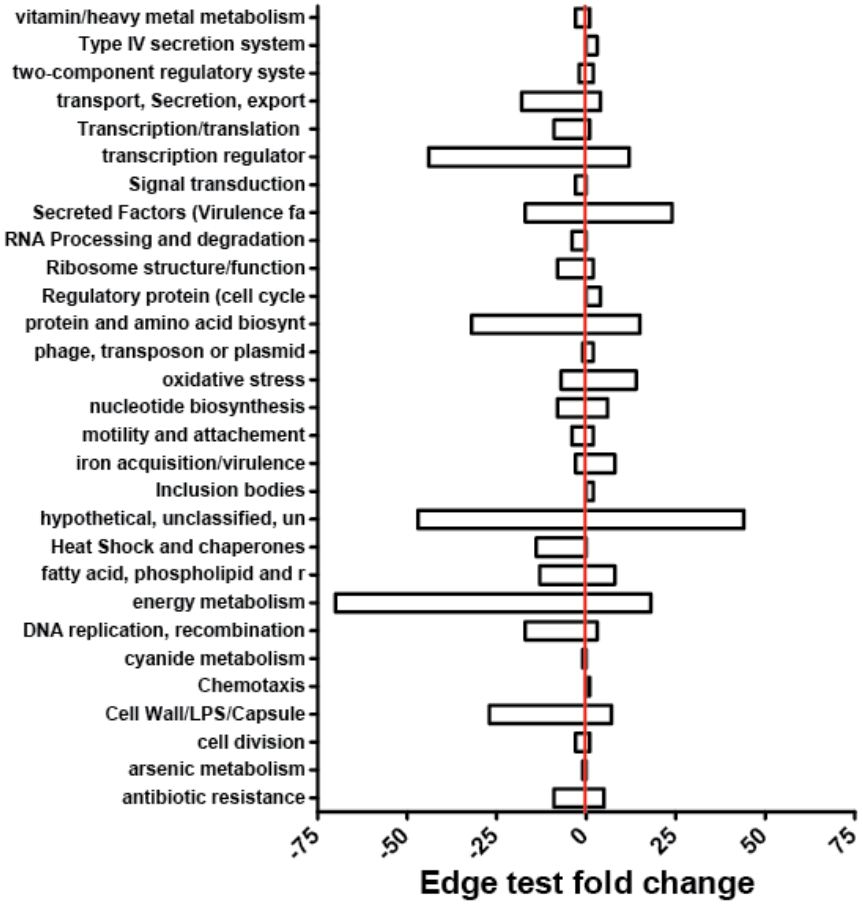

Figure 5-45-4 Function classification of genes differentially regulated in SCV relative to NH
An EDGE test was performed using CLC Software and the differentially expressed groups organised into functional categories. Groups with a positive EDGE test fold change are those which are upregulated in the SCVs. Groups with a negative EDGE test fold change are downregulated in SCVs relative to NH.

Conversely, genes that function in the response to oxidative stress and those that encode secreted virulence factors are largely upregulated in SCVJan/SCVFeb. Indeed, five of the ten most highly upregulated genes in SCVJan/SCVFeb are those associated with the response to oxidative stress (Table 5-1). Highly upregulated oxidative stress genes include, *katA*[344] which encodes the major catalase of *P. aeruginosa*, *ahpB*, *ahpC* and *ahpF*[304,345,346], which encode subunits of alkyl hydroperoxide reductase and *trxB2* that encodes thioredoxin reductase 2[192,347,348]. Consistent with the observed transcriptional changes, catalase activity was strongly increased in SCVJan relative to NH (Figure 3-10a).

Genes encoding a number of secreted virulence factors such as the proteases LasA, LasB and AprA, the fructose-binding lectin LecB[349] and the chitin binding protein CbpD and chitinase ChiC[350] were also highly upregulated. Similarly genes encoding hydrogen cyanide synthase and a number of enzymes that function in phenazine biosynthesis are also upregulated (Table 5-1)[50,60,104,106,293,351]. Phenazines have previously been shown to enhance killing of *Caenorhabditis elegans* by *P. aeruginosa*[352]. The apparent increase in the production of virulence factors by SCVJan/SCVFeb relative to NH suggests increased virulence of the SCV. To directly test this we used an infection model based on infection of the murine macrophage cell line J774A.1. Cell death of J774A.1 through LDH release was measured at 4 and 10 hours post infection with NH and SCVJan. At 4 hours, levels of LDH release were similar for NH and SCVJan, whereas at 10 hours LDH release was significantly increased for SCVJan; 96% vs 38%, $p < 0.0001$ (Figure 3-10b).

To determine if the increased virulence of the SCV observed against a murine cell line translated to increased virulence in an animal model of infection, we utilised an invertebrate model of infection utilising the larva of the wax moth *Galleria mellonella*. Similar to the macrophage infection assay, SCVJan displayed increased virulence in the *G. mellonella* infection model. Mortality of larvae was measured at 24, 48 and 72 hours post infection. No significant differences in mortality were detected at 24 or 48 hours, whereas at 72 hours % mortality was 86% and 63% ($p < 0.01$) for SCVJan and NH infected larvae, respectively (Figure 3-10c). Data from both infection models shows that SCVJan shows increased virulence, relative to NHMuc, which is consistent with the phenotype of SCVs obtained from the human host.[156,296]

Table 5-1 Top 35 representative genes upregulated in SCV versus NH

Feature/gene ID[a]	Fold Change[b]	P-Value[c]	Protein description and/or interspecies homology
NHmuc_04720	62	3.24 -16	hypothetical protein
trxB2	55	3.9 8-16	thioredoxin reductase 2
NHmuc_01300	35	3.74 -15	putative alkyl hydroperoxide reductase
NHmuc_02350	28	1.36 -26	putative acyl carrier protein
ahpF	28	8.39 -13	alkyl hydroperoxide reductase subunit F
kata	23	7.12 -10	catalase
NHmuc_03862	20	6.84 -21	putative ankyrin domain-containing protein
NHmuc_03863	19	1.81 -18	putative hydrolase
NHmuc_00257	19	1.36 -12	putative CBS domain protein
ahpC	18	8.97 -08	alkyl hydroperoxide reductase subunit C
chiC	17	1.45 -09	chitinase
NHmuc_04185	17	6.67 -06	RNA polymerase sigma factor RpoS
aprA	12	5.10 -08	alkaline metalloproteinase
NHmuc_04924	11	3.24 -16	CsbD family protein
NHmuc_04718	11	1.47 -11	hypothetical protein
NHmuc_04925	11	2.20 -08	transport-associated
NHmuc_00127	10	5.84 -07	putative hemolysin
Snr1	10	4.84 -07	cytochrome c Snr1
lecB	9	5.93 -08	fucose-binding lectin PA-IIL
NHmuc_03413	8	9.13 -15	Phage terminase, small subunit
katB	8	9.04 -15	catalase
NHmuc_04074	8	9.04 -06	leucyl-tRNA synthetase
phzG2_2	7	2.23 -12	pyridoxamine 5'-phosphate oxidase
NHmuc_03358	7	3.34 -06	putative protein associated with synthesis and assembly of refractile inclusion bodies
phzE1_1	7	3.15 -06	phenazine biosynthesis protein PhzE
NHmuc_00055	7	6.09 -07	hypothetical protein
NHmuc_01628	7	1.29 -08	hypothetical protein
cbpD	7	4.11 -06	chitin-binding protein CbpD
NHmuc_00546	6	0.0020	LysR transcriptional regulator
rhlR	6	0.0001	transcriptional regulator RhlR
gcdH	6	4.26 -05	glutaryl-CoA dehydrogenase
NHmuc_01422	6	0.0004	putative dna-binding stress protein
NHmuc_04078	6	1.51 -10	oxidoreductase probably involved in sulfite reduction
rsaL	6	0.01	regulatory protein RsaL

a See appendix for corresponding PAO1 feature ID/gene ID

b The magnitude of gene expression (fold change) was determined by comparing transcription in three replicates of NH with that in three replicates each of the two SCV strains.

c P values were assessed by performing an EDGE test using CLC software

Table 4-2 Top 35 representative genes downregulated in SCV versus NH

Feature/gene ID[a]	Fold Change[b]	P-Value[c]	Protein description and/or interspecies homology
NHmuc_01025	-75	2.59 -11	putative acetyltransferase
mexC	-53	1.07 -11	Resistance-Nodulation-Cell Division (RND) multidrug efflux membrane fusion protein MexC precursor
ibpA	-31	1.09 -07	heat-shock protein IbpA
algD	-30	1.01 -09	GDP-mannose 6-dehydrogenase AlgD
NHmuc_05385	-29	8.47 -08	17 kDa surface antigen
NHmuc_04138	-29	1.25 -10	periplasmic metal-binding protein
grpE	-25	1.22 -07	heat shock protein GrpE
htpG	-23	3.58 -07	heat shock protein 90
NHmuc_0100	-22	1.76 -05	hypothetical, unclassified, unknown
clpB	-20	6.45 -06	ClpB protein
nfxB	-20	3.72 -07	transcriptional regulator NfxB
fsxA	-18	7.85 -08	FxsA protein
NHmuc_04950	-17	3.34 -06	molecular chaperone DnaK
NHmuc_05744	-17	5.76 -05	putative lipoprotein
dapB	-17	2.75 -06	dihydrodipicolinate reductase
hslV	-17	4.13 -07	ATP-dependent protease peptidase subunit
NHmuc_01173	-16	4.70 -06	hypothetical protein
NHmuc_01024	-16	6.05 -07	putative transporter
NHmuc_04180	-16	3.30 -06	recombinase A
mexD	-15	9.52 -07	Resistance-Nodulation-Cell Division (RND) multidrug efflux transporter MexD
NHmuc_04776	-15	6.06 -06	PAS/PAC sensor signal transduction histidine kinase
rsmA	-14	0.0007	carbon storage regulator
NHmuc_01174	-14	3.26 -07	hypothetical protein
NHmuc_01594	-13	2.08 -05	putative oxidoreductase
mucA	-12	7.40 -05	anti-sigma factor MucA
NHmuc_03262	-12	2.48 -09	hypothetical protein
NHmuc_04386	-12	6.83 -05	Surface antigen
amrZ	-12	3.01 -05	alginate and motility regulator Z
glnA	-12	5.84 -06	glutamine synthetase
groES	-12	3.92 -05	co-chaperonin GroES
dnaJ	-12	7.54 -05	chaperone protein DnaJ
algU	-11	0.00002	RNA polymerase sigma factor AlgU
clpX	-11	0.00004	ATP-dependent protease ATP-binding subunit ClpX
NHmuc_04521	-10	1.92 -06	periplasmic ligand-binding sensor protein

a See appendix for corresponding PAO1 feature ID/gene ID

b The magnitude of gene expression (fold change) was determined by comparing transcription in three replicates of NH with that in three replicates each of the two SCV strains.

c P values were assessed by performing an EDGE test using CLC software

In an attempt to establish whether the large genomic inversion in the SCVs resulted in any local effects on gene expression close to the inversion site, a map of the genome with corresponding gene expression levels was constructed as shown in figure 5-5. This failed to identify any specific local effects on gene expression at the inversion site and instead demonstrated that differentially expressed genes are distributed relatively evenly throughout the genome indicating that global changes in gene transcription are responsible for conversion to the SCV phenotype.

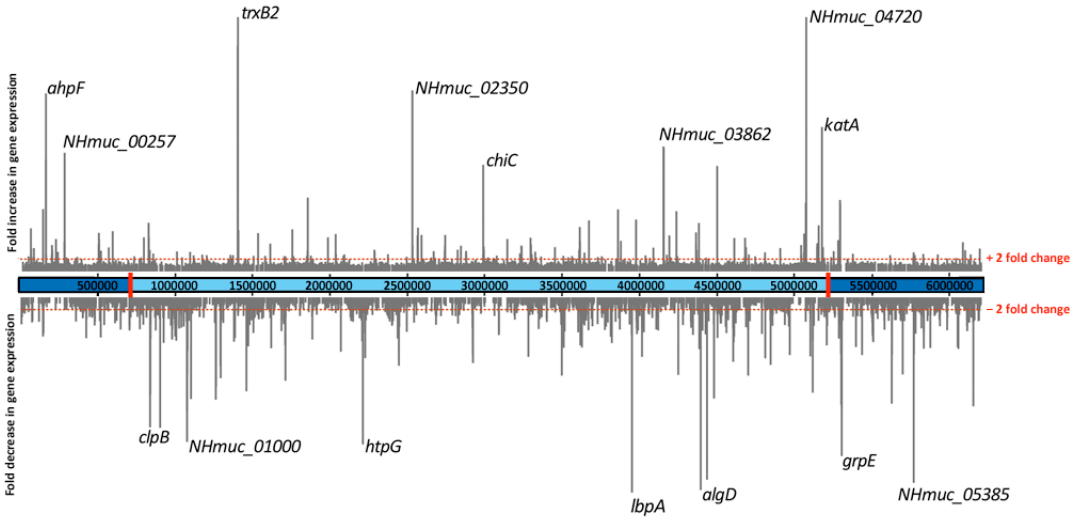

Figure 5-55-5 Global changes in gene transcription on conversion to the SCV phenotype. Fold-changes in gene expression for SCVJan/Feb relative to NHMuc are shown in the context of the NHMuc genome. Breakpoints that define the genomic inversion present in SCVJan and SCVFeb are indicated by red rectangles.

5.3 Discussion

In this study we demonstrate that the differential gene expression of a naturally occurring SCV from a mouse model in comparison with its wild type counterpart correlates with several other studies[156,246] which also found that functional properties such as iron uptake, resistance against oxidative stress, cytotoxicity and reduced growth are all upregulated on conversion to the SCV phenotype.

SCVs for many bacteria are well known for adopting a slow-growing phenotype which has altered carbon metabolism, antibiotic resistance and increased intracellular persistence[176,287]. Persister cells are able to enter a dormant state making them almost refractory to the effects of the immune system and antibiotics[66,229,281,282]. Genes involved in energy metabolism, growth, replication and recombination and cell biosynthesis were all downregulated in both SCV isolates which together are consistent with the slow growth rate observed for SCVs.

This slow growth rate, and lack of protein production and defective ribosomes seen in the SCV phenotype would also account for the genes encoding heat shock proteins and other molecular chaperones (IbpA, GrpE, HtpG, ClpB, DnaK, GroES, DnaJ and ClpX) being amongst the most highly downregulated genes in the SCV. The ability of bacteria to rapidly adapt to changes in their environment is essential for survival and they have evolved complex regulatory circuits to induce the synthesis of heat shock proteins after a sudden increase in ambient temperatures. The principle function of these heat shock proteins is to assist in protein folding, assembly, transport and degradation during normal growth[353].

Several studies have suggested that exposure of bacteria to sublethal concentrations of hydrogen peroxide can lead to formation of SCV's via a mutagenic DNA repair pathway and enhancing the size of the SCV population[192,222,354]. Responses to oxidative stress involve complex mechanisms which include alterations in gene expression patterns and the activation of a cascade of enzymes which prevent ROS accumulation. Genes that function in the response to oxidative stress and those that encode secreted virulence factors are largely upregulated in the SCV in this study. Five of the ten most highly upregulated genes in the SCV are those associated with the response to oxidative stress. Highly upregulated oxidative stress genes include, *katA*[344] which encodes the major catalase of *P.*

aeruginosa, *ahpB*, *ahpC* and *ahpF*[304,345,346], which encode subunits of alkyl hydroperoxide reductase and *trxB2* that encodes thioredoxin reductase 2[192,347,348]. *S. aureus* is also known to utilise a number of defence molecules including catalase (KatA) to combat reactive oxygen species[354]. Consistent with the observed transcriptional changes, catalase activity was strongly increased in SCV relative to NHMuc**.** It has been proposed that bactericidal antibiotics can induce cell death through a common oxidative damage mechanism that relies on the production of ROS. Antibiotics are able to activate cellular respiration, leading to superoxide formation and release of iron. Iron is then able to activate a chemical reaction to produce ROS in the form of hydroxyl radicals which can damage proteins, lipids and DNA[188,240,241]. Bacteria are able to protect themselves from ROS by upregulating anti-oxidant molecules therefore there is potential to target these bacterial defence mechanisms as means of enhancing killing efficacy of bactericidal agents.

One of the most important micronutrients for bacterial growth is iron, which is an important cofactor playing an essential role in many cellular processes. Bacteria employ a wide variety of mechanisms to regulate intracellular iron concentrations preventing the toxic effects and also sequestration through the production and secretion of siderophores[247,302,303]. In this study, there are a number of genes involved in iron acquisition upregulated in the SCV as compared to the mucoid strain including *hemH*, *feoC*, *napF*, *ccmH* and *cycH*. These all enable the SCV to persist within a more hostile environment, with a slower growth rate and conserving vital nutrients. There have been numerous studies investigating the effect of iron limitation on the global gene expression in *P. aeruginosa* showing differential expression of over 554 genes[247,355]. Certain genes have further been implicated as part of the regulon involved in the iron response, including those coding for siderophore receptors, iron transport, regulators, sensors and sigma factors[239,246].

Previous studies have suggested that SCVs are typically less virulent due to their slower growth and reduced expression of virulence factors however the SCVs isolated in this study reveal increased virulence as seen in chapter 3 which is also reflected in the transcriptome results. Genes encoding a number of secreted virulence factors such as the proteases LasA, LasB and AprA, the frucose-binding lectin LecB[349] and the chitin binding protein CbpD and chitinase ChiC[350] were also highly upregulated. Similarly genes encoding hydrogen cyanide synthase and a number of enzymes that function in phenazine biosynthesis are also upregulated[50,60,104,106,293,351]. Phenazines have previously been shown

to enhance killing of *Caenorhabditis elegans* by *P. aeruginosa*[352] and are well characterized virulence factors. Phenazines are nitrogen containing secondary metabolites that serve as signalling molecules influencing gene expression during environmental adaptations and biofilm formation. They are capable of producing ROS toxic to eukaryotic cells and other bacteria[60,106]. The apparent increase in the production of virulence factors by SCVJan/SCVFeb relative to NHMuc suggests increased virulence of the SCV. To directly test this we used an infection model based on infection of the murine macrophage cell line J774A.1. Cell death of J774A.1 through LDH release was measured at 4 and 10 hours post infection with NHMuc and SCVJan. At 4 hours, levels of LDH release were similar for NHMuc and SCVJan, whereas at 10 hours LDH release was significantly increased for SCVJan; 96% vs 38%, $p < 0.0001$.

To determine if the increased virulence of the SCV observed against a murine cell line translated to increased virulence in an animal model of infection, we utilised an invertebrate model of infection utilising the larva of the wax moth *Galleria mellonella*. Similar to the macrophage infection assay, SCVJan displayed increased virulence in the *G. mellonella* infection model. Mortality of larvae was measured at 24, 48 and 72 hours post infection. No significant differences in mortality were detected at 24 or 48 hours, whereas at 72 hours % mortality was 86% and 63% ($p < 0.01$) for SCVJan and NHMuc infected larvae, respectively. Data from both infection models shows that SCVJan shows increased virulence, relative to NHMuc, which is consistent with the phenotype of SCVs obtained from the human host.[156,296]

5.4 Conclusion and future work

From the results in this chapter we can conclude that it is likely that the large genome inversion found in the isolated SCVs results in a global change in gene transcription. We are unsure as to exactly how this has occurred or to what extent different transcriptional regulators are involved. RsmA has been previously described as a small post-transcriptional regulatory protein which controls the expression of many virulence genes and QS signalling molecule synthesis and a global transcriptional regulator[35,39,356]. In this study, the expression of RsmA is markedly downregulated in the SCV which may account for the global reduction in gene expression in this phenotype.

Collectively, the phenotypic data in combination with the whole genome analysis and transcriptome data has allowed us to get an in depth correlation between phenotypic traits (antibiotic resistance, type III secretion expression, biofilm formation, cell cytotoxicity) and gene expression data. Given the large genome rearrangement and the resultant gross phenotypic change with altered gene expression, it would appear the change in orientation of part of the genome functions as a 'switch' for gene expression and control.

Further work is required to produce a high-resolution transcriptome map with detailed operon organisation, coding and non-coding transcripts and their sites of transcription initiation to further establish the effects of the inversion on the control of major transcriptional regulators. Identification and characterisation of essential genes for the establishment and/or maintenance of chronic infection may be the basis to elaborate novel and effective antimicrobials against bacteria, especially if these are conserved genes between different bacterial species.

Chapter 6 Optimisation of RNA extraction from CF sputum samples

6.1 Introduction

The cystic fibrosis (CF) lung provides a well characterised and clinically relevant environment to study bacterial transcriptional responses to antibiotic challenge. CF patients are peculiarly susceptible to infection with the Gram-negative bacterium *Pseudomonas aeruginosa* and chronic infection with this opportunistic pathogen can lead to progressive lung damage and ultimately respiratory failure. *P. aeruginosa* has a large genome, with 6.26 million base pairs, comprising almost 90 percent protein coding genes[19]. The large genome size at least partly explains the ability of *P. aeruginosa* to adapt and thrive in a wide range of diverse environments. Initially, during teenage years, CF patients show transient colonization with *P. aeruginosa* that can be cleared by antibiotic therapy. However, as the disease develops, chronic colonization occurs in about 80% of patients that cannot be eradicated by antibiotics. Frequent respiratory exacerbations occur in association with chronic colonization and although these may respond to anti-pseudomonal treatment, increasing levels of multidrug resistance present a considerable therapeutic challenge. Such patients are maintained on regular inhaled antibiotics and receive intravenous treatment for exacerbations. Resistance rates of *P. aeruginosa* strains from CF patients are significantly higher than those from non-CF patients which is a direct consequence of the extensive use of antibiotics in this patient group and the consequent selective pressure for the development of resistance.

Recent years have witnessed a revolution in the field of bacterial transcriptomics, starting with the development of DNA microarrays, which provides a tool to globally quantify gene expression. In 2008, RNA-Seq was introduced, which involves deep sequencing of cDNA generated from RNA preparations and has overcome some of the drawbacks of microarrays: providing single-base resolution and improved signal to noise ratio owing to a reduced background and a higher dynamic range[236,340].

Since mRNA has both a short half-life and makes up only a small fraction of the total RNA, one of the main hurdles in the use of these technologies remains the extraction of sufficient bacterial mRNA to enable meaningful transcriptomic analysis. This may be particularly problematic when studying host-pathogen interactions using infection models or patient derived samples where the presence of host RNA and DNA is a complicating factor. In addition, mRNA enrichment is challenging in prokaryotes, as prokaryotic mRNA lacks the 3'-end poly (A) tail that marks mature mRNA in eukaryotes and

amplification of microbial RNA by methods that utilise synthetic polyadenylation is not applicable for samples containing large amounts of eukaryotic mRNA. A study by Wei Lim et al, published in July 2012 explored numerous different methods to successfully extract and purify RNA directly from a cystic fibrosis sputum sample[275]. They found that following RNA extraction and further rRNA depletion precluded subsequent rRNA-based analysis of the sample as there was bias and relative abundance of certain microbial taxa in the sample. In other published attempts to analyse microbial metatranscriptomics from infected animal tissues, the results highlighted the difficulty in obtaining meaningful microbial data. In a study by Wittekindt et al (2010), 99.3% of the taxonomically assigned reads were host derived and only <0.01% were of microbial origin[357].

The initial aim of the work described in this chapter was to optimise bacterial DNA and mRNA extraction from human CF sputum samples by implementing various methods of enrichment, targeting and depletion whilst minimizing contamination with host nucleic acid. In summary, the original aims were:

1. To optimize the recovery and sequencing of *P. aeruginosa* mRNA from patients chronically colonized with this microbe and to follow the stability of this transcriptional profile over time and in response to inhaled antibiotics.
2. To determine the transcriptional changes following antibiotic therapy in patients newly colonized with *Pseudomonas aeruginosa*.
3. To determine the transcriptional changes following antibiotic therapy in chronically colonized patients who are receiving intravenous antibiotics for a respiratory exacerbation.

6.2 Results

6.2.1 RNA extraction from CF sputum

In order to obtain samples for RNA extraction ten sputum samples were collected from five CF volunteers (CF1 through to CF5) at the adult CF clinic (Gartnavel General Hospital, Glasgow) by expectoration into a sterile cup. All collection was in accordance with the University of Glasgow Ethics Committee Review panel, reference 13/WS/0051. Patient information sheets (Appendix A) and consent forms (Appendix B) were distributed as per policy. Each sample was from a patient who was known to be colonised with *P. aeruginosa*. Following collection, samples were immediately placed on ice to prevent RNA degradation. Each sample was syringe homogenised and divided into aliquots for transcriptomic analysis, culture and storage. Samples were then processed according to the protocol outlined in section 2.6.3.1.

Ideally, high quality transcriptomic data contain relatively few rRNA reads and an unbiased sampling of different RNAs. The initial amplification step during preparation of a cDNA sequencing library is, however, a potential source of transcript size induced bias. In addition, the sputum samples obtained were from patients undergoing an infective exacerbation, which reduces the chance of obtaining a high proportion of microbial RNA, given the large quantity of human immune and epithelial cells that are invariably present in such samples.

In order to begin to develop a method to extract high levels of total RNA from CF sputum samples, three commercially available RNA extraction kits were tested and the RNA yields compared. As shown in Table 6-1 a much greater RNA yield was obtained using the Zymo Clean and Concentrator method than either the Qiagen Saliva kit or the Ribo pure kit. One possible reason for the low yields obtained using the Qiagen Saliva kit and RiboPure kit is that the enzymatic sputum lysis stage may have been inadequate given the purulence of the sputum. Cystic fibrosis sputum samples, especially from patients undergoing an infective exacerbation have highly viscous sputum with a high proportion of human inflammatory cells and DNA[358]. Prior to the Zymo Clean and Concentrator spin column, the sputum was digested chemically using Trizol and the purulent nature with dense inflammatory cell infiltrates was physically disrupted using zirconia beads.

Table 6-1: Comparison of total RNA yield between Qiagen Saliva Kit, Ribo Pure and Zymo Clean and Concentrator.

Sample 1: RNA isolated directly from the cystic fibrosis sputum (CF1), Sample 2: RNA isolated from the sputum (CF1) inoculated into LB broth, Sample 3: RNA isolated directly from the cystic fibrosis sputum (CF2), Sample 4: RNA isolated from the sputum (CF2) inoculated into LB broth, Sample 5: RNA isolated directly from the cystic fibrosis sputum (CF3), Sample 6: RNA isolated from the sputum (CF3) inoculated into LB broth.

	Total RNA Yield µg		
Sample	**Qiagen Saliva Kit**	**Ribo Pure**	**Zymo Clean and Concentrator**
1	0.10	0.56	26.12
2	0.28	0.72	41.11
3	0.25	1.08	34.52
4	0.34	1.12	12.54
5	0.67	1.15	9.87
6	0.55	1.24	24.29

Having established that sufficiently high RNA yields could be obtained from CF sputum samples using the Zymo Clean and Concentrator kit, RNA purified by this method was treated in order to deplete rRNA levels. rRNA depletion is an essential step prior to sequencing as this makes up a significant proportion of the total RNA. Table 6-2 shows the total RNA yield of the extracted RNA before and after rRNA depletion. The ratio of absorbance at 260nm and 280nm is used to assess the purity (not quality) of both DNA and RNA. A ratio of ~1.8 is generally accepted as 'pure' for DNA and a ratio of ~2.0 is generally accepted as 'pure' for RNA. If the ratio is significantly lower in either case it may indicate the presence of protein, phenol or other contaminants that absorb strongly at 280nm. The A_{260}/A_{280} ratios are inadequate confirmation of quality prior to sequencing.

Table 6-2: RNA concentration before and after rRNA depletion using Epicentre Ribozero Epidemiology Kit. Sample 1: RNA isolated directly from the cystic fibrosis sputum (CF1), Sample 2: RNA isolated from the sputum (CF1) inoculated into LB broth, Sample 3: RNA isolated directly from the cystic fibrosis sputum (CF2), Sample 4: RNA isolated from the sputum (CF2) inoculated into LB broth, Sample 5: RNA isolated directly from the cystic fibrosis sputum (CF3), Sample 6: RNA isolated from the sputum (CF3) inoculated into LB broth.

	Before rRNA depletion		**After rRNA depletion**	
Sample	**Total RNA µg**	**A_{260}/A_{280}**	**Total RNA µg**	**A_{260}/A_{280}**
1	**26.15**	**1.93**	**1.59**	**1.71**
2	**41.11**	**1.59**	**0.29**	**1.56**
3	**10.08**	**2.08**	**0.71**	**0.47**
4	**10.50**	**2.09**	**0.78**	**1.71**
5	**8.38**	**2.08**	**0.36**	**1.75**
6	**8.25**	**2.01**	**0.44**	**1.89**

In an attempt to further enrich for microbial mRNA, different combinations of methods including Zymo Clean and Clear with Microbenrich, Ribozero then MEGAclear were tested to obtain optimum yields of microbial mRNA. MEGAclear is designed for final cleanup of RNA from any residual buffers, enzymes or other inhibitory factors. However, this was unfortunately found to reduce the final yield of purified RNA to a level insufficient for sequencing. The final method which was implemented consisted of the following steps:

1. Trizol and zirconia bead treatment of CF sputum
2. Zymo Clean and Clear
3. Microbenrich
4. Ribozero

Following rRNA depletion, qPCR was performed to ensure that Pseudomonal RNA was present in the samples. The primers used were targeted against *gyrB* which is specific for Pseudomonas spp. The amplification plot is shown in Figure 1, which shows amplification in each of samples 1-5 confirming the presence of Pseudomonal mRNA.

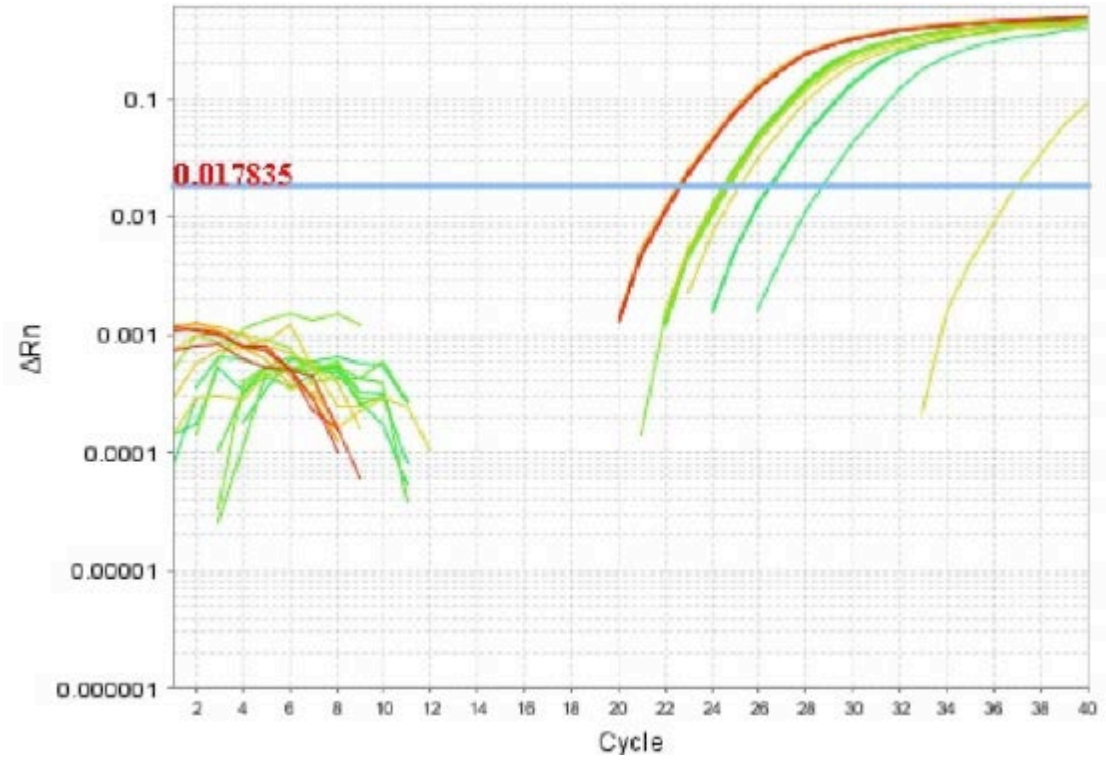

Figure 6-10-1: Amplification plot showing *Pseudomonas aeruginosa* RNA present in each of the samples tested as confirmed by successful amplification of all samples.

From left (red line) to right (yellow line) samples are 2, 1, 6, 5, 4 and 3, respectively as listed in Table 6-2.

6.3 Transcriptomic analysis

Following mRNA extraction, rRNA depletion and microbial mRNA enrichment, samples were sent to Liverpool University Genomics Research laboratory for preparation of RNAseq libraries using the Epicentre kit to prepare strand specific cDNA. Paired end sequencing (2 x 100bp) of RNAseq libraries on the Illumina Hi-Seq platform was performed, which generated data in excess of 120M clusters per lane. Post processing of the reads including QC, resolution of indexes and transfer of fastq files was additionally performed.

Initial QC results from Liverpool using an Agilent Bioanalyser suggested very poor quality, degraded RNA. An example of a Bioanalyser trace using these samples is shown in figure 6-2. This indicates due to the absence of distinct peaks that the RNA was most likely significantly degraded. However, on further investigation it was evident that this may not be the case and the analysis was likely compromised due the carryover of ethanol

in the sample from the ethanol precipitation step during the rRNA depletion[275,359]. Subsequently, the quality of the extracted RNA samples was confirmed by successful generation of high quality cDNA libraries and transcriptomic analysis.

a)

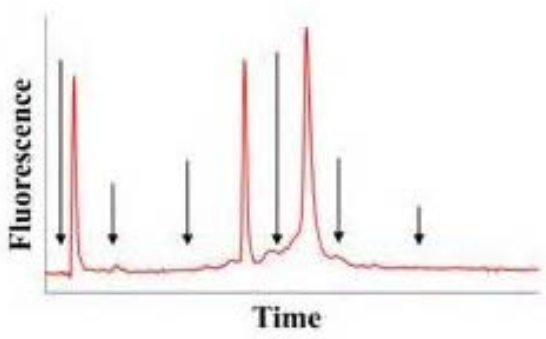

b)

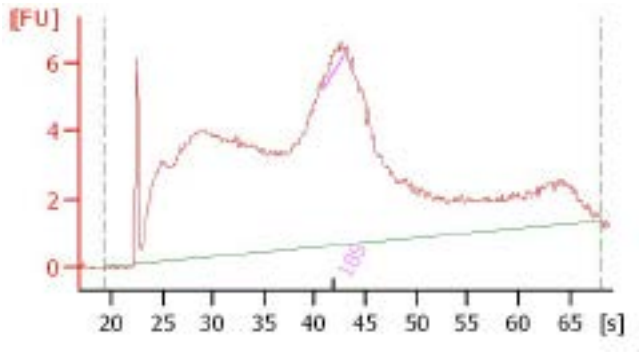

c)

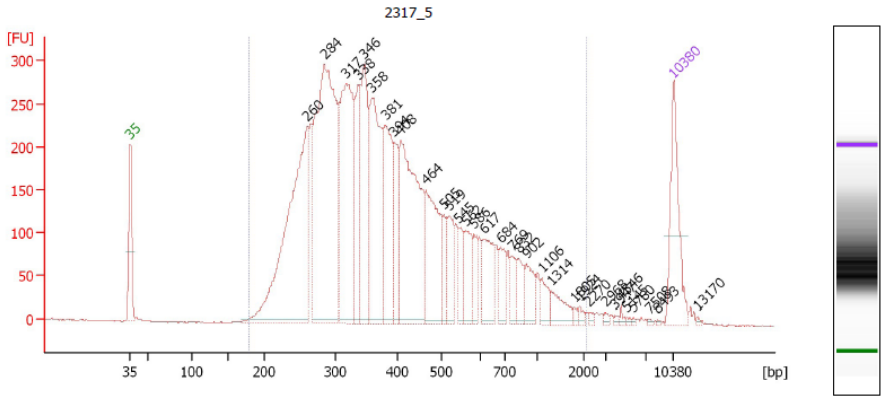

Figure 6-20-2 Agilent Bioanalyser Traces

Trace a) shows the ideal total RNA trace from the Agilent Bioanalyser. Ideally the traces would reveal defined peaks in the 18S and 28S in a human sample and 16S and 23S in a microbial sample.

Trace b) an example of the trace from the Agilent Bioanalyser following total RNA from human CF sputum samples and rRNA depletion. The trace reveals no peaks corresponding to high molecular weight rRNA and lots of small sized RNA (a wide smear at <20 nucleotides) which indicates RNA degradation. Trace c) following cDNA library preparation, which represents high quality RNA to cDNA conversion suitable for downstream transcriptomic analysis.

After establishing the quality of purified RNA obtained from CF sputum samples using the above methods, RNAseq was performed using an Illumina HiSeq 2000 platform. Sequencing was performed with paired end reads, 100bp length and raw reads were QC checked for read quality and degradation using FastQC (Babraham Bioinformatics). As shown in Table 6-3 a large number of reads were obtained and data analysed using CLC Workbench 7 (CLC Bio). Sequences were imported, trimmed accordingly and aligned against the human genome and the PA01 genome to establish the relative proportions of transcripts present. Unfortunately despite extensive optimisation of methods, enrichment procedures and rRNA depletion, sufficient *P. aeruginosa* RNA reads could not be obtained from these samples to allow for meaningful transcriptomic analysis. Given the cost associated with the process, it was felt that this line of investigation would not be financially viable in this particular project.

Table 6-3: Proportion of human and PA transcripts isolated from human CF sputum samples.

Sample	Preparation	Total number of Reads	Human Reads (%)	*P. aeruginosa* Reads (%)
1	Trizol, Zymo, Ribozero	16,168,456	99.56	0.01
2	Trizol, Zymo, Ribozero	16,539,890	99.23	0.02
3	Trizol, Zymo, MicrobEnrich, Ribozero	12,503,240	98.35	0.04
4	Trizol, Zymo, MicrobEnrich, Ribozero	18,033,754	98.95	0.05
5	Trizol, Zymo, Ribozero	14,305,226	99.45	0.01

Analysis using Metaphlam revealed the most common bacterial taxa found within theses samples included *P. aeruginosa*, Bacteroides, Prevotella, Firmicutes, Staphylococcus and Streptococcus, with Pseudomonas being the lowest percentage.

6.4 Discussion

As discussed throughout this chapter, extraction and purification of adequate concentrations and quality of bacterial RNA from CF sputum samples is an extremely difficult process. Following extensive method optimization, it was apparent that the initial processing step using two of the commercial kits (Ribopure and Qiagen Saliva Kit) failed to produce adequate concentrations of RNA and this was likely due to inadequate enzyme lysis of the purulent sputum sample and inflammatory cells. The Trizol bead beating method on the other hand combines both enzymatic and mechanical lysis, enabling disruption of the human cells and DNA present in the purulent samples. There is very little published data surrounding this to date and the main paper from Lim et al[275] in 2013 suggests they experienced similar difficulties when trying to sequence the metatranscriptome from CF sputum samples during an exacerbation.

The additional problem of the apparent poor quality of the purified RNA, as determined from Agilent Bioanalyser traces was shown to be an artifact, likely due carryover of ethanol at the precipitation stage, as high quality cDNA libraries could be obtained from these samples. It is well known that use of low-quality RNA compromises the derived expression results, reproducibility and relevance of gene expression results. Reliable isolation techniques must yield intact, high quality RNA that is free of RNases, proteins and genomic DNA. Spectrophometric methods often fail in sensitivity, are highly variable and give no indication as to the basic integrity of the RNA. The Agilent Bioanalyser and the Experion (Bio-Rad Laboratories) allow analysis of very small amounts of RNA and are becoming standard for analysis.

RNA purified by the methods outlined in this chapter were then sent to Liverpool Genomics for RNA-Seq using the HiSeq platform. Following successful construction of high quality cDNA libraries, it was immediately apparent that the samples were highly contaminated with human genetic material. Numerous studies have shown that saturation of sequence data by abundant transcripts remains a major limiting factor as when analyzing bacterial gene expression within host tissue.

Ideally, high quality transcriptomic data contains relatively few rRNA reads and an unbiased sampling of different RNAs. The initial amplification step during preparation of a cDNA sequencing library, however, is a potential source of transcript size induced bias. In

addition, the sputum samples obtained were from patients undergoing an infective exacerbation, which reduces the chance of obtaining a high proportion of microbial RNA given the large quantity of human immune and epithelial cells that are invariably present in such samples.

Given the financial restraints of this particular research project it was not feasible to continue optimizing methods for RNA extraction from the CF sputum samples. Efforts are being made to look at isolating RNA from a single bacterial cell within host tissue which would reduce the quantity of starting material required and reduce the contamination from human genetic material and in this case other bacteria present within the specimen. Use of single cell transcriptomics however would not give an indication of the microbial community present and the gross changes in gene expression which would have been vital in this research project as each different bacteria within a biofilm utilizes a different number of genes.

Chapter 7 Final Discussion

In this work we show that *P. aeruginosa* SCVs, that share key phenotypic features with SCVs isolated from chronically infected CF patients, can be isolated from a chronic murine lung infection model in the absence of antibiotic selection. Interestingly, SCVs were isolated significantly less from the bronchoalveolar lavage fluid (53%) of chronically infected mice compared with the lung homogenate samples (88%). Clinically this is likely to be highly significant, as it suggests that the presence of SCVs, in lung infection may be widely underestimated as sputum samples, rather than deeper tissue samples which are routinely used for bacterial isolation. The general upregulation of virulence associated genes in the SCVs, relative to the mucoid parent strain, and the increased virulence demonstrated in two infection models may begin to explain the link between the appearance of SCVs in chronic lung infection and the associated decline in lung function[360]. In addition, the upregulation of genes that mediate the response to oxidative stress immediately suggests why the isolated SCVs are rapidly selected for in a chronic infection model in which the host immune system is strongly activated.

From a clinical microbiology point of view, it would seem that CF microbiology and current culturing techniques are somewhat redundant. The swarming of the agar plates by the mucoid colonies and of other potential pathogens makes interpretation very difficult. The difficulty in obtaining a suitable sample for culturing results in inappropriate testing of isolated from thick upper airway secretions rather than deep samples from the lung tissue which contain the persister cells and small colony variants. Bronchoscopy and deeper sampling is not appropriate in this patient cohort given the high mortality associated with the procedure. Although next generation sequencing is advancing, the same problems would arise given the difficulty of sampling. The PEG biofilm assay also highlights a major problem with interpreting sensitivity results from automated systems such as the Vitek. Given their slow growth and biofilm form, the SCV's are significantly more resistant to antibiotics in the form found in the host. Clinical laboratories would release these isolates as antibiotic sentitive.

A key strength of our study was the availability of the parent strain used to establish infection for sequencing. This allowed a meaningful comparative genetic analysis to be performed enabling the determination the genetic basis of conversion to the SCV phenotype. Surprisingly, SNPs and INDELs were not identified in the SCV genome

by Illumina sequencing and single-molecule real-time sequencing was subsequently used to show that the two sequenced SCVs carried a large genomic inversion within 16S rRNA genes. Interestingly, the transcriptional changes associated with genomic inversion and that drive conversion to the SCV phenotype are not restricted to genes close to or within the inversion breakpoints, with major upregulated and downregulated genes distributed relatively evenly throughout the genome. Instead the major changes in gene expression are largely restricted to specific functional classes of genes including those that mediate the response to oxidative stress, virulence, DNA repair and recombination, the chaperone network and metabolism. This global rewiring of the cellular transcriptomic output results in concerted transcriptional changes to these normally differentially regulated genes. The mechanistic details of how the observed genomic inversion lead to these coordinated expression changes is currently not known, but the observation that a clinical SCV strain (SCV20265) obtained from the lung of a CF patient strain recently sequenced using the same strategy of combining SMRT and Illumina sequencing possesses a similar 16S rRNA based inversion, indicates that this inversion may be a highly clinically relevant route to the SCV phenotype[181]. A reversible genomic inversion has also recently been shown to mediate the reversible conversion between normal colony and SCV phenotypes in *S. aureus*[184]. However, in the case of the SCVs isolated in our work the SCV phenotype is stable and revertants to the parent phenotype are not observed. A possible explanation for this observation is that a number of genes encoding proteins involved in DNA repair and recombination, including RecA, are downregulated in the SCV relative to the parent strain.

It is generally accepted that the habitat of a chronically infected CF lung selects for less virulent *P. aeruginosa* phenotypes, with previous studies showing lower levels of protease, elastase and exotoxinA[93,306] and lower levels of type III secretion toxins including ExoS, ExoT and ExoU. However, the results of this study, in agreement with some other SCV studies[155,156] reveals that these SCV morphotypes exhibit an increased virulence potential and therefore would explain why the presence of these phenotypes have an adverse effect on the mortality of CF patients. Given the impact on prognosis and the difficulties in detection within the clinical laboratory, there should be strict precautions in place to ensure adequate detection of this otherwise easily missed phenotype.

It is currently common knowledge that growth of microorganisms in biofilm can enhance their resistnace to antimicrobial agents. Numerous studies[361,362] have discussed the role of quorum sensing inhibitors in biofilm formation and these molecules have also been shown to be promising antibiofilm agents and may be of great value in the future treatment of bacterial infections. A major benefit of quorum sensing inhibitors is that they are not directly involved in the inhibition of bacterial growth therefore do not impose harsh selective pressure for the development of resistance. The activities and pathways of microorganisms in biofilms present many novel drug targets because the activities and pathways are distinct from those important in free-floating microbial cells. From this study it is clear that rather than focusing on the mucoid *P. aeruginosa* we need to concentrate on the persistent small colony variant which is able to adopt a non-growing phase. It should be possible to potentiate the action of a conventional antibiotic by providing appropriate metabolic stimuli to 'wake up' persister cells. A further potential target would be to prevent the attachment or adhesion of a bacterial cell to a surface whether it be the lung epithelium or biomaterial. Microorganisms in biofilms are protected from killing by antimicrobial agents therefore another potential strategy would be to disrupt the biofilm matrix. Currently DNAses are used in CF, however there are many different pathways which could be explored.

Future work that may lead from this area of research could include setting up a respiratory tissue cell culture to look at whether small colony variants can be isolated from a tissue culture rather than a living host. From here it would be possible to establish other factors involved in the phenotypic switch and large scale genome rearrangement. It would be interesting to look at adjuncts to antibiotic therapy which could be able to target the intricate biofilm and extracellular matrix as antibiotics in general only target the bacteria specifically. Currently in Glasgow University there is work underway to establish whether synthetic lamellar bodies have any effect on the composition of the biofilm. There are numerous studies looking into compounds such as Manuka honey[363] which has the ability to reduce the oxidative stress and break down the biofilm structure therefore other potential compounds could be trialled in a similar fashion to be used in the human host. If small molecules can be identified that potentiate oxidative stress or subvert cellular processes that protect against reactive oxygen species, these small molecules have the potential to effectively eradicate infections that currently defy our antibiotic arsenal. These new agents may serve the dual function of acting on bacteria as primary antibiotics as well as impairing the bacterial defence to host immunity.

References

1. ANDERSEN, D. H. CYSTIC FIBROSIS OF THE PANCREAS AND ITS RELATION TO CELIAC DISEASE. *Am. J. Dis. Child.* **56,** 344 (1938).
2. Smyth, A. R. *et al.* European Cystic Fibrosis Society Standards of Care: Best Practice guidelines. *J. Cyst. Fibros.* **13 Suppl 1,** S23-42 (2014).
3. Boucher, R. . An overview of the pathogenesis of cystic fibrosis lung disease. *Adv. Drug Deliv. Rev.* **54,** 1359–1371 (2002).
4. Sobonya RE, Taussig LM (1986) Quantitative aspects of lung pathology in cystic fibrosis. Am Rev Respir Dis 134: 290-295. PubMed: 3740655. - Open Access Library. at <http://www.oalib.com/references/10863319>
5. O'Sullivan, B. P. & Freedman, S. D. Cystic fibrosis. *Lancet* **373,** 1891–904 (2009).
6. Davies, J. C. Pseudomonas aeruginosa in cystic fibrosis: pathogenesis and persistence. *Paediatr. Respir. Rev.* **3,** 128–134 (2002).
7. Pressler, T. *et al.* Chronic Pseudomonas aeruginosa infection definition: EuroCareCF Working Group report. *J. Cyst. Fibros.* **10,** S75–S78 (2011).
8. CF Registry - Annual Data Reports - Cystic Fibrosis Trust. at <http://www.cysticfibrosis.org.uk/research-care/uk-cf-registry/cf-registry-reports>
9. Waters, V. *et al.* Chronic Stenotrophomonas maltophilia infection and mortality or lung transplantation in cystic fibrosis patients. *J. Cyst. Fibros.* **12,** 482–6 (2013).
10. Livermore, D. M. Multiple mechanisms of antimicrobial resistance in Pseudomonas aeruginosa: our worst nightmare? *Clin. Infect. Dis.* **34,** 634–40 (2002).
11. Häussler, S. *et al.* Fatal outcome of lung transplantation in cystic fibrosis patients due to small-colony variants of the Burkholderia cepacia complex. *Eur. J. Clin. Microbiol. Infect. Dis.* **22,** 249–53 (2003).
12. Pinto-de-Oliveira, A. *et al.* 109 The Burkholderia cepacia small colony variants (SCV) are a more pathogenic bacterial form that may facilitate persistent respiratory infections in CF patients. *J. Cyst. Fibros.* **12,** S76 (2013).
13. Chaparro, C. *et al.* Infection with Burkholderia cepacia in cystic fibrosis: outcome following lung transplantation. *Am. J. Respir. Crit. Care Med.* **163,** 43–8 (2001).
14. MRSA in Patients With Cystic Fibrosis Linked to Shorter Survival Time. at <http://www.medscape.org/viewarticle/723623>
15. Goss, C. H. & Muhlebach, M. S. Review: Staphylococcus aureus and MRSA in cystic fibrosis. *J. Cyst. Fibros.* **10,** 298–306 (2011).
16. Cullen, A. R., Cannon, C. L., Mark, E. J. & Colin, A. A. Mycobacterium abscessus infection in cystic fibrosis. Colonization or infection? *Am. J. Respir. Crit. Care Med.* **161,** 641–5 (2000).

17. Gellatly, S. L. & Hancock, R. E. W. Pseudomonas aeruginosa: new insights into pathogenesis and host defenses. *Pathog. Dis.* **67,** 159–73 (2013).

18. Smith, E. E. *et al.* Genetic adaptation by Pseudomonas aeruginosa to the airways of cystic fibrosis patients. *Proc. Natl. Acad. Sci. U. S. A.* **103,** 8487–92 (2006).

19. Stover, C. K. *et al.* Complete genome sequence of Pseudomonas aeruginosa PAO1, an opportunistic pathogen. *Nature* **406,** 959–64 (2000).

20. Lee, D. G. *et al.* Genomic analysis reveals that Pseudomonas aeruginosa virulence is combinatorial. *Genome Biol.* **7,** R90 (2006).

21. Darling, A. E., Miklós, I. & Ragan, M. A. Dynamics of Genome Rearrangement in Bacterial Populations. *PLoS Genet.* **4,** e1000128 (2008).

22. Juhas, M., Eberl, L. & Tummler, B. Quorum sensing: the power of cooperation in the world of Pseudomonas. *Environ. Microbiol.* **7,** 459–471 (2005).

23. Wolfgang, M. C. *et al.* Conservation of genome content and virulence determinants among clinical and environmental isolates of Pseudomonas aeruginosa. *Proc. Natl. Acad. Sci. U. S. A.* **100,** 8484–9 (2003).

24. Hogardt, M. & Heesemann, J. Adaptation of Pseudomonas aeruginosa during persistence in the cystic fibrosis lung. *Int. J. Med. Microbiol.* **300,** 557–62 (2010).

25. Strateva, T. & Mitov, I. Contribution of an arsenal of virulence factors to pathogenesis of Pseudomonas aeruginosa infections. *Ann. Microbiol.* **61,** 717–732 (2011).

26. Kipnis, E., Sawa, T. & Wiener-Kronish, J. Targeting mechanisms of Pseudomonas aeruginosa pathogenesis. *Médecine Mal. Infect.* **36,** 78–91 (2006).

27. Persat, A., Inclan, Y. F., Engel, J. N., Stone, H. A. & Gitai, Z. Type IV pili mechanochemically regulate virulence factors in Pseudomonas aeruginosa. *Proc. Natl. Acad. Sci. U. S. A.* **112,** 7563–8 (2015).

28. Déziel, E., Comeau, Y. & Villemur, R. Initiation of biofilm formation by Pseudomonas aeruginosa 57RP correlates with emergence of hyperpiliated and highly adherent phenotypic variants deficient in swimming, swarming, and twitching motilities. *J. Bacteriol.* **183,** 1195–204 (2001).

29. Chiang, P. & Burrows, L. L. Biofilm Formation by Hyperpiliated Mutants of Pseudomonas aeruginosa. *J. Bacteriol.* **185,** 2374–2378 (2003).

30. Burrows, L. L. Pseudomonas aeruginosa twitching motility: type IV pili in action. *Annu. Rev. Microbiol.* **66,** 493–520 (2012).

31. Feldman, M. *et al.* Role of Flagella in Pathogenesis of Pseudomonas aeruginosa Pulmonary Infection. *Infect. Immun.* **66,** 43–51 (1998).

32. Drake, D. & Montie, T. C. Flagella, motility and invasive virulence of Pseudomonas aeruginosa. *J. Gen. Microbiol.* **134,** 43–52 (1988).

33. Montie, T. C., Doyle-Huntzinger, D., Craven, R. C. & Holder, I. A. Loss of virulence associated with absence of flagellum in an isogenic mutant of Pseudomonas aeruginosa in the burned-mouse model. *Infect. Immun.* **38,** 1296–1298 (1982).

34. Wagner, V. E., Bushnell, D., Passador, L., Brooks, A. I. & Iglewski, B. H. Microarray analysis of Pseudomonas aeruginosa quorum-sensing regulons: effects of growth phase and environment. *J. Bacteriol.* **185,** 2080–95 (2003).

35. Pessi, G. *et al.* The global posttranscriptional regulator RsmA modulates production of virulence determinants and N-acylhomoserine lactones in Pseudomonas aeruginosa. *J. Bacteriol.* **183,** 6676–83 (2001).

36. Pesci, E. C., Pearson, J. P., Seed, P. C. & Iglewski, B. H. Regulation of las and rhl quorum sensing in Pseudomonas aeruginosa. *J. Bacteriol.* **179,** 3127–32 (1997).

37. Ben Haj Khalifa, A., Moissenet, D., Vu Thien, H. & Khedher, M. [Virulence factors in Pseudomonas aeruginosa: mechanisms and modes of regulation]. *Ann. Biol. Clin. (Paris).* **69,** 393–403

38. Gambello, M. J. & Iglewski, B. H. Cloning and characterization of the Pseudomonas aeruginosa lasR gene, a transcriptional activator of elastase expression. *J. Bacteriol.* **173,** 3000–9 (1991).

39. Burrowes, E., Baysse, C., Adams, C. & O'Gara, F. Influence of the regulatory protein RsmA on cellular functions in Pseudomonas aeruginosa PAO1, as revealed by transcriptome analysis. *Microbiology* **152,** 405–18 (2006).

40. Lalaouna, D., Fochesato, S., Barakat, M., Ortet, P. & Achouak, W. Multiple transcription-activating sequences regulate the RsmZ regulatory small RNA of Pseudomonas brassicacearum. *J. Bacteriol.* **194,** 4888–93 (2012).

41. Duss, O. *et al.* Structural basis of the non-coding RNA RsmZ acting as a protein sponge. *Nature* **509,** 588–92 (2014).

42. Heurlier, K. *et al.* Positive control of swarming, rhamnolipid synthesis, and lipase production by the posttranscriptional RsmA/RsmZ system in Pseudomonas aeruginosa PAO1. *J. Bacteriol.* **186,** 2936–45 (2004).

43. Lequette, Y. & Greenberg, E. P. Timing and localization of rhamnolipid synthesis gene expression in Pseudomonas aeruginosa biofilms. *J. Bacteriol.* **187,** 37–44 (2005).

44. Caiazza, N. C., Merritt, J. H., Brothers, K. M. & O'Toole, G. A. Inverse regulation of biofilm formation and swarming motility by Pseudomonas aeruginosa PA14. *J. Bacteriol.* **189,** 3603–12 (2007).

45. Boles, B. R., Thoendel, M. & Singh, P. K. Rhamnolipids mediate detachment of Pseudomonas aeruginosa from biofilms. *Mol. Microbiol.* **57,** 1210–23 (2005).

46. McKnight, S. L., Iglewski, B. H. & Pesci, E. C. The Pseudomonas Quinolone Signal Regulates rhl Quorum Sensing in Pseudomonas aeruginosa. *J. Bacteriol.* **182,** 2702–2708 (2000).

47. Wei, Q. *et al.* Phenotypic and genome-wide analysis of an antibiotic-resistant small colony variant (SCV) of Pseudomonas aeruginosa. *PLoS One* **6,** e29276 (2011).

48. Meyer, J., Neely, A., Stintzi, A., Georges, C. & Holder, I. Pyoverdin is essential for virulence of Pseudomonas aeruginosa. *Infect. Immun.* **64,** 518–523 (1996).

49. Taguchi, F. *et al.* The siderophore pyoverdine of Pseudomonas syringae pv. tabaci 6605 is an intrinsic virulence factor in host tobacco infection. *J. Bacteriol.* **192,** 117–26 (2010).

50. Pessi, G. *et al.* The global posttranscriptional regulator RsmA modulates production of virulence determinants and N-acylhomoserine lactones in Pseudomonas aeruginosa. *J. Bacteriol.* **183,** 6676–83 (2001).

51. Christiaen, S. E. A. *et al.* Bacteria that inhibit quorum sensing decrease biofilm

formation and virulence in Pseudomonas aeruginosa PAO1. *Pathog. Dis.* **70,** 271–9 (2014).

52. Mikkelsen, H. *et al.* Biofilms and type III secretion are not mutually exclusive in Pseudomonas aeruginosa. *Microbiology* **155,** 687–98 (2009).

53. Høiby, N., Bjarnsholt, T., Givskov, M., Molin, S. & Ciofu, O. Antibiotic resistance of bacterial biofilms. *Int. J. Antimicrob. Agents* **35,** 322–32 (2010).

54. Wozniak, D. J. *et al.* Alginate is not a significant component of the extracellular polysaccharide matrix of PA14 and PAO1 Pseudomonas aeruginosa biofilms. *Proc. Natl. Acad. Sci. U. S. A.* **100,** 7907–12 (2003).

55. Colvin, K. M. *et al.* The Pel and Psl polysaccharides provide Pseudomonas aeruginosa structural redundancy within the biofilm matrix. *Environ. Microbiol.* **14,** 1913–28 (2012).

56. Starkey, M. *et al.* Pseudomonas aeruginosa rugose small-colony variants have adaptations that likely promote persistence in the cystic fibrosis lung. *J. Bacteriol.* **191,** 3492–503 (2009).

57. Ventre, I. *et al.* Multiple sensors control reciprocal expression of Pseudomonas aeruginosa regulatory RNA and virulence genes. *Proc. Natl. Acad. Sci. U. S. A.* **103,** 171–6 (2006).

58. Wong, A., Rodrigue, N. & Kassen, R. Genomics of adaptation during experimental evolution of the opportunistic pathogen Pseudomonas aeruginosa. *PLoS Genet.* **8,** e1002928 (2012).

59. Malone, J. G. *et al.* YfiBNR mediates cyclic di-GMP dependent small colony variant formation and persistence in Pseudomonas aeruginosa. *PLoS Pathog.* **6,** e1000804 (2010).

60. Wang, D. *et al.* Adaptation genomics of a small-colony variant in a Pseudomonas chlororaphis 30-84 biofilm. *Appl. Environ. Microbiol.* **81,** 890–9 (2015).

61. Tralau, T. *et al.* Transcriptomic analysis of the sulfate starvation response of Pseudomonas aeruginosa. *J. Bacteriol.* **189,** 6743–50 (2007).

62. Martin, D. W., Schurr, M. J., Yu, H. & Deretic, V. Analysis of promoters controlled by the putative sigma factor AlgU regulating conversion to mucoidy in Pseudomonas aeruginosa: relationship to sigma E and stress response. *J. Bacteriol.* **176,** 6688–96 (1994).

63. Werner, E. *et al.* Stratified growth in Pseudomonas aeruginosa biofilms. *Appl. Environ. Microbiol.* **70,** 6188–96 (2004).

64. Folsom, J. P. *et al.* Physiology of Pseudomonas aeruginosa in biofilms as revealed by transcriptome analysis. *BMC Microbiol.* **10,** 294 (2010).

65. Borriello, G. *et al.* Oxygen limitation contributes to antibiotic tolerance of Pseudomonas aeruginosa in biofilms. *Antimicrob. Agents Chemother.* **48,** 2659–64 (2004).

66. Keren, I., Kaldalu, N., Spoering, A., Wang, Y. & Lewis, K. Persister cells and tolerance to antimicrobials. *FEMS Microbiol. Lett.* **230,** 13–8 (2004).

67. Diaz, M. H. & Hauser, A. R. Pseudomonas aeruginosa cytotoxin ExoU is injected into phagocytic cells during acute pneumonia. *Infect. Immun.* **78,** 1447–56 (2010).

68. Wong-Beringer, A., Wiener-Kronish, J., Lynch, S. & Flanagan, J. Comparison of

type III secretion system virulence among fluoroquinolone-susceptible and -resistant clinical isolates of Pseudomonas aeruginosa. *Clin. Microbiol. Infect.* **14,** 330–6 (2008).

69. Jain, M. *et al.* Type III secretion phenotypes of Pseudomonas aeruginosa strains change during infection of individuals with cystic fibrosis. *J. Clin. Microbiol.* **42,** 5229–37 (2004).

70. Galle, M., Carpentier, I. & Beyaert, R. Structure and function of the Type III secretion system of Pseudomonas aeruginosa. *Curr. Protein Pept. Sci.* **13,** 831–42 (2012).

71. Coburn, B., Sekirov, I. & Finlay, B. B. Type III secretion systems and disease. *Clin. Microbiol. Rev.* **20,** 535–49 (2007).

72. Hauser, A. R. The type III secretion system of Pseudomonas aeruginosa: infection by injection. *Nat. Rev. Microbiol.* **7,** 654–65 (2009).

73. Hauser, A. R. & Engel, J. N. Pseudomonas aeruginosa induces type-III-secretion-mediated apoptosis of macrophages and epithelial cells. *Infect. Immun.* **67,** 5530–7 (1999).

74. Feltman, H. *et al.* Prevalence of type III secretion genes in clinical and environmental isolates of Pseudomonas aeruginosa. *Microbiology* **147,** 2659–69 (2001).

75. Miyata, S., Casey, M., Frank, D. W., Ausubel, F. M. & Drenkard, E. Use of the Galleria mellonella Caterpillar as a Model Host To Study the Role of the Type III Secretion System in Pseudomonas aeruginosa Pathogenesis. *Infect. Immun.* **71,** 2404–2413 (2003).

76. McCaw, M. L., Lykken, G. L., Singh, P. K. & Yahr, T. L. ExsD is a negative regulator of the Pseudomonas aeruginosa type III secretion regulon. *Mol. Microbiol.* **46,** 1123–33 (2002).

77. Kudoh, I., Wiener-Kronish, J. P., Hashimoto, S., Pittet, J. F. & Frank, D. Exoproduct secretions of Pseudomonas aeruginosa strains influence severity of alveolar epithelial injury. *Am. J. Physiol.* **267,** L551-6 (1994).

78. Allewelt, M., Coleman, F. T., Grout, M., Priebe, G. P. & Pier, G. B. Acquisition of expression of the Pseudomonas aeruginosa ExoU cytotoxin leads to increased bacterial virulence in a murine model of acute pneumonia and systemic spread. *Infect. Immun.* **68,** 3998–4004 (2000).

79. Phillips, R. M., Six, D. A., Dennis, E. A. & Ghosh, P. In vivo phospholipase activity of the Pseudomonas aeruginosa cytotoxin ExoU and protection of mammalian cells with phospholipase A2 inhibitors. *J. Biol. Chem.* **278,** 41326–32 (2003).

80. Sawa, T. *et al.* Active and passive immunization with the Pseudomonas V antigen protects against type III intoxication and lung injury. *Nat. Med.* **5,** 392–8 (1999).

81. Roy-Burman, A. *et al.* Type III protein secretion is associated with death in lower respiratory and systemic Pseudomonas aeruginosa infections. *J. Infect. Dis.* **183,** 1767–74 (2001).

82. Vance, R. E., Rietsch, A. & Mekalanos, J. J. Role of the type III secreted exoenzymes S, T, and Y in systemic spread of Pseudomonas aeruginosa PAO1 in vivo. *Infect. Immun.* **73,** 1706–13 (2005).

83. Miao, E. A. *et al.* Innate immune detection of the type III secretion apparatus

through the NLRC4 inflammasome. *Proc. Natl. Acad. Sci. U. S. A.* **107,** 3076–80 (2010).

84. Sutterwala, F. S. *et al.* Immune recognition of Pseudomonas aeruginosa mediated by the IPAF/NLRC4 inflammasome. *J. Exp. Med.* **204,** 3235–45 (2007).

85. Faure, E. *et al.* Pseudomonas aeruginosa type-3 secretion system dampens host defense by exploiting the NLRC4-coupled inflammasome. *Am. J. Respir. Crit. Care Med.* **189,** 799–811 (2014).

86. Twining, S. S. Fluorescein isothiocyanate-labeled casein assay for proteolytic enzymes. *Anal. Biochem.* **143,** 30–4 (1984).

87. Tang, H. *et al.* Contribution of specific Pseudomonas aeruginosa virulence factors to pathogenesis of pneumonia in a neonatal mouse model of infection. *Infect. Immun.* **64,** 37–43 (1996).

88. Van Delden, C. & Iglewski, B. H. Cell-to-cell signaling and Pseudomonas aeruginosa infections. *Emerg. Infect. Dis.* **4,** 551–60

89. Hobden, J. A. Pseudomonas aeruginosa proteases and corneal virulence. *DNA Cell Biol.* **21,** 391–6

90. Baltch, A. L. *et al.* Production of cytotoxin by clinical strains of Pseudomonas aeruginosa. *Can. J. Microbiol.* **33,** 104–111 (1987).

91. King, J. D., Kocíncová, D., Westman, E. L. & Lam, J. S. Review: Lipopolysaccharide biosynthesis in Pseudomonas aeruginosa. *Innate Immun.* **15,** 261–312 (2009).

92. Cryz, S. J., Pitt, T. L., Fürer, E. & Germanier, R. Role of lipopolysaccharide in virulence of Pseudomonas aeruginosa. *Infect. Immun.* **44,** 508–13 (1984).

93. Pier, G. B. Pseudomonas aeruginosa lipopolysaccharide: a major virulence factor, initiator of inflammation and target for effective immunity. *Int. J. Med. Microbiol.* **297,** 277–95 (2007).

94. Hao, Y., King, J. D., Huszczynski, S., Kocíncová, D. & Lam, J. S. Five new genes are important for common polysaccharide antigen biosynthesis in Pseudomonas aeruginosa. *MBio* **4,** e00631-12 (2013).

95. Tang, H. B. *et al.* Contribution of specific Pseudomonas aeruginosa virulence factors to pathogenesis of pneumonia in a neonatal mouse model of infection. *Infect. Immun.* **64,** 37–43 (1996).

96. Young, L. S. Human Immunity to Pseudomonas aeruginosa. II. Relationship between Heat-Stable Opsonins and Type-Specific Lipopolysaccharides. *J. Infect. Dis.* **126,** 277–287 (1972).

97. Pennington, J. E., Reynolds, H. Y., Wood, R. E., Robinson, R. A. & Levine, A. S. Use of a Pseudomonas Aeruginosa vaccine in pateints with acute leukemia and cystic fibrosis. *Am. J. Med.* **58,** 629–36 (1975).

98. Young, L. S., Meyer, R. D. & Armstrong, D. Pseudomonas aeruginosa vaccine in cancer patients. *Ann. Intern. Med.* **79,** 518–27 (1973).

99. Pier, G. B., Sidberry, H. F. & Sadoff, J. C. Protective immunity induced in mice by immunization with high-molecular-weight polysaccharide from Pseudomonas aeruginosa. *Infect. Immun.* **22,** 919–25 (1978).

100. Schaad, U. B., Lang, A. B., Wedgwood, J., Buehlamnn, U. & Fuerer, E. Serotype-

specific serum IgG antibodies to lipopolysaccharides of Pseudomonas aeruginosa in cystic fibrosis: correlation to disease, subclass distribution, and experimental protective capacity. *Pediatr. Res.* **27,** 508–13 (1990).

101. Schalk, I. J. & Guillon, L. Pyoverdine biosynthesis and secretion in Pseudomonas aeruginosa: implications for metal homeostasis. *Environ. Microbiol.* **15,** 1661–73 (2013).

102. Usher, L. R. *et al.* Induction of neutrophil apoptosis by the Pseudomonas aeruginosa exotoxin pyocyanin: a potential mechanism of persistent infection. *J. Immunol.* **168,** 1861–8 (2002).

103. Wilson, R. *et al.* Measurement of Pseudomonas aeruginosa phenazine pigments in sputum and assessment of their contribution to sputum sol toxicity for respiratory epithelium. *Infect. Immun.* **56,** 2515–7 (1988).

104. Lau, G. W., Ran, H., Kong, F., Hassett, D. J. & Mavrodi, D. Pseudomonas aeruginosa pyocyanin is critical for lung infection in mice. *Infect. Immun.* **72,** 4275–8 (2004).

105. Lau, G. W., Hassett, D. J., Ran, H. & Kong, F. The role of pyocyanin in Pseudomonas aeruginosa infection. *Trends Mol. Med.* **10,** 599–606 (2004).

106. Mavrodi, D. V *et al.* Functional analysis of genes for biosynthesis of pyocyanin and phenazine-1-carboxamide from Pseudomonas aeruginosa PAO1. *J. Bacteriol.* **183,** 6454–65 (2001).

107. Williams, H. D., Zlosnik, J. E. A. & Ryall, B. Oxygen, cyanide and energy generation in the cystic fibrosis pathogen Pseudomonas aeruginosa. *Adv. Microb. Physiol.* **52,** 1–71 (2007).

108. Lenney, W. & Gilchrist, F. J. Pseudomonas aeruginosa and cyanide production. *Eur. Respir. J.* **37,** 482–3 (2011).

109. Gallagher, L. A. & Manoil, C. Pseudomonas aeruginosa PAO1 kills Caenorhabditis elegans by cyanide poisoning. *J. Bacteriol.* **183,** 6207–14 (2001).

110. Williams, B. J., Dehnbostel, J. & Blackwell, T. S. Pseudomonas aeruginosa: host defence in lung diseases. *Respirology* **15,** 1037–56 (2010).

111. Barton, A. D., Ryder, K., Lourenço, R. V, Dralle, W. & Weiss, S. G. Inflammatory reaction and airway damage in cystic fibrosis. *J. Lab. Clin. Med.* **88,** 423–6 (1976).

112. Murphy, T. F. *et al.* Pseudomonas aeruginosa in chronic obstructive pulmonary disease. *Am. J. Respir. Crit. Care Med.* **177,** 853–60 (2008).

113. Valderrey, A. D. *et al.* Chronic colonization by Pseudomonas aeruginosa of patients with obstructive lung diseases: cystic fibrosis, bronchiectasis, and chronic obstructive pulmonary disease. *Diagn. Microbiol. Infect. Dis.* **68,** 20–7 (2010).

114. Martínez-Solano, L., Macia, M. D., Fajardo, A., Oliver, A. & Martinez, J. L. Chronic Pseudomonas aeruginosa infection in chronic obstructive pulmonary disease. *Clin. Infect. Dis.* **47,** 1526–33 (2008).

115. Cohen, T. S. & Prince, A. Cystic fibrosis: a mucosal immunodeficiency syndrome. *Nat. Med.* **18,** 509–19 (2012).

116. Linnane, B. M. *et al.* Lung function in infants with cystic fibrosis diagnosed by newborn screening. *Am. J. Respir. Crit. Care Med.* **178,** 1238–44 (2008).

117. Hartl, D. *et al.* Innate immunity in cystic fibrosis lung disease. *J. Cyst. Fibros.* **11,**

363–82 (2012).

118. Ratner, D. & Mueller, C. Immune Responses in Cystic Fibrosis. *Am. J. Respir. Cell Mol. Biol.* (2012). at <http://www.atsjournals.org/doi/full/10.1165/rcmb.2011-0399RT#.VfBQ1-mNeS0>

119. Massengale, A. R. *et al.* Reduced interleukin-8 production by cystic fibrosis airway epithelial cells. *Am. J. Respir. Cell Mol. Biol.* **20,** 1073–80 (1999).

120. Kelly, E., Greene, C. M. & McElvaney, N. G. Targeting neutrophil elastase in cystic fibrosis. *Expert Opin. Ther. Targets* **12,** 145–57 (2008).

121. Gifford, A. M. & Chalmers, J. D. The role of neutrophils in cystic fibrosis. *Curr. Opin. Hematol.* **21,** 16–22 (2014).

122. Gaggar, A. *et al.* The role of matrix metalloproteinases in cystic fibrosis lung disease. *Eur. Respir. J.* **38,** 721–7 (2011).

123. Conese, M., Copreni, E., Di Gioia, S., De Rinaldis, P. & Fumarulo, R. Neutrophil recruitment and airway epithelial cell involvement in chronic cystic fibrosis lung disease. *J. Cyst. Fibros.* **2,** 129–35 (2003).

124. Moser, C. *et al.* The immune response to chronic Pseudomonas aeruginosa lung infection in cystic fibrosis patients is predominantly of the Th2 type. *APMIS* **108,** 329–35 (2000).

125. Milagres, L. G. *et al.* Antibody response to Pseudomonas aeruginosa in children with cystic fibrosis. *Pediatr. Pulmonol.* **44,** 392–401 (2009).

126. Amin, R., Lam, M., Dupuis, A. & Ratjen, F. The effect of early Pseudomonas aeruginosa treatment on lung function in pediatric cystic fibrosis. *Pediatr. Pulmonol.* **46,** 554–8 (2011).

127. Powderly, W. G., Schreiber, J. R., Pier, G. B. & Markham, R. B. T cells recognizing polysaccharide-specific B cells function as contrasuppressor cells in the generation of T cell immunity to Pseudomonas aeruginosa. *J. Immunol.* **140,** 2746–52 (1988).

128. Wientzen, R., Prestidge, C. B., Kramer, R. I., McCracken, G. H. & Nelson, J. D. Acute pulmonary exacerbations in cystic fibrosis. A double-blind trial of tobramycin and placebo therapy. *Am. J. Dis. Child.* **134,** 1134–8 (1980).

129. Gold, R., Carpenter, S., Heurter, H., Corey, M. & Levison, H. Randomized trial of ceftazidime versus placebo in the management of acute respiratory exacerbations in patients with cystic fibrosis. *J. Pediatr.* **111,** 907–13 (1987).

130. Elphick, H. E. & Tan, A. Single versus combination intravenous antibiotic therapy for people with cystic fibrosis. *Cochrane database Syst. Rev.* CD002007 (2005). doi:10.1002/14651858.CD002007.pub2

131. Blumer, J. L., Saiman, L., Konstan, M. W. & Melnick, D. The efficacy and safety of meropenem and tobramycin vs ceftazidime and tobramycin in the treatment of acute pulmonary exacerbations in patients with cystic fibrosis. *Chest* **128,** 2336–46 (2005).

132. Cheng, K. *et al.* Spread of beta-lactam-resistant Pseudomonas aeruginosa in a cystic fibrosis clinic. *Lancet* **348,** 639–42 (1996).

133. Banjanac, M. *et al.* Anti-inflammatory mechanism of action of azithromycin in LPS-stimulated J774A.1 cells. *Pharmacol. Res.* **66,** 357–62 (2012).

134. Yamauchi, K. *et al.* Azithromycin suppresses interleukin-12p40 expression in

lipopolysaccharide and interferon-gamma stimulated macrophages. *Int. J. Biol. Sci.* **5,** 667–78 (2009).

135. Murphy, B. S. *et al.* Azithromycin alters macrophage phenotype. *J. Antimicrob. Chemother.* **61,** 554–60 (2008).

136. Ianaro, A. *et al.* Anti-inflammatory activity of macrolide antibiotics. *J. Pharmacol. Exp. Ther.* **292,** 156–63 (2000).

137. Cystic fibrosis: long-term azithromycin | Key-points-from-the-evidence | Advice | NICE. at <https://www.nice.org.uk/advice/esuom37/chapter/key-points-from-the-evidence>

138. Lumacaftor–Ivacaftor in Patients with Cystic Fibrosis Homozygous for Phe508del CFTR — NEJM. at <http://www.nejm.org/doi/full/10.1056/NEJMoa1409547#t=articleBackground>

139. Eckford, P. D. W., Li, C., Ramjeesingh, M. & Bear, C. E. Cystic fibrosis transmembrane conductance regulator (CFTR) potentiator VX-770 (ivacaftor) opens the defective channel gate of mutant CFTR in a phosphorylation-dependent but ATP-independent manner. *J. Biol. Chem.* **287,** 36639–49 (2012).

140. Yu, H. *et al.* Ivacaftor potentiation of multiple CFTR channels with gating mutations. *J. Cyst. Fibros.* **11,** 237–45 (2012).

141. Wang, Y. *et al.* CFTR potentiators partially restore channel function to A561E-CFTR, a cystic fibrosis mutant with a similar mechanism of dysfunction as F508del-CFTR. *Br. J. Pharmacol.* **171,** 4490–503 (2014).

142. Eckford, P. D. W., Li, C., Ramjeesingh, M. & Bear, C. E. Cystic fibrosis transmembrane conductance regulator (CFTR) potentiator VX-770 (ivacaftor) opens the defective channel gate of mutant CFTR in a phosphorylation-dependent but ATP-independent manner. *J. Biol. Chem.* **287,** 36639–49 (2012).

143. Lumacaftor–Ivacaftor in Patients with Cystic Fibrosis Homozygous for Phe508del CFTR — NEJM.

144. Cystic fibrosis (F508del mutation) - lumacaftor (with ivacaftor) [ID786] | Guidance and guidelines | NICE. at <https://www.nice.org.uk/guidance/indevelopment/gid-tag530>

145. Yu, H. *et al.* Ivacaftor potentiation of multiple CFTR channels with gating mutations. *J. Cyst. Fibros.* **11,** 237–45 (2012).

146. Wang, Y. *et al.* CFTR potentiators partially restore channel function to A561E-CFTR, a cystic fibrosis mutant with a similar mechanism of dysfunction as F508del-CFTR. *Br. J. Pharmacol.* **171,** 4490–503 (2014).

147. Henke, M. O. & Ratjen, F. Mucolytics in cystic fibrosis. *Paediatr. Respir. Rev.* **8,** 24–9 (2007).

148. Robinson, P. J. Dornase alfa in early cystic fibrosis lung disease. *Pediatr. Pulmonol.* **34,** 237–41 (2002).

149. Konstan, M. W. *et al.* Clinical use of dornase alpha is associated with a slower rate of FEV1 decline in cystic fibrosis. *Pediatr. Pulmonol.* **46,** 545–53 (2011).

150. Chernick, W. S. & Barbero, G. J. COMPOSITION OF TRACHEOBRONCHIAL SECRETIONS IN CYSTIC FIBROSIS OF THE PANCREAS AND BRONCHIECTASIS. *Pediatrics* **24,** 739–745 (1959).

151. Kirchner, K. K., Wagener, J. S., Khan, T. Z., Copenhaver, S. C. & Accurso, F. J. Increased DNA levels in bronchoalveolar lavage fluid obtained from infants with cystic fibrosis. *Am. J. Respir. Crit. Care Med.* **154,** 1426–9 (1996).

152. Rosenfeld, M. *et al.* Early pulmonary infection, inflammation, and clinical outcomes in infants with cystic fibrosis. *Pediatr. Pulmonol.* **32,** 356–66 (2001).

153. Nash, E. F., Stephenson, A., Ratjen, F. & Tullis, E. Nebulized and oral thiol derivatives for pulmonary disease in cystic fibrosis. *Cochrane database Syst. Rev.* CD007168 (2009). doi:10.1002/14651858.CD007168.pub2

154. Flume, P. A. *et al.* Cystic fibrosis pulmonary guidelines: airway clearance therapies. *Respir. Care* **54,** 522–37 (2009).

155. Haussler, S. Highly adherent small-colony variants of Pseudomonas aeruginosa in cystic fibrosis lung infection. *J. Med. Microbiol.* **52,** 295–301 (2003).

156. von Götz, F. *et al.* Expression analysis of a highly adherent and cytotoxic small colony variant of Pseudomonas aeruginosa isolated from a lung of a patient with cystic fibrosis. *J. Bacteriol.* **186,** 3837–47 (2004).

157. Hogardt, M. *et al.* Stage-specific adaptation of hypermutable Pseudomonas aeruginosa isolates during chronic pulmonary infection in patients with cystic fibrosis. *J. Infect. Dis.* **195,** 70–80 (2007).

158. Murray, T. S., Ledizet, M. & Kazmierczak, B. I. Swarming motility, secretion of type 3 effectors and biofilm formation phenotypes exhibited within a large cohort of Pseudomonas aeruginosa clinical isolates. *J. Med. Microbiol.* **59,** 511–520 (2010).

159. Miyata, S., Casey, M., Frank, D. W., Ausubel, F. M. & Drenkard, E. Use of the Galleria mellonella Caterpillar as a Model Host To Study the Role of the Type III Secretion System in Pseudomonas aeruginosa Pathogenesis. *Infect. Immun.* **71,** 2404–2413 (2003).

160. Boucher, J. C. *et al.* Two distinct loci affecting conversion to mucoidy in Pseudomonas aeruginosa in cystic fibrosis encode homologs of the serine protease HtrA. *J. Bacteriol.* **178,** 511–23 (1996).

161. Schurr, M. J., Martin, D. W., Mudd, M. H. & Deretic, V. Gene cluster controlling conversion to alginate-overproducing phenotype in Pseudomonas aeruginosa: functional analysis in a heterologous host and role in the instability of mucoidy. *J. Bacteriol.* **176,** 3375–82 (1994).

162. Déziel, E., Comeau, Y. & Villemur, R. Initiation of biofilm formation by Pseudomonas aeruginosa 57RP correlates with emergence of hyperpiliated and highly adherent phenotypic variants deficient in swimming, swarming, and twitching motilities. *J. Bacteriol.* **183,** 1195–204 (2001).

163. Maduka-Ezeh, A. N. *et al.* Antimicrobial susceptibility and biofilm formation of Staphylococcus epidermidis small colony variants associated with prosthetic joint infection. *Diagn. Microbiol. Infect. Dis.* **74,** 224–9 (2012).

164. Allegrucci, M. & Sauer, K. Formation of Streptococcus pneumoniae non-phase-variable colony variants is due to increased mutation frequency present under biofilm growth conditions. *J. Bacteriol.* **190,** 6330–9 (2008).

165. Zbinden, A. *et al.* Characterization of Streptococcus tigurinus small-colony variants causing prosthetic joint infection by comparative whole-genome analyses. *J. Clin. Microbiol.* **52,** 467–74 (2014).

166. Wellinghausen, N. *et al.* Characterization of clinical Enterococcus faecalis small-colony variants. *J. Clin. Microbiol.* **47,** 2802–11 (2009).

167. Rea, R., Hill, C. & Gahan, C. G. M. Listeria monocytogenes PerR mutants display a small-colony phenotype, increased sensitivity to hydrogen peroxide, and significantly reduced murine virulence. *Appl. Environ. Microbiol.* **71,** 8314–22 (2005).

168. Cano, D. A., Pucciarelli, M. G., Martínez-Moya, M., Casadesús, J. & García-del Portillo, F. Selection of small-colony variants of Salmonella enterica serovar typhimurium in nonphagocytic eucaryotic cells. *Infect. Immun.* **71,** 3690–8 (2003).

169. Roggenkamp, A., Hoffmann, H. & Hornef, M. W. Growth control of small-colony variants by genetic regulation of the hemin uptake system. *Infect. Immun.* **72,** 2254–62 (2004).

170. Jacob, J., Hort, G. M., Overhoff, P. & Mielke, M. E. A. In vitro and in vivo characterization of smooth small colony variants of Brucella abortus S19. *Microbes Infect.* **8,** 363–71 (2006).

171. Morton, H. E. & Shoemaker, J. The Identification of Neisseria gonorrhoeae by Means of Bacterial Variation and the Detection of Small Colony Forms in Clinical Material. *J. Bacteriol.* **50,** 585–7 (1945).

172. Day, M. Yeast petites and small colony variants: for everything there is a season. *Adv. Appl. Microbiol.* **85,** 1–41 (2013).

173. Kahl, B. C. Small colony variants (SCVs) of Staphylococcus aureus--a bacterial survival strategy. *Infect. Genet. Evol.* **21,** 515–22 (2014).

174. Tuchscherr, L. *et al.* Staphylococcus aureus small-colony variants are adapted phenotypes for intracellular persistence. *J. Infect. Dis.* **202,** 1031–40 (2010).

175. Seifert, H., Wisplinghoff, H., Schnabel, P. & von Eiff, C. Small colony variants of Staphylococcus aureus and pacemaker-related infection. *Emerg. Infect. Dis.* **9,** 1316–8 (2003).

176. Brouillette, E., Martinez, A., Boyll, B. J., Allen, N. E. & Malouin, F. Persistence of a Staphylococcus aureus small-colony variant under antibiotic pressure in vivo. *FEMS Immunol. Med. Microbiol.* **41,** 35–41 (2004).

177. Gröbner, S., Beck, J., Schaller, M., Autenrieth, I. B. & Schulte, B. Characterization of an Enterococcus faecium small-colony variant isolated from blood culture. *Int. J. Med. Microbiol.* **302,** 40–4 (2012).

178. Benes, J. *et al.* Relapsing endocarditis caused by Enterococcus faecalis forming small colony variants. *Scand. J. Infect. Dis.* **45,** 800–3 (2013).

179. Roggenkamp, A. *et al.* Chronic prosthetic hip infection caused by a small-colony variant of Escherichia coli. *J. Clin. Microbiol.* **36,** 2530–4 (1998).

180. Häussler, S., Tümmler, B., Weissbrodt, H., Rohde, M. & Steinmetz, I. Small-colony variants of Pseudomonas aeruginosa in cystic fibrosis. *Clin. Infect. Dis.* **29,** 621–5 (1999).

181. Eckweiler, D., Bunk, B., Spröer, C., Overmann, J. & Häussler, S. Complete Genome Sequence of Highly Adherent Pseudomonas aeruginosa Small-Colony Variant SCV20265. *Genome Announc.* **2,** e01232-13 (2014).

182. Malone, J. G. *et al.* YfiBNR mediates cyclic di-GMP dependent small colony

variant formation and persistence in Pseudomonas aeruginosa. *PLoS Pathog.* **6,** e1000804 (2010).

183. Schaaff, F., Bierbaum, G., Baumert, N., Bartmann, P. & Sahl, H.-G. Mutations are involved in emergence of aminoglycoside-induced small colony variants of Staphylococcus aureus. *Int. J. Med. Microbiol.* **293,** 427–35 (2003).

184. Cui, L., Neoh, H., Iwamoto, A. & Hiramatsu, K. Coordinated phenotype switching with large-scale chromosome flip-flop inversion observed in bacteria. *Proc. Natl. Acad. Sci. U. S. A.* **109,** E1647-56 (2012).

185. Wolter, D. J. *et al.* Staphylococcus aureus small-colony variants are independently associated with worse lung disease in children with cystic fibrosis. *Clin. Infect. Dis.* **57,** 384–91 (2013).

186. Sadowska, B. *et al.* Characteristics of Staphylococcus aureus , isolated from airways of cystic fibrosis patients, and their small colony variants. *FEMS Immunol. Med. Microbiol.* **32,** 191–197 (2002).

187. Bayston, R., Ashraf, W. & Smith, T. Triclosan resistance in methicillin-resistant Staphylococcus aureus expressed as small colony variants: a novel mode of evasion of susceptibility to antiseptics. *J. Antimicrob. Chemother.* **59,** 848–53 (2007).

188. Grant, S. S. & Hung, D. T. Persistent bacterial infections, antibiotic tolerance, and the oxidative stress response. *Virulence* **4,** 273–83 (2013).

189. Salunkhe, P. *et al.* A cystic fibrosis epidemic strain of Pseudomonas aeruginosa displays enhanced virulence and antimicrobial resistance. *J. Bacteriol.* **187,** 4908–20 (2005).

190. Palma, M., DeLuca, D., Worgall, S. & Quadri, L. E. N. Transcriptome Analysis of the Response of Pseudomonas aeruginosa to Hydrogen Peroxide. *J. Bacteriol.* **186,** 248–252 (2003).

191. Drenkard, E. & Ausubel, F. M. Pseudomonas biofilm formation and antibiotic resistance are linked to phenotypic variation. *Nature* **416,** 740–3 (2002).

192. Zhou, A. *et al.* Hydrogen peroxide-induced oxidative stress responses in Desulfovibrio vulgaris Hildenborough. *Environ. Microbiol.* **12,** 2645–57 (2010).

193. Folkesson, A. *et al.* Adaptation of Pseudomonas aeruginosa to the cystic fibrosis airway: an evolutionary perspective. *Nat. Rev. Microbiol.* **10,** 841–51 (2012).

194. Simpson, J. A., Smith, S. E. & Dean, R. T. Scavenging by alginate of free radicals released by macrophages. *Free Radic. Biol. Med.* **6,** 347–353 (1989).

195. Meshulam, T., Verbrugh, H. A. & Verhoef, J. Opsonization and phagocytosis of mucoid and non-mucoidPseudomonas aeruginosa strains. *Eur. J. Clin. Microbiol.* **1,** 112–117 (1982).

196. Meshulam, T., Obedeanu, N., Merzbach, D. & Sobel, J. D. Phagocytosis of mucoid and nonmucoid strains of Pseudomonas aeruginosa. *Clin. Immunol. Immunopathol.* **32,** 151–165 (1984).

197. Wood, L. F. & Ohman, D. E. Identification of genes in the σ^{22} regulon of Pseudomonas aeruginosa required for cell envelope homeostasis in either the planktonic or the sessile mode of growth. *MBio* **3,** e00094-12- (2012).

198. Starkey, M. *et al.* Pseudomonas aeruginosa rugose small-colony variants have adaptations that likely promote persistence in the cystic fibrosis lung. *J. Bacteriol.*

191, 3492–503 (2009).

199. Häussler, S. Biofilm formation by the small colony variant phenotype of Pseudomonas aeruginosa. *Environ. Microbiol.* **6,** 546–51 (2004).

200. Besier, S. *et al.* Prevalence and clinical significance of Staphylococcus aureus small-colony variants in cystic fibrosis lung disease. *J. Clin. Microbiol.* **45,** 168–72 (2007).

201. Kahl, B. *et al.* Persistent infection with small colony variant strains of Staphylococcus aureus in patients with cystic fibrosis. *J. Infect. Dis.* **177,** 1023–9 (1998).

202. WHO | Antimicrobial resistance: global report on surveillance 2014. at <http://www.who.int/drugresistance/documents/surveillancereport/en/>

203. Harris, S. R. *et al.* Evolution of MRSA during hospital transmission and intercontinental spread. *Science* **327,** 469–74 (2010).

204. Scottish Medicines Consortium About the Scottish Antimicrobial Prescribing Group (SAPG). at <https://www.scottishmedicines.org.uk/SAPG/Scottish_Antimicrobial_Prescribing_Group__SAPG_>

205. Technical Report The bacterial challenge: Time to react. at <http://ecdc.europa.eu/en/publications/Publications/0909_TER_The_Bacterial_Challenge_Time_to_React.pdf>

206. Lister, P. D., Wolter, D. J. & Hanson, N. D. Antibacterial-resistant Pseudomonas aeruginosa: clinical impact and complex regulation of chromosomally encoded resistance mechanisms. *Clin. Microbiol. Rev.* **22,** 582–610 (2009).

207. Giwercman, B., Lambert, P. A., Rosdahl, V. T., Shand, G. H. & Høiby, N. Rapid emergence of resistance in Pseudomonas aeruginosa in cystic fibrosis patients due to in-vivo selection of stable partially derepressed beta-lactamase producing strains. *J. Antimicrob. Chemother.* **26,** 247–59 (1990).

208. Giwercman, B., Meyer, C., Lambert, P. A., Reinert, C. & Høiby, N. High-level beta-lactamase activity in sputum samples from cystic fibrosis patients during antipseudomonal treatment. *Antimicrob. Agents Chemother.* **36,** 71–6 (1992).

209. Stewart, P. S. Mechanisms of antibiotic resistance in bacterial biofilms. *Int. J. Med. Microbiol.* **292,** 107–13 (2002).

210. Delcour, A. H. Outer membrane permeability and antibiotic resistance. *Biochim. Biophys. Acta* **1794,** 808–16 (2009).

211. Schwartz, T. *et al.* Whole genome and transcriptome analyses of environmental antibiotic sensitive and multi-resistant Pseudomonas aeruginosa isolates exposed to waste water and tap water. *Microb. Biotechnol.* **8,** 116–30 (2015).

212. Hancock, R. E. W. & Brinkman, F. S. L. Function of pseudomonas porins in uptake and efflux. *Annu. Rev. Microbiol.* **56,** 17–38 (2002).

213. Li, H., Luo, Y.-F., Williams, B. J., Blackwell, T. S. & Xie, C.-M. Structure and function of OprD protein in Pseudomonas aeruginosa: from antibiotic resistance to novel therapies. *Int. J. Med. Microbiol.* **302,** 63–8 (2012).

214. El Amin, N. *et al.* Carbapenem resistance mechanisms in Pseudomonas aeruginosa: alterations of porin OprD and efflux proteins do not fully explain resistance patterns

observed in clinical isolates. *APMIS* **113,** 187–96 (2005).

215. MacLeod, D. L. *et al.* Aminoglycoside-resistance mechanisms for cystic fibrosis Pseudomonas aeruginosa isolates are unchanged by long-term, intermittent, inhaled tobramycin treatment. *J. Infect. Dis.* **181,** 1180–4 (2000).

216. Boles, B. R., Thoendel, M. & Singh, P. K. Self-generated diversity produces 'insurance effects' in biofilm communities. *Proc. Natl. Acad. Sci. U. S. A.* **101,** 16630–16635 (2004).

217. Zhao, K. *et al.* Psl trails guide exploration and microcolony formation in Pseudomonas aeruginosa biofilms. *Nature* **497,** 388–91 (2013).

218. Haussler, S. Highly adherent small-colony variants of Pseudomonas aeruginosa in cystic fibrosis lung infection. *J. Med. Microbiol.* **52,** 295–301 (2003).

219. Davies, D. Understanding biofilm resistance to antibacterial agents. *Nat. Rev. Drug Discov.* **2,** 114–22 (2003).

220. Driffield, K., Miller, K., Bostock, J. M., O'Neill, A. J. & Chopra, I. Increased mutability of Pseudomonas aeruginosa in biofilms. *J. Antimicrob. Chemother.* **61,** 1053–6 (2008).

221. Molin, S. & Tolker-Nielsen, T. Gene transfer occurs with enhanced efficiency in biofilms and induces enhanced stabilisation of the biofilm structure. *Curr. Opin. Biotechnol.* **14,** 255–61 (2003).

222. Ciofu, O., Riis, B., Pressler, T., Poulsen, H. E. & Høiby, N. Occurrence of hypermutable Pseudomonas aeruginosa in cystic fibrosis patients is associated with the oxidative stress caused by chronic lung inflammation. *Antimicrob. Agents Chemother.* **49,** 2276–82 (2005).

223. Oliver, A., Cantón, R., Campo, P., Baquero, F. & Blázquez, J. High frequency of hypermutable Pseudomonas aeruginosa in cystic fibrosis lung infection. *Science* **288,** 1251–4 (2000).

224. de Beer, D., Stoodley, P. & Lewandowski, Z. Measurement of local diffusion coefficients in biofilms by microinjection and confocal microscopy. *Biotechnol. Bioeng.* **53,** 151–8 (1997).

225. Bagge, N. *et al.* Pseudomonas aeruginosa biofilms exposed to imipenem exhibit changes in global gene expression and beta-lactamase and alginate production. *Antimicrob. Agents Chemother.* **48,** 1175–87 (2004).

226. Wood, L. F., Leech, A. J. & Ohman, D. E. Cell wall-inhibitory antibiotics activate the alginate biosynthesis operon in Pseudomonas aeruginosa: Roles of sigma (AlgT) and the AlgW and Prc proteases. *Mol. Microbiol.* **62,** 412–26 (2006).

227. Hansen, C. R., Pressler, T. & Høiby, N. Early aggressive eradication therapy for intermittent Pseudomonas aeruginosa airway colonization in cystic fibrosis patients: 15 years experience. *J. Cyst. Fibros.* **7,** 523–30 (2008).

228. Al-Dhaheri, R. S. & Douglas, L. J. Absence of amphotericin B-tolerant persister cells in biofilms of some Candida species. *Antimicrob. Agents Chemother.* **52,** 1884–7 (2008).

229. Lewis, K. Multidrug tolerance of biofilms and persister cells. *Curr. Top. Microbiol. Immunol.* **322,** 107–31 (2008).

230. Roberts, M. E. & Stewart, P. S. Modelling protection from antimicrobial agents in

biofilms through the formation of persister cells. *Microbiology* **151,** 75–80 (2005).

231. Motta, S. S. *et al.* Adaptive Resistance in Bacteria Requires Epigenetic Inheritance, Genetic Noise, and Cost of Efflux Pumps. *PLoS One* **10,** e0118464 (2015).

232. Turner, K. H., Vallet-Gely, I. & Dove, S. L. Epigenetic control of virulence gene expression in Pseudomonas aeruginosa by a LysR-type transcription regulator. *PLoS Genet.* **5,** e1000779 (2009).

233. Veening, J.-W., Smits, W. K. & Kuipers, O. P. Bistability, epigenetics, and bet-hedging in bacteria. *Annu. Rev. Microbiol.* **62,** 193–210 (2008).

234. Fang, G. *et al.* Genome-wide mapping of methylated adenine residues in pathogenic Escherichia coli using single-molecule real-time sequencing. *Nat. Biotechnol.* **30,** 1232–9 (2012).

235. Motta, S. S. *et al.* Adaptive Resistance in Bacteria Requires Epigenetic Inheritance, Genetic Noise, and Cost of Efflux Pumps. *PLoS One* **10,** e0118464 (2015).

236. Croucher, N. J. & Thomson, N. R. Studying bacterial transcriptomes using RNA-seq. *Curr. Opin. Microbiol.* **13,** 619–24 (2010).

237. Woolhouse, M. & Farrar, J. Policy: An intergovernmental panel on antimicrobial resistance. *Nature* **509,** 555–557 (2014).

238. Gilbert, K. B., Kim, T. H., Gupta, R., Greenberg, E. P. & Schuster, M. Global position analysis of the Pseudomonas aeruginosa quorum-sensing transcription factor LasR. *Mol. Microbiol.* **73,** 1072–85 (2009).

239. Yu, X. *et al.* Transcriptional analysis of the global regulatory networks active in Pseudomonas syringae during leaf colonization. *MBio* **5,** e01683-14 (2014).

240. Kalghatgi, S. *et al.* Bactericidal antibiotics induce mitochondrial dysfunction and oxidative damage in Mammalian cells. *Sci. Transl. Med.* **5,** 192ra85 (2013).

241. Side effects of long-term antibiotic use linked to oxidative stress | Scope Blog. at <http://scopeblog.stanford.edu/2013/07/05/side-effects-of-long-term-antibiotic-use-linked-to-oxidative-stress/>

242. Hassett, D. J. & Imlay, J. A. Bactericidal antibiotics and oxidative stress: a radical proposal. *ACS Chem. Biol.* **2,** 708–10 (2007).

243. Kuczyńska-Wiśnik, D. *et al.* Antibiotics promoting oxidative stress inhibit formation of Escherichia coli biofilm via indole signalling. *Res. Microbiol.* **161,** 847–53 (2010).

244. Nguyen, D. *et al.* Active starvation responses mediate antibiotic tolerance in biofilms and nutrient-limited bacteria. *Science* **334,** 982–6 (2011).

245. Shatalin, K., Shatalina, E., Mironov, A. & Nudler, E. H2S: a universal defense against antibiotics in bacteria. *Science* **334,** 986–90 (2011).

246. Ochsner, U. A., Wilderman, P. J., Vasil, A. I. & Vasil, M. L. GeneChip expression analysis of the iron starvation response in Pseudomonas aeruginosa: identification of novel pyoverdine biosynthesis genes. *Mol. Microbiol.* **45,** 1277–87 (2002).

247. Palma, M., Worgall, S. & Quadri, L. E. N. Transcriptome analysis of the Pseudomonas aeruginosa response to iron. *Arch. Microbiol.* **180,** 374–9 (2003).

248. Teitzel, G. M. *et al.* Survival and growth in the presence of elevated copper: transcriptional profiling of copper-stressed Pseudomonas aeruginosa. *J. Bacteriol.*

188, 7242–56 (2006).

249. Aspedon, A., Palmer, K. & Whiteley, M. Microarray analysis of the osmotic stress response in Pseudomonas aeruginosa. *J. Bacteriol.* **188,** 2721–5 (2006).

250. Dötsch, A. *et al.* The Pseudomonas aeruginosa Transcriptome in Planktonic Cultures and Static Biofilms Using RNA Sequencing. *PLoS One* **7,** e31092 (2012).

251. Wurtzel, O. *et al.* The single-nucleotide resolution transcriptome of Pseudomonas aeruginosa grown in body temperature. *PLoS Pathog.* **8,** e1002945 (2012).

252. Koboldt, D. C., Steinberg, K. M., Larson, D. E., Wilson, R. K. & Mardis, E. R. The next-generation sequencing revolution and its impact on genomics. *Cell* **155,** 27–38 (2013).

253. Next Generation Sequencing Channel, A Revolution in Technology | Bitesize Bio. at <http://bitesizebio.com/13543/introducing-the-next-generation-sequencing-channel-part-1-ngs-a-revolution-in-technology/>

254. Mardis, E. R. Next-generation sequencing platforms. *Annu. Rev. Anal. Chem. (Palo Alto. Calif).* **6,** 287–303 (2013).

255. Quick, J. *et al.* Real-time, portable genome sequencing for Ebola surveillance. *Nature* **530,** 228–232 (2016).

256. Azarian, T. *et al.* Whole-genome sequencing for outbreak investigations of methicillin-resistant Staphylococcus aureus in the neonatal intensive care unit: time for routine practice? *Infect. Control Hosp. Epidemiol.* **36,** 777–85 (2015).

257. Harris, S. R. *et al.* Whole-genome sequencing for analysis of an outbreak of meticillin-resistant Staphylococcus aureus: a descriptive study. *Lancet. Infect. Dis.* **13,** 130–6 (2013).

258. Peacock, S. J. & Weinstock, G. M. Microbial sequencing to improve individual and population health. *Genome Med.* **6,** 103 (2014).

259. Quail, M. A. *et al.* A tale of three next generation sequencing platforms: comparison of Ion Torrent, Pacific Biosciences and Illumina MiSeq sequencers. *BMC Genomics* **13,** 341 (2012).

260. Korlach, J. *et al.* Real-time DNA sequencing from single polymerase molecules. *Methods Enzymol.* **472,** 431–55 (2010).

261. Roberts, R., Carneiro, M. & Schatz, M. The advantages of SMRT sequencing. *Genome Biol.* **14,** 405 (2013).

262. Koren, S. *et al.* Reducing assembly complexity of microbial genomes with single-molecule sequencing. *Genome Biol.* **14,** R101 (2013).

263. Powers, J. G. *et al.* Efficient and accurate whole genome assembly and methylome profiling of E. coli. *BMC Genomics* **14,** 675 (2013).

264. Murray, I. A. *et al.* The methylomes of six bacteria. *Nucleic Acids Res.* **40,** 11450–62 (2012).

265. van Heeckeren, A. M. & Schluchter, M. D. Murine models of chronic Pseudomonas aeruginosa lung infection. *Lab. Anim.* **36,** 291–312 (2002).

266. Davis, M. R. & Goldberg, J. B. Purification and visualization of lipopolysaccharide from Gram-negative bacteria by hot aqueous-phenol extraction. *J. Vis. Exp.* (2012). doi:10.3791/3916

267. Erlandsen, S. L., Kristich, C. J., Dunny, G. M. & Wells, C. L. High-resolution visualization of the microbial glycocalyx with low-voltage scanning electron microscopy: dependence on cationic dyes. *J. Histochem. Cytochem.* **52,** 1427–35 (2004).

268. Secretion Assay in Shigella flexneri —BIO-PROTOCOL. at <http://www.bio-protocol.org/e1302>

269. Dasgupta, N., Ashare, A., Hunninghake, G. W. & Yahr, T. L. Transcriptional induction of the Pseudomonas aeruginosa type III secretion system by low Ca2+ and host cell contact proceeds through two distinct signaling pathways. *Infect. Immun.* **74,** 3334–41 (2006).

270. Ramarao, N., Nielsen-Leroux, C. & Lereclus, D. The insect Galleria mellonella as a powerful infection model to investigate bacterial pathogenesis. *J. Vis. Exp.* e4392 (2012). doi:10.3791/4392

271. Jander, G., Rahme, L. G. & Ausubel, F. M. Positive correlation between virulence of Pseudomonas aeruginosa mutants in mice and insects. *J. Bacteriol.* **182,** 3843–5 (2000).

272. Hoegy, F., Mislin, G. L. A. & Schalk, I. J. Pyoverdine and pyochelin measurements. *Methods Mol. Biol.* **1149,** 293–301 (2014).

273. Grothues, D., Koopmann, U., von der Hardt, H. & Tümmler, B. Genome fingerprinting of Pseudomonas aeruginosa indicates colonization of cystic fibrosis siblings with closely related strains. *J. Clin. Microbiol.* **26,** 1973–7 (1988).

274. Grothues, D., Koopmann, U., von der Hardt, H. & Tümmler, B. Genome fingerprinting of Pseudomonas aeruginosa indicates colonization of cystic fibrosis siblings with closely related strains. *J. Clin. Microbiol.* **26,** 1973–7 (1988).

275. Lim, Y. W. *et al.* Metagenomics and metatranscriptomics: Windows on CF-associated viral and microbial communities. *J. Cyst. Fibros.* **12,** 154–164 (2013).

276. Livak, K. J. & Schmittgen, T. D. Analysis of relative gene expression data using real-time quantitative PCR and the 2(-Delta Delta C(T)) Method. *Methods* **25,** 402–8 (2001).

277. Mortazavi, A., Williams, B. A., McCue, K., Schaeffer, L. & Wold, B. Mapping and quantifying mammalian transcriptomes by RNA-Seq. *Nat. Methods* **5,** 621–8 (2008).

278. Li, H. & Durbin, R. Fast and accurate short read alignment with Burrows-Wheeler transform. *Bioinformatics* **25,** 1754–60 (2009).

279. Koboldt, D. C. *et al.* VarScan 2: somatic mutation and copy number alteration discovery in cancer by exome sequencing. *Genome Res.* **22,** 568–76 (2012).

280. Seemann, T. Prokka: rapid prokaryotic genome annotation. *Bioinformatics* **30,** 2068–9 (2014).

281. Balaban, N. Q., Merrin, J., Chait, R., Kowalik, L. & Leibler, S. Bacterial persistence as a phenotypic switch. *Science* **305,** 1622–5 (2004).

282. Lewis, K. Persister cells: molecular mechanisms related to antibiotic tolerance. *Handb. Exp. Pharmacol.* 121–33 (2012). doi:10.1007/978-3-642-28951-4_8

283. Dawson, C. C., Intapa, C. & Jabra-Rizk, M. A. 'Persisters': survival at the cellular level. *PLoS Pathog.* **7,** e1002121 (2011).

284. Marrakchi, M., Liu, X. & Andreescu, S. Oxidative stress and antibiotic resistance in bacterial pathogens: state of the art, methodologies, and future trends. *Adv. Exp. Med. Biol.* **806,** 483–98 (2014).

285. Nelson, L. K. *et al.* Phenotypic diversification in vivo: Pseudomonas aeruginosa gacS- strains generate small colony variants in vivo that are distinct from in vitro variants. *Microbiology* **156,** 3699–709 (2010).

286. Moisan, H. *et al.* Transcription of virulence factors in Staphylococcus aureus small-colony variants isolated from cystic fibrosis patients is influenced by SigB. *J. Bacteriol.* **188,** 64–76 (2006).

287. Malone, J. G. Role of small colony variants in persistence of Pseudomonas aeruginosa infections in cystic fibrosis lungs. *Infect. Drug Resist.* **8,** 237–47 (2015).

288. Hoffmann, N. *et al.* Novel mouse model of chronic Pseudomonas aeruginosa lung infection mimicking cystic fibrosis. *Infect. Immun.* **73,** 2504–14 (2005).

289. Boucher, J. C., Yu, H., Mudd, M. H. & Deretic, V. Mucoid Pseudomonas aeruginosa in cystic fibrosis: characterization of muc mutations in clinical isolates and analysis of clearance in a mouse model of respiratory infection. *Infect. Immun.* **65,** 3838–46 (1997).

290. Bjarnsholt, T. *et al.* Pseudomonas aeruginosa biofilms in the respiratory tract of cystic fibrosis patients. *Pediatr. Pulmonol.* **44,** 547–58 (2009).

291. Meyer, J. M., Neely, A., Stintzi, A., Georges, C. & Holder, I. A. Pyoverdin is essential for virulence of Pseudomonas aeruginosa. *Infect. Immun.* **64,** 518–23 (1996).

292. Cryz, S. J. J., Pitt, T. L., Furer, E. & Germanier, R. Role of lipopolysaccharide in virulence of Pseudomonas aeruginosa. *Infect. Immun.* **44,** 508–513 (1984).

293. Wang, D. *et al.* Adaptation genomics of a small-colony variant in a Pseudomonas chlororaphis 30-84 biofilm. *Appl. Environ. Microbiol.* **81,** 890–9 (2015).

294. Besier, S. *et al.* Prevalence and clinical significance of Staphylococcus aureus small-colony variants in cystic fibrosis lung disease. *J. Clin. Microbiol.* **45,** 168–72 (2007).

295. Morris, J. F., Barnes, C. G. & Sellers, T. F. An Outbreak of Typhoid Fever Due to the Small Colony Variety of Eberthella typhosa*. (1943).

296. Sabra, W., Haddad, A. M. & Zeng, A.-P. Comparative physiological study of the wild type and the small colony variant of Pseudomonas aeruginosa 20265 under controlled growth conditions. *World J. Microbiol. Biotechnol.* **30,** 1027–36 (2014).

297. Mah, T. F. & O'Toole, G. A. Mechanisms of biofilm resistance to antimicrobial agents. *Trends Microbiol.* **9,** 34–9 (2001).

298. Neut, D., Hendriks, J. G. E., van Horn, J. R., van der Mei, H. C. & Busscher, H. J. Pseudomonas aeruginosa biofilm formation and slime excretion on antibiotic-loaded bone cement. *Acta Orthop.* **76,** 109–14 (2005).

299. Schwarzmann, S. & Boring, J. R. Antiphagocytic Effect of Slime from a Mucoid Strain of Pseudomonas aeruginosa. *Infect. Immun.* **3,** 762–7 (1971).

300. LaFleur, M. D., Kumamoto, C. A. & Lewis, K. Candida albicans biofilms produce antifungal-tolerant persister cells. *Antimicrob. Agents Chemother.* **50,** 3839–46 (2006).

301. Gerber, A. U., Vastola, A. P., Brandel, J. & Craig, W. A. Selection of Aminoglycoside-Resistant Variants of Pseudomonas aeruginosa in an in Vivo Model. *J. Infect. Dis.* **146,** 691–697 (1982).

302. Britigan, B. E., Rasmussen, G. T., Olakanmi, O. & Cox, C. D. Iron acquisition from Pseudomonas aeruginosa siderophores by human phagocytes: an additional mechanism of host defense through iron sequestration? *Infect. Immun.* **68,** 1271–5 (2000).

303. Matthijs, S. *et al.* Siderophore-mediated iron acquisition in the entomopathogenic bacterium Pseudomonas entomophila L48 and its close relative Pseudomonas putida KT2440. *Biometals* **22,** 951–64 (2009).

304. Vinckx, T., Matthijs, S. & Cornelis, P. Loss of the oxidative stress regulator OxyR in Pseudomonas aeruginosa PAO1 impairs growth under iron-limited conditions. *FEMS Microbiol. Lett.* **288,** 258–65 (2008).

305. Luzar, M. A. & Montie, T. C. Avirulence and altered physiological properties of cystic fibrosis strains of Pseudomonas aeruginosa. *Infect. Immun.* **50,** 572–6 (1985).

306. Burke, V., Robinson, J. O., Richardson, C. J. & Bundell, C. S. Longitudinal studies of virulence factors of Pseudomonas aeruginosa in cystic fibrosis. *Pathology* **23,** 145–8 (1991).

307. Burke, V., Robinson, J. O., Richardson, C. J. & Bundell, C. S. Longitudinal studies of virulence factors of Pseudomonas aeruginosa in cystic fibrosis. *Pathology* **23,** 145–8 (1991).

308. Kay, E. *et al.* Two GacA-dependent small RNAs modulate the quorum-sensing response in Pseudomonas aeruginosa. *J. Bacteriol.* **188,** 6026–33 (2006).

309. Schmidt, K. D., Tümmler, B. & Römling, U. Comparative genome mapping of Pseudomonas aeruginosa PAO with P. aeruginosa C, which belongs to a major clone in cystic fibrosis patients and aquatic habitats. *J. Bacteriol.* **178,** 85–93 (1996).

310. Römling, U., Schmidt, K. D. & Tümmler, B. Large genome rearrangements discovered by the detailed analysis of 21 Pseudomonas aeruginosa clone C isolates found in environment and disease habitats. *J. Mol. Biol.* **271,** 386–404 (1997).

311. Mahan, M. J. & Roth, J. R. Ability of a bacterial chromosome segment to invert is dictated by included material rather than flanking sequence. *Genetics* **129,** 1021–32 (1991).

312. Schmidt, K. D., Tümmler, B. & Römling, U. Comparative genome mapping of Pseudomonas aeruginosa PAO with P. aeruginosa C, which belongs to a major clone in cystic fibrosis patients and aquatic habitats. *J. Bacteriol.* **178,** 85–93 (1996).

313. Malone, J. G. *et al.* The YfiBNR signal transduction mechanism reveals novel targets for the evolution of persistent Pseudomonas aeruginosa in cystic fibrosis airways. *PLoS Pathog.* **8,** e1002760 (2012).

314. Smania, A. M. Emergence of phenotypic variants upon mismatch repair disruption in Pseudomonas aeruginosa. *Microbiology* **150,** 1327–1338 (2004).

315. Martínez-Granero, F. *et al.* The Gac-Rsm and SadB signal transduction pathways converge on AlgU to downregulate motility in Pseudomonas fluorescens. *PLoS One* **7,** e31765 (2012).

316. Pseudomonas aeruginosa DK2 - Ensembl Genomes. at <http://bacteria.ensembl.org/Pseudomonas_aeruginosa_dk2/Info/Index>

317. Carver, T., Thomson, N., Bleasby, A., Berriman, M. & Parkhill, J. DNAPlotter: circular and linear interactive genome visualization. *Bioinformatics* **25,** 119–20 (2009).

318. Davis, B. M., Chao, M. C. & Waldor, M. K. Entering the era of bacterial epigenomics with single molecule real time DNA sequencing. *Curr. Opin. Microbiol.* **16,** 192–8 (2013).

319. ANGERS, B., CASTONGUAY, E. & MASSICOTTE, R. Environmentally induced phenotypes and DNA methylation: how to deal with unpredictable conditions until the next generation and after. *Mol. Ecol.* **19,** 1283–1295 (2010).

320. Bierne, H., Hamon, M. & Cossart, P. Epigenetics and bacterial infections. *Cold Spring Harb. Perspect. Med.* **2,** a010272 (2012).

321. Casadesús, J. & Low, D. A. Programmed heterogeneity: epigenetic mechanisms in bacteria. *J. Biol. Chem.* **288,** 13929–35 (2013).

322. Melter, O. & Radojevič, B. Small colony variants of Staphylococcus aureus--review. *Folia Microbiol. (Praha).* **55,** 548–58 (2010).

323. Mena, A. *et al.* Genetic adaptation of Pseudomonas aeruginosa to the airways of cystic fibrosis patients is catalyzed by hypermutation. *J. Bacteriol.* **190,** 7910–7 (2008).

324. Marvig, R. L., Sommer, L. M., Molin, S. & Johansen, H. K. Convergent evolution and adaptation of Pseudomonas aeruginosa within patients with cystic fibrosis. *Nat. Genet.* **47,** 57–64 (2014).

325. Barekzi, N. *et al.* High-Frequency Flp Recombinase-Mediated Inversions of the oriC-Containing Region of the Pseudomonas aeruginosa Genome. *J. Bacteriol.* **182,** 7070–7074 (2000).

326. B, R.-C., N, K. & GM, C. Appropriate maturation and folding of 16S rRNA during 30S subunit biogenesis are critical for translational fidelity. *Proc. Natl. Acad. Sci. U. S. A.* **107,** 4567–4572 (2010).

327. Gerasimova, Y. V & Kolpashchikov, D. M. Folding of 16S rRNA in a signal-producing structure for the detection of bacteria. *Angew. Chem. Int. Ed. Engl.* **52,** 10586–8 (2013).

328. Roy-Chaudhuri, B., Kirthi, N. & Culver, G. M. Appropriate maturation and folding of 16S rRNA during 30S subunit biogenesis are critical for translational fidelity.

329. Iorio, M. V., Piovan, C. & Croce, C. M. Interplay between microRNAs and the epigenetic machinery: An intricate network. *Biochim. Biophys. Acta - Gene Regul. Mech.* **1799,** 694–701 (2010).

330. Chuang, J. C. & Jones, P. A. Epigenetics and microRNAs. *Pediatr. Res.* **61,** 24R–29R (2007).

331. Sato, F., Tsuchiya, S., Meltzer, S. J. & Shimizu, K. MicroRNAs and epigenetics. *FEBS J.* **278,** 1598–609 (2011).

332. Non-Coding RNA | What is Epigenetics? at <http://www.whatisepigenetics.com/non-coding-rna/>

333. Alonso, A., Rojo, F. & Martínez, J. L. Environmental and clinical isolates of Pseudomonas aeruginosa show pathogenic and biodegradative properties irrespective of their origin. *Environ. Microbiol.* **1,** 421–30 (1999).

334. Gripenland, J. *et al.* RNAs: regulators of bacterial virulence. *Nat. Rev. Microbiol.* **8,** 857–66 (2010).

335. Waters, L. S. & Storz, G. Regulatory RNAs in bacteria. *Cell* **136,** 615–28 (2009).

336. Lease, R. A., Cusick, M. E. & Belfort, M. Riboregulation in Escherichia coli: DsrA RNA acts by RNA:RNA interactions at multiple loci. *Proc. Natl. Acad. Sci. U. S. A.* **95,** 12456–61 (1998).

337. Sonnleitner, E. *et al.* Detection of small RNAs in Pseudomonas aeruginosa by RNomics and structure-based bioinformatic tools. *Microbiology* **154,** 3175–87 (2008).

338. van Vliet, A. H. M. Next generation sequencing of microbial transcriptomes: challenges and opportunities. *FEMS Microbiol. Lett.* **302,** 1–7 (2010).

339. Loman, N. J. *et al.* High-throughput bacterial genome sequencing: an embarrassment of choice, a world of opportunity. *Nat. Rev. Microbiol.* **10,** 599–606 (2012).

340. Giannoukos, G. *et al.* Efficient and robust RNA-seq process for cultured bacteria and complex community transcriptomes. *Genome Biol.* **13,** R23 (2012).

341. Mathee, K., McPherson, C. J. & Ohman, D. E. Posttranslational control of the algT (algU)-encoded sigma22 for expression of the alginate regulon in Pseudomonas aeruginosa and localization of its antagonist proteins MucA and MucB (AlgN). *J. Bacteriol.* **179,** 3711–20 (1997).

342. Stintzi, A., Evans, K., Meyer, J. & Poole, K. Quorum-sensing and siderophore biosynthesis in Pseudomonas aeruginosa: lasRllasI mutants exhibit reduced pyoverdine biosynthesis. *FEMS Microbiol. Lett.* **166,** 341–345 (1998).

343. Deep, A., Chaudhary, U. & Gupta, V. Quorum sensing and Bacterial Pathogenicity: From Molecules to Disease. *J. Lab. Physicians* **3,** 4–11 (2011).

344. Lee, J.-S., Heo, Y.-J., Lee, J. K. & Cho, Y.-H. KatA, the major catalase, is critical for osmoprotection and virulence in Pseudomonas aeruginosa PA14. *Infect. Immun.* **73,** 4399–403 (2005).

345. Ochsner, U. A., Vasil, M. L., Alsabbagh, E., Parvatiyar, K. & Hassett, D. J. Role of the Pseudomonas aeruginosa oxyR-recG Operon in Oxidative Stress Defense and DNA Repair: OxyR-Dependent Regulation of katB-ankB, ahpB, and ahpC-ahpF. *J. Bacteriol.* **182,** 4533–4544 (2000).

346. Ochsner, U. A., Vasil, M. L., Alsabbagh, E., Parvatiyar, K. & Hassett, D. J. Role of the Pseudomonas aeruginosa oxyR-recG operon in oxidative stress defense and DNA repair: OxyR-dependent regulation of katB-ankB, ahpB, and ahpC-ahpF. *J. Bacteriol.* **182,** 4533–44 (2000).

347. Chung, J.-S. *et al.* Interaction domain on thioredoxin for Pseudomonas aeruginosa 5'-adenylylsulfate reductase. *J. Biol. Chem.* **284,** 31181–9 (2009).

348. Hishinuma, S., Ohtsu, I., Fujimura, M. & Fukumori, F. OxyR is involved in the expression of thioredoxin reductase TrxB in Pseudomonas putida. *FEMS Microbiol. Lett.* **289,** 138–45 (2008).

349. Tielker, D. *et al.* Pseudomonas aeruginosa lectin LecB is located in the outer membrane and is involved in biofilm formation. *Microbiology* **151,** 1313–23 (2005).

350. Frederiksen, R. F. *et al.* Bacterial chitinases and chitin-binding proteins as virulence

factors. *Microbiology* **159,** 833–47 (2013).

351. Sanchez, P. Fitness of in vitro selected Pseudomonas aeruginosanalB and nfxB multidrug resistant mutants. *J. Antimicrob. Chemother.* **50,** 657–664 (2002).

352. Cezairliyan, B. *et al.* Identification of Pseudomonas aeruginosa phenazines that kill Caenorhabditis elegans. *PLoS Pathog.* **9,** e1003101 (2013).

353. Ulanova, M. *et al.* The clonal antibody response to Pseudomonas aeruginosa heat shock protein is highly diverse in cystic fibrosis patients. *APMIS* **105,** 449–56 (1997).

354. Painter, K. L. *et al.* Staphylococcus aureus adapts to oxidative stress by producing H2O2-resistant small colony variants via the SOS response. *Infect. Immun.* **83,** 1830–1844 (2015).

355. Lim, C. K. *et al.* The Effect of Iron Limitation on the Transcriptome and Proteome of Pseudomonas fluorescens Pf-5. *PLoS One* **7,** e39139 (2012).

356. Mikkelsen, H., Sivaneson, M. & Filloux, A. Key two-component regulatory systems that control biofilm formation in Pseudomonas aeruginosa. *Environ. Microbiol.* **13,** 1666–81 (2011).

357. Wittekindt, N. E. *et al.* Nodeomics: pathogen detection in vertebrate lymph nodes using meta-transcriptomics. *PLoS One* **5,** e13432 (2010).

358. SANDERS, N. N. *et al.* Cystic Fibrosis Sputum. *http://dx.doi.org/10.1164/ajrccm.162.5.9909009* (2012).

359. Chen, Z. & Duan, X. Ribosomal RNA depletion for massively parallel bacterial RNA-sequencing applications. *Methods Mol. Biol.* **733,** 93–103 (2011).

360. Small Colony Variants of Pseudomonas aeruginosa in Cystic Fibrosis. at <http://cid.oxfordjournals.org/content/29/3/621.full.pdf>

361. Brackman, G. & Coenye, T. Quorum sensing inhibitors as anti-biofilm agents. *Curr. Pharm. Des.* **21,** 5–11 (2015).

362. Høiby, N., Bjarnsholt, T., Givskov, M., Molin, S. & Ciofu, O. Antibiotic resistance of bacterial biofilms. *Int. J. Antimicrob. Agents* **35,** 322–32 (2010).

363. Mandal, M. D. & Mandal, S. Honey: its medicinal property and antibacterial activity. *Asian Pac. J. Trop. Biomed.* **1,** 154–60 (2011).

Appendices

A. Participant Information Leaflet

Please reply to: Dr Sharon Irvine
B429, Level 4
Biomedical Research Centre
University of Glasgow
G12 8QQ
Tel: 01413308133, Mobile: 07736231751
E-mail: Sharon.irvine@glasgow.ac.uk

Participant Information Leaflet

1. Study title

A study to look at the changes in RNA production of bacteria within the cystic fibrosis lung and mechanisms by which bacteria become resistant to antibiotics.

Study Doctor: Sharon Irvine
Chief Investigator: Dr D Walker

You are being invited to take part in a research study. Before you decide it is important for you to understand why the research is being done and what it will involve. Please take time to read the following information carefully and discuss it with others if you wish. Ask us if there is anything that is not clear or if you would like more information. Take time to decide whether or not you wish to take part.

2. What is the purpose of the study?

This project aims to discover the mechanisms by which bacteria become resistant to antibiotics. Such resistance is widespread and growing and the development of novel antibiotics is much needed. Rather than study the changes in the DNA of bacteria that

underlie resistance, we will study the changes in RNA produced by bacteria following antibiotics. RNA is the 'messenger' of DNA that directs which proteins the bacteria makes. The pattern of RNA production alters depending on the bacterial environment. We will study these changes in the bacterium *Pseudomonas aeruginosa* found in the airways of patients with cystic fibrosis, an inherited disease that leads to infection in the airways with this microbe. By following the changes in the pattern of RNA produced in patients following antibiotic exposure, we will identify novel targets for drugs that can prevent bacterial growth.

This study will be carried out over a period of approximately 2 years.

3. Why have I been chosen?

You have been chosen because you have cystic fibrosis and are aged between 16 and 40. The bacteria which we are interested in is found in high numbers within the airways of cystic fibrosis patients which allows us to look at the genetic material within this organism. We hope to recruit approximately 20 patients to this study.

4. Do I have to take part?

It is up to you whether or not to take part. If you decide to take part you will be given this information sheet to keep and be asked to sign a consent form. If you decide to take part you are still free to withdraw at any time without giving a reason.

5. What will happen to me if I take part?

If you are happy with the information and agree to participate you will attend the Cystic Fibrosis Unit in Gartnavel General where any remaining queries will be discussed.

We are looking to recruit 3 different groups of patient. The first group will be stable, on regular nebulised antibiotics only. An initial sputum sample will be routinely obtained on day 1 and then following inhaled therapy at weekly intervals over a 3-week period. This will be repeated approximately 1 year later. The second group will be patients who have been newly colonised with *Pseudomonas aeruginosa*. Sputum samples will be obtained on day 1 and then at regular intervals during routine visits while on therapy until sputum production ceases. The third group will be chronically colonised patients who are undergoing an infective exacerbation. Samples will be routinely collected on day 1 and then at regular intervals during the exacerbation until resolution.

Sputum samples will be obtained during your routine visits to the Cystic Fibrosis Unit during the study period. It is essential that the sputum samples are immediately frozen following expectoration to ensure the bacteria remain in a stable state to give us an idea of how they behave inside your lungs. Once the sputum samples have been collected they will be analysed within a separate laboratory.

6. What do I have to do?

You can carry on as normal and there are no restrictions on your daily activities. The only thing we ask is that you are able to attend the unit to enable collection of the sputum sample.

7. What are the possible disadvantages and risks of taking part?

The only disadvantage of taking part is the inconvenience of having to attend the unit to provide the sputum samples. No blood sampling or other invasive samples are required.

8. What are the possible benefits of taking part?

The information gained during this study will hopefully enable future research into developing new antibiotic targets to treat the complex bacterial infections in cystic fibrosis.

9. Will my taking part be kept confidential?

All information which is collected about you during the course of the research will be kept strictly confidential. You will be identified by an ID number and any information about you will have your name and address removed so that you cannot be recognised from it.

10. What will happen to the results of the research study?

The results of the study will be published and used in further research aimed at antibiotic development. We will also provide full feedback from the study to all participants.

11. What will happen to my samples after the study has finished?

The sputum samples which you provide for this study will be processed to extract information from the bacteria within the samples. The samples will be analysed in such a way that the results will not be directly traceable to you. This information may then be used for future research. A separate aliquot of the sample will be stored for the entire period of the research project.

12. What will happen if I don't want to carry on with the study?

You can withdraw at any time from the study. If you wish to withdraw from the study, we will retain the data that has been collected up to your withdrawal. However, should you wish for samples and data to be destroyed we will comply with this request.

13. Who is organising and funding the research?

The study is funded by the Medical Research Council (MRC)

14. Further information

If you wish to ask further information about the study now or at any time, please contact the study doctor, Dr Sharon Irvine. She can be contacted as above, by phone or e-mail, to discuss anything or meet in person. You can also contact Professor T Evans at any time to discuss any other details:

Details: Dr D Walker
Level 2 GBRC
120 University Place
G12 8TA

Other Contact: Dr Neil Ritchie
Level 4 GBRC
120 University place
G12 8TA
E-mail: neil.ritchie@glasgow.ac.uk

Thank you for taking time to read this information sheet and for agreeing to take part in this study…

B. Consent Form

Centre Number:

Study Number:

Patient Identification number for this trial:

CONSENT FORM

Title of Project: Transcriptome analysis of Pseudomonas aeruginosa under antibiotic pressure

Name of Researcher: Dr Sharon Irvine

Principal Investigator: Dr D Walker

Please initial box

1. I confirm that I have read and understood the information sheet (version 1, 08/01/13) for the above study and have had the opportunity to ask questions. ☐

2. I understand that my participation is voluntary and that I am free to withdraw at any time, without giving any reason and without my medical care or legal rights being affected ☐

3. I understand that sections of any medical notes may be looked at by responsible individuals involved directly with this study where it is relevant to my taking part in this research study. I give permission for these individuals to have access to my records. ☐

4. I agree to take part in the above study. ☐

_____	_____	_____
Name of subject	Date	Signature
_____	_____	_____
Name of researcher/Person taking consent	Date	Signature

C. Gene expression values following analysis on CLC Workbench. Fold change negative values suggest down regulation in SCV as compared to NH.

Feature ID	EDGE test: group 2 vs group 1, tagwise dispersions - Fold change	EDGE test: group 2 vs group 1, tagwise dispersions - FDR p-value correction	Functional group	PA01 Mapping ID	Annotations - Source reference id
dnaA	-4.417184334	0.01439246	DNA replication, recombination, modification and repair	PA0001	NHmuc_00001
NHmuc_00055	6.912988853	6.09029E-07	hypothetical, unclassified, unknown	PA0050	NHmuc_00055
NHmuc_00056	3.797302019	0.000467657	hypothetical, unclassified, unknown	PA0050	NHmuc_00056
NHmuc_00058	2.403837681	0.026370836	Cell Wall/LPS/Capsule	PA0052	NHmuc_00058
osmC	-4.124303156	0.005184752	oxidative stress	PA0059	NHmuc_00064
NHmuc_00065	-2.695360637	0.025427029	hypothetical, unclassified, unknown	PA0060	NHmuc_00065
NHmuc_00067	-3.947267164	0.000196897	Cell Wall/LPS/Capsule	PA0062	NHmuc_00067
NHmuc_00073	3.815671061	0.000341974	transcription regulator	PA0068	NHmuc_00073
NHmuc_00107	-4.006235926	0.014124146	energy metabolism	PA0102	NHmuc_00107
NHmuc_00127	9.938974956	5.84887E-07	Secreted Factors (Virulence factors, toxins, biofilm enzymes, alginate)	PA0122	NHmuc_00127
NHmuc_00129	-2.078320785	0.03616119	phage, transposon or plasmid	PA0124	NHmuc_00129
NHmuc_00130	-6.325768289	0.000829674	transcription regulator	PA0125	NHmuc_00130
NHmuc_00133	-5.819174966	0.009065186	fatty acid, phospholipid and rhamnolipid metabolism	PA0128	NHmuc_00133
ahpC	17.64515406	8.97871E-08	oxidative stress	PA0139	NHmuc_00144
ahpF	28.06951992	8.39621E-13	oxidative stress	PA0140	NHmuc_00145
ppk2	2.765805026	0.030434916	Energy metabolism	PA0141	NHmuc_00146
aer2	2.754846702	0.029845438	Energy metabolism	PA0176	NHmuc_00180
NHmuc_00181	4.296568205	3.1021E-06	Chemotaxis	PA0177	NHmuc_00181
NHmuc_00182	2.977963715	0.004102209	two-component regulatory system	PA0178	NHmuc_00182
NHmuc_00183	3.58660234	2.73725E-06	two-component regulatory system	PA0179	NHmuc_00183
NHmuc_00205	5.252044554	8.46278E-06	hypothetical, unclassified, unknown	PA0200	NHmuc_00205
NHmuc_00206	-2.140455628	0.034475291	energy metabolism	PA0201	NHmuc_00206
NHmuc_00215	2.618696816	0.023708185	Energy metabolism	PA0209	NHmuc_00215
mdcC	3.239568263	0.008933071	protein and amino	PA0210	NHmuc_00216

			acid biosynthesis and metabolism		
NHmuc_00256	4.84646436	4.05693E-09	protein and amino acid biosynthesis and metabolism	PA0249	NHmuc_00256
NHmuc_00257	18.74050045	1.36694E-12	Regulatory protein (cell cycle, immune response)	PA0250	NHmuc_00257
NHmuc_00269	2.336141528	0.003241178	hypothetical, unclassified, unknown	PA0261	NHmuc_00269
NHmuc_00280	2.082581884	0.022599324	antibiotic resistance	PA0271	NHmuc_00280
NHmuc_00329	-3.96395054	0.013287939	hypothetical, unclassified, unknown		NHmuc_00329
NHmuc_00333	2.410674132	0.001860987	hypothetical, unclassified, unknown	PA0320	NHmuc_00333
NHmuc_00359	2.178176936	0.02503635	Energy metabolism	PA0344	NHmuc_00359
pfpI	-3.455682413	0.011493221	Protein and amino acid biosynthesis and metabolism	PA0355	NHmuc_00370
mutM	-3.292712577	0.022121784	DNA replication, recombination, modification and repair	PA0357	NHmuc_00372
NHmuc_00374	-2.612659909	0.01732446	antibiotic resistance	PA0359	NHmuc_00374
rpoH	-6.582541497	0.007450432	transcription regulator	PA0376	NHmuc_00392
NHmuc_00393	-3.606447893	0.001476058	hypothetical, unclassified, unknown	PA0377	NHmuc_00393
pilH	-2.777035298	0.015147122	motility and attachement	PA0409	NHmuc_00426
mexA_1	-4.580523043	0.002188593	antibiotic resistance		NHmuc_00442
mexA_2	-3.997796433	0.004328301	antibiotic resistance		NHmuc_00443
NHmuc_00462	4.394215943	7.44869E-05	protein and amino acid biosynthesis and metabolism	PA0446	NHmuc_00462
gcdH	6.21517268	4.26321E-05	protein and amino acid biosynthesis and metabolism	PA0447	NHmuc_00463
NHmuc_00465	5.235417877	0.008316796	protein and amino acid biosynthesis and metabolism	PA0449	NHmuc_00465
NHmuc_00476	3.425778412	0.026370836	Energy metabolism	PA0459	NHmuc_00476
NHmuc_00479	-6.47893064	0.001072343	Ribosome structure/function	PA0462	NHmuc_00479
glcB	-4.527515853	0.014774233	fatty acid, phospholipid and rhamnolipid metabolism	PA0482	NHmuc_00500
NHmuc_00523	3.921597223	4.45334E-07	hypothetical, unclassified, unknown	PA0505	NHmuc_00523
NHmuc_00546	6.486084936	0.002005233	transcription regulator		NHmuc_00546
NHmuc_00565	-4.226238871	0.02311624	energy metabolism	PA0545	NHmuc_00565
NHmuc_00574	-3.2189795	0.008966678	Cell Wall/LPS/Capsule	PA0554	NHmuc_00574
fda	-3.868306178	0.016265295	energy metabolism	PA0555	NHmuc_00575
rpoD	-5.217847143	0.008037573	transcription regulator	PA0576	NHmuc_00599
NHmuc_00652	-5.3703391	0.006700525	motility and attachement	PA0646	NHmuc_00652
NHmuc_00653	-4.649814117	0.002938608	hypothetical, unclassified, unknown	PA0645	NHmuc_00653
trpG	-2.439994206	0.019127209	protein and amino acid biosynthesis and metabolism	PA0649	NHmuc_00654
NHmuc_00658	-2.757112638	0.025731279	oxidative stress	PA0653	NHmuc_00658

NHmuc_00715	-5.182420296	0.003271859	energy metabolism	PA4657	NHmuc_00715
NHmuc_00716	-2.934437584	0.038795247	energy metabolism	PA4656	NHmuc_00716
hemH	2.34321811	0.022137328	iron acquisition/virulence	PA4655	NHmuc_00717
upp	-2.829747194	0.030156143	nucleotide biosynthesis	PA4646	NHmuc_00726
NHmuc_00733	-3.119627003	0.010261734	Cell Wall/LPS/Capsule	PA4639	NHmuc_00733
NHmuc_00734	5.522850153	3.86682E-07	hypothetical, unclassified, unknown	PA4970	NHmuc_00734
NHmuc_00735	-4.489544412	0.000178199	Cell Wall/LPS/Capsule	PA4637	NHmuc_00735
NHmuc_00754	-3.331648614	0.029757251	energy metabolism	PA4621	NHmuc_00754
NHmuc_00756	-3.360049742	0.01515352	energy metabolism	PA4619	NHmuc_00756
katB	7.785278283	9.04805E-06	oxidative stress	PA4613	NHmuc_00763
NHmuc_00764	5.483471901	4.81596E-09	Regulatory protein (cell cycle, immune response)	PA4612	NHmuc_00764
NHmuc_00769	3.52970777	0.028270492	hypothetical, unclassified, unknown	PA4607	NHmuc_00769
nfxB	-20.58306321	3.72094E-07	transcription regulator	PA4600	NHmuc_00776
mexC	-52.82022287	1.07118E-11	antibiotic resistance	PA4599	NHmuc_00777
mexD	-15.43872456	9.52068E-07	antibiotic resistance	PA4598	NHmuc_00778
oprJ	-4.3861873	0.001144294	antibiotic resistance	PA4597	NHmuc_00779
NHmuc_00780	-6.708913648	0.001348001	transcription regulator	PA4596	NHmuc_00780
ccpR	2.987365074	0.003065934	oxidative stress	PA4587	NHmuc_00790
fklB	-3.375765517	0.005873078	Protein and amino acid biosynthesis and metabolism	PA4572	NHmuc_00806
rplU	-5.378661115	0.023536876	Ribosome structure/function	PA4568	NHmuc_00810
rluD	-3.568246296	0.033070963	RNA Processing and degradation	PA4544	NHmuc_00835
clpB	-20.67680515	6.45696E-06	Heat Shock and chaperones	PA4542	NHmuc_00837
nadC	-7.308412635	0.001094572	energy metabolism	PA4524	NHmuc_00859
mreB	-4.612192835	0.012778889	Cell Wall/LPS/Capsule	PA4481	NHmuc_00902
NHmuc_00908	-3.331458138	0.039710924	energy metabolism	PA4475	NHmuc_00908
NHmuc_00909	-6.812659917	0.002604302	hypothetical, unclassified, unknown	PA4474	NHmuc_00909
NHmuc_00910	-3.09977908	0.021356826	Protein and amino acid biosynthesis and metabolism	PA4473	NHmuc_00910
pmbA	-5.162599437	0.001476058	Protein and amino acid biosynthesis and metabolism	PA4472	NHmuc_00911
NHmuc_00925	-3.555247885	0.034475291	energy metabolism	PA4458	NHmuc_00925
NHmuc_00926	-4.424490025	0.023570287	energy metabolism	PA4457	NHmuc_00926
NHmuc_00928	-6.339799586	0.002212046	transport, Secretion, export	PA4456	NHmuc_00928
ttg2C	-2.862358721	0.020689842	transport, Secretion, export	PA4454	NHmuc_00930
NHmuc_00934	-5.082510518	0.004991789	DNA replication, recombination, modification and repair	PA4451	NHmuc_00934
murA	-6.996152938	0.000820513	energy metabolism	PA4450	NHmuc_00935
hisG	-4.579490199	0.000153815	energy metabolism	PA4449	NHmuc_00936

rplM	-5.084477772	0.010534557	Ribosome structure/function	PA4433	NHmuc_00952
NHmuc_00963	-2.63122443	0.038264587	DNA replication, recombination, modification and repair	PA4422	NHmuc_00963
NHmuc_00965	-4.935622795	0.011389538	cell division	PA4421	NHmuc_00965
lpxC	-4.735781813	0.016628566	energy metabolism	PA4406	NHmuc_00980
NHmuc_00996	-3.822944761	0.014157681	Transcription/translation	PA4390	NHmuc_00996
fabG_2	-4.024183578	0.006222881	fatty acid, phospholipid and rhamnolipid metabolism	PA4389	NHmuc_00997
NHmuc_00998	-2.281200463	0.027606805	protein and amino acid biosynthesis and metabolism	PA4388	NHmuc_00998
fxsA	-18.00374256	7.85429E-08	Cell Wall/LPS/Capsule	PA4387	NHmuc_00999
NHmuc_01000	-22.88183657	1.70096E-05	hypothetical, unclassified, unknown		NHmuc_01000
groES	-12.23549685	3.92972E-05	Heat Shock and chaperones	PA4386	NHmuc_01001
NHmuc_01002	-8.64006117	0.00031396	Heat Shock and chaperones	PA4385	NHmuc_01002
NHmuc_01010	-3.276970611	0.032909106	DNA replication, recombination, modification and repair	PA4379	NHmuc_01010
inaA	-3.869942007	0.015655542	energy metabolism	PA4378	NHmuc_01011
NHmuc_01012	3.218781827	0.003749137	Hypothetical, unclassified, Unknown	PA4377	NHmuc_01012
NHmuc_01024	-16.1325674	6.05419E-07	transport, Secretion, export	PA4365	NHmuc_01024
NHmuc_01025	-75.16156702	2.59164E-11	energy metabolism	PA4364	NHmuc_01025
feoC	2.684424557	0.010672553	iron acquisition/virulence	PA4357	NHmuc_01033
purU	-3.027127956	0.036332027	energy metabolism	PA4314	NHmuc_01076
flp	2.806111225	0.012156795	motility and attachement	PA4306	NHmuc_01085
NHmuc_01112	2.715747751	0.008918753	hypothetical, unclassified, unknown		NHmuc_01112
NHmuc_01167	-4.197802177	0.015223029	hypothetical, unclassified, unknown	PA0731	NHmuc_01167
NHmuc_01173	-16.24166877	4.70777E-06	hypothetical, unclassified, unknown	PA2756	NHmuc_01173
NHmuc_01174	-14.2488547	3.26594E-07	hypothetical, unclassified, unknown	PA0737	NHmuc_01174
NHmuc_01175	-3.706217666	0.00149126	Cell Wall/LPS/Capsule	PA0738	NHmuc_01175
algU	-11.01533341	0.000182745	Secreted Factors (Virulence factors, toxins, biofilm enzymes, alginate)	PA0762	NHmuc_01201
mucA	-12.88423353	7.40696E-05	transcription regulator	PA0763	NHmuc_01202
mucB	-4.557460593	0.012661257	Secreted Factors (Virulence factors, toxins, biofilm enzymes, alginate)	PA0764	NHmuc_01203
lepA	-3.780130196	0.033183495	Transcription/translation	PA0767	NHmuc_01206
NHmuc_01218	-4.198920945	0.019010709	Protein and amino acid biosynthesis and metabolism	PA0779	NHmuc_01218
NHmuc_01255	2.764333982	0.012156795	nucleotide	PA0814	NHmuc_01255

			biosynthesis		
NHmuc_01265	2.28085322	0.017085558	hypothetical, unclassified, unknown	PA3300	NHmuc_01265
coaB	2.70384762	0.002586297	phage, transposon or plasmid	PA0723	NHmuc_01270
NHmuc_01284	-7.136382142	0.001110397	Cell Wall/LPS/Capsule	PA0833	NHmuc_01284
slyD	-6.534345885	0.008156815	Protein and amino acid biosynthesis and metabolism	PA0837	NHmuc_01289
NHmuc_01290	-2.609395295	0.034375835	oxidative stress	PA0838	NHmuc_01290
NHmuc_01300	35.58361869	3.74161E-15	oxidative stress	PA0848	NHmuc_01300
trxB2	54.81523674	3.98306E-16	oxidative stress	PA0849	NHmuc_01301
cbpD	6.610567731	4.11705E-06	Secreted Factors (Virulence factors, toxins, biofilm enzymes, alginate)	PA0852	NHmuc_01304
rsmA	-14.93915724	0.000746199	transcription regulator	PA0905	NHmuc_01359
NHmuc_01360	-4.900166645	0.000183243	hypothetical, unclassified, unknown		NHmuc_01360
NHmuc_01361	-4.609022852	0.000637352	hypothetical, unclassified, unknown		NHmuc_01361
NHmuc_01364	-3.64401698	0.001392162	hypothetical, unclassified, unknown	PA0907	NHmuc_01364
mgtE	-7.863457474	0.000433862	transport, Secretion, export	PA0913	NHmuc_01370
NHmuc_01379	-4.521229961	0.001204117	transcription regulator	PA0922	NHmuc_01379
cysM	-3.800231505	0.027112295	protein and amino acid biosynthesis and metabolism	PA0932	NHmuc_01390
NHmuc_01396	2.605107146	0.029013593	transcription regulator	PA0938	NHmuc_01396
NHmuc_01401	-5.784237538	0.002938608	transcription regulator	PA0942	NHmuc_01401
NHmuc_01402	-3.65809684	0.029709357	energy metabolism	PA0943	NHmuc_01402
wrbA	-3.183162038	0.004118766	energy metabolism	PA0949	NHmuc_01408
NHmuc_01409	-3.335953213	0.016510761	arsenic metabolism	PA0950	NHmuc_01409
NHmuc_01422	6.184556714	0.000406335	oxidative stress	PA0962	NHmuc_01422
NHmuc_01434	-3.597560136	0.021356826	Cell Wall/LPS/Capsule	PA0974	NHmuc_01434
phnB	-2.578358098	0.025076641	protein and amino acid biosynthesis and metabolism	PA1002	NHmuc_01452
mvfR	-3.570357336	0.02503635	transcription regulator	PA1003	NHmuc_01453
NHmuc_01495	4.535217414	3.646E-07	Cell Wall/LPS/Capsule	PA1041	NHmuc_01495
NHmuc_01508	-8.160000738	0.002909878	Cell Wall/LPS/Capsule	PA1053	NHmuc_01508
NHmuc_01523	-2.959928862	0.023952779	Heat Shock and chaperones	PA1068	NHmuc_01523
NHmuc_01571	-5.497764274	5.12623E-05	Cell Wall/LPS/Capsule	PA1114	NHmuc_01571
NHmuc_01572	-3.797682932	0.029988851	Protein and amino acid biosynthesis and metabolism	PA1115	NHmuc_01572
NHmuc_01584	-4.362185577	0.001456352	energy metabolism	PA1127	NHmuc_01584
NHmuc_01586	2.046359001	0.032080301	antibiotic resistance	PA1129	NHmuc_01586
rhlC	2.490172951	0.001465559	fatty acid, phospholipid and rhamnolipid metabolism	PA1130	NHmuc_01587
NHmuc_01593	-7.672642989	2.47166E-05	transcription regulator	PA1136	NHmuc_01593
NHmuc_01594	-13.29593162	2.08823E-05	energy metabolism	PA1137	NHmuc_01594

NHmuc_01596	-3.37854828	0.001144294	Secreted Factors (Virulence factors, toxins, biofilm enzymes, alginate)	PA1139	NHmuc_01596
NHmuc_01628	6.776299037	1.29335E-08	hypothetical, unclassified, unknown	PA1168	NHmuc_01628
napB	2.59548182	0.000738088	Energy metabolism	PA1173	NHmuc_01633
napD	2.241452819	0.013677427	protein and amino acid biosynthesis and metabolism	PA1175	NHmuc_01635
napF	2.280340144	0.025427029	iron acquisition/virulence	PA1176	NHmuc_01636
NHmuc_01717	2.251167363	0.005877206	hypothetical, unclassified, unknown	PA1245	NHmuc_01717
aprE	2.180551102	0.012481039	transport, Secretion, export	PA1247	NHmuc_01719
aprF	3.471657702	2.60049E-05	Cell Wall/LPS/Capsule	PA1248	NHmuc_01720
aprA	11.71633006	5.10912E-08	Secreted Factors (Virulence factors, toxins, biofilm enzymes, alginate)	PA1249	NHmuc_01721
NHmuc_01736	-2.518645973	0.018900082	transcription regulator	PA1264	NHmuc_01736
NHmuc_01739	2.656807799	0.02677326	iron acquisition/virulence	PA2193	NHmuc_01739
cobU	2.141040954	0.036481054	Energy metabolism	PA1278	NHmuc_01752
cobS	-3.206297988	0.002752124	energy metabolism	PA1281	NHmuc_01755
NHmuc_01757	-6.807554907	0.000270892	transcription regulator	PA1283	NHmuc_01757
NHmuc_01783	-2.902006306	0.018900082	transcription regulator	PA1309	NHmuc_01783
NHmuc_01843	5.51137458	0.005265267	hypothetical, unclassified, unknown	PA2500	NHmuc_01843
rsaL	6.047906396	0.011907376	Regulatory protein (cell cycle, immune response)	PA1431	NHmuc_01889
NHmuc_01929	-8.730001291	1.70018E-08	Cell Wall/LPS/Capsule	PA1471	NHmuc_01929
ccmH	2.125556767	0.024299075	iron acquisition/virulence	PA1482	NHmuc_01940
cycH	2.828875063	0.000562129	iron acquisition/virulence	PA1483	NHmuc_01941
hcpC_2	2.055387573	0.017628142	Type IV secretion system	PA1511	NHmuc_01971
NHmuc_02000	-3.170950536	0.004216376	transcription regulator	PA1539	NHmuc_02000
NHmuc_02001	-3.348894816	0.018561762	antibiotic resistance	PA1540	NHmuc_02001
NHmuc_02002	-3.996697211	0.000301358	antibiotic resistance	PA1541	NHmuc_02002
NHmuc_02052	-2.993159578	0.013173308	hypothetical, unclassified, unknown		NHmuc_02052
sucC	-3.81566461	0.035295519	energy metabolism	PA1588	NHmuc_02053
NHmuc_02057	-7.115936005	0.000178199	Cell Wall/LPS/Capsule	PA1592	NHmuc_02057
htpG	-23.28094446	3.58411E-07	Heat Shock and chaperones	PA1596	NHmuc_02061
NHmuc_02062	-2.621308324	0.015282819	energy metabolism	PA1597	NHmuc_02062
NHmuc_02074	-5.865210601	0.00251593	fatty acid, phospholipid and rhamnolipid metabolism	PA1609	NHmuc_02074
fabA	-9.712881246	1.20881E-05	fatty acid, phospholipid and rhamnolipid metabolism	PA1610	NHmuc_02075
gpsA	-3.787295825	0.028046734	energy metabolism	PA1614	NHmuc_02079

NHmuc_02119	-2.927687842	0.013970729	transcription regulator	PA1653	NHmuc_02119
NHmuc_02122	3.559520708	0.003329986	DNA replication, recombination, modification and repair	PA1656	NHmuc_02122
impB3	3.222670815	1.49419E-05	DNA replication, recombination, modification and repair	PA1657	NHmuc_02123
NHmuc_02197	-2.494485198	0.036332027	protein and amino acid biosynthesis and metabolism	PA1729	NHmuc_02197
NHmuc_02204	2.882381314	0.000467782	hypothetical, unclassified, unknown	PA2108	NHmuc_02204
NHmuc_02208	-2.919519093	0.003414642	energy metabolism	PA1739	NHmuc_02208
NHmuc_02217	-3.492152455	0.02503635	fatty acid, phospholipid and rhamnolipid metabolism	PA1748	NHmuc_02217
cysB	-3.959456548	0.030317032	transcription regulator	PA1754	NHmuc_02223
NHmuc_02224	-3.595810992	0.006792633	hypothetical, unclassified, unknown	PA1755	NHmuc_02224
NHmuc_02238	-4.619928432	0.01250702	energy metabolism	PA1769	NHmuc_02238
ppsA	-4.392060187	0.019900789	energy metabolism	PA1770	NHmuc_02239
NHmuc_02271	-6.641639409	1.70096E-05	hypothetical, unclassified, unknown	PA3678	NHmuc_02271
NHmuc_02272	-2.878996229	0.012156795	Secreted Factors (Virulence factors, toxins, biofilm enzymes, alginate)	PA3319	NHmuc_02272
clpP	-3.948610443	0.029013593	Protein and amino acid biosynthesis and metabolism	PA1801	NHmuc_02277
clpX	-10.93022828	0.000449626	Secreted Factors (Virulence factors, toxins, biofilm enzymes, alginate)	PA1802	NHmuc_02278
lon	-9.404774021	0.000577797	DNA replication, recombination, modification and repair	PA1803	NHmuc_02279
hupB	-4.05696024	0.039633641	DNA replication, recombination, modification and repair	PA1804	NHmuc_02280
ppiD	-4.836174321	0.005722003	Heat Shock and chaperones	PA1805	NHmuc_02282
NHmuc_02316	2.458266941	0.01982077	hypothetical, unclassified, unknown	PA2847	NHmuc_02316
NHmuc_02317	2.039027757	0.023708185	hypothetical, unclassified, unknown	PA0072	NHmuc_02317
NHmuc_02326	-5.607963032	0.00415351	oxidative stress/iron acquisition	PA1847	NHmuc_02326
NHmuc_02350	28.53120916	1.3634E-26	fatty acid, phospholipid and rhamnolipid metabolism	PA1869	NHmuc_02350
lasA	4.301121418	0.000350216	Secreted Factors (Virulence factors, toxins, biofilm enzymes, alginate)	PA1871	NHmuc_02352
NHmuc_02370	-4.161076002	0.002572734	hypothetical, unclassified, unknown	PA1889	NHmuc_02370
phzB1_1	4.582647863	0.002122241	Secreted Factors (Virulence factors, toxins, biofilm	PA1900	NHmuc_02381

			enzymes, alginate)		
phzC1_1	5.810319852	6.24453E-06	Secreted Factors (Virulence factors, toxins, biofilm enzymes, alginate)	PA4212	NHmuc_02382
phzD1_1	3.80043932	0.000763431	Secreted Factors (Virulence factors, toxins, biofilm enzymes, alginate)	PA4213	NHmuc_02383
phzE1_1	7.015658355	3.15044E-06	Secreted Factors (Virulence factors, toxins, biofilm enzymes, alginate)	PA4214	NHmuc_02384
NHmuc_02465	2.348114795	0.028169864	protein and amino acid biosynthesis and metabolism	PA1985	NHmuc_02465
NHmuc_02479	3.356269444	7.34043E-05	protein and amino acid biosynthesis and metabolism	PA1999	NHmuc_02479
maiA	2.312535177	0.039710924	Energy metabolism	PA2007	NHmuc_02487
fahA	2.042346251	0.014870066	Protein and amino acid biosynthesis and metabolism	PA2008	NHmuc_02488
galU	-4.492685043	0.011797459	energy metabolism	PA2023	NHmuc_02503
NHmuc_02511	2.139675735	0.011686936	hypothetical, unclassified, unknown	PA2031	NHmuc_02511
cynR	-3.109134891	0.013103741	transcription regulator	PA2054	NHmuc_02533
NHmuc_02545	3.494192334	9.04805E-06	hypothetical, unclassified, unknown	PA2066	NHmuc_02545
NHmuc_02546	4.231453845	1.4957E-05	protein and amino acid biosynthesis and metabolism	PA2067	NHmuc_02546
NHmuc_02547	2.591372267	0.006680858	Secreted Factors (Virulence factors, toxins, biofilm enzymes, alginate)	PA2068	NHmuc_02547
NHmuc_02548	5.870527406	2.17334E-06	nucleotide biosynthesis	PA2069	NHmuc_02548
NHmuc_02589	2.030340731	0.01982077	hypothetical, unclassified, unknown	PA2116	NHmuc_02589
cupA1	-3.012679093	0.008823471	motility and attachement	PA2128	NHmuc_02602
NHmuc_02622	-3.126282845	0.019010709	hypothetical, unclassified, unknown	PA0845	NHmuc_02622
NHmuc_02623	3.577050193	0.001866626	oxidative stress	PA2146	NHmuc_02623
NHmuc_02636	-4.304387204	0.004229683	Signal transduction	PA2159	NHmuc_02636
NHmuc_02643	4.192987849	6.05419E-07	hypothetical, unclassified, unknown	PA2166	NHmuc_02643
NHmuc_02644	-2.991739486	0.017628142	fatty acid, phospholipid and rhamnolipid metabolism	PA2167	NHmuc_02644
hcnA	3.396840965	9.87829E-05	Secreted Factors (Virulence factors, toxins, biofilm enzymes, alginate)	PA2193	NHmuc_02673
hcnB	2.978577379	0.000551741	Secreted Factors (Virulence factors, toxins, biofilm enzymes, alginate)	PA2194	NHmuc_02674
hcnC	2.589282848	0.018900082	Secreted Factors (Virulence factors, toxins, biofilm enzymes, alginate)	PA2195	NHmuc_02675
bkdR	-2.87474868	0.036168641	transcription regulator	PA2246	NHmuc_02721

bkdA1	-4.854043842	0.010701216	energy metabolism	PA2247	NHmuc_02723
bkdA2	-7.544732073	0.001329842	protein and amino acid biosynthesis and metabolism	PA2248	NHmuc_02724
bkdB	-9.207888483	0.000332406	energy metabolism	PA2249	NHmuc_02725
lpdV	-10.49827825	5.76107E-05	energy metabolism	PA2250	NHmuc_02726
chiC	16.87708596	1.45256E-09	Secreted Factors (Virulence factors, toxins, biofilm enzymes, alginate)	PA2300	NHmuc_02776
NHmuc_02777	2.74763445	0.000837484	transcription, RNA processing	PA2301	NHmuc_02777
NHmuc_02778	3.658376992	0.007289717	Secreted Factors (Virulence factors, toxins, biofilm enzymes, alginate)	PA2302	NHmuc_02778
NHmuc_02779	4.058868107	7.66919E-06	Regulatory protein (cell cycle, transcription, immune response)	PA2303	NHmuc_02779
NHmuc_02780	2.2227256	0.018142306	transcription regulator	PA2304	NHmuc_02780
NHmuc_02781	3.536534985	0.001247642	Secreted Factors (Virulence factors, toxins, biofilm enzymes, alginate)	PA2305	NHmuc_02781
NHmuc_02803	2.135429429	0.033385201	transport, Secretion, export	PA2327	NHmuc_02803
NHmuc_02806	2.356392155	0.002540432	fatty acid, phospholipid and rhamnolipid metabolism	PA2330	NHmuc_02806
NHmuc_02807	2.331557238	0.013287939	oxidative stress	PA2331	NHmuc_02807
impJ	2.208912982	0.027112295	Type IV secretion system	PA2363	NHmuc_02839
impB	2.175508851	0.029709357	DNA replication, recombination, modification and repair	PA2365	NHmuc_02841
NHmuc_02856	-3.07709124	0.016419271	energy metabolism	PA2379	NHmuc_02856
NHmuc_02858	2.64977315	0.001456352	Energy metabolism	PA2381	NHmuc_02858
NHmuc_02881	-2.548744985	0.020430505	hypothetical, unclassified, unknown	PA2405	NHmuc_02881
NHmuc_02882	-6.119914005	0.000178199	Cell Wall/LPS/Capsule	PA2406	NHmuc_02882
NHmuc_02883	-5.580165379	0.008588433	Cell Wall/LPS/Capsule	PA2407	NHmuc_02883
NHmuc_02922	5.271546147	0.000355611	hypothetical, unclassified, unknown	PA4734	NHmuc_02922
NHmuc_02957	-2.621738075	0.025885357	Secreted Factors (Virulence factors, toxins, biofilm enzymes, alginate)	PA2463	NHmuc_02957
NHmuc_02976	-2.969068298	0.005026094	energy metabolism	PA2482	NHmuc_02976
NHmuc_02978	-3.684561603	0.023916663	transcription regulator	PA2484	NHmuc_02978
NHmuc_02980	-2.740258634	0.004950684	hypothetical, unclassified, unknown	PA2486	NHmuc_02980
NHmuc_02991	-2.659018459	0.015223029	transcription regulator	PA2497	NHmuc_02991
NHmuc_02998	2.976340437	4.908E-05	hypothetical, unclassified, unknown	PA2504	NHmuc_02998
antA	4.238259049	0.002714362	Energy metabolism	PA2512	NHmuc_03006
antB	2.442460011	0.034998279	Energy metabolism	PA2513	NHmuc_03007
antC	4.064440595	4.86797E-07	Energy metabolism	PA2514	NHmuc_03008

cigR	-9.542501423	0.00043664	Cell Wall/LPS/Capsule	PA2562	NHmuc_03060
tam	5.426198486	7.9258E-06	nucleotide biosynthesis	PA2564	NHmuc_03062
NHmuc_03063	3.54922096	6.02961E-06	hypothetical, unclassified, unknown	PA2565	NHmuc_03063
NHmuc_03064	4.348191152	2.08823E-05	nucleotide biosynthesis	PA2566	NHmuc_03064
NHmuc_03068	-2.986636015	0.008097799	hypothetical, unclassified, unknown	PA2569	NHmuc_03068
lecA	2.852771271	0.004612404	Secreted Factors (Virulence factors, toxins, biofilm enzymes, alginate)	PA2570	NHmuc_03069
NHmuc_03090	3.262625173	0.000507241	transcription regulator	PA2588	NHmuc_03090
infA	-5.155983482	0.001631867	Transcription/translation	PA2619	NHmuc_03122
mnmA	-3.622328348	0.038795247	Transcription/translation	PA2626	NHmuc_03129
NHmuc_03170	-3.612671473	0.033836706	energy metabolism	PA2666	NHmuc_03170
NHmuc_03171	-4.039889721	0.000799893	transcription regulator	PA2667	NHmuc_03171
infC	-4.475492554	0.023536876	Transcription/translation	PA2743	NHmuc_03257
NHmuc_03262	-12.46367915	2.4886E-09	hypothetical, unclassified, unknown	PA3505	NHmuc_03262
NHmuc_03267	-3.35657899	0.018387567	hypothetical, unclassified, unknown	PA1644	NHmuc_03267
NHmuc_03272	-4.426147087	0.005930671	RNA Processing and degradation	PA2751	NHmuc_03272
NHmuc_03273	-8.101736164	3.86682E-07	hypothetical, unclassified, unknown	PA2701	NHmuc_03273
eco	-5.560186916	0.005219523	Secreted Factors (Virulence factors, toxins, biofilm enzymes, alginate)	PA2755	NHmuc_03279
NHmuc_03311	2.586515523	0.010729427	hypothetical, unclassified, unknown	PA2781	NHmuc_03311
NHmuc_03316	2.277060446	0.005834829	Energy metabolism	PA2786	NHmuc_03316
NHmuc_03337	2.15962559	0.021690603	cell division	PA2805	NHmuc_03337
NHmuc_03353	3.482275145	8.7395E-05	hypothetical, unclassified, unknown		NHmuc_03353
NHmuc_03356	3.790543246	0.000162736	hypothetical, unclassified, unknown	PA2633	NHmuc_03356
NHmuc_03358	7.141090705	2.02246E-08	Inclusion bodies	PA2188	NHmuc_03358
NHmuc_03359	4.881351634	7.49282E-07	Inclusion bodies	PA3779	NHmuc_03359
NHmuc_03369	-2.561010762	0.025427029	oxidative stress	PA2826	NHmuc_03369
htpX	-7.736662523	0.000359382	Heat Shock and chaperones	PA2830	NHmuc_03373
NHmuc_03383	-8.069092737	3.23529E-05	Transcription/translation	PA2840	NHmuc_03383
NHmuc_03386	3.116362519	0.007299763	protein and amino acid biosynthesis and metabolism	PA2843	NHmuc_03386
NHmuc_03389	-3.862659651	0.002325968	transcription regulator	PA2846	NHmuc_03389
efp	-4.362809676	0.030156143	Transcription/translation	PA2851	NHmuc_03394
NHmuc_03398	-4.588589233	0.021339705	Protein and amino acid biosynthesis and metabolism	PA2854	NHmuc_03398
NHmuc_03409	-3.827955873	0.013287939	DNA replication, recombination, modification and repair	PA2865	NHmuc_03409
NHmuc_03410	-2.922739761	0.009303747	hypothetical,	PA5141	NHmuc_03410

			unclassified, unknown		
NHmuc_03413	8.169395697	9.13076E-15	phage, transposon or plasmid	PA2868	NHmuc_03413
NHmuc_03422	-5.320059031	0.000236161	transcription regulator	PA2877	NHmuc_03422
NHmuc_03441	-3.558989295	0.030156143	transcription regulator	PA2896	NHmuc_03441
NHmuc_03446	-4.726218374	0.003783375	fatty acid, phospholipid and rhamnolipid metabolism	PA2901	NHmuc_03446
NHmuc_03466	2.422396137	0.008189319	hypothetical, unclassified, unknown	PA2919	NHmuc_03466
NHmuc_03478	-4.390146886	0.000233627	transcription regulator	PA2931	NHmuc_03478
NHmuc_03491	2.548459126	0.033842846	hypothetical, unclassified, unknown		NHmuc_03491
fabD	-5.28912888	0.003034677	fatty acid, phospholipid and rhamnolipid metabolism	PA2968	NHmuc_03521
NHmuc_03524	-4.053484541	0.015546538	iron acquisition/virulence	PA2971	NHmuc_03524
rluC	-4.79376696	0.013075478	Ribosome structure/function	PA2975	NHmuc_03528
NHmuc_03537	-3.871514371	0.02311624	transport, Secretion, export	PA2983	NHmuc_03537
NHmuc_03539	-4.127793724	0.003089575	hypothetical, unclassified, unknown	PA2985	NHmuc_03539
NHmuc_03556	-6.366718441	0.003762449	energy metabolism	PA3001	NHmuc_03556
NHmuc_03560	-4.017712562	0.006598764	protein and amino acid biosynthesis and metabolism	PA3005	NHmuc_03560
lexA	-2.49110919	0.021339705	DNA replication, recombination, modification and repair	PA3007	NHmuc_03562
NHmuc_03563	-7.362109338	4.97353E-06	cell division	PA3008	NHmuc_03563
NHmuc_03577	2.094805313	0.013287939	zinc/nitrogen metabolism	PA3022	NHmuc_03577
NHmuc_03586	-4.027562386	0.020368376	Cell Wall/LPS/Capsule	PA3031	NHmuc_03586
snr1	9.892182014	4.84724E-07	oxidative stress	PA3032	NHmuc_03588
NHmuc_03605	4.962311898	4.26321E-05	Hypothetical, unclassified, Unknown		NHmuc_03605
NHmuc_03611	-4.613794522	0.005165378	hypothetical, unclassified, unknown	PA3055	NHmuc_03611
NHmuc_03612	-5.216960425	0.003414642	DNA replication, recombination, modification and repair	PA3056	NHmuc_03612
NHmuc_03649	-2.799117393	0.010701216	cyanide metabolism	PA3093	NHmuc_03649
NHmuc_03671	-4.468931496	0.008296333	energy metabolism	PA3112	NHmuc_03671
NHmuc_03683	-6.063303937	0.000746199	transcription regulator	PA3124	NHmuc_03683
ibpA	-30.86511182	1.09581E-07	Heat Shock and chaperones	PA3126	NHmuc_03685
NHmuc_03712	-3.843031509	0.027360342	vitamin/heavy metal metabolism	PA4097	NHmuc_03712
NHmuc_03713	-4.997319328	0.011907376	hypothetical, unclassified, unknown	PA5449	NHmuc_03713
NHmuc_03714	-5.959215244	0.016834283	energy metabolism	PA1091	NHmuc_03714
NHmuc_03719	-2.648229505	0.017715584	hypothetical, unclassified, unknown	PA3538	NHmuc_03719
wzz	-5.384355659	0.008231901	Cell Wall/LPS/Capsule	PA3160	NHmuc_03721
NHmuc_03731	-3.092982635	0.018561762	hypothetical, unclassified, unknown		NHmuc_03731

NHmuc_03744	-2.448786365	0.022137328	protein and amino acid biosynthesis and metabolism	PA3181	NHmuc_03744
pgl	-5.12505861	3.03066E-06	energy metabolism	PA3182	NHmuc_03745
zwf	-9.541037984	7.08974E-05	energy metabolism	PA3183	NHmuc_03746
NHmuc_03753	2.683365054	0.023384293	Energy metabolism	PA3190	NHmuc_03753
edd	-5.657261045	0.00147933	energy metabolism	PA3194	NHmuc_03757
NHmuc_03778	2.286167248	0.011493221	motility and attachement	PA3214	NHmuc_03778
NHmuc_03801	3.898905706	0.007525246	Cell Wall/LPS/Capsule	PA3237	NHmuc_03801
NHmuc_03806	-2.713849794	0.026289545	fatty acid, phospholipid and rhamnolipid metabolism	PA3242	NHmuc_03806
NHmuc_03832	-5.237851201	0.007233958	Protein and amino acid biosynthesis and metabolism	PA3262	NHmuc_03832
NHmuc_03834	-3.347983813	0.025725564	hypothetical, unclassified, unknown		NHmuc_03834
NHmuc_03843	-5.371565336	3.29044E-05	energy metabolism	PA3270	NHmuc_03843
NHmuc_03862	19.73740243	6.8494E-21	oxidative stress	PA3287	NHmuc_03862
NHmuc_03863	19.56925506	1.80626E-18	Cell Wall/LPS/Capsule	PA3288	NHmuc_03863
NHmuc_03896	5.800672948	4.80787E-06	hypothetical, unclassified, unknown	PA3318	NHmuc_03896
lecB	9.59332893	5.9344E-08	Secreted Factors (Virulence factors, toxins, biofilm enzymes, alginate)	PA3361	NHmuc_03939
NHmuc_03948	2.027326745	0.025766114	hypothetical, unclassified, unknown	PA3369	NHmuc_03948
amrZ	-12.34248743	3.0104E-05	Secreted Factors (Virulence factors, toxins, biofilm enzymes, alginate)	PA3385	NHmuc_03964
NHmuc_03993	-4.511721246	0.009065186	DNA replication, recombination, modification and repair	PA3413	NHmuc_03993
NHmuc_03994	-2.570923693	0.02503635	hypothetical, unclassified, unknown	PA3414	NHmuc_03994
NHmuc_03995	-2.869435014	0.011897811	hypothetical, unclassified, unknown	PA4700	NHmuc_03995
NHmuc_04041	-4.020975863	0.018047309	energy metabolism	PA3460	NHmuc_04041
NHmuc_04042	-4.96172051	0.004642075	Protein and amino acid biosynthesis and metabolism	PA3461	NHmuc_04042
NHmuc_04053	-6.078803146	0.002338068	Cell Wall/LPS/Capsule	PA3472	NHmuc_04053
NHmuc_04054	-2.63177412	0.006267371	antibiotic resistance	PA3473	NHmuc_04054
rhlL	4.27426147	7.6398E-08	transcription regulator	PA3476	NHmuc_04057
rhlR	6.304817418	0.000121182	transcription regulator	PA3477	NHmuc_04058
rhlB	2.948971743	0.025300743	fatty acid, phospholipid and rhamnolipid metabolism	PA3478	NHmuc_04059
rhlA	3.541824596	0.01439246	fatty acid, phospholipid and rhamnolipid metabolism	PA3479	NHmuc_04060
NHmuc_04074	7.744181754	2.23045E-12	protein and amino acid biosynthesis and metabolism	PA3496	NHmuc_04074

NHmuc_04079	-2.262660414	0.020516325	vitamin/heavy metal metabolism	PA3519	NHmuc_04079
bfrB	-8.323042492	0.006845427	iron acquisition/virulence	PA3531	NHmuc_04091
NHmuc_04092	-8.099816012	0.00123197	transport, Secretion, export	PA3532	NHmuc_04092
NHmuc_04093	-4.612712281	0.029895396	oxidative stress	PA3533	NHmuc_04093
algD	-30.44578348	1.01598E-09	Secreted Factors (Virulence factors, toxins, biofilm enzymes, alginate)	PA3540	NHmuc_04100
NHmuc_04101	-4.214291274	0.003052935	Secreted Factors (Virulence factors, toxins, biofilm enzymes, alginate)	PA3541	NHmuc_04101
algE	-3.207155053	0.023536876	Secreted Factors (Virulence factors, toxins, biofilm enzymes, alginate)	PA3544	NHmuc_04104
algX	-3.473695945	0.007697403	Secreted Factors (Virulence factors, toxins, biofilm enzymes, alginate)	PA3546	NHmuc_04106
algL	-2.671378868	0.016628566	energy metabolism	PA3547	NHmuc_04107
algF	-5.424078423	2.08823E-05	Secreted Factors (Virulence factors, toxins, biofilm enzymes, alginate)	PA3550	NHmuc_04110
algA	-5.34709863	0.001961357	protein and amino acid biosynthesis and metabolism	PA3551	NHmuc_04111
NHmuc_04118	2.324453559	0.017829678	fatty acid, phospholipid and rhamnolipid metabolism	PA3558	NHmuc_04118
NHmuc_04129	-5.795427756	0.001933383	Secreted Factors (Virulence factors, toxins, biofilm enzymes, alginate)	PA3566	NHmuc_04129
NHmuc_04130	-5.999199792	6.38087E-05	energy metabolism	PA3567	NHmuc_04130
NHmuc_04137	-4.552348941	0.00020543	transcription regulator	PA3574	NHmuc_04137
NHmuc_04138	-28.84538749	1.2516E-10	transport, Secretion, export	PA3520	NHmuc_04138
NHmuc_04143	-3.787913066	0.002586297	protein and amino acid biosynthesis and metabolism	PA3580	NHmuc_04143
glpD	-3.944052639	0.028525891	fatty acid, phospholipid and rhamnolipid metabolism	PA3584	NHmuc_04147
recX	-4.466619396	3.10711E-05	DNA replication, recombination, modification and repair	PA3616	NHmuc_04179
NHmuc_04180	-16.07969736	3.3064E-06	DNA replication, recombination, modification and repair	PA3617	NHmuc_04180
NHmuc_04181	-2.526983646	0.039118729	DNA replication, recombination, modification and repair	PA3618	NHmuc_04181
NHmuc_04185	16.68827501	6.6701E-06	transcription regulator		NHmuc_04185
NHmuc_04201	-6.537941929	0.001524962	nucleotide biosynthesis	PA3637	NHmuc_04201
tsf	-3.592454364	0.029845438	Transcription/translati	PA3655	NHmuc_04219

			on		
rpsB	-4.289274841	0.018801312	Ribosome structure/function	PA3656	NHmuc_04220
NHmuc_04221	-3.279946179	0.01982077	hypothetical, unclassified, unknown		NHmuc_04221
map	-4.233866306	0.028839065	Protein and amino acid biosynthesis and metabolism	PA3657	NHmuc_04222
NHmuc_04228	-3.038842109	0.024687056	motility and attachement	PA3663	NHmuc_04228
NHmuc_04250	-3.361544302	0.005026094	Protein and amino acid biosynthesis and metabolism	PA3685	NHmuc_04250
adk	-4.825103304	0.003101391	nucleotide biosynthesis	PA3686	NHmuc_04251
cadA2	-5.765438836	0.00184906	transcription regulator	PA3690	NHmuc_04255
prfB	-3.74772747	0.029513801	Protein and amino acid biosynthesis and metabolism	PA3701	NHmuc_04266
NHmuc_04287	2.101946485	0.03625249	Energy metabolism	PA3723	NHmuc_04287
lasB	5.4083324	0.000143769	Secreted Factors (Virulence factors, toxins, biofilm enzymes, alginate)	PA3724	NHmuc_04288
NHmuc_04295	-5.044114205	0.000551741	Heat Shock and chaperones	PA3731	NHmuc_04295
NHmuc_04296	-10.30190036	0.000638522	hypothetical, unclassified, unknown	PA3732	NHmuc_04296
NHmuc_04298	-7.21675114	4.49396E-05	hypothetical, unclassified, unknown	PA2747	NHmuc_04298
dsbC	-6.357639387	0.002212046	Protein and amino acid biosynthesis and metabolism	PA3737	NHmuc_04302
ffh	-4.249819748	0.019245838	Signal transduction	PA3746	NHmuc_04311
NHmuc_04327	-2.260437248	0.026302118	hypothetical, unclassified, unknown	PA3762	NHmuc_04327
NHmuc_04330	-2.124043799	0.035010105	hypothetical, unclassified, unknown	PA3765	NHmuc_04330
NHmuc_04351	2.450457945	0.003171616	hypothetical, unclassified, unknown	PA3784	NHmuc_04351
NHmuc_04352	5.43842799	1.89208E-07	Cell Wall/LPS/Capsule	PA3785	NHmuc_04352
NHmuc_04353	2.55202055	0.002055513	hypothetical, unclassified, unknown	PA3786	NHmuc_04353
NHmuc_04355	2.870284038	0.000181839	hypothetical, unclassified, unknown	PA3788	NHmuc_04355
oprC	2.507869567	0.010310287	transport, Secretion, export	PA3790	NHmuc_04357
NHmuc_04358	3.960203547	1.09581E-07	iron acquisition/virulence	PA3791	NHmuc_04358
ndk	-4.854242673	0.00705587	nucleotide biosynthesis	PA3807	NHmuc_04374
NHmuc_04375	2.838575954	0.000616273	iron acquisition/virulence	PA3808	NHmuc_04375
NHmuc_04385	-5.149851173	0.004991789	transcription regulator	PA3818	NHmuc_04385
NHmuc_04386	-12.45456645	6.83353E-05	transport, Secretion, export	PA3819	NHmuc_04386
yajC	-2.771058156	0.020688736	transport, Secretion, export	PA3822	NHmuc_04389
NHmuc_04396	-3.917395951	0.028544519	transport, Secretion, export	PA3828	NHmuc_04396
NHmuc_04413	2.55408797	0.001067257	Secreted Factors (Virulence factors, toxins, biofilm enzymes, alginate)	PA3844	NHmuc_04413
NHmuc_04470	-5.912053209	8.18586E-05	Secreted Factors	PA3902	NHmuc_04470

			(Virulence factors, toxins, biofilm enzymes, alginate)		
NHmuc_04472	3.165634912	0.000120594	Type IV Secretion system	PA3904	NHmuc_04472
NHmuc_04489	-9.730187002	3.13656E-05	energy metabolism	PA3920	NHmuc_04489
NHmuc_04520	-3.798234732	0.001144294	Transcription/translation	PA3951	NHmuc_04520
NHmuc_04521	-10.77256168	1.92605E-06	transport, Secretion, export	PA3952	NHmuc_04521
NHmuc_04533	-4.637766106	0.01439246	hypothetical, unclassified, unknown	PA1846	NHmuc_04533
NHmuc_04557	-2.706306551	0.036264195	hypothetical, unclassified, unknown	PA3979	NHmuc_04557
NHmuc_04564	3.833921619	2.63289E-06	hypothetical, unclassified, unknown	PA3986	NHmuc_04564
ppa	-4.540826459	0.013075478	energy metabolism	PA4031	NHmuc_04607
nusB	-2.868580009	0.024687056	transcription regulator	PA4052	NHmuc_04628
ribH	-3.174719819	0.022137328	energy metabolism	PA4053	NHmuc_04629
ribB	-2.414616216	0.029895396	energy metabolism	PA4054	NHmuc_04630
ribC	-4.728478409	0.000363344	vitamin/heavy metal metabolism	PA4055	NHmuc_04631
NHmuc_04637	-9.242285213	0.000153815	oxidative stress	PA4061	NHmuc_04637
ampC	4.287109347	0.001646686	antibiotic resistance	PA4110	NHmuc_04689
NHmuc_04690	2.685363352	0.010118755	hypothetical, unclassified, unknown	PA4111	NHmuc_04690
NHmuc_04707	3.119692004	9.87829E-05	protein and amino acid biosynthesis and metabolism	PA4128	NHmuc_04707
NHmuc_04708	6.09181152	1.5135E-10	Energy metabolism	PA4129	NHmuc_04708
NHmuc_04711	2.73821285	0.004122396	transcription regulator	PA4132	NHmuc_04711
NHmuc_04712	3.454751116	0.008706714	Energy metabolism	PA4133	NHmuc_04712
NHmuc_04713	5.659064105	2.50923E-09	hypothetical, unclassified, unknown	PA4134	NHmuc_04713
NHmuc_04718	10.92503714	1.4704E-11	hypothetical, unclassified, unknown	PA4139	NHmuc_04718
NHmuc_04720	62.47174884	3.24397E-16	hypothetical, unclassified, unknown	PA4141	NHmuc_04720
NHmuc_04733	-4.000671454	8.18586E-05	transport, Secretion, export	PA4154	NHmuc_04733
NHmuc_04745	-2.301747237	0.025300743	fatty acid, phospholipid and rhamnolipid metabolism	PA4166	NHmuc_04745
NHmuc_04760	-2.701592985	0.00187657	DNA replication, recombination, modification and repair	PA4181	NHmuc_04760
NHmuc_04761	-9.451508195	7.45465E-05	transcription regulator	PA4182	NHmuc_04761
NHmuc_04762	-4.066699062	8.18586E-05	Secreted Factors (Virulence factors, toxins, biofilm enzymes, alginate)	PA4183	NHmuc_04762
NHmuc_04775	-6.977326226	7.118E-07	two-component regulatory system	PA4196	NHmuc_04775
NHmuc_04776	-15.15225768	6.0636E-06	Signal transduction	PA4197	NHmuc_04776
NHmuc_04781	-4.649806111	0.000264072	fatty acid, phospholipid and rhamnolipid metabolism	PA4202	NHmuc_04781
NHmuc_04782	-4.619689968	0.000133509	transcription regulator	PA4203	NHmuc_04782

mexH	4.073102208	2.17334E-06	antibiotic resistance	PA4206	NHmuc_04785
mexI	3.039168715	0.025427029	antibiotic resistance	PA4207	NHmuc_04786
opmD	4.614094841	1.8488E-07	Cell Wall/LPS/Capsule	PA4208	NHmuc_04787
phzE1_2	2.530379352	0.027047635	Secreted Factors (Virulence factors, toxins, biofilm enzymes, alginate)	PA4214	NHmuc_04793
phzF1_2	3.81485457	0.001524962	Secreted Factors (Virulence factors, toxins, biofilm enzymes, alginate)	PA4215	NHmuc_04794
phzG2_2	7.397533527	3.34419E-06	Secreted Factors (Virulence factors, toxins, biofilm enzymes, alginate)	PA1905	NHmuc_04795
ssb	-3.854195764	0.002794904	DNA replication, recombination, modification and repair	PA4232	NHmuc_04811
katA	22.80862551	7.12639E-10	oxidative stress	PA4236	NHmuc_04815
rpmJ_2	3.987906644	0.00200701	Ribosome structure/function	PA4242	NHmuc_04821
rpsN	2.314606081	0.018665522	Ribosome structure/function	PA4250	NHmuc_04829
tuf2_2	-7.716427272	0.000505605	transcription regulator	PA4277	NHmuc_04860
NHmuc_04863	-4.631211615	0.00705587	hypothetical, unclassified, unknown		NHmuc_04863
NHmuc_04886	3.33655998	0.006786276	Hypothetical, unclassified, Unknown		NHmuc_04886
NHmuc_04912	5.067236288	0.028169864	transcription regulator		NHmuc_04912
NHmuc_04924	11.35638131	3.24397E-16	hypothetical, unclassified, unknown	PA4738	NHmuc_04924
NHmuc_04925	10.74361491	2.20628E-08	transport, Secretion, export	PA4739	NHmuc_04925
NHmuc_04933	-6.640887399	0.00408448	Ribosome structure/function	PA4746	NHmuc_04933
NHmuc_04935	-2.725651884	0.025319825	hypothetical, unclassified, unknown		NHmuc_04935
tpiA	-4.117484338	0.018665522	energy metabolism	PA4748	NHmuc_04936
NHmuc_04940	-4.556690059	0.011907376	Ribosome structure/function	PA4752	NHmuc_04940
NHmuc_04941	-3.600301931	0.028046734	RNA Processing and degradation	PA4753	NHmuc_04941
NHmuc_04942	-3.255479377	0.003271859	transport, Secretion, export	PA4754	NHmuc_04942
NHmuc_04945	-2.95852575	0.025731279	protein and amino acid biosynthesis and metabolism	PA4757	NHmuc_04945
NHmuc_04946	-9.042416191	0.000270892	nucleotide biosynthesis	PA4758	NHmuc_04946
NHmuc_04947	-6.762360152	0.000318762	hypothetical, unclassified, unknown		NHmuc_04947
dapB	-17.0356775	2.75982E-06	energy metabolism	PA4759	NHmuc_04948
dnaJ	-11.95228098	7.45465E-05	Heat Shock and chaperones	PA4760	NHmuc_04949
NHmuc_04950	-17.59238009	3.34419E-06	Heat Shock and chaperones	PA4761	NHmuc_04950
grpE	-25.1319909	1.22598E-07	Heat Shock and chaperones	PA4762	NHmuc_04951
NHmuc_04967	2.161522462	0.019655562	transcription regulator	PA4778	NHmuc_04967
fdnH	2.938079851	0.000917438	protein and amino acid biosynthesis and metabolism	PA4811	NHmuc_05001
NHmuc_05019	-3.206480443	0.001329842	hypothetical, unclassified, unknown	PA4826	NHmuc_05019

NHmuc_05036	-4.479050782	0.008220392	hypothetical, unclassified, unknown	PA4842	NHmuc_05036
NHmuc_05037	-7.992546431	0.000433862	hypothetical, unclassified, unknown	PA1387	NHmuc_05037
accB	-3.111667039	0.001832216	energy metabolism	PA4847	NHmuc_05042
NHmuc_05046	-3.11209978	0.016834283	transcription regulator	PA4851	NHmuc_05046
NHmuc_05065	-3.215499207	0.015393726	transcription regulator	PA4870	NHmuc_05065
NHmuc_05073	-9.214901049	0.000376385	transcription regulator	PA4878	NHmuc_05073
NHmuc_05135	-4.095672986	0.01420864	nucleotide biosynthesis	PA4938	NHmuc_05135
hisZ	-5.575182461	0.001150362	energy metabolism	PA4939	NHmuc_05136
NHmuc_05137	-6.162445331	0.000551741	transport, Secretion, export	PA4940	NHmuc_05137
NHmuc_05140	-6.883278059	0.001204117	energy metabolism	PA4943	NHmuc_05140
NHmuc_05141	-7.21776827	0.002586297	transcription regulator	PA4944	NHmuc_05141
NHmuc_05167	-2.387492012	0.025805715	energy metabolism	PA4970	NHmuc_05167
aspP	-3.577195257	0.005616748	energy metabolism	PA4971	NHmuc_05168
NHmuc_05205	-2.19076535	0.038818698	energy metabolism	PA5007	NHmuc_05205
NHmuc_05206	-2.804926636	0.010676471	Cell Wall/LPS/Capsule	PA5008	NHmuc_05206
waaP	-3.847140006	0.012156795	Secreted Factors (Virulence factors, toxins, biofilm enzymes, alginate)	PA5009	NHmuc_05207
waaG	-5.274565797	0.004102209	Protein and amino acid biosynthesis and metabolism	PA5010	NHmuc_05208
NHmuc_05225	2.717887425	0.007375163	oxidative stress	PA5027	NHmuc_05225
gltB	-3.86550244	0.019570838	protein and amino acid biosynthesis and metabolism	PA5036	NHmuc_05234
hslV	-16.88301086	4.13225E-07	Heat Shock and chaperones	PA5053	NHmuc_05252
hslU	-9.188294167	6.72388E-05	Heat Shock and chaperones	PA5054	NHmuc_05253
NHmuc_05272	-3.767009273	0.035008372	hypothetical, unclassified, unknown	PA5073	NHmuc_05272
NHmuc_05275	-3.257805589	0.027988263	transport, Secretion, export	PA5076	NHmuc_05275
mdoD	-3.719137484	0.024655919	energy metabolism	PA5078	NHmuc_05277
blc	-3.766031801	0.004723299	Cell Wall/LPS/Capsule	PA5107	NHmuc_05306
NHmuc_05307	-2.292737845	0.019208813	Cell Wall/LPS/Capsule	PA5108	NHmuc_05307
fbp	-3.898648784	0.031413472	energy metabolism	PA5110	NHmuc_05309
glnA	-12.30100677	5.84838E-06	protein and amino acid biosynthesis and metabolism	PA5119	NHmuc_05318
ntrB	-3.186654488	0.01653863	two-component regulatory system	PA5124	NHmuc_05323
NHmuc_05324	-2.768129412	0.030434916	Protein and amino acid biosynthesis and metabolism	PA5125	NHmuc_05324
grx	-3.909947953	0.005838259	energy metabolism	PA5129	NHmuc_05328
rmlD	2.477580729	0.017085558	fatty acid, phospholipid and rhamnolipid metabolism	PA5162	NHmuc_05365
rmlA	2.548992766	0.012156795	Energy metabolism	PA5163	NHmuc_05366
rmlC	3.173655128	0.000153815	nucleotide biosynthesis	PA5164	NHmuc_05367

arcA	2.738312052	0.027360342	protein and amino acid biosynthesis and metabolism	PA5171	NHmuc_05374
NHmuc_05385	-29.31646515	8.47921E-08	transport, Secretion, export	PA5182	NHmuc_05385
NHmuc_05386	-9.142058711	1.58886E-08	DNA replication, recombination, modification and repair	PA5183	NHmuc_05386
pckA	-5.870222012	0.005265267	energy metabolism	PA5192	NHmuc_05396
gcvH1	-2.561356603	0.030434916	Protein and amino acid biosynthesis and metabolism	PA5214	NHmuc_05418
NHmuc_05424	2.904126995	0.000363344	hypothetical, unclassified, unknown	PA5220	NHmuc_05424
NHmuc_05425	2.128565137	0.012857887	oxidative stress	PA5221	NHmuc_05425
NHmuc_05426	2.090050077	0.014157681	transcription regulator	PA5426	NHmuc_05426
NHmuc_05431	-5.029373784	0.000703254	cell division	PA5227	NHmuc_05431
NHmuc_05433	-3.162367856	0.034847811	energy metabolism	PA5228	NHmuc_05433
rho	-5.725244627	0.003749137	transcription regulator	PA5239	NHmuc_05445
NHmuc_05446	-8.250197002	0.000317519	hypothetical, unclassified, unknown		NHmuc_05446
hemC	-3.886425859	0.03383863	iron acquisition/virulence	PA5260	NHmuc_05468
lppL	-8.136777734	0.000908998	Cell Wall/LPS/Capsule	PA5276	NHmuc_05485
NHmuc_05512	2.848091794	0.000700034	nucleotide biosynthesis	PA5222	NHmuc_05512
NHmuc_05515	-2.896954142	0.027047635	Cell Wall/LPS/Capsule	PA5306	NHmuc_05515
pyrE	-3.669096132	0.022137328	nucleotide biosynthesis	PA5331	NHmuc_05540
rph	-4.694549778	0.006764943	RNA Processing and degradation	PA5334	NHmuc_05543
yicC	-2.775364896	0.010484845	hypothetical, unclassified, unknown	PA5335	NHmuc_05544
gmk	-2.295010127	0.025427029	nucleotide biosynthesis	PA5336	NHmuc_05545
NHmuc_05568	2.20696566	0.013287939	Secreted Factors (Virulence factors, toxins, biofilm enzymes, alginate)	PA5359	NHmuc_05568
betA	-5.346222992	0.003089575	protein and amino acid biosynthesis and metabolism	PA5372	NHmuc_05586
betB	-4.328697101	0.017085558	energy metabolism	PA5373	NHmuc_05587
NHmuc_05650	-7.984398594	0.001173191	energy metabolism	PA5435	NHmuc_05650
NHmuc_05652	-4.525188909	0.010701216	transcription regulator	PA5437	NHmuc_05652
NHmuc_05654	-8.261639183	0.000820513	transcription regulator	PA5438	NHmuc_05654
NHmuc_05663	4.728439825	7.08974E-05	hypothetical, unclassified, unknown	PA5446	NHmuc_05663
NHmuc_05677	3.497446692	2.18019E-05	hypothetical, unclassified, unknown	PA5460	NHmuc_05677
NHmuc_05697	2.089840528	0.038166819	Secreted Factors (Virulence factors, toxins, biofilm enzymes, alginate)	PA5481	NHmuc_05697
cc4	-3.725494621	0.038264587	energy metabolism	PA5490	NHmuc_05706
NHmuc_05707	-4.712631469	0.002212046	energy metabolism	PA5491	NHmuc_05707
engB	-5.496461139	0.001860987	Ribosome structure/function	PA5492	NHmuc_05708
NHmuc_05719	-4.160315895	0.004018062	Cell Wall/LPS/Capsule	PA5502	NHmuc_05719

NHmuc_05743	-4.087740302	0.000687276	transcription regulator	PA5525	NHmuc_05743
NHmuc_05744	-17.30352723	5.76107E-05	Cell Wall/LPS/Capsule	PA5526	NHmuc_05744
NHmuc_05746	-3.985684245	0.037072056	transport, Secretion, export	PA5528	NHmuc_05746
NHmuc_05751	-3.770535747	0.012085973	energy metabolism	PA5533	NHmuc_05751
NHmuc_05764	3.764297241	0.011948526	fatty acid, phospholipid and rhamnolipid metabolism	PA5546	NHmuc_05764
glmR	-2.253629907	0.035035864	transcription regulator	PA5550	NHmuc_05768
atpH	-3.592367501	0.03625249	energy metabolism	PA5557	NHmuc_05775
atpF	-3.914812343	0.017223443	energy metabolism	PA5558	NHmuc_05776
atpB	-3.836825345	0.023536876	energy metabolism	PA5560	NHmuc_05778